RHEOLOGICAL PROPERTIES AND PERMEABILITY PROPERTIES OF CEMENTED AND UNCEMENTED HIGH-DENSITY PASTE TAILINGS: EFFECT OF SULPHIDE MINERALS

MIRACLE OYEWALE

Thesis submitted to the University of Ottawa in partial fulfilment of the requirements for the degree of ***Doctor of Philosophy in Environmental Engineering.***

Thesis Supervisor: Prof. Mamadou Fall
Thesis Co-supervisor: Dr. Alireza Ghirian

uOttawa

Ottawa-Carleton Institute for Environmental Engineering (OCIENE)
Department of Civil Engineering
Faculty of Engineering
University of Ottawa

ABSTRACT

The sustainable management of sulphide-bearing mine tailings remains one of the most pressing environmental and geotechnical challenges in modern mining. This challenge arises from the reactive nature of iron sulphide minerals, particularly pyrite (FeS_2), which oxidizes to produce acid, leading to structural instability and environmental degradation. To curb these impacts, several tailings management strategies have been developed. Among the emerging approaches, paste tailings (PT) technology has emerged as a sustainable solution as it repurposes tailings into a dense, often cemented material that provides structural support for underground excavations, enhances storage stability, and mitigates acid mine drainage risks. Beyond its technical benefits, this approach contributes to environmental protection and supports the mining industry's transition toward more sustainable waste management practices.

PTs can be used underground as cemented paste backfill (CPB) or on the surface as uncemented (UPT) or lightly cemented paste tailings (LCPT). CPB and LCPT are composed of tailings, binder, and water, while UPT contains no binder. Preparation occurs at surface backfill plants, and the mixtures are transported to deposition sites by pumping or gravity flow. Consequently, flowability (or rheological properties) is a key design parameter. Once placed, PTs must exhibit low permeability to limit the movement of water and air, which can trigger acid generation and contaminant leaching. Therefore, understanding and optimizing both rheology and permeability properties are critical to the safe and sustainable design of PT systems.

However, there is limited knowledge about these properties, particularly when reactive pyrite-bearing tailings are incorporated. Pyrite addition may significantly alter the rheological and permeability behaviour of PTs. To address this knowledge gap, this study conducted a comprehensive laboratory investigation of PTs containing pyrite under various mix conditions (tailings type, binder composition, curing time, and pyrite content) that simulate field

environments. Tests included rheological (vane shear, viscosity), hydraulic (permeability), and physicochemical (pH, electrical conductivity, porosity, and void ratio) measurements. Complementary microstructural analyses, including thermogravimetric (TG/DTG), X-ray diffraction (XRD), and scanning electron microscopy (SEM), were performed to interpret the mechanisms governing the behaviour.

Results showed that increasing pyrite content elevated yield stress and viscosity, reducing flowability. Slag–Portland cement blends exhibited better flow characteristics than pure Portland cement systems. Permeability increased with higher pyrite and sulphate levels due to ettringite and gypsum formation, which caused microcracking and pore enlargement. Air exposure intensified oxidation and matrix weakening. Overall, binder type, sulphate concentration, and oxidation control were identified as critical factors for ensuring the long-term stability and durability of sulphide-bearing paste tailings.

ACKNOWLEDGMENTS

This PhD journey has been one of resilience, faith, and profound growth, and I am deeply grateful to everyone who has contributed to this achievement.

First and foremost, I thank God Almighty for His boundless grace, wisdom, and strength that sustained me throughout this academic pursuit. Every breakthrough, discovery, and moment of clarity came through His divine guidance.

I would like to express my deepest gratitude to my supervisor, Professor Mamadou Fall, for his invaluable guidance, encouragement, and mentorship throughout my doctoral journey. His profound expertise, insightful feedback, and unwavering support were instrumental in shaping the direction and quality of this research. I am equally thankful to my co-supervisor Dr. Alireza Ghirian for his technical advice and encouragement that greatly enriched my work.

My heartfelt gratitude extends to my colleagues, specifically Dr. Sada Haruna and Weizhou Quan, and to my friends in the Geotechnical Engineering Laboratory at the University of Ottawa for their collaboration, inspiring discussions, and camaraderie throughout this research journey. I also wish to thank the laboratory's technical staff, Mr. Jean Claude Celestin**,** for his assistance during sample preparation, testing, and analysis, as well as Dr. Wendy Pell and Mr. Glenn Poirier from other University of Ottawa laboratories for their generous technical support and guidance in conducting various experimental tests for this research.

I am sincerely thankful to my former professors from the University of Lagos, Professor J.K. Saliu, Dr. Nnamdi Amaeze, and Professor Ebuehi, whose recommendation letters opened the doors that led me to this remarkable opportunity. Their belief in my potential and continuous encouragement laid the foundation for this academic achievement.

To my family, I am eternally grateful. I especially thank my mum, Princess E.A. Olateru-Olagbegi, for her sacrifices, unconditional love, and unwavering belief in my dreams. To my loved ones and friends, thank you for your endless prayers, patience, and encouragement. Your support gave me the strength and courage to keep going, even when the journey was difficult.

This achievement is dedicated to everyone who continues to dream big and to those who supported me in turning mine into reality.

TABLE OF CONTENTS

LIST OF FIGURES

CHAPTER ONE

CHAPTER TWO

CHAPTER THREE

CHAPTER FOUR

CHAPTER FIVE

CHAPTER SIX

LIST OF TABLES

LIST OF SYMBOLS AND ABBREVIATIONS

Abbreviation	Description
%	Percentage
°C	Degree Celsius (temperature)
AMD	Acid Mine Drainage
ARD	Acid Rock Drainage
ASTM	American Society for Testing and Materials
C_2S	Dicalcium Silicate or Belite
C_3S	Tricalcium Silicate
$Ca(OH)_2$)/CH	Portlandite (Calcium Hydroxide)
CPB	Cemented Paste Backfill
C-S-H	Calcium Silicate Hydrate
DTG	Derivative Thermogravimetric
e	Void ratio
EC	Electrical Conductivity
Fe^{2+} / Fe^{3+}	Ferrous / Ferric ions
FeS_2	Pyrite/Iron disulphide
GHG	Green House Gases
G_s	Specific Gravity
k_{sat}	Saturated hydraulic conductivity
LCPT	Lightly Cemented Paste Tailings
MIP	Mercury Intrusion Porosimetry
NT	Natural Tailings
PC	Portland Cement Type I
PC-LCPT	Portland Cement–Lightly Cemented Paste Tailings
pH	Hydrogen Ion Concentration
Ppm	Parts per million
PT	Paste Tailings
SEM	Scanning Electron Microscopy
SG	Slag
SG-LCPT	Slag–Lightly Cemented Paste Tailings
SO_4^2	Sulphate
SPD	Surface Paste Disposal
ST	Silica Tailings
TG	Thermogravimetric
UPT	Uncemented Paste Tailings
Vol%	Volumetric Percentage
W	Water
W/C	Water to Cement ratio
XRD	X-ray Diffraction

CHAPTER ONE.
GENERAL INTRODUCTION

1.1 BACKGROUND OF STUDY

The mining sector has continued to play a pivotal role in human civilization throughout millennia (Morrice et al., 2013; Qi et al., 2016). In ancient civilizations, mining was instrumental in driving economic development in Classic Greece and the Roman Empire, particularly through the extraction of materials like lead, copper, and gold for currency production and construction (Fernandez-Lozano et al., 2015; Carvalho et al., 2017). As the Industrial Revolution era unfolded, mining assumed a greater significance by supplying essential raw materials needed for manufacturing and infrastructure development (Carvalho et al., 2017). The 20th century marked a significant turning point for the mining sector because the sector underwent global expansion and adoption of cutting-edge technologies that facilitated the feasibility of excavating valuable resources from remote and challenging environments (EB, 2017; Carvalho et al., 2017). This era also witnessed the emergence of mining conglomerates and the ascendancy of resource-rich nations as influential global players (Osama and Elhassan, 2022; Gilbria, 2014). Today, the mining sector has evolved into a global economic powerhouse, driving job creation, fueling economic expansion and promoting technological innovation through the extraction and processing of valuable minerals, metals and energy sources from within the earth's crust (Coelho et al., 2011; Haddaway et al., 2019; Hossain et al., 2013; Worlanyo and Jiangfeng, 2021).

According to data collated by Statista, in 2021, the global revenue generated from leading mining companies, representing a vast majority of the whole industry, was about 925 billion U.S.

dollars (Statista, 2023). On a national scale, the mining sector accounts for a dominant share of national wealth in both developing and developed countries. Ericsson and Löf (2018) stated that mining contributes approximately 10-20% of a nation's Gross domestic product (GDP), accounts for 50% or more of a country's exports and countries like China, America, Russia, Brazil, and Canada are leading mining hubs. The Canadian mining sector is a global leader in producing a diverse range of more than 60 minerals and metals (Natural Resources Canada, 2023). The economic significance of minerals and metals to Canada's economy falls within a range of 2.7% to 4.5% of the nation's real GDP (Marshall, 2021), which is about $91 billion (Natural Resources Canada, 2023). Furthermore, the broader extractive industry, which encompasses mineral, oil, and gas extraction, substantially contributed about $148.4 billion, equivalent to 7.9% of Canada's real GDP in 2020 (Marshall, 2021). Although the mining sector stands as a fundamental driver of Canada's economy and provides employment to nearly 403,000 Canadians (Natural Resources Canada, 2023), it is also noteworthy to know that mining activities have severe global ecological footprints (Carvalho et al., 2017).

Past mining operations have left a lasting imprint on the environment. Among the numerous issues that have emerged, the problems of mine waste (tailings) disposal and acid mine drainage (AMD) are of global concern (Carvalho et al., 2017). Tailings are voluminous waste products of mining process and typically contain toxic elements like acid-generating sulphides (e.g., pyrite, pyrrhotite), heavy metals (e.g., arsenic (As) and cadmium (Cd)), and other contaminants that may cause severe environmental issues like acid mine drainage if leached into the surrounding environment (e.g., surface and groundwater, soil) (Nordstrom, 2011; Jain et al., 2016; Carvalho et al., 2017). Among the different types of mine waste, sulphide-bearing tailings are the most hazardous due to their potential to cause AMD (Dold, 2014; Ohlander et al., 2012). This elevated

risk is attributed to the fact that when sulphidic tailings (containing pyrite) are exposed to air and water, they are known to undergo oxidation processes, resulting in AMD (Buckby et al., 2003). Although AMD can be generated naturally, it is also a known fact that mining activities increase the rate of acid formation by exposing a large volume of sulphide waste to the biogeosphere (Kumari et al., 2010). Therefore, it is imperative that mine tailings must be appropriately managed to prevent or minimize environmental, social and economic impacts (Benzaazoua et al., 2008).

Several mining disposal and mine waste management methods like desulphurization, dry stacking, paste tailings (cemented paste backfills (CPBs) and uncemented paste tailings (UPTs)), and/or a combination of these approaches have been proposed or put into practice to prevent/minimize the negative impacts of sulphidic tailings like AMD (Benzaazoua et al., 2008; Bois et al., 2012). Among these technologies, paste tailings (PTs) is one of the most innovative, cost-effective, and environmentally beneficial approaches adopted for reducing voluminous mine wastes and disposing hazardous sulphidic tailings generated during mining (Fall et al., 2005; Nasir and Fall, 2008). PTs can be used for backfilling underground mines in the form of cemented paste backfill (CPB) or for surface tailings disposal in the form of uncemented paste tailings (UPT) or lightly cemented paste tailings (LCPT) (Tariq and Ernest, 2013). CPB and LCPT are cementitious materials composed of tailings (usually 70%–85% of the total solid content), binder (2%–7% (for CPB)/ $\leq$ 1% (for LCPT) of the total solid mass), and water (Hassani and Archibald, 1998; Benzaazoua et al., 2004; Fall et al., 2010), while UPT is similar to CPB and LCPT in terms of composition and preparation, but do not contain cement or binder. PT (e.g., CPB, UPT and LCPT) preparation is usually completed at the ground surface (e.g., backfill plant) and then transported to final deposition sites (by pumping or/and gravity) (Liu and Fall, 2022). Hence, the transportability (which depends on rheological properties) of PT is a specific characteristic/property to consider

when transporting PT because if the transported material does not have suitable transportability/flowability, clogging of the pipelines might occur, which will lead to significant financial losses (e.g. flow delays/ interruption of the progress of PT production which may require possible replacement of the pipelines) (Li and Fall 2016; Haruna and Fall 2020; Bannister, 1980).

Aside from transportability (flowability), other key performance characteristics/properties to consider in preparing paste tailings are its mechanical stability (usually evaluated by strength), cost (depends on binder consumption) and, just as importantly, the environmental performance of the PT mixture (Fall et al., 2014). The environmental performance of PT is generally evaluated by its permeability and reactivity (Fall et al., 2005). This encompasses different mechanisms, including susceptibility to acid mine drainage, oxygen transport capacity and leaching potential. The aforementioned mechanisms are strongly influenced by the permeation properties of the PT, specifically its saturated hydraulic conductivity (Yilmaz, 2011; Ghirian and Fall, 2014; Fall et al., 2009; Levens et al., 1996). The saturated hydraulic conductivity provides essential information about the pore structure (e.g., coarseness, pore connectivity, presence of cracks) of PT. Deficient pore structure and cracks can result in rapid transfer of fluid (e.g., water and oxygen) between PT and adjacent rock, ore or environment which may increase the oxidation risk of sulphides (pyrite) present in the backfill material, thereby reducing the CPB/UPT/LCPT service life or increasing its ability to release contaminants into surrounding water bodies (Fall et al., 2009; Levens et al., 1996). Thus, improving the knowledge of PT approach by studying key performance properties (like rheological and permeability) of various mixture components and aspects of PT preparation would benefit the mining industry by enabling more environmentally friendly design of CPBs/LCPTs/UPTs and better tailings management practices.

1.2 STATEMENT OF PROBLEM

Paste-based technologies such as UPT, LCPT, and CPB are increasingly used in mine waste management because of their advantages in disposal efficiency and environmental control. However, their performance is strongly influenced by the nature of the tailings used, particularly when the tailings contain sulphide minerals such as pyrite. Sulphide-rich tailings present a high risk of acid mine drainage (AMD) generation and may alter the movement of oxygen and water within the paste matrix. These processes play a crucial role in determining both the short- and long-term behaviour of paste materials.

While several studies have examined the general rheological and hydraulic characteristics of paste mixtures, very little work has examined how pyrite content affects these properties. This gap is significant because rheological behaviour directly influences paste transport and deposition, whereas permeation behaviour governs fluid ingress, which drives sulphide oxidation and AMD development. Without a clear understanding of how pyrite-bearing tailings modify these key properties, designing reliable and environmentally sound paste disposal systems remains challenging.

Currently, there is limited experimental evidence describing the effects of varying pyrite contents on the yield stress, viscosity, and permeation characteristics of UPT, LCPT, and CPB used for surface and underground disposal. This lack of targeted information restricts the development of optimized mixture designs and predictive tools that could improve both operational performance and long-term environmental protection in mines handling sulphide-rich tailings.

This study addresses this critical knowledge gap by experimentally examining how pyrite minerals and their content influence the rheological and permeation behaviour of UPT and LCPT for surface paste disposal, as well as CPB for underground paste disposal.

1.3 RESEARCH OBJECTIVES

The overall goal of this research is to acquire an in-depth understanding of the effect of pyrite minerals on the rheological and permeability properties of CPB, LCPT and UPT. The specific objectives are:

- To investigate the effect of pyrite content on the rheological properties of paste tailings intended for surface disposal.
- To evaluate the influence of pyrite on the rheological behaviour of underground cemented paste tailings.
- To examine the impact of pyrite on the permeability characteristics of paste tailings designed for surface disposal.
- To assess the effect of pyrite content on the permeability properties of underground cemented paste tailings.

1.4 RESEARCH APPROACH

The research approaches and methods implemented in this study are illustrated schematically in Figure 1. To accomplish the listed study objectives in section 1.3, laboratory testing procedures for paste mixtures with pyrite have been utilized to assess its critical engineering design properties (rheological and permeability properties) under several mix components (tailings, binder type and pyrite content), and various curing conditions close to those encountered in the field. Preliminary review of the literature and a study of the theoretical background on the subject facilitated the selection of appropriate test methods for the investigations. Non-reactive synthetic silica tailings were used to prepare the paste mixtures. The use of non-reactive synthetic silica tailings can generally provide a certain level of confidence in the obtained results by controlling the effects of various reactive minerals that can be found in the natural tailings, which may alter the cement hydration process. Portland cement type I (PCI) and blast furnace slag (SG) in different proportions were used as binders. The mixing water type used was tap water. The main engineering properties investigated were yield stress, viscosity, and saturated hydraulic conductivity. The PT mixtures were prepared and cured under room temperature.

Microstructural analyses and monitoring tests were employed to have a better understanding of the mechanisms responsible for the behaviors observed from various tests. Zeta potential, electrical conductivity, and pH monitoring were performed on fresh PT mixtures to examine changes caused by binder hydration under the influence of the pyrite and different curing times. Mercury intrusion porosimetry (MIP), thermal analyses (TG/DTG), and X-ray diffraction (XRD) were conducted on some selected dried PT samples. Detailed description of all the experimental tests conducted are presented in the respective chapters.

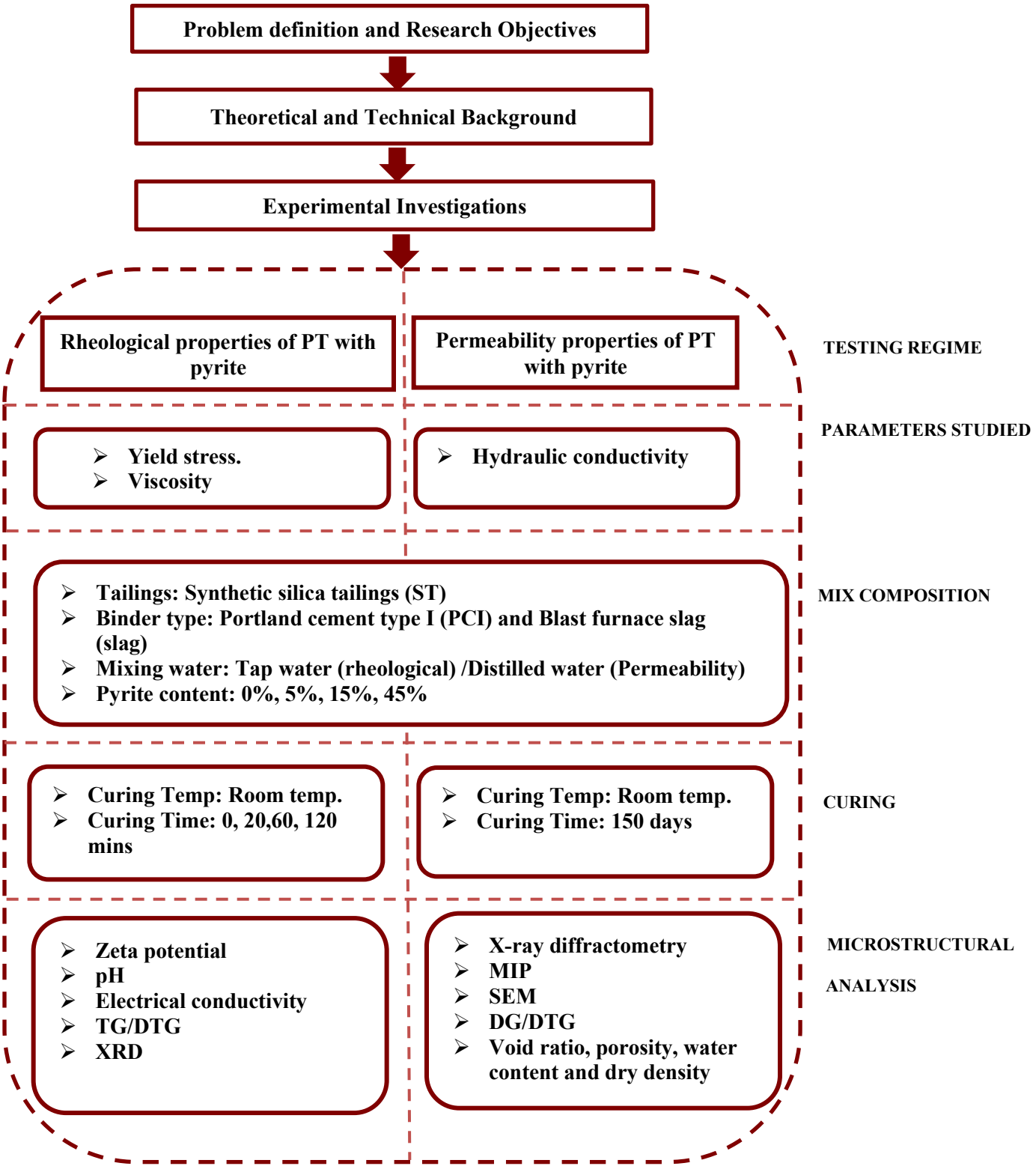

Figure 1: Research and study approach

1.5 ORGANIZATION OF THESIS MANUSCRIPT

This Ph.D. thesis is structured into eight chapters, which contain discussions of the different tasks and objectives of the current PhD research. Figure 2 presents the structure of the flowchart of this thesis. **Chapter One** is a general introduction, which contains problem statements, objectives, and research methods employed in this research. **Chapter Two** is structured to provide a comprehensive literature review and/or background information on tailings, sulphide minerals, tailings management methods, CPB technique and performance, binder hydration and past studies on the rheological and permeability properties of paste tailings. **Chapters Three to Six** are structured into a manuscript-based thesis format, which comprises four technical manuscripts. Each manuscript includes an introduction, materials and methods, results, and discussion, as well as a summary and conclusions. Therefore, some information in these manuscripts may be repeated as each paper is independently written following the manuscript preparation instructions of the corresponding publication journal. **Chapters Three and Four** present the experimental works and results on the effects of pyrite on the rheological properties of paste tailings for surface disposal (Chapter Three) and underground disposal (Chapter Four). **Chapters Five and Six** cover the experimental works and results on the effects of pyrite on the permeability properties of paste tailings for surface disposal (Chapter Five) and underground disposal (Chapter Six). **Chapter Seven** of this dissertation synthesizes and discusses the overall results obtained from this thesis. Finally, **Chapter Eight** presents the conclusion and future suggestions for advancing future works on the effect of pyrite on the material properties of paste tailings for surface and underground disposal. This chapter will also give recommendations for future studies.

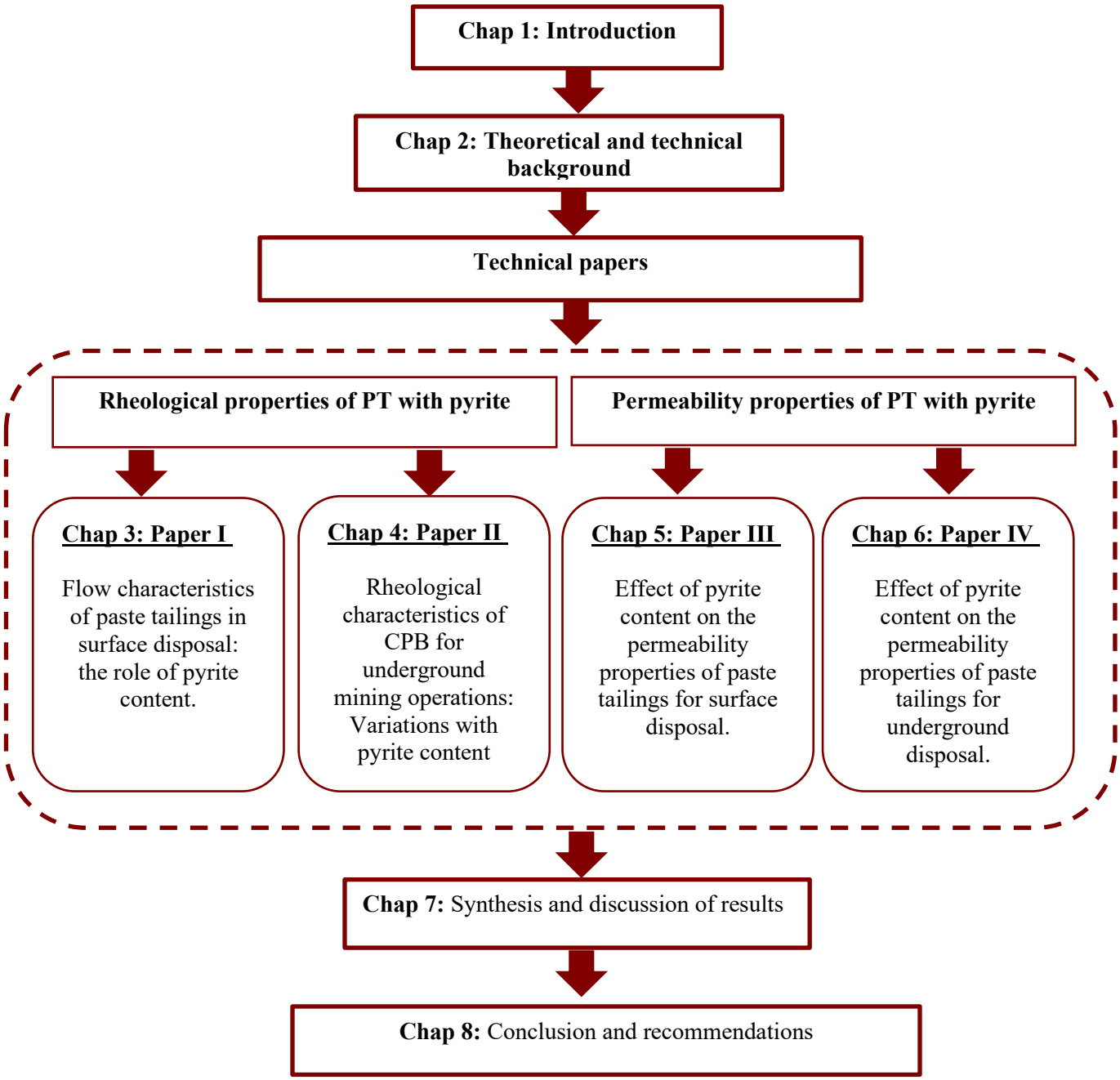

Figure 2: Thesis Organization

1.6 REFERENCES

Aldhafeeri, Z., and Fall, M. (2016). Time and damage induced changes in the chemical reactivity of cemented paste backfill. *Journal of Environmental Chemical Engineering*, 4(4), 4038- 4049

Aldhafeeri, A., and Fall, M., (2017). Sulphate induced changes in the reactivity of cemented tailings backfill. *International Journal of Mineral Processing,* 166 (10),13-23.

Ali, G., Fall, M., and Alainachi, I. (2021). Time- And Temperature-Dependence of Rheological Properties of Cemented Tailings Backfill with Sodium Silicate. *Journal of Materials in Civil Engineering,* 33(3), 04020498. doi:10.1061/(ASCE)MT.1943-5533.0003605.

Benzaazoua, M., Bussière, B., Demers, I., Aubertin, M., Fried, É., and Blier, A. (2008). Integrated mine tailings management by combining environmental desulphurization and cemented paste backfill: Application to mine Doyon, Quebec, Canada. *Minerals Engineering*, 21(4), 330–340. https://doi.org/10.1016/j.mineng.2007.11.012

Benzaazoua, M., Fall, M., and Belem, T. (2004). A contribution to understanding the hardening process of cemented pastefill. *Minerals Engineering*, 17(2), 141–152. https://doi.org/10.1016/j.mineng.2003.10.022

Bois, D., Benzaazoua, M., Bussiere, B., Kongolo, M., and Poirier, P. (2005). A feasibility study on the use of desulphurized tailings to control acid mine drainage. *CIM Bulletin*, 98(1087), 74–74.

Buckby, T., Black, S., Coleman, M. L., and Hodson, M. E. (2003). Fe-sulphate-rich evaporative mineral precipitates from the Rio Tinto, Southwest Spain. *Mineralogical Magazine*, 67(2), 263–278. https://doi.org/10.1180/0026461036720104

Carvalho, F. P. (2017). Mining Industry and Sustainable Development: Time for Change. *Food and Energy Security, 6*(2), 61–77. https://doi.org/10.1002/fes3.109.

Cazacliu, B. (2008). In-mixer measurements for describing mixture evolution during concrete mixing. *Chemical Engineering Research and Design*, 86(12), 1423–1433. https://doi.org/10.1016/j.cherd.2008.08.021

Cazacliu, B., and Roquet, N. (2009). Concrete mixing kinetics by means of power measurement. *Cement and Concrete Research*, 39(3), 182–194. https://doi.org/10.1016/j.cemconres.2008.12.005.

Chopin, D., de Larrard, F., and Cazacliu, B. (2004). Why do HPC and SCC require a longer mixing time? *Cement and Concrete Research*, 34(12), 2237–2243. https://doi.org/10.1016/j.cemconres.2004.02.012

Coelho, P.C.S., Teixeira, J.P.F., and Gonçalves, O.N.B.S.M. (2011). Mining activities: health impacts. In: Nriagu, J.O. (Ed.), *Encyclopedia of Environmental Health*, 3, 788–802.

Dold, B. (2014). Evolution of Acid Mine Drainage Formation in Sulphidic Mine Tailings. *Minerals*, 4(3), 621–641. http://doi.org/10.3390/min4030621

E.B. (2017). Mining. *Encyclopaedia Britannica* Online. Encyclopaedia Britannica Inc. Available at https://www.britannica.com/technology/mining (accessed 15 March 2017).

Ericsson, M., and Löf, O. (2018). Mining's Contribution to Low- and Middle-income Economies. In T. Addison and A. Roe (Eds.), Extractive Industries: The Management of Resources as a Driver of Sustainable Development (pp. 1-33). *Oxford Academic*. https://doi.org/10.1093/oso/9780198817369.003.0003

Fall, M., Benzaazoua, M., and Ouellet, S. (2005). Experimental characterization of the influence of tailings fineness and density on the quality of cemented paste backfill. *Minerals Engineering*, 18(1), 41–44. https://doi.org/10.1016/j.mineng.2004.05.012

Fall, M., Adrien, D., Célestin, J. C., Pokharel, M., and Touré, M. (2009). Saturated hydraulic conductivity of cemented paste backfill. *Minerals Engineering*, 22(15), 1307–1317. https://doi.org/10.1016/j.mineng.2009.08.002

Fall, M., Célestin, J. C., Pokharel, M., and Touré, M. (2010). A contribution to understanding the effects of curing temperature on the mechanical properties of mine cemented tailings backfill. *Engineering Geology*, 114(3), 397–413. https://doi.org/10.1016/j.enggeo.2010.05.016

Fall, M, Wu, D., and Pokharel, M. (2014). 'Effect of deep mine temperature conditions on the heat development in cemented paste backfill and its properties', in M Hudyma and Y Potvin (eds), *Deep Mining 2014: Proceedings of the Seventh International Conference on Deep and High Stress Mining*, Australian Centre for Geomechanics, Perth, pp. 559-573, https://doi.org/10.36487/ACG_rep/1410_39_Fall

Fernández-Lozano, J., Gutiérrez-Alonso, G., and Fernández-Morán, M. Á. (2015). Using airborne LiDAR sensing technology and aerial orthoimages to unravel Roman water supply systems and gold works in NW Spain (Eria valley, León). *Journal of Archaeological Science*, *53*, 356–373. https://doi.org/10.1016/j.jas.2014.11.003

Ghirian, A., and Fall, M. (2014). Coupled thermo-hydro-mechanical‒chemical behaviour of cemented paste backfill in column experiments Part II: Mechanical, chemical and microstructural processes and characteristics. *Engineering Geology*, 170, 11–23. https://doi.org/10.1016/j.enggeo.2013.12.004

Gibria, G. (2014). Mining: Friend or Foe?. Economic, Environmental and Social Impacts. https://www.researchgate.net/publication/265379518.

Haddaway, N.R., Cooke, S.J., Lesser, P., Macura, B., Nilsson, N.E., Taylor, J.J., and Kaisa, R, (2019). Evidence of the impact of mental mining and the effectiveness of mining mitigation

measures on social-ecological systems in Artic and Arboreal regions; a systematic map protocol. *Environ. Evid*. 8, 9. https://doi.org/10.1186/ s13750-019-0152-8.

Haiqiang, J., Fall, M., and Cui, L. (2016). Yield stress of cemented paste backfill in sub-zero environments: Experimental results. *Minerals Engineering*, 92, 141–150. https://doi.org/10.1016/j.mineng.2016.03.014

Han, D.,vand Ferron, R. D. (2016). Influence of high mixing intensity on rheology, hydration, and microstructure of fresh state cement paste. *Cement and Concrete Research*, 84, 95–106. https://doi.org/10.1016/j.cemconres.2016.03.004

Haruna, S., and Fall, M. (2020). Time- and temperature-dependent rheological properties of cemented paste backfill that contains superplasticizer. *Powder Technology*, 360, 731–740. https://doi.org/10.1016/j.powtec.2019.09.025

Hassani, F., and Archibald, J. (1998). *Mine Backfill*. Canadian Institute of Mining, Metallurgy, and Petroleum, Canada.

Hossain, D., Gorman, D., Chapelle, B., Mann, W., Saal, R., and Penton, G. (2013). Impact of the mining industry on the mental health of landholders and rural communities in southwest Queensland. *Australas. Psychiatr,* 21, 32–37.

Jain, R.K., Cui, Z. "Cindy", and Domen, J.K. (2016). Chapter 4 - Environmental Impacts of Mining. In Environmental Impact of Mining and Mineral Processing (pp. 53–157). *Elsevier Inc*. https://doi.org/10.1016/B978-0-12-804040-9.00004-8.

Kumari, S., Udayabhanu, G., and Prasad, B. (2010). Studies on environmental impact of acid mine drainage generation and its treatment: an appraisal. *Indian Journal of Environmental Protection*, 30(11), 953–967

Levens, R. L., Marcy, A. D., and Boldt, C. M. K. (1996). Environmental impacts of cemented mine waste backfill.

Liu, S. and Fall, M. (2022). Fresh and hardened properties of cemented paste backfill: Links to mixing time. *Construction and Building Materials*, 324, 126688–. https://doi.org/10.1016/j.conbuildmat.2022.126688

Marshall, B. (2021). Facts and Figures 2021 of the Canadian Mining Industry. Ottawa, Canada. Retrieved from www.mining.ca

Morrice, E., and Colagiuri, R. (2013). Coal Mining, Social Injustice and Health: A Universal Conflict of Power and Priorities. *Health and Place, 19*, 74–79. https://doi.org/10.1016/j.healthplace.2012.10.006.

Nasir, O., and Fall, M. (2008). Shear behaviour of cemented pastefill-rock interfaces. *Engineering Geology*, 101(3), 146–153. https://doi.org/10.1016/j.enggeo.2008.04.010

Natural Resources Canada. (2023). Minerals and the economy. https://natural-resources.canada.ca/our-natural-resources/minerals-mining/mining-data-statistics-and-analysis/minerals-and-the-economy/20529

Nordstrom, D. K. (2011). Mine waters; acidic to circmneutral. *Elements (Quebec)*, *7*(6), 393–398. https://doi.org/10.2113/gselements.7.6.393

Öhlander, B., Chatwin, T., and Alakangas, L. (2012). Management of Sulfide-Bearing Waste, a Challenge for the Mining Industry. Minerals (Basel), 2(1), 1–10. https://doi.org/10.3390/min2010001

Osama, M., and Elhassan, B. (2022). A review study in Mining Industry. *American Journal of Applied Sciences*, 7, 1-14.

Ouattara, D., Yahia, A., Mbonimpa, M., and Belem, T. (2017). Effects of superplasticizer on rheological properties of cemented paste backfills. *International Journal of Mineral Processing*, 161, 28–40. https://doi.org/10.1016/j.minpro.2017.02.003

Ouattara, D., Mbonimpa, M., Yahia, A., and Belem, T. (2018). Assessment of rheological parameters of high density cemented paste backfill mixtures incorporating superplasticizers. *Construction and Building Materials*, 190, 294–307. https://doi.org/10.1016/j.conbuildmat.2018.09.066

Ouellet, S., Bussiere, B., Benzaazoua, M., Aubertin, M., Fall, M., and Belem, T. (2003). Sulphide reactivity within cemented paste backfill: oxygen consumption test results. *In Proceedings of 56th Canadian geotechnical conference* (pp. 176-183).

Ouellet, S., Bussière, B., Mbonimpa, M., Benzaazoua, M., and Aubertin, M. (2006). Reactivity and mineralogical evolution of an underground mine sulphidic cemented paste backfill. *Minerals engineering*, 19(5), 407-419

Qi, Y., Stern, N., Wu, T., Lu, J and Green, F. (2016). China's post-coal growth. *Nature Geoscience*, 9 (8), 564-566. https://doi.org/10.1038/ngeo2777.

Roshani, A., and Fall, M. (2020). Flow ability of cemented pastefill material that contains nano-silica particles. *Powder Technology*, 373, 289–300. https://doi.org/10.1016/j.powtec.2020.06.050

Statista. (2023). Mining industry worldwide- statistics and facts. https://www.statista.com/topics/1143/mining/#topicoverview.

Tariq, A, and Ernest, K. Y. (2013). A Review of Binders Used in Cemented Paste Tailings for Underground and Surface Disposal Practices. *Journal of Environmental Management*, 131, 138–149. https://doi.org/10.1016/j.jenvman.2013.09.039

Veenstra, RL, Grabinsky, MW, Bawden, WF and Thompson, BD. (2014). A numerical analysis of how permeability affects the development of pore water pressure in early age cemented paste backfill in a backfilled stope', in Y PotvinandT Grice (eds), *Mine Fill 2014: Proceedings of the Eleventh International Symposium on Mining with Backfill*, Australian Centre for Geomechanics, Perth, pp. 83-95, https://doi.org/10.36487/ACG_rep/1404_05_Veenstra

Worlanyo, A. S., and Jiangfeng, L. (2021). Evaluating the environmental and economic impact of mining for post-mined land restoration and land-use: A review. *Journal of Environmental Management,* 279, 111623–. https://doi.org/10.1016/j.jenvman.2020.111623

Xiapeng, P., Fall, M., and Haruna, S. (2019). Sulphate induced changes of rheological properties of cemented paste backfill. *Minerals Engineering*, 141, 105849–. https://doi.org/10.1016/j.mineng.2019.105849

Yang, L., Wang, H., Li, H., and Zhou, X. (2019). Effect of High Mixing Intensity on Rheological Properties of Cemented Paste Backfill. *Minerals (Basel)*, 9(4), 240.

CHAPTER TWO.
THEORETICAL AND TECHNICAL BACKGROUND

2.1 INTRODUCTION

This chapter provides a comprehensive review of the theoretical and technical background information pertaining to cemented and uncemented paste tailings. The information provided is required for a better understanding of the investigations performed and reported in this thesis. Section 2.2 provides a general overview of tailings, their properties, how tailings are generated, and environmental impacts of mine tailings. In Section 2.3, an in-depth literature review is done on sulphide minerals, which are among the most hazardous components of tailings. Section 2.4 delves into the types of surface and underground tailings management techniques that have been utilized over the years, while Section 2.5 focuses on CPB technology, including its design criteria and the key properties that govern its engineering performance. The concluding section of this chapter (Section 2.6) provides a concise literature review on the rheological and permeability properties of cemented and uncemented paste tailings and finally pinpoints the specific research gap that this current study aims to address.

2.2 TAILINGS

Tailings are unwanted by-products (e.g., silicates, oxides, hydroxides, carbonates, and sulphides) of ore beneficiation processes (Gou et al., 2019; Dimitrova and Yanful, 2012; Lottermoser, 2010). These waste materials are the remnants left behind after the economic fraction

of a mineral ore has been extracted, and they are known for their voluminous quantity (Oberle et al., 2020), as depicted in Figure 1. Tailings are a composite mixture of ground rock slurries, water, and chemical reagents generated through a mineral concentration process which encompasses several steps (Oberle et al., 2020). First, the mineral-bearing rock or ore is removed from the Earth through open-pit mining, underground mining, or other specialized methods (EC, 2009).

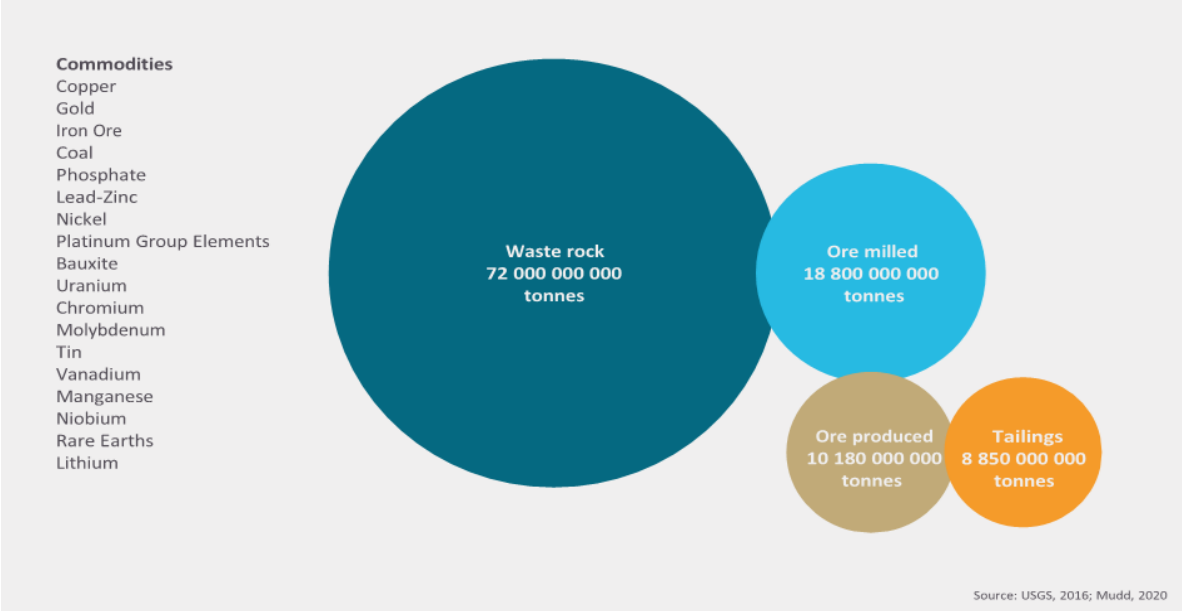

Figure 1: Estimate of the volume of tailings and waste rock produced in 2016 (USGS, 2016).

Then the mine ore is reduced in size to facilitate the separation of the desired mineral from the host rock through crushing and grinding processes. The final steps of the mineral concentration process include ore separation and concentrate dewatering. Tailings are generated in the ore separation step, as this step entails the separation of the valuable material (generally referred to as head) from the waste slurry material (tail) known as tailings illustrated in Figure 2 (EC, 2009). The characteristics and compositions of tailings are dependent on the mineralogy of the ore deposit, the geochemistry, the particle size of the crushed material, the type of chemicals used in mineral processing, and the nature of the processing steps (James et al., 2013; Kiventerä et al., 2020). The

grain particle size of tailings ranges from colloids and silts (less than 0.001–0.002 mm) to fine sands (> 0.075 mm) and their grain shape is generally more angular than natural soil particles (Rodriguez and Edeskär, 2013). In PT technology, tailings constitute about 70–85% by weight of the paste fill mixture (Aldea, 2010); hence, their characteristics/properties play a significant role in determining the stability and performance of UPT/CPB (Kesimal et al., 2005; Fall et al., 2004). These properties are briefly discussed in Section 2.2.1.

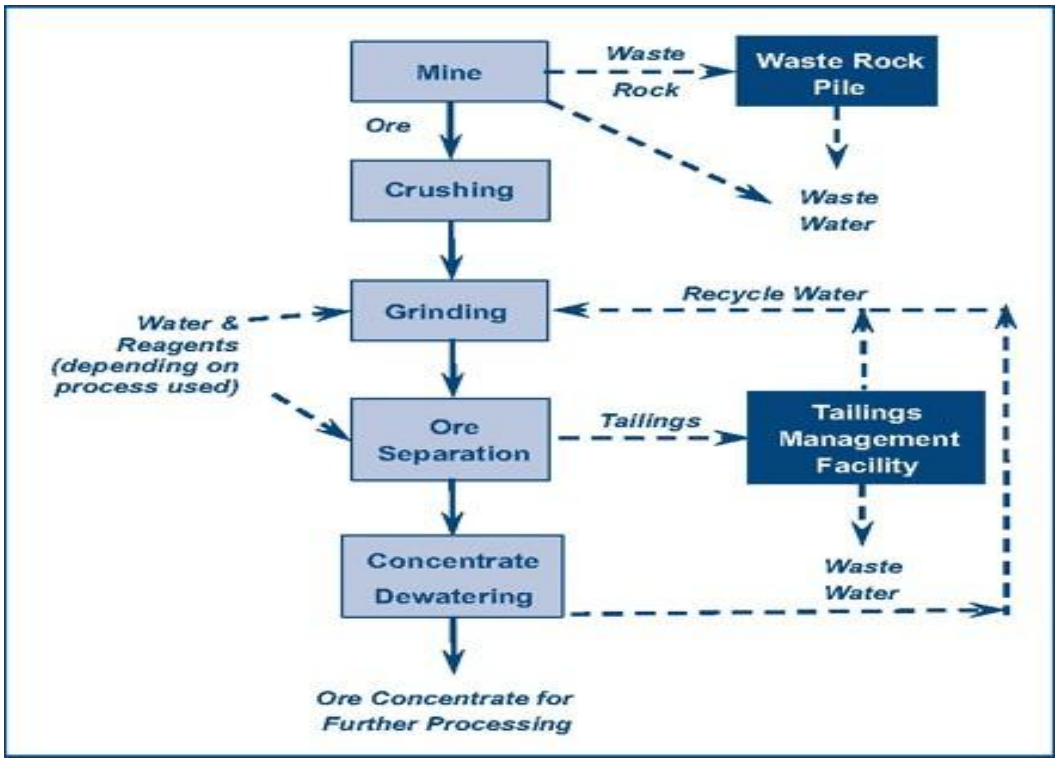

Figure 2: Typical activities in mining operations (Environment Canada, 2009).

2.2.1 PROPERTIES OF TAILINGS

2.2.1.1 PHYSICAL PROPERTIES

The physical properties of tailings are integral to the success of UPT/CPB technology. These properties such as particle size distribution, specific gravity, porosity, specific surface area,

and density are known to have a significant impact on the transportability, dimensional stability, strength, cost, and water volume requirements for UPT/CPB systems (Fall et al., 2005). Various researchers, such as Kesimal et al. (2005), Fall et al. (2004), and Benzaazoua and Kongolo (2003), have investigated the impact of these properties on PT system performance. The particle size distribution of PT backfill material influences the backfill performance, and this is mainly due to varying specific surface area with varying particle size distribution (Kesimal et al., 2003; Sivakugan et al., 2006). It was revealed that the percentage of fine particles in tailings played a vital role in PT performance because the presence of fine particles (< 20μm) is essential in preventing the segregation of the paste constituents. This enhances the water-holding capacity, prevents bleeding of water in paste fill and facilitates the flow characteristics of paste fill (Landriault et al., 2000; Fall et al., 2004). The shape of tailings particles also affects consolidation, settling of backfill and the durability of paste pipeline as irregular and angular particle creates high wear and tear of paste fill pipeline (Fall et al., 2005).

The presence of fine particles also influences microstructure of PT, particularly its pore size distribution and porosity. The porosity and pore size distribution further influences the drainage capacity of UPT/CPB (Fall et al., 2004). Most published research has revealed that cementitious mixtures containing tailings as fine aggregate had a higher water absorption percentage due to capillarity (Fontes et al., 2016) or higher fine content and specific surface area values of tailings (Argane et al., 2016). Shettima et al. (2016) described that concrete with tailings absorbed more water than control specimen; but water absorption decreased with increase in age because tailings occupy the macro and micro pores of cementitious concrete. Additionally, a proportional relationship exists between an increase in the volume of fine particles in tailings and the water demand of the paste. Similarly, there's also a proportional connection between the water consumption of the hydraulic binder and the density of tailings in the mixture. This implies that

the use of high-density tailings leads to higher cement consumption in cemented paste backfill (CPB) production, resulting in increased costs for CPB (Fall et al., 2004).

2.2.1.2 CHEMICAL PROPERTIES

The chemical properties of tailings are also vital properties to consider in PT technology. The chemical properties (e.g acidity, reactivity, potential for metal leaching and presence of specific contaminants like heavy metals) of tailings depend on the mineralogy of the ore body, the nature of the processing fluids used to extract the economic metals, the efficiency of the extraction process and the degree of weathering during storage (Kossoff et al., 2014). Aldea (2010) revealed that the chemical properties of tailings need to be identified to ensure compatibility with the binders used in the paste mix. For instance, the presence of sulphur in the tailings increases the density of UPT/CPB mixtures as well as enhances the strength of the paste due to the addition of more binder (Fall et al., 2004). On the other hand, a high sulphur content can cause degradation of CPB because of sulphate attacks.

2.2.1.3 MINERALOGICAL PROPERTIES

The mineral properties of tailings play a crucial role in shaping the characteristics and performance of backfill because specific minerals present have a significant influence on the properties and functioning of backfill operations (Lu et al., 2018; Zhang et al., 2017; Xu et al., 2018; Nouairi et al., 2018). For example, the abundance of clay minerals and quartz can respectively affect the water retention capacity and abrasiveness (leading to pipeline wear and tear) of PT backfill (Mishra et al., 2010; Qi et al., 2018; Wu et al., 2019). Similarly, excessive sulphide in waste materials may result in a long-term reduction of the strength of the backfill mass. This reduction in strength occurs due to the generation of acid when sulphide-rich waste reacts with

water and the acid weakens the calcium silicate hydrate (C-S-H) bonds (Ouellet et al., 2006; Burchfield et al., 1979, Fourie et al., 2001; Roa et al., 2006).

2.2.2 ENVIRONMENTAL IMPACTS OF MINE TAILINGS

Mining operations and their resulting by-products (tailings) are known to greatly contribute to environmental pollution, which may lead to serious human health risks, loss of biodiversity and long-term impairment of waterways (Hatje et al., 2017). The foremost impacts of this process include acid mine drainage (AMD) and potential contamination of soil, water (surface/underground water), and air from enriched mine tailings (Singer and Stumm, 1970; Cacciuttolo and Cano, 2022). The composition of tailings is known to encompass various chemicals, such as sodium ethyl xanthate, sodium cyanide, copper sulphate, pine oil tar, fatty acid soaps, dithiophosphates, collectors, foaming agents, and lime, as well as elevated concentrations of naturally occurring heavy metals (like cadmium, chromium, manganese, arsenic, lead, and zinc) (Ayres et al., 2002; Cacciuttolo and Cano, 2022). These substances are recognized as highly toxic and hazardous to the ecosystem. For example, research has shown that the release of toxic chemicals like cyanide into water and soil from tailings can lead to water contamination, adversely affecting aquatic life. Aquatic life, such as fish and marine invertebrates, are particularly vulnerable to cyanide exposure, with concentrations as low as 5.0 to 7.2 µg/L impacting swimming ability and reproduction, and concentrations above 200 µg/L causing rapid toxic effects for most aquatic species. Terrestrial birds and mammals can also face toxic levels of cyanide inhalation through the food chain, with specific toxic levels for inhalation related to body weight (Medina and Anderson, 2020; Cacciuttolo and Cano, 2022). In humans, exposure to cyanide concentrations of 20-40 ppm in air after several hours may cause respiratory distress, while concentrations above 250 ppm can lead to death within minutes (Cacciuttolo and Cano, 2022). Other chemicals found

In tailings, such as sodium ethyl xanthate, dithiophosphate-1404, methyl isobutyl carbinol (MIBC), and Dowfroth 250 (a foaming agent), are also recognized as toxic, presenting potential risks to both human health and the environment (Chockalingam et al., 2003; Dopson et al., 2006). A more serious impact of tailings is the generation of AMD, resulting from the exposure of sulphide-bearing tailings to the surrounding environment (Xu et al., 2019). This process creates acidic conditions that harm human health and ecosystems. Ongoing acid-generating reactions associated with acid mine drainage (AMD) promote the migration of dissolved elements into nearby receptors, including surface runoff, soils, sediments, and local ecosystems (Abraham and Susan 2017; Torres et al. 2018; Park et al. 2019). As a result, this phenomenon has long-lasting and harmful consequences on public health and the ecological environment, as highlighted in comprehensive reviews (Liao et al. 2016, 2017). Section 2.3 gives extensive information on sulphide minerals and pyrite, which are known to be the dominant cause of AMD.

2.3 SULPHIDE MINERALS

Sulphide minerals are a class of minerals containing sulphide (S^{2-}) or disulphide (S_2^{2-}) as the major anion. They are an important group of ore minerals because they are responsible for the concentration of a wide range of mineable deposits like nonferrous and precious metals such as gold, silver, copper, zinc etc (Chanturiya et al., 2022). In ore mining and mineral processing, sulphide-containing ores are also known to be one of the most environmentally hazardous types of metallurgical wastes. This is largely attributed to the fact that during waste storage, sulphide minerals (particularly pyrite and pyrrhotite), oxidize forming sulphuric acid (acid mine drainage (AMD)), ferrous and non-ferrous sulphates (Kalinnikov et al., 2001; Parbhakar-Fox et al., 2013; Chanturiya et al., 2022). Several hundred sulphide minerals have been reported in literature, but

only five are sufficiently abundant accessory minerals to have been categorized as 'rock forming' (Bowles et al. 2011). These five are pyrite, pyrrhotite (iron ore), galena (lead ore), sphalerite (zinc ore) and chalcopyrite (copper ore), with iron sulphides (pyrite and pyrrhotite) being dominant (Vaughan and Corkhill, 2017). Table 2.1 shows the main types of ore deposits that contain significant amounts of sulphide minerals, their major ore minerals and the metals extracted from them.

Table 1: The major types of sulphide ore deposits.

TYPE	MAJOR ORE MINERALS*	METALS EXTRACTED
Ores related to mafic and ultramafic intrusions		
Sulphide nickel deposits	Po, Pn, Py, Cpy, Viol	Ni, Cu, Co, Pgm
Merensky reef platinum	Po, Pn, Cpy	Ni, Cu, Pgm
Ores related to felsic intrusive rocks		
Tin and tungsten skarns	Py, Cass, Sph, Cpy, Wf	Sn, W
Zinc–lead skarns	Py, Sph, Gn	Zn, Pb
Copper skarns	Py, Cpy	Cu, Au
Porphyry copper/molybdenum	Py, Cpy, Bn, Mbd	Cu, Mo, Au
Polymetallic veins	Py, Cpy, Gn, Sph, Ttd	Cu, Pb, Zn, Ag
High sulfidation ores	Py, Enar, Cov, Ten, Au	Cu, Au, Ag
Ores related to marine mafic extrusive rocks		
Cyprus-type massive sulphides	Py, Cpy	Cu
Besshi-type massive sulphides	Py, Cpy, Sph, Gn	Cu, Pb, Zn
Ores related to subaerial felsic to mafic extrusive rocks		
Creede-type epithermal veins	Py, Sph, Gn, Cpy, Ttd, Asp	Cu, Pb, Zn, Ag, Au
Ores related to marine felsic to mafic extrusive rocks		
Kuroko-type	Py, Cpy, Gn, Sph, Ttd, Asp	Cu, Pb, Zn, Ag, Au
Ores in clastic sedimentary rocks		
Quartz pebble U–gold	Py, Uran, Gold	Au, U
Sandstone-hosted lead–zinc	Py, Sph, Gn	Pb, Zn, Cd
Sedimentary exhalative lead–zinc	Py, Sph, Gn, Cpy, Asp, Ttd, Po	Cu, Pb, Zn, Au, Ag
Ores in carbonate rocks		
Mississippi Valley type	Py, Gn, Sph	Zn, Pb, Cd, Ga, Ge

Source: (Vaughan and Corkhill, 2017).

*Abbreviations used are as follows: Asp–Arsenopyrite, Au–Gold, Bn–Bornite, Cass–Cassiterite, Cov–Covellite, Cpy–Chalcopyrite, Enar–Enargite, Gn–Galena, Mbd–Molybdenite, PGM–Platinum Group Minerals, Pn–Pentlandite, Po–Pyrrhotite, Py–Pyrite, Sph–Sphalerite, Ten–Tennantite, Ttd–Tetrahedrite, Uran–Uraninite, Viol–Violarite, Wf–Wolframite

2.3.1 MAJOR TYPES OF SULPHIDE MINERALS

2.3.1.1 IRON SULPHIDES

Iron sulphides are accessory minerals that play a crucial role in mining activities, particularly in the extraction of valuable metals. They are known to exist in different oxidation states (Fe^{2+} and Fe^{3+}) and different forms such as pyrite, marcasite (FeS_2), greigite (Fe_3S_4), pyrrhotite ($Fe_{1x}S$), mackinawite (FeS_{1-x}), and troilite (FeS) (Esmaeely and Nesic, 2017). Numerous studies have shown that pyrite and pyrrhotite are the two most reactive (Agboola et al., 2020) and abundant iron sulphide minerals found in mined aggregates (Jeyakaran et al., 2023; Chanturiya et al., 2022; Cohn et al., 2006; Schoonen et al., 2006; Schoonen et al., 2010). In geotechnical engineering design and concrete or CPB technology, studies have shown that utilization of aggregates containing iron sulphides may be detrimental to concrete structures. According to Kleiv (2021), aggregates containing iron sulphide minerals like pyrite can undergo oxidative reactions, which may cause expansion of concrete structures. This expansion may affect the service life (Jeyakaran et al., 2023) and structural performance of concrete by causing map cracking, progressive decline in theconcrete's strength and stiffness, pop-outs and rust stains (Jeyakaran et al., 2021; Saengsoy et al., 2021; Mosallamy and Shehata, 2020).

2.3.1.2 COPPER SULPHIDES

Copper is a common toxic element found in tailings from mining operations (Smuda et al., 2008), due to the current technological challenges associated with fully extracting the metal from the ore (Smuda et al., 2008). In economic ores, it exists as an oxide, sulphate, or sulphide, with copper sulphide ore constituting 80% of the overall copper resource and major source of metallic copper (Davenport et al., 2002). In tailings, copper is commonly found in the Cu^{+2} oxidation state, in the form of oxides (CuO), sulphates ($CuSO_4$) and sulphides such as chalcopyrite ($CuFeS_2$),

bornite (Cu_5FeS_4), covellite (CuS), and chalcocite (Cu_2S) (Chen et al., 2020). Academic research has shown that the presence of copper in hydrated cement causes strength loss at replacement levels over 1% (Ma et al., 2010). Furthermore, a study conducted by Onuaguluchi and Eren (2012) reported that concrete mixtures with a 10% replacement level of copper tailing (% by mass of cement replaced by tailing), showed higher resistance to acid attack, and lower resistance to sulphate attack compared to concrete mixtures with no replacement. Further studies by Vargas and Lopez (2018) showed that concrete mixtures with a 40% replacement level of treated copper tailings showed a minimum loss of mechanical strength, depending on the nature of the tailing.

2.3.1.3 LEAD SULPHIDES

Lead sulphide is an inorganic compound with the chemical formula PbS. It is commonly found in mineral deposits such as galena, and research studies have shown that lead sulphides exhibit different chemical transformations in varying environmental conditions (Buckley and Woods, 1984; Fornasiero et al., 1994; Kim et al., 1995; Nowak and Laajalehto, 2000, Shapter et al., 2000, Boa et al., 2021). In natural oxygenated environments, galena tends to transform into anglesite, which is weakly soluble below pH 6 (Lin, 1997; Shapter et al., 2000). Galena may also undergo oxidation in acidic conditions facilitated by Fe (III) (Rimstidt et al., 1994). The oxidation of Galena in air may lead to the formation of lead hydroxide and lead oxide products (Evans and Raftery, 1982; Buckley and Woods, 1984a; Laajalehto et al., 1993), while oxidation in aqueous solutions leads to potential formation of lead oxides and lead sulphate surface products (Fornasiero et al., 1994; Kartio et al., 1996; Kim et al., 1995; Nowak and Laajalehto, 2000). Lastly, the oxidation of galena in the absence of oxygen may result in the release of lead and sulphide ions into solutions as free lead ions and hydrogen sulphide (Fornasiero et al., 1994).

In the context of mine tailings management, the presence of lead sulphide in paste tailings has been proven to degrade the mechanical properties of cemented materials. More specifically, increased lead sulphide content in tailings used for CPB decreases the overall strength and structural integrity of cemented materials (Dong et al., 2019).

2.3.1.4 ZINC SULPHIDES

Zinc sulphide/Sphalerite (ZnS) is the principal source of Zn and Cd in tailings and acidic runoff from mining activities (Jambor et al., 2005). It can undergo oxidation through different mechanisms, including exposure to dissolved molecular oxygen (O_2) or ferric iron (Fe (III)) in the environment (Seal and Hammarstrom, 2003; Malmström and Collin, 2004; Schippers and Sand,2002). During this oxidation process, zinc sulphide releases zinc (Zn) and sulphate ions (SO_4^{2-}) into the surrounding environment, posing a pollution risk to rivers and oceans (Martin et al., 2001). Zinc sulphide also oxidizes under acidic conditions (Seal and Hammarstrom, 2003; Malmström and Collin, 2004). Similar to pyrrhotite, sphalerite is acid soluble and can dissolve to produce hydrogen sulphide (H_2S) under acidic pH conditions (Nordstrom and Alpers, 1999). In weathered tailing deposits sphalerite oxidizes under acidic conditions to release sulphur, zinc, iron and other metal(loid) into tailings pore waters (Lindsay et al., 2015). This underscores the environmental implications of sphalerite oxidation in mining waste.

2.3.2 PYRITE MINERAL

Pyrite, also known as iron disulphide (FeS_2), is the most abundant sulphide mineral in nature that has a major influence on the biogeochemical cycles of iron, sulphur and oxygen. It is present in various geological formations, including sedimentary, igneous, and metamorphic structures, as well as in deep sea vents (Rickard and Luther 2007). Pyrite oxidation and the factors

affecting the kinetics of oxidation (O_2, Fe^{3+}, temperature, pH, E_h, and the presence or absence of microorganisms) have been extensively studied by researchers (e.g, Buckley and Woods, 1987; Brown and Jurinak, 1989; McKibben and Barnes, 1986; Moses et al., 1987; Sasaki et al., 1995) due to its environmental significance in causing AMD (Vaughan 2005; Rimstidt et al., 2003). Pyrite oxidation occurs when the mineral surface is exposed to an oxidizing agent and water, in both oxygenated and anoxic systems. This oxidation process is complex and can involve several chemical, biological and electrochemical reactions. As pyrite begins to oxidize, it yields protons (H^+), Fe^{2+} ions, and sulphates, leading to decreases in pH of the surrounding environment. Fe^{2+} can be oxidized further, releasing Fe^{3+} ions that can act as further catalysts and oxidize more pyrite minerals in the surroundings (Park et al., 2019). The step-by-step biogeochemistry of pyrite oxidation is given in the following equations.

The overall reaction of pyrite by atmospheric oxygen produces one mole of Fe^{2+}, two moles of $2SO_4^{2-}$ and two moles of H^+ for every mole of pyrite oxidized (Nordstrom, 1982):

$$FeS_{2\,(S)} + \frac{7}{2}O_2 + H_2O \longrightarrow Fe^{2+} + 2SO_4^{2-} + 2H^+ \qquad \textbf{equation 2.1}$$

The Fe(II) thus released may be oxidized to Fe (III):

$$Fe^{2+} + \frac{1}{4}O_2 + H^+ \longleftrightarrow Fe^{3+} + \frac{1}{2}H_2O \qquad \textbf{equation 2.2}$$

Fe (III) oxyhydroxides such as ferrihydrite (nominally $5Fe_2O_3 \cdot 9H_2O$) may precipitate:

$$Fe^{3+} + 3H_2O \longleftrightarrow Fe(OH)_3 + 3H^+ \qquad \textbf{equation 2.3}$$

where $Fe(OH)_3$ is a surrogate for ferrihydrite. Adding Equations (1)– (3) yields the overall reaction.

$$FeS_{2\,(S)} + \frac{15}{4}O_{2(aq)} + \frac{7}{2}H_2O_{(aq)} \longrightarrow 2SO_4^{2-} + Fe(OH)_{3(S)} + 4H^+_{(aq)} \qquad \textbf{equation 2.4}$$

This overall reaction results in the release of 4 mol of H^+ for each mole of pyrite oxidized.

2.4 TAILINGS MANAGEMENT METHODS

According to Vick (1990), the improper management of tailings is a primary contributor to environmental issues in mining operations. Historically, tailings were routinely discharged directly into the nearest surface watercourse (Vick, 1990). However, this type of storage method creates vast environmental liabilities and costs associated with remediation and reclamation (Jakubick et al. 2003). These methods have also generated substantial opposition that has contributed to the general negative public perception of the mining industry, thus harming its reputation. Presently, tailing management methods are selected to meet site-specific factors and stringent environmental regulations. These strategies generally include surface management methods, or underground management methods (Dixon-Hardy and Engels, 2007, EC 2004). Some of these methods are reviewed in the following section.

2.4.1 SURFACE TAILINGS MANAGEMENT METHODS

Surface tailings management methods are containment methods for storing and handling waste on the Earth's surface. Some of these methods include slurry, thickened, paste and dry stack management methods. Tailings stored on the surface are usually deposited within purpose-built retaining embankments. Conventional impoundment storage is the most common, and normally has higher embankments than thickened, paste, and dry-stack storage facilities. Embankments for conventional storage facilities are designed to retain tailings and water (Vick 1990), whereas thickened, paste, and dry-stack facilities have embankments designed to retain runoff, bleed water and fines, rather than the weight of the tailings mass itself. The design principles of surface thickened, paste, and dry-stack are to create a self-supporting mound of tailings (ICOLD and UNEP 2001) rather than relying on the retaining forces of embankments to prevent mobilization.

2.4.2.1 SLURRY TAILINGS DISPOSAL TECHNOLOGY

Conventional slurry tailings remain the predominant approach for tailings disposal in the global mining sector. Compared to paste, dry stacking and thickening disposal methods, this method is widely used because of the simplicity in the disposal process and its cost effectiveness (Kheirkhah et al., 2020; Gomes et al., 2016). Slurry tailings are a mixture of water and ground tailings that are generated during ore processing, they typically range from 20 to 50% solids content by weight and are characterized by a yield stress less than 40 Pa (MEND, 2017). Conventional slurry tailings disposal process involves transportation of tailings-to-tailings storage facility (TSF) in a slurry pipeline by gravity or using centrifugal pumps. Dams, embankments or surface impoundments are typically used to contain the tailings solids and process water. The containment structures may be constructed of waste rock, locally excavated borrow materials, a portion of the tailings or a combination of these materials and may be lined or unlined depending on construction technique and operating requirements. Upon deposition slurry tailings segregate with the coarsest particles settling near the discharge points and finer particles settling further from the discharge points (IAAC,2021). In conventional systems, water recoveries can be as high as 65-75% and water at the settling pond is decanted by floating pumps, or decant towers, and dam seepages are collected by a drainage system and cutoff trench systems. However, a high seasonal evaporation rate can substantially reduce water recovery from the pond area, and infiltration from the pond in contact with natural soil can produce water losses (Cacciuttolo and Valuenzuela, 2022). Slurry tailings disposal offers advantages such as its affordability, widespread adoption, and a longstanding history that has yielded valuable insights for numerous successful operations. Despite its widespread use, slurry tailings disposal has drawbacks (Watson et al., 2010). One notable disadvantage is its reliance on large volumes of water for transportation and disposal. This factor

makes the method costly, especially in regions with limited water supply. In areas facing water scarcity, the use of slurry tailings disposal may not be practical or economically feasible (Watson et al., 2010). Moreover, these conventional slurry tailings disposal facilities have caused severe geotechnical failures (e.g. dam failures) in many parts of the world, with serious social and economic consequences for the mining industry and society (Fourie et al. 2001; Welch 2003).

2.4.2.2 THICKENED TAILINGS DISPOSAL TECHNOLOGY

Thickened tailings are defined as tailings that have been significantly dewatered to a point where they form a homogeneous non-segregated mass when deposited from the end of a pipe (Welch 2003). This method aims to enhance the hydrogeotechnical properties of tailings by reducing the water content to obtain thickened tailings (Ouattara et al., 2017). Thickened tailings have a solid content of 40 to 60% by weight and a yield stress ranging from 20 to 200 Pa (IAAC, 2021; MEND, 2017). They are produced by the mechanical process of dewatering low-solids concentrated slurry (Fourie 2003). This is normally achieved by using compression thickeners or a combination of thickeners and filter presses (DPI 2003). The concept of thickened tailings disposal is to stack the pulp to form a self-supporting conical pile, thus reducing the required height and retention forces of the containing perimeter embankments. The tailings are generally discharged from topographical high points within the TSF or by riser towers or central ramps (ICOLD and UNEP 2001). Water remaining after deposition, and any surface runoff, are collected in a pond at the toe of the pile. The primary advantage of this disposal method is that water is conserved and environmental problems such as seepage, spillage of process water and the potential for water to act as a transporter for tailings flows (e.g. embankment breach) are significantly reduced (Welch 2003, Dixon-Hardy and Engels, 2007). Furthermore, due to their much lower water content than conventional slurry tailings, surface thickened tailings structures exhibit much

stronger geotechnical stability under both static and dynamic conditions than slurry tailings. However, the high operating costs associated with dewatering and substantial land requirements for implementing this method may limit its feasibility for mine operators (Dixon-Hardy and Engels, 2007).

2.4.2.3 PASTE TAILINGS DISPOSAL TECHNOLOGY

Surface paste disposal evolved from the technology developed for underground backfilling of voids (Welch 2003). In the context of tailings, paste tailings are defined as tailings that have been significantly dewatered to a point where they lack a critical flow velocity during pumping. This means that they do not segregate upon deposition and generate minimal bleed water when discharged through a pipe. They have solid contents of 60 to 75% solids by weight with a yield stress of 200 Pa or greater (IAAC, 2021; MEND, 2017). The process of paste tailings involves utilizing positive displacement pumps to transport paste due to the increased viscosity of the tailings resulting from high dewatering. This in turn, limits the distance that the paste can be transported economically (Theriault et al. 2003). Paste tailings generally form a homogenous and non-segregated mass when deposited, with limited volumes of bleed water following deposition (IAAC, 2021). In paste tailings disposal, additives such as flocculants and coagulants are usually added to the tailings feed or the thickener to dewater the tailings to higher densities. The types of additives used reflect how the paste behaves when pumped and how the tailings will flow once at the storage facility (Fourie 2003). The major advantage of this method is that it can be cheaper than conventional low-density methods; however, the affordable cost is dependent on the additives used, the distance that the paste is required to be pumped, and the storage space available (Dixon-Hardy and Engels, 2007). This disposal method also offers several additional advantages which include; the substantial reduction or complete elimination of water storage and retaining ponds,

reduction of facility footprint due to higher slope angles regardless of material volume, enhancement of the geotechnical stability of surface paste tailings disposal facilities due the reduced water content of the paste tailings, rreduced risk of environmental damage due to limited water to aid the transport of tailings in the case of an embankment breach and reduced seepage from the stored paste tailings (Dixon-Hardy and Engels, 2007).

2.4.2.4 DRY STACK/FILTERED TAILINGS DISPOSAL TECHNOLOGY

Dry stacking, also known as filtered tailings disposal, is a tailings disposal method that involves mechanically dewatering tailings to a point at which they no longer behave as a slurry and are more characteristic of a partially saturated soil. They typically have solids contents of 75% by weight or greater and a yield stress >1000 Pa (IAAC, 2021). This process entails mechanically dewatering tailings by using a combination of belt, drum, horizontal and vertically stacked pressure plates, vacuum filtration systems or centrifuges. As a result, it produces a filtered wet (saturated) and dry cake (unsaturated) that can no longer be transported by pipeline due to its low moisture content (Martin et al. 2002, IAAC, 2021). These filtered tailings are then transported by conveyor or hauled by truck to the TSF, where they are placed and compacted as a homogenous, non-segregated and partially saturated mass (Davies and Rice 2001; IAAC, 2021). A major disadvantage of utilizing this method is the high mechanical dewatering operational costs associated with producing wet and dry cakes. Additionally, the dry stacking method has the potential to cause air pollution in the form of airborne dust to surrounding land users. However, dry stacking facilities are also easier to close and rehabilitate, eliminate the possibility of groundwater contamination through seepage, improve the geotechnical stability of the tailings disposal facilities, and can be utilized in aggressive environments (e.g. undulating and steep terrain), and generate better regulatory and public perceptions of tailings storage (Davies and Rice 2001).

Figure 3 illustrates the dewatering tailings technologies for surface disposal.

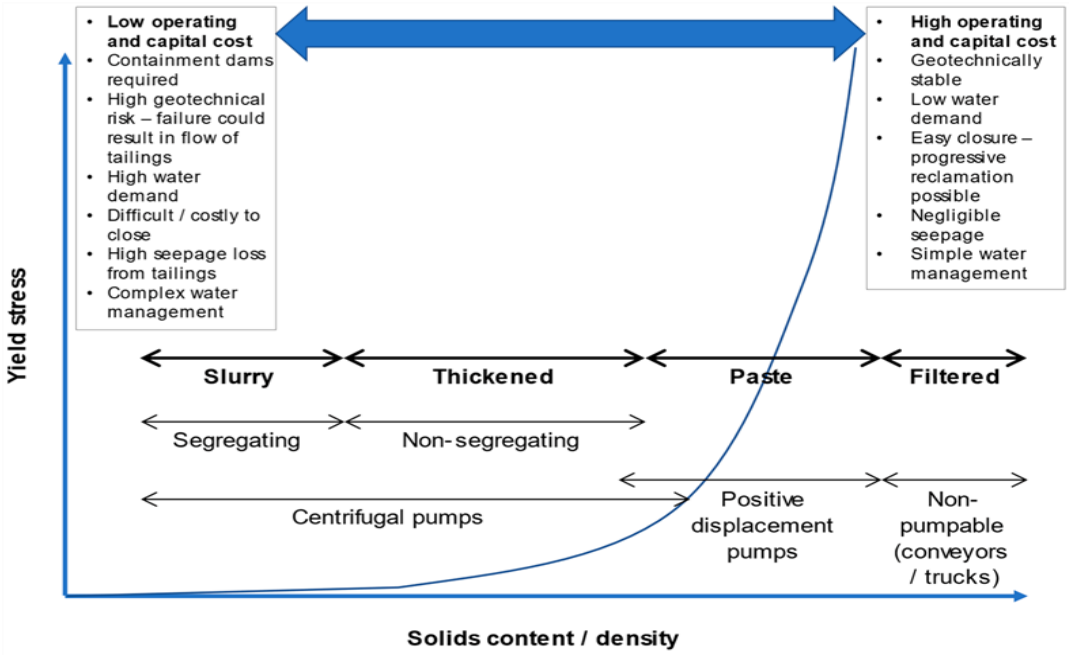

Figure 3: The tailings continuum for surface disposal (Burden and Wilson, 2023).

2.4.3 UNDERGROUND TAILINGS MANAGEMENT METHODS

Tailings can also be stored below ground in previously worked out voids in form of mine backfills. The tailings are generally mixed with a binder, usually cement, and then pumped underground to fill voids and help support an underground mine. Mine backfills are typically classified into three main types: rock fill, hydraulic fill (slurry backfill) and paste fill (or paste backfill). The selection among these three types depends on several factors, including geometry/depth/orientation/grade of the ore bodies, mining method, stope sequence and size, available filling materials, and operational costs (Landriault, 2001).

2.4.3.1 ROCK BACKFILL DISPOSAL TECHNOLOGY

Rock fill consists of waste rock, tailings, or unclassified sand. The primary requirement for rock backfilling is the presence of waste rock at mining sites. Consequently, it proves to be an

effective approach for handling mine wastes in underground mining. The key benefits of this backfilling method include straightforward preparation, high strength, and the absence of stope dewatering. Rock fill can exist in either cemented (CRF) or uncemented (URF) forms. Typically, a 4% to 8% cement is added to strengthen rock fill. Cement paste can be introduced via pipelines and mixed with waste rock before placement. The required strength ranges from 0.2 to 4.0 MPa, which is influenced by stope size, mining technique, and stope recovery time (Hassani and Archibald, 1998; Stone, 2007). Achieving good quality control and preventing segregation pose challenges (Belem and Benzaazoua, 2008; Hassani and Archibald, 1998). CRF strength is controlled by factors such as grain size distribution, binder content, rock type, placement method, segregation, and water-to-cement ratio (Henderson et al., 1998; Chen et al., 2004). Additionally, the expenses associated with rock crushing, transportation, and the need for fine materials as filler in rock backfilling are considerable. The implementation of an appropriate placement method and the regulation of moisture content can mitigate segregation potential (Landriault et al., 1997; 2001).

2.4.3.2 CEMENTED HYDRAULIC BACKFILL DISPOSAL TECHNOLOGY

Hydraulic backfill or slurry backfill is classified as a material with high permeability and low density. Deriving its name from the mode of transportation, hydraulic backfilling describes a method that uses mainly water to facilitate the transport of the fill materials. It is a mix of aggregate (tailings), water and binder (if cemented) (Potvin et al., 2005). This mixture is usually prepared at the ground level and then transported by pipeline to the underground voids**.** To facilitate the removal of excess water, perforated drainage pipes are installed in mine stopes. The main advantages of this backfilling method are simplicity of installation and operation, ease in supervision, ease of quality control, availability of solid parts as mine waste and reduction in surface waste disposal (Hassani and Archibald, 1998). Disadvantages of this backfilling method

are the high amount of excess water, segregation of cement from the solid phase and cement washout (Landriault et al., 1997; Hassani and Archibald, 1998; Landriault, 2001).

2.4.3.3 CEMENTED PASTE BACKFILL DISPOSAL TECHNOLOGY

Cemented paste backfilling is another prevalent type of backfilling used in underground mining operations. CPB technology is broadly discussed in detail in the following section (section 2.5).

2.5 CEMENTED PASTE BACKFILL TECHNOLOGY

Cemented paste backfill (CPB) is one of the broadly used methods in modern mines with the purpose of waste disposal and ground support (Haruna and Fall, 2020). CPB is comprised of full mill tailings, mixed with a small percentage of binder (usually 3–7% by weight cement), and water. This material is dense and has a toothpaste consistency (Fall et al., 2015). A fresh CPB can be transported through the pipeline into the cavities. In static state, the CPB ingredients are not separated, as the colloidal electrical charges can retain all the water between the particles. To create such a state, at least 15% of particles should be smaller than 20 microns (Landriault, 2001; Grice, 1998). As less water is required (compared to other types of backfills) for transporting the CPB through the pipelines, mechanical strength is attained faster since most of the water would be used for cement hydration (Grice, 1998). It should be noted that the chemical and mineralogical properties of the tailings have a significant impact on the engineering properties (strength, permeability, reactivity, etc.) of CPB. Two main issues when implementing CPB are optimization of ore recovery and consideration of the miners' safety. Moreover, pipelines that transfer CPB materials underground require frequent inspection (Landriault, 2001; Cui and Fall, 2018). Fig. 2.6 shows a fresh CPB being pumped through a pipeline.

2.5.1 DESIGN CRITERIA FOR CPB STRUCTURES

The design criteria of the CPB are influenced by its physical, mechanical, hydraulic, and chemical properties. Therefore, CPB must fulfill specific requirements during the design phase (Fang et al., 2020). These properties are explained in the following sections.

2.5.1.1 PHYSICAL PROPERTIES

Physical properties, such as porosity (or void ratio), unit weight, water content and degree of saturation are known to influence the strength and performance of CPB. According to Yilmaz et al. (2009), who investigated the variation of physical properties with respect to binder content (3, 4.5, 7 and 10%), for both unconsolidated and consolidated CPB samples over 28 days showed that unconsolidated samples prepared with ordinary Portland cement (OPC), had a porosity range from 0.42 to 0.47, degree of saturation ranges between 90% and 97% and gravimetric water content varies from 38% to 46%. For consolidated samples (cured under pressure) the porosity ranged from 0.41 to 0.45, degree of saturation was between 80% and 94% and gravimetric water content was from 33% to 42%. The review in this research showed that the physical properties (porosity, void ratio, degree of saturation, unit weight) influenced CPB by decreasing as cement content increased due to the effect of desaturation caused by cement hydration (in unconsolidated samples). Also, a comparison between the unconsolidated and consolidated tests showed that the drainage due to consolidation reduces the values of the physical properties. Furthermore, another research by Yilmaz et al. (2014) who studied the physical properties of CPB samples prepared with a blend of Slag-Portland cement (3, 4.5 and 7%) with respect to curing times of 7, 14 and 28 days and different drainage conditions (drained, undrained and consolidated) also confirmed that factors such as curing time, drainage and consolidation affects the physical properties of CPB which in turn affects the strength and performance of CPB. Hence, the need to study the physical

properties of CPB is an important design criterion for the performance of CPB.

2.5.1.1 MECHANICAL PROPERTIES

Mechanical stability is one of the most important design criteria for paste backfill (Fall et al., 2007), this is because mine safety is dependent on the CPB's mechanical properties, which play a vital role in preventing buckling or collapse, thereby preventing potential harm, entrapment, or fatalities among miners (Pokharel & Fall, 2011). The most common and direct method to determine the mechanical strength of backfill materials is to measure its unconfined compressive strength (Belem et al., 2002). Previous studies on CPB mechanical strength showed that UCS values mostly vary between 0.2 and 4 MPa (Klein and Simon, 2006; Belem and Benzaazoua, 2008; Pokharel and Fall, 2011) and short-term and longterm mechanical strength can be significantly affected by variation of several factors. For example, tailings characteristics, including mineralogy, chemical content (e.g., suphide-rich tailings), fineness and density can affect strength development (Fall et al., 2005; Kesimal et al., 2005). The presence of sulphide minerals, as well as soluble sulphates has a harmful effect on the CPB strength due to sulphate attacks (Benzaazoua et al., 2002; Kesimal et al., 2004). Fall et al. (2005) reported that increasing tailings fineness (particles < 20 μm) to more than approximately 55% can reduce the UCS due to deleterious effects on porosity and pore size distribution. Also, higher tailings density can lead to higher binder consumption which generally provides a higher strength to the CPB (Fall et al., 2004). Yilmaz et al. (2009) reported that curing stress has a significant impact on the UCS of CPB. Binder properties, such as binder type and content, and the chemical characteristics of binders (e.g., soluble sulphate concentration) are one of the most important factors that can influence CPB strength. Higher binder content generally produces higher strength (Benzaazoua et al., 2004). Furthermore, binder type (i.e., ordinary Portland cement (OPC), Slag, Fly ash (FA) or their combination) can deliver different strength to CPB. Benzaazoua et al. (2002) found that OPC and FA/OPC mixture are

appropriate for high sulphate-rich tailings in terms of compressive strength. Mixing water properties and contents including chemical concentration (e.g., sulphate content) and water to binder ratio can affect the strength acquisition process. Water chemistry can alter the cement chemistry and hydration processes. It can affect the formation of the primary and secondary cement hydration products which are responsible for backfill strengthening (Benzaazoua et al., 2002). Furthermore, increase in the w/c ratio as the main factor in mixing can considerably decrease the strength values. Previous studies (e.g., Fall and Samb, 2006; Fall et al., 2007; Fall et al., 2010) have revealed that the curing temperature significantly influences the short-term and long-term mechanical strength and pore structure of CPB materials. The coupled effect of curing temperature and sulphate significantly affects the strength of CPB. This effect can be positive (strength increase) or negative (strength decrease) depending on the initial amount of sulphate content, the curing temperature, and type of binder (Fall and Pokharel, 2010).

2.5.1.2 HYDRAULIC PROPERTIES

Hydraulic properties, particularly the saturated hydraulic conductivity, is also an important criterion for the design of CPB. Saturated hydraulic conductivity (k_{sat}) is used to assess the fluid transportability of backfills, which can be used to investigate the environmental performance of CPB, the groundwater flow within the backfill and/or between the CPB and surrounding rock, after mine flooding. Also, it is required to estimate the drainage ability and leakage potential of metal ions from the backfill into the groundwater (Levens et al., 1996). Several factors can affect the saturated hydraulic conductivity of CPB. For example, the k_{sat} value decreases as the curing time increases. Also, the k_{sat} value decreases when curing temperature increases. Saturated conductivity can also be affected by the mix components (Pokharel and Fall, 2013), for instance, CPB permeability decreases as binder content increases or the w/c ratio

decreases, tailings with finer particles produce lower permeability, while sulphate content can have both positive and negative impacts on CPB. Sulphate content can reduce the k_{sat} value at early ages (< 28 days). However, high sulphate content at an advanced age (90 days) can increase the k_{sat} due to the secondary formation of cement products and development of micro-cracks (Fall et al., 2009; Pokharel and Fall, 2013).

2.5.1.3 CHEMICAL PROPERTIES

The chemical properties or factors of CPB depend on the chemical and mineralogical characteristics of its constituents, such as the mixing water, tailings chemistry and mineralogy, and binder chemical compositions and reactions. These chemical factors can significantly influence the short and long-term strength of CPB (Benzaazoua et al., 2002). Two chemical mechanisms can take place to alter the mechanical strength of the backfill. These can be either direct or indirect. In the former, CPB prepared with sulphide-rich tailings (e.g., pyrite) can be oxidized in the presence of oxygen (also called weathering). The degree of oxidation is mainly a function of pyrite percentage and degree of saturation. The weathering causes release of metal ions and acid mine drainage into the environment (Ouellet et al., 2003). In the latter, the initial chemical compositions (e.g., sulphides, sulphate) in the CPB ingredients (i.e., tailings, binder and mixing water) can negatively affect the CPB strength development due to sulphate attacks (Benzaazoua et al., 2004). For example, sulphate in the initial CPB matrix can inhibit cement hydration reactions at early ages and therefore reduce its strength (Fall and Benzaazoua, 2005; Pokharel and Fall, 2011). In advanced ages, the formation of secondary expansive minerals in the backfill pores, such as ettringite and gypsum, can cause internal cracks and eventually lead to strength deterioration (Fall and Benzaazoua, 2005). However, usage of sulphate resistance binders can help to maintain a long-term strength thereby mitigating the impact of strength degradation (Ercikdi et al., 2009).

2.5.2 MIX DESIGN OF CPB

The paste used in CPB is a carefully formulated mixture comprising three primary ingredients: mine tailings containing 70% to 85% solid content, a hydraulic binder, typically cement, constituting 3% to 7% of the total paste weight and water (freshwater or mine processed water), which is added to achieve the desired rheological and strength characteristics (Benzaazoua et al., 2002). These components are combined and mixed at the surface of mine sites and then the final paste is transported by gravity or pumping to fill designated excavated stopes. Figure 4 illustrates a schematic of CPB mixture components.

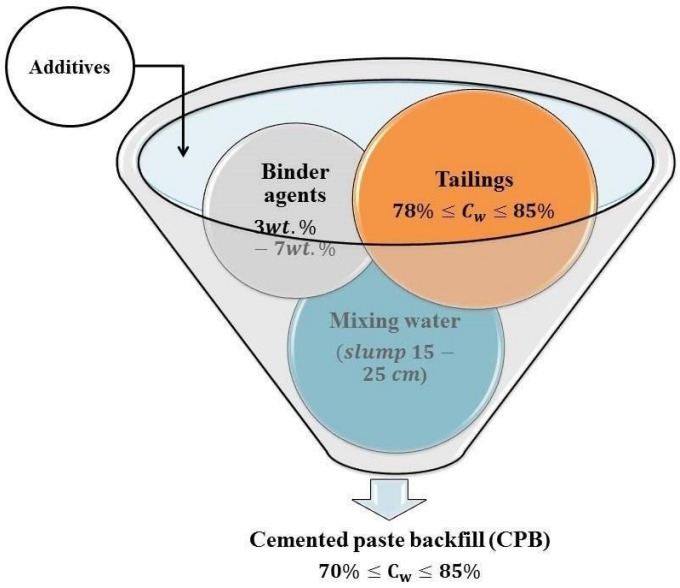

Figure 4. Schematic diagram of CPB mixture components with typical portions (Adapted from Benzaazoua et al., 2002).

2.5.3 PREPARATION OF CPB

CPB is prepared using dewatered mine tailings with solid percentage of ≥ 70%. Various processes, involving high-capacity thickeners, disk filters, and gravity settling tanks, are employed to consolidate mill tailings into filter cakes. Subsequently, these filter cakes undergo mixing in a spiral (or screw) mixer, where a combination of binder and water is introduced to achieve a specific

consistency (slump) for the CPB. Following the preparation of CPB, it is conveyed into the stope through an underground distribution system, either by gravity or through pumping (Landriault et al., 1997). Figure 5 shows the layout of a CPB system.

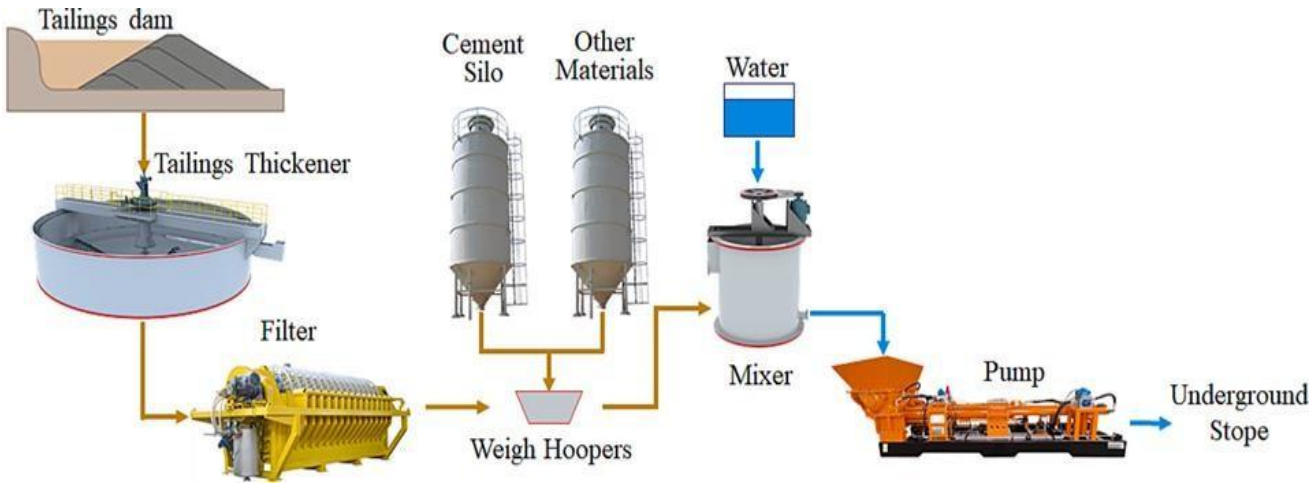

Figure 5: Typical layout of CPB plant (Fang et al., 2023).

2.6 BINDERS AND HYDRATION PROCESS

Binders are materials capable of binding solid particles together to form a whole cohesive solid material. In general, there are two main types of binders used in construction: hydraulic and nonhydraulic. Hydraulic binders, such as Portland cement, are a type of material that sets and hardens when mixed with water as a result of a chemical reaction (hydration process). Non-hydraulic binders (e.g., lime and gypsum plaster) are a type of material that hardens without contact with water (Aldhafeeri, 2018). Portland cement type I (PCI, in accordance with ASTM standards) are the most commonly used hydraulic binders used in tailings management, and most times, they are used alone or blended with pozzolanic materials (e.g blast furnace slag) to increase the final

strength and reduce the binder cost (Kesimal et al., 2005; Bellem and Benzaazoua, 2004 & 2008). The following sections provide a detailed review of binders used in this research study.

2.6.1 BLAST FURNACE SLAG

Ground granulated blast furnace slag is a nonmetallic byproduct of iron manufacturing and consists essentially of silicates and aluminosilicates of calcium and other bases, which is developed in a molten condition simultaneously with iron in a blast furnace, then water chilled rapidly by immersion in water to form glassy granular particles, and then ground to cement fineness or finer (ACI Committee 233; Bouzoubaa and Simon, 2005). Most slags hydrate by themselves, while some need activators (alkalis or lime) for their hydration mechanisms. In the PC-slag systems, the PC component begins to hydrate first followed by reaction with slag, which releases calcium and aluminium ions into solution. Later on, slag reacts with alkali hydroxide and is followed by a reaction with Ca $(OH)_2$ to form more C-S-H gel (Neville, 1995). The release of alkali (Ca^{2+}) and hydroxyl (OH^-) ions during the hydration of PC raises the pH of the pore solutions that triggers the hydration reactions for cement-slag systems. The silica glasses become soluble in the alkaline solution, giving rise to secondary growths of C-S-H, which further fills the capillary pore space left by prior hydration products of PC (Hooton, 2000). Slag develops its cementitious properties far too slowly to be of practical use unless its hydration is activated by the addition of calcium compounds such as PC. Research substantiates that the partial replacement of cement with slag is promising in mine tailings CPB formulations (Nantel and Lecuyer, 1983; Douglas and Malhotra, 1989; Uusitalo et al., 1993; Benzaazoua et al., 2002; Godbout et al., 2007).

2.6.2 ORDINARY PORTLAND CEMENT

Portland cement (CSA Type GU (General use) or ASTM Type I) is the most widely utilized binding agent due to its availability and versatility. It has a longstanding history of being the most suitable binder for addressing mine waste management issues, including the disposal of sulphidic tailings (Weaver and Luka, 1970; Aylmer, 1973; Manca et al., 1983; Atkinson et al., 1989; Lamos and Clark, 1989; Benzaazoua et al., 2004; Rankine and Sivakugan, 2007; Grabinsky et al., 2007). According to ASTM 150 Portland cement is defined "*as a hydraulic cement (cement that not only hardens by reacting with water but also forms a water-resistant product) produced by pulverizing clinkers consisting essentially of hydraulic calcium silicates, usually containing one or more of the forms of calcium sulphate as an inter ground addition*". The binder is used principally to develop sufficient mechanical strength for PT to meet certain dynamic and static load resistance requirements. In cement-based solidification, water chemically reacts with Portland cement to form hydrated calcium silicate and aluminate compounds, while the solids act as aggregates to form 'concrete' (Conner, 1993). The addition of Portland cement (PC) has been found to enhance the cohesive component of the shear strength and intensify the stiffness of mine tailings paste. (Hassani et al., 2007; Ouellet et al., 1998).

2.6.2.1 CHEMICAL COMPOSITION OF PORTLAND CEMENT

The chemical composition of Portland cement involves both major and minor oxides (Punmatharith et al., 2010). The major oxides include CaO, SiO_2, Al_2O_3, and Fe_2O_3, whereas the minor oxides also include MgO, SO_3, and some alkali oxides (K_2O and Na_2O) and sometimes the inclusion of other compounds, P_2O_5, Cl, TiO_2, MnO_3, and so forth (Punmatharith et al., 2010). At high temperatures of 2,600º F, each of the oxides chemically interacts with each other to produce

greyish-black pellets known as clinker. The cement clinker formed is known to be composed of tricalcium silicate (C_3S), dicalcium silicate (C_2S), tricalcium aluminate (C_3A) and tetracalcium aluminoferrite (C_4AF). Although there are other compounds in the final cement product, the silicates and aluminates are largely responsible for the hydration reaction of the PCI (Bergold et al., 2017). Hydration occurs when these compounds come in contact with water, generating new products that are responsible for the setting and hardening of the mixture.

2.6.2.2 PORTLAND CEMENT HYDRATION PROCESS

Cement hydration can be defined as the chemical reactions between solid compounds (clinkers) and the liquid phase (Chen and Brouwers, 2010). It is an exothermic chemical process that occurs when cement particles come in contact with water and cement, thereby gaining binding, setting, and hardening properties. In this process, the main components of cement, such as tricalcium silicate (Ca_3SiO_5, Alite, C_3S), dicalcium silicate (Ca_2SiO_4, Belite, C_2S), tricalcium aluminate ($Ca_3Al_2O_6$, Aluminate, C_3A), tetracalcium aluminoferrite ($Ca_2AlFeO5$, Ferrite, C_4AF) react with water and generate hydration products which are accountable for the setting and hardening of paste (Li et al., 2017; Ma et al., 2016; Sharma and Kothiyal, 2015). Cement hydration reaction generates three main types of cement hydration products, they include; calcium silicate hydrate (C-S-H), calcium hydroxide ($Ca(OH)_2$ or CH), and calcium sulphoaluminate known as ettringite ($3CaO.Al_2O_3.3CaSO_4.31H_2O$). C-S-H is formed by the hydration of C_3S and C_2S at different rates. It occupies approximately 60% (by volume) of the total cement hydration products in hardened cement (Beaudoin et al., 2011; Alizadeh, 2009). CH is a by-product of the hydration of calcium silicates and takes up to 20% of the cement hydration products (Double, 1983).

Ettringite is the product of the hydration of the aluminate phases and gypsum. (Double, 1983).

Figure 6 shows the schematic diagram of cement hydration products.

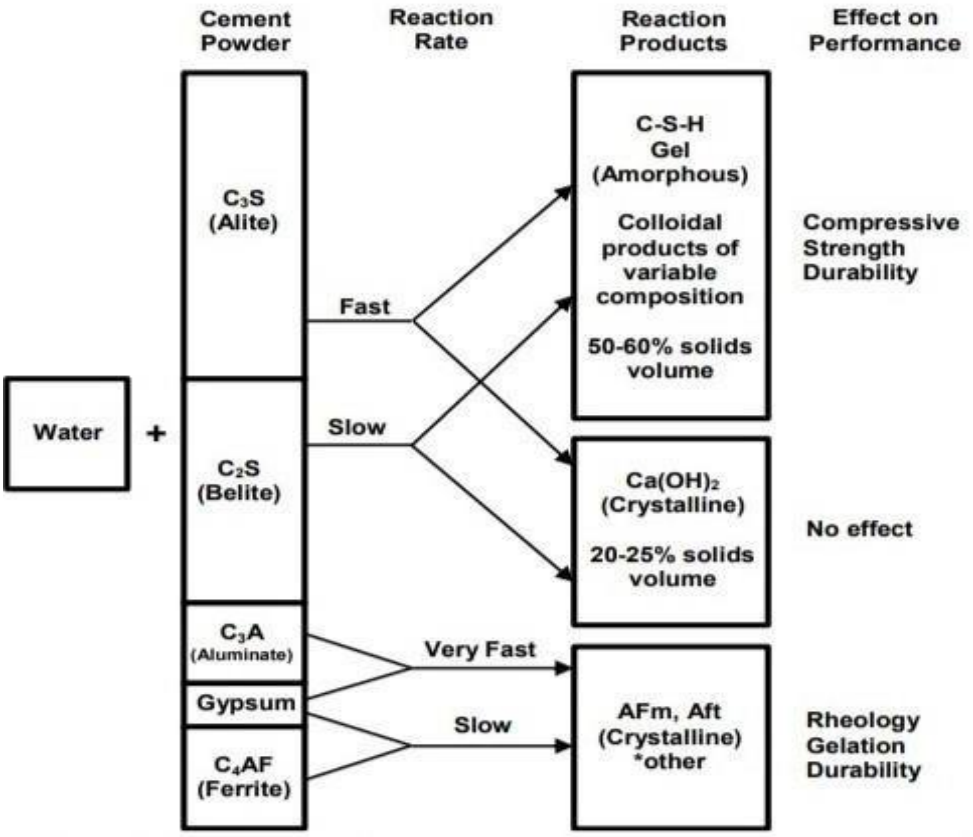

Figure 6 Schematic diagram of cement hydration process and products (Double, 1983).

2.6.2.2.1 SETTING, HARDENING AND HEAT OF CEMENT HYDRATION

Understanding the basics of hydration is essential to ensure the strength and durability of paste backfill (Bull and Fall, 2020; Yilmaz et al., 2011). There are several methods to evaluate the progress of cement hydration, such as the amount of Ca $(OH)_2$ in the paste, thermal changes due to hydration, measurement of the strength of the hydrated paste (i.e., UCS test), thermogravimetric techniques, XRD and scanning electron microscopy (SEM) (Ercikdi et al., 2009). The hydration

process of Portland cement and the generated heat of hydration typically take place in five distinct stages, namely; the initial, induction, acceleration (or setting), deceleration (or hardening) and densification stages (Figure 7) (Mehta and Monteiro, 1993).

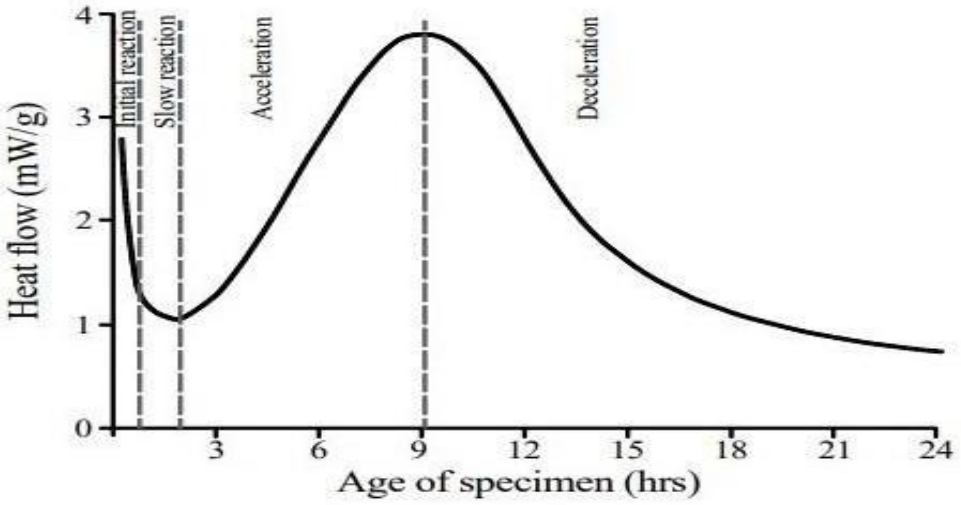

Figure 7: Rate of cement hydration with curing time (Bullard et al., 2011).

The summary of various stages is outlined based on the works of Soroka (1980), Neville (1995), Swaddiwudhipong et al. (2002), Bullard et al. (2011), and Winter (2012).

Stage I- Initial reaction (0 to 30 min.): This occurs almost immediately after water is added during the mixing period. At this stage, the rapid dissolution of aluminates and gypsum occurs, leading to the release of substantial heat, along with Na, K, Ca, OH and SO_4 ions, into the pore solution.

Stage II-Induction (dormant period, 30 min to 3 hrs): This stage involves the reaction of calcium silicates (C_3S and C_2S), leading to the initial formation of C-S-H gel and a supersaturated solution of Ca and OH. Also, reactions between gypsum and C_3A result in the formation of

ettringite. The formation of C-S-H and ettringite around the C_3S and C_3A particles separates them from the pore solution, which in turn, retards the further rapid migration of the ions into the pore solution. During this time, the paste is plastic and does not generate heat.

Stage III-Acceleration (setting period, 3 to 17 hrs): This stage begins at the end of the dormant period, where a preventive coating formed around the cement grains is ruptured due to excess pressure. A significant amount of heat is generated due to the reaction of the C_3A and gypsum, and later on, C_3A and ettringite, which leads to a specific heat of 1495 kJ/kg. C-S-H and CH are formed as a result of the hydration of alites and belites. In this period of hydration, the porosity decreases and strength increases, thus resulting in the setting of the paste.

Stage IV-Deceleration (hardening period, 17 to 48 hrs): At the deceleration stage, the C-S-H and CH continue to grow at a slower rate, which limits the access of water to undissolved cement grains. The sulphate ions are also depleted and the remaining aluminate reacts with C-S-H. Less stable ettringite converts into more stable monosulphate. The heat of hydration reaches its peak value and then starts to drop. The hydration products gradually fill the pores, thus resulting in further pore refinement at a slower rate.

Stage V-Densification (48 hrs to several months/years): In this phase, belites and alites dissolve at very slow rates, which form a solid mass of C-S-H and CH products. High strength, very low porosity and low hydraulic conductivity evolve in this stage and may take up to several years.

2.6.3 MAIN FACTORS THAT AFFECT CEMENT HYDRATION

Cement hydration can be affected by several factors, such as w/c ratio, fineness of cement, and curing temperature (Lin and Meyer, 2009).

Cement fineness

Cement fineness can affect the final degree of hydration and the hydration rate. Cement with finer particles has a higher surface area. This can result in greater surface contact with water

and higher hydration rate. Also, finer cement particles have cement hydration products with less thickness, which in turn, increases the final degree of hydration. Therefore, finer cement particles reduce the setting time, accelerate the hardening process and increase the mechanical strength (Ginebra et al., 2004; Bentz et al., 2008; Lin and Meyer, 2009).

Water-cement ratio

A lower w/c ratio can increase the rate of hydration, which in turn, increases the heat of hydration. Furthermore, a decrease in the w/c ratio can reduce the porosity (decrease the hydraulic conductivity) and increase the mechanical strength (Goto and Roy, 1981; Bentz et al., 2009).

Curing temperature

Curing temperature can accelerate the rate of cement hydration reaction. Also, it increases the density of cement hydration products and short-term compressive strength. However, high curing temperatures (e.g., above 85°C) can reduce the mechanical strength at advanced ages. This can be attributed to higher porosity, less uniform microstructure and coarser pore structure, which can lead to decreases in mechanical strength (Kjellsen et al., 1990; Maltais and Marchand, 1997; Elkhadiri et al., 2009).

Curing pressure

Curing under high pressure can increase the rate of hydration. For example, experimental studies have shown that the hydration of C_3S increases under pressure. Also, precipitation of cement hydration products (C-S-H and CH) is faster under the application of pressure (Bresson et al., 2002). The time of the application of pressure can also affect the rate of hydration, and it is more effective during the first 48 hrs of curing under pressure. The applied pressure can increase the accessibility of cement grains to water required for hydration which can lead to hydration of the unreacted cement particles, which in turn, increases the degree of hydration (Zhou and

Beaudoin, 2003). Furthermore, curing pressure can increase the compressive strength through the formation of denser cement gel around the unhydrated cement particles, as well as decrease the porosity (Roy et al., 1972).

2.7 RHEOLOGICAL AND PERMEABILITY PROPERTIES OF PASTE TAILINGS

2.7.1 RHEOLOGICAL PROPERTIES

The rheological properties of paste tailings and cemented paste backfill (CPB) are important properties, which determine its flow ability or ease of transport in pipelines. These properties can be measured by key parameters like yield stress and viscosity (Xiaoping et al. 2019).

2.7.1.1 Definition of yield stress

Yield stress is defined as the minimum shear stress required to initiate flow (Simon and Grabinsky, 2013). It is a key parameter used in the evaluation of the flowability or transportability of CPB and can be employed as a quantitative criterion for quality control and evaluation (Liddel and Boger, 1996). In pipeline design, changes in the yield stress of fluid PT are commonly associated with changes in friction loss due to the diameter of the pipes (Li and Moerman, 2002). Several factors contribute to the yield stress of paste tailings. Some studies have suggested a correlation between the yield stress of thickened tailings and grinding fineness (Ding et al., 2007), while others have explored the impact of additives such as limestone on rheology (Elmakki et al., 2016). Simultaneously, various researchers have asserted that the yield stress of thickened tailings is intricately linked to a range of factors, including physical properties (solid fraction, particle gradient, and particle shape), intergranular forces (type and value), chemical and physical properties of cement, inner structure, physical ageing, and other considerations (Sofra and Boger 2002; Kwak et al., 2005; Simon and Grabinsky, 2013; Crowder, 2004; Lee et al., 2017; Mbasha et

al., 2015; Malkin et al., 2017; Joshi and Petekidis, 2018). In the context of CPB technology, yield stress of a CPB is determined by the mixture components such as tailings, binders, water and other additives. Furthermore, a previous study by Xiaoping et al. (2019) highlighted that regardless of curing time, sulphate content in tailings can also cause significant changes to yield stress. Hence, the contents of CPB mixtures must be taken into consideration for the successful application of CPB technology.

2.7.1.2 Definition of viscosity

Another important parameter for the evaluation of the transportability of PT is viscosity. Viscosity is a measure of the fluid's resistance to flow. More specifically, viscosity refers to the resistance of a fluid towards being deformed when subjected to a shearing force (Wong, 2013). In pipeline design, the ability to transport a specific paste is significantly influenced by the paste's viscosity. High viscosity affects the pump performance and can lead to high pressures in pipelines. Moreover, excessive viscosity can result in pipeline blockages and shutdown (e.g., Andrade, 1947; McKetta, 1992; Hassani and Archibald, 1998; Jacobsen et al., 2008). Several research studies have indicated that the viscosity of a PT mixture is affected by different factors. For example, Deng et al. (2018) studied the role of particle size on the rheological properties of CPB. The authors highlighted that the larger the size of the particles, the higher the viscosity of CPB. They further cited that packing density is essential for the efficient transport of the mining materials. Deng et al. (2018) research work is supported by Cao et al. (2018), who also focus on the distribution of materials and the importance of evaluating the particle size before transport. These two studies agree that the viscosity of PT depends on particle size and packing density. Additionally, Cao et al. (2018) also highlighted that the slurry of cemented tailings backfill, along with the cement-to-tailings ratio (c/t), and solid content (SD) are important parameters that need to be examined to ensure cost-efficiency of operations.

2.7.2 PERMEABILITY PROPERTIES

Permeability properties are critical characteristics that define the ability of a material to allow the flow or movement of fluids through it. This is an important parameter for determining the flow of a fluid in porous media and the ability of the fluid to pass through the porous medium (Bürger et al., 2001). These properties can be measured by saturated hydraulic conductivity (Fall et al., 2009).

2.7.1.1 Definition of saturated hydraulic conductivity

The saturated hydraulic conductivity of paste tailings is a measure of the ease with which water can flow through the paste tailings, and it is a critical parameter in understanding the permeability characteristics of paste tailings. Changes in hydraulic conductivity influence the effectiveness of PT for both surface and underground PT applications (Chakilam and Cui, 2020). Sheshpari (2015) highlighted the importance of designing CPB so that its drainage has the appropriate hydraulic conductivity to prevent retailing wall destruction and facilitate drainage. Similarly, Pokharel and Fall (2013) argue that temperature and sulphate significantly influence hydraulic conductivity and can either increase or decrease it. For instance, a decrease in temperature increases hydraulic conductivity (Jiang et al., 2017). As a result, it is critical to keep the temperature at an optimum level in order to avoid a negative impact on the CPB.

Fall et al. (2009) conducted a comprehensive examination of hydraulic conductivity and identified various factors that influence this property. Their findings reveal that the hydraulic conductivity of CPB is typically time-dependent, decreasing with increasing time. Additionally, the authors also highlighted other factors which affect hydraulic conductivity, include, binder content, tailings fineness, and curing temperature. It was seen that an elevation in the water-to-cement ratio corresponds to an increase in hydraulic conductivity. Furthermore, the authors also cited that the

time-dependent initial sulphate content study had differing effects on hydraulic conductivity. In the early stages, up to 28 days of curing, CPB containing sulphate exhibited lower hydraulic conductivity due to reduced porosity resulting from the precipitation of secondary cement hydration products. However, at later curing ages (90 days and beyond), CPB with high sulphate content became more permeable, attributed to the development of microcracks resulting from an excess of expansive hydration products.

2.8 PREVIOUS STUDIES ON RHEOLOGICAL AND PERMEABILITY PROPERTIES

Paste tailings are commonly transported through pumping or gravity, necessitating a pipeline reticulation system. However, due to the non-Newtonian behaviour of paste tailings, the design parameters for pipeline transportation depend on the control of certain material properties like rheological properties (e.g. yield stress and viscosity). Additionally, to prevent the susceptibility of PT to AMD and their potential to release contaminants into mine areas or groundwater, it is crucial to thoroughly study their permeability properties, such as saturated hydraulic conductivity. Therefore, for the successful application of PT, researchers have delved into investigating two critical aspects: 1) permeability and 2) rheological properties. This section provides a comprehensive review of previous studies on the rheological and permeability properties of uncemented and cemented paste tailings.

2.8.1 Review studies on rheological and permeability properties of uncemented paste tailings.

To improve the PT knowledge for successful application of uncemented paste tailings, numerous researchers have looked at several factors that can affect the rheological and permeability properties of UPT. Such factors include chemical functional groups, pore volume, pore fluid, pH and particle surface potential of the material (Goudoulas et al. 2003, Huynh et al. 2006). Amongst the rheological studies, authors like Kwak et al. (2005) aimed to optimize the

surface disposal of uncemented paste tailings by applying vane geometry to investigate how water content affects the flow behaviour and depositional geometry of tailings and kaolinite pastes. According to the authors, a higher water content in paste affects the flow properties and settling of paste. Furthermore, the authors also highlighted that the angle at which the paste settles (depositional angle) and the forces within the paste (yield stress) decrease as more water is added to the paste. Another study by Huynh et al. (2006) focused on studying the effect of polymer addition on uncemented thickened tailings in order to change their flow properties. Specifically, the researchers looked at how altering the pH and using certain polymer dispersants affected the yield stress of these uncemented tailings. The research demonstrated that the use of specific polymer dispersants proved effective in reducing the rheological properties (yield stress) of uncemented paste tailings. Ding et al. (2006) also provided insights into how specific parameters in the wet ultra-fine grinding process impact the rheological properties of pyrite–heptane slurry. The parameters investigated included the concentration of solid particles, the amount of dispersant added, grinding time, and the type of organic acid used as a dispersant. The results revealed that an increase in solid concentration increased the rheological behaviour of the slurry. The rheological behaviour and particle size of the slurry were also influenced by the grinding time and the carbon numbers of the organic acids used as dispersants.

Some noteworthy research works on the permeability studies of uncemented paste tailings include research works by Benzaazoua et al. (2004), who aimed to study the leaching potential of pyrite and arsenopyrite in tailings from a European gold mine. The study aimed to understand how the geochemical behaviour of the tailings is affected before and after including cementitious components. The research extensively characterized the tailings and examined the solidification and stabilization processes (SSP) by studying leaching processes, microstructure evolution, and chemical composition changes in paste samples. The findings highlighted that leaching is

minimized in paste containing cemented components compared to uncemented samples as leaching tests showed that samples with cement had higher retention potential. The studies of Benzaazoua et al. (2004) are supported by Deschamps et al. (2008), who concluded that uncemented paste disposal is not a necessarily good technique to prevent AMD. The authors further suggested that the use of uncemented paste tailings for surface paste disposal could become an adequate method to manage acid generating tailings if small binder quantities are added to tailings mixture.

2.8.2 Review studies on rheological and permeability properties of cemented paste tailings.

In order to optimize the knowledge of cemented paste tailings, several studies have conducted rheological and permeability tests to study specific factors that can affect the flowability and porosity of cemented paste tailings. In the areas of rheology researchers have successfully explored factors like, the influence of type and content of binders, tailings, initial sulphate content, and superplasticizers on the rheological characteristics of CPB (Haiqiang et al., 2016; Bian et al., 2021; Ali et al., 2021; Haruna and Fall 2020; Ouattara et al., 2017; Xiao et al., 2021; Xiapeng, Ouattara et al., 2018; Roshani and Fall, 2020).

Yang et al. (2019) and (2020) successfully studied the mixing process (such as mixing time, mixing speed) and its influence on the rheological performance of CPB. Some studies have focused on the mixing power (Cazacliu, 2008, mixing time (Chopin et al., 2004), mixing velocity (Han and Ferron, 2016) and mixer parameters (Cazacliu and Roquet, 2009). Furthermore, Han and Ferron, (2016) proposed that the fluidity of cement paste was affected by mixing power as they highlighted that the fluidity properties of cement paste deteriorated when the mixing power increased to a threshold value. Takahashi et al. (2011) investigated how the mixing energy affected the fluidity and hardened behaviours of cement-containing grouts and showed that a longer mixing time reduced the

rheological parameters of the cement-containing grouts. The mixing time was inversely proportional to energy consumption and production efficiency. Therefore, an increase in mixing time increases energy consumption and decreases production efficiency during mixing (Cazacliu, 2008; Cazacliu and Roquet, 2009).

The permeability properties of CPB can be evaluated using knowledge of its hydraulic conductivity. Hydraulic conductivity is a crucial factor that governs the rate of groundwater flow through the CPB structure. This parameter provides valuable insights into the CPB's pore structure, including coarseness, connectivity, and any potential cracking. Previous studies on the permeability properties of CPB include works by Fall et al. (2009). The authors who experimentally studied the permeability properties of CPB by assessing its hydraulic conductivity reported that the hydraulic conductivity of CPB is time-dependent, decreasing with increasing curing time. They further highlighted that the permeability of CPB is influenced by factors such as CPB mix components, water to cement ratio, binder type, tailings fineness, and sulphate concentration. Curing temperature and time were also reported to impact hydraulic conductivity, particularly in early age samples. Initial sulphate was found to have two opposite effects on the hydraulic conductivity. At an early age, up to 28 days of curing, CPB containing sulphate has lower hydraulic conductivity due to low porosity caused by precipitation of secondary cement hydration products. At old curing age (90 days and above), the CPB containing high sulphate content becomes more permeable due to the development of microcracks as the amount of expansive hydration products becomes excessive.

Other researchers have also experimentally shown that changes in hydraulic conductivity influence the effectiveness of the CPB (Chakilam and Cui, 2020). For example, Sheshpari (2015) emphasized the importance of designing CPB so that its drainage has the appropriate hydraulic conductivity to prevent retaining wall destruction and facilitate drainage. Similarly, Pokharel and

Fall (2013) argue that temperature and sulphate significantly influence hydraulic conductivity and can either increase or decrease it. For instance, a decrease in temperature increases hydraulic conductivity (Jiang et al., 2017). As a result, it is critical to keep the temperature at an optimum level to avoid a negative impact on the CPB.

2.9 CONCLUSION

The shift towards paste for surface and underground disposal of tailings as an alternative to traditional methods signifies a transformative phase in mine waste management practice. While this approach offers significant advantages across operational, environmental, and regulatory aspects in mineral extraction and processing, there is still a major challenge of fully understanding the behaviour of paste tailings. This challenge is particularly evident in the preparation of paste tailings that meet suitable flowability and porosity standards in order to avoid cost problems from pipeline clogging during PT transportation and environmental leaching through AMD. To tackle these problems the knowledge of paste tailings technology must be continually optimized through laboratory-scale studies that focus on how several factors affect the material properties and behaviours of PT. Specifically, investigations into the effects of pyrite content in tailings, binder types, binder replacement, and the combined synergistic effects of these components are essential. Examining how these factors influence the rheological and permeability properties of paste tailings is pivotal for overcoming the challenges associated with successful understanding and application of PT for both surface and underground disposal. Therefore, investigation of these factors would be the focus of this PhD research. Findings from the study will provide beneficial information for proper and sustainable design of PT.

2.10 REFRENCES

Abraham, M. R., and Susan, T. B. (2017). Water contamination with heavy metals and trace elements from Kilembe copper mine and tailing sites in Western Uganda; implications for domestic water quality. *Chemosphere (Oxford)*, *169*, 281–287. https://doi.org/10.1016/j.chemosphere.2016.11.077

ACI Committee 233R, 2000. Ground Granulated Blast Furnace Slag as a Cementitious Constituent in Concrete. American Concrete Institute (ACI), Farmington Hills, Michigan

Agboola, O., Babatunde, D. E., Isaac Fayomi, O. S., Sadiku, E. R., Popoola, P., Moropeng, L., Yahaya, A., and Mamudu, O. A. (2020). A review on the impact of mining operation: Monitoring, assessment and management. *Results in Engineering*, *8*, 100181-. https://doi.org/10.1016/j.rineng.2020.100181

Aldea, C. (2010). Paste backfill mix From concept through closure. International Mining, (April), 79–80.

Aldhafeeri, Z. (2018). Reactivity of Cemented Paste Backfill. Doctoral dissertation, University of Ottawa.

Ali, G., Fall, M., and Alainachi, I. (2021). Time- and temperature-dependence of rheological properties of cemented tailings backfill with sodium silicate. *Journal of Materials in Civil Engineering, 33*(3), 04020498. https://doi.org/10.1061/(ASCE)MT.1943-5533.0003605

Alizadeh, R., 2009. Nanostructure and Engineering Properties of Basic and Modified CalciumSilicate-Hydrate Systems. PhD thesis, University of Ottawa, 252 p.

Andrade, E.N.da C., 1947. Viscosity and Plasticity. Heffer, Cambridge

Argane, R., Benzaazoua, M., Hakkou, R., and Bouamrane, A. (2016). A comparative study on the practical use of low sulfide base-metal tailings as aggregates for rendering and masonry mortars. *Journal of Cleaner Production*, *112*(Part 1), 914–925. https://doi.org/10.1016/j.jclepro.2015.06.004

Aylmer, F. L. (1973, August). Cement properties related to the behaviour of cemented fill. In *Proceedings Jubilee Symposium on Mine Filling, Mount Isa, North West Queensland Branch, The AusIMM, August* (pp. 59-63).

Ayres, R. U., Ayres, L. W., and Råde, I. (2002). The Life Cycle of Copper, Its Co-Products and By-Products. Mining, Minerals and Sustainable Development. International Institute for Environment and Development: London, UK, 210.

Bao, Z., Al, T., Couillard, M., Poirier, G., Bain, J., Shrimpton, H. K., Finfrock, Y. Z., Lanzirotti, A., Paktunc, D., Saurette, E., Hu, Y., Ptacek, C. J., and Blowes, D. W. (2021). A cross-scale investigation of galena oxidation and controls on mobilization of lead in mine waste rock. *Journal of Hazardous Materials*, *412*, 125130–125130. https://doi.org/10.1016/j.jhazmat.2021.125130

Bascetin A., Tuylu S., Adıguzel D., and Ozdemir O. (2016). New Technologies on Mine Process Tailing Disposal. Journal of Geological Resource and Engineering, 4(2). https://doi.org/10.17265/2328-2193/2016.02.002

Beaudouin J. J., Patarachao, B., Raki, L., Alizadeh, R., 2011. Adsorption of methylene blue as a descriptor C-S-H nanostructure. Cement and Concrete Composites, 33(2): 246-250.

Belem, T., and Benzaazoua, M. (2008). Design and Application of Underground Mine Paste Backfill Technology. *Geotechnical and Geological Engineering*, *26*(2), 147–174. https://doi.org/10.1007/s10706-007-9154-3

Belem, T., Bussière, B., and Benzaazoua, M. (2001). The effect of microstructural evolution on the physical properties of paste backfill. In Proceedings of the Tailings and Mine Waste ’01 (pp. 365–374). Fort Collins, Colorado, Balkema, Rotterdam

Bentz, D.P., 2008. A review of early-age properties of cement-based materials. Cement and Concrete Research, 38(2): 196–204

Benzaazoua, M., and Kongolo, M. (2003). Physico-chemical properties of tailing slurries during environmental desulphurization by froth flotation. International Journal of Mineral Processing, 69(1–4), 221–234. http://doi.org/10.1016/S0301-7516(02)00129-1

Benzaazoua, M., Belem, T., and Bussière, B. (2002). Chemical factors that influence the performance of mine sulphidic paste backfill. *Cement and Concrete Research*, *32*(7), 1133–1144. https://doi.org/10.1016/S0008-8846(02)00752-4

Benzaazoua, M., Fall, M., and Belem, T. (2004). A contribution to understanding the hardening process of cemented pastefill. *Minerals Engineering*, *17*(2), 141–152. https://doi.org/10.1016/j.mineng.2003.10.022

Benzaazoua, M., Marion, P., Picquet, I., and Bussière, B. (2004). The use of pastefill as a solidification and stabilization process for the control of acid mine drainage. *Minerals Engineering*, *17*(2), 233–243. https://doi.org/10.1016/j.mineng.2003.10.027

Bergold, S. T., Goetz-Neunhoeffer, F., and Neubauer, J. (2017). Interaction of silicate and aluminate reaction in a synthetic cement system: Implications for the process of alite hydration. Cement and Concrete Research, 93, 32-44

Bian, J., Fall, M., and Haruna, S. (2021). Sulfate-induced changes in rheological properties of fibre-reinforced cemented paste backfill. *Magazine of Concrete Research, 73*(11), 574–583.

Bouzoubaa, N., and Foo, S. (2004). Use of fly ash and slag in concrete: A Best Practice Guide. *Materials and Technology Laboratory, MTL*, *16*.

Bowles, J. F. W., Howie, R. A., Vaughan, D. J., and Zussman, J. (2011). Non-silicates: Oxides, Hydroxides and Sulphides. In Rock-Forming Minerals Vol. 5A. Geological Society, London. 920 pp. https://doi.org/10.3749/canmin.49.5.1335

Bresson, E., Stern, J., and Szydlo, M. (2002). Threshold Ring Signatures and Applications to Ad-hoc Groups. *Annual International Cryptology Conference*.

Brown, A. D., and Jurinak, J. J. (1989). Mechanism of Pyrite Oxidation in Aqueous Mixtures. *Journal of Environmental Quality*, *18*(4), 545–550. https://doi.org/10.2134/jeq1989.00472425001800040028x

Buckley, A. N., and Woods, R. (1984). An x-ray photoelectron spectroscopic study of the oxidation of galena. *Applications of Surface Science*, *17*(4), 401–414. https://doi.org/10.1016/0378-5963(84)90003-5

Buckley, A. N., and Woods, R. (1987). The surface oxidation of pyrite. *Applied Surface Science*, *27*(4), 437–452. https://doi.org/10.1016/0169-4332(87)90153-X

Bull, A. J., and Fall, M. (2020). Thermally induced changes in metalloid leachability of cemented paste backfill that contains blast furnace slag. *Minerals Engineering, 156*, 106520. https://doi.org/10.1016/j.mineng.2020.106520.

Bullard, J. W., Jennings, H. M., Livingston, R. A., Nonat, A., Scherer, G. W., Schweitzer, J. S., Scrivener, K. L., and Thomas, J. J. (2011). Mechanisms of cement hydration. *Cement and Concrete Research, 41*(12), 1208–1223. https://doi.org/10.1016/j.cemconres.2010.09.011.

Burchfield, T. E., and Hepler, L. G. (1979). Some chemical and physical properties of tailings water from oil sands extraction plants. *Fuel (Guildford)*, *58*(10), 745–747. https://doi.org/10.1016/0016-2361(79)90074-7

Burden, R., and Wilson, G. W. (2023). Commingling of Waste Rock and Tailings to Improve "Dry Stack" Performance: Design and Evaluation of Mixtures. *Minerals (Basel)*, *13*(2), 295-. https://doi.org/10.3390/min13020295

Bürger, R., Concha, F., and Tiller, F. M. (2000). Applications of the phenomenological theory to several published experimental cases of sedimentation processes. *Chemical Engineering Journal, 80*, 105–117. https://doi.org/10.1016/S1383-5866(00)00090-3..

Bürger, R., Liu, C., and Wendland, W. L. (2001). Existence and Stability for Mathematical Models of Sedimentation–Consolidation Processes in Several Space Dimensions. *Journal of Mathematical Analysis and Applications*, *264*(2), 288–310. https://doi.org/10.1006/jmaa.2001.7646

Cacciuttolo, C., and Cano, D. (2022). Environmental Impact Assessment of Mine Tailings Spill Considering Metallurgical Processes of Gold and Copper Mining: Case Studies in the Andean Countries of Chile and Peru. *Water (Basel)*, *14*(19), 3057-. https://doi.org/10.3390/w14193057

Cacciuttolo, C., and Valenzuela, F. (2022). Efficient Use of Water in Tailings Management: New Technologies and Environmental Strategies for the Future of Mining. *Water (Basel)*, *14*(11), 1741- https://doi.org/10.3390/w14111741

Cao, S., Yilmaz, E., and Song, W. (2018). Evaluation of viscosity, strength and microstructural properties of cemented tailings backfill. Minerals, 8(8), 352.

Cazacliu, B. (2008). In-mixer measurements for describing mixture evolution during concrete mixing. *Chemical Engineering Research and Design, 86*(12), 1423–1433.

Cazacliu, B., and Roquet, N. (2009). Concrete mixing kinetics by means of power measurement. *Cement and Concrete Research, 39*(3), 182–194.

Chakilam, S., and Cui, L. (2020). Effect of polypropylene fiber content and fiber length on the saturated hydraulic conductivity of hydrating cemented paste backfill. Construction and Building Materials, 262, 120854

Chanturiya, V. A., Krasavtseva, E. A., and Makarov, D. V. (2022). Electrochemistry of Sulfides: Process and Environmental Aspects. *Sustainability (Basel, Switzerland)*, *14*(18), 11285-. https://doi.org/10.3390/su141811285

Chen, J., Xu, Z. and Chen, Y. (2020). Electronic Structure and Surfaces of Sulfide Minerals, edited by Y. Chen, J. Chen and Z. Xu, pp. 13–81. Amsterdam: Elsevier. http://dx.doi.org/10.1016/B978-0-12-817974-1.00002-8

Chen, W., and Brouwers, H. J. H. (2010). Alkali binding in hydrated Portland cement paste. *Cement and Concrete Research*, *40*(5), 716–722. https://doi.org/10.1016/j.cemconres.2009.12.007

Chockalingam, E., Subramanian, S., and Natarajan, K. A. (2003). Studies on biodegradation of organic flotation collectors using Bacillus polymyxa. *Hydrometallurgy*, *71*(1), 249–256. https://doi.org/10.1016/S0304-386X(03)00163-4

Chopin, D., de Larrard, F., and Cazacliu, B. (2004). Why do HPC and SCC require a longer mixing time? *Cement and Concrete Research, 34*(12), 2237–2243.

Chougnet, A., Audibert, A. and Moan, M. 2007. Linear and non linear rheological behavior of cement and silica suspensions: effect of polymer addition. Rheologica acta, 46: 793-802

Cohn, C. A., Laffers, R., Simon, S. R., et al. (2006). Role of pyrite in formation of hydroxyl radicals in coal: possible implications for human health. *Part Fibre Toxicol, 3*(1), 16. https://doi.org/10.1186/1743-8977-3-16

Conner, J. R. (1990). *Chemical fixation and solidification of hazardous wastes* (p. 692). New York: Van Nostrand Reinhold.

Cooke, R., Spearing, A.J.S., and Gericke, D. 1992. The Influence of Binder Addition on the Hydraulic Transport of Classified-Tailings Backfill. Journal of the South African Institute of Mining and Metallurgy, 92 (11/12): 325–329.

Crowder, J. (2004). Deposition, consolidation, and strength of a nonplastic tailings paste for surface disposal. Ph.D. thesis, University of Toronto, Toronto, ON, Canada.

Cui, L., and Fall, M. (2018). Modeling of self-desiccation in a cemented backfill structure. *International Journal for Numerical and Analytical Methods in Geomechanics*, *42*(3), 558–583. https://doi.org/10.1002/nag.2756

Davenport, W. G., King, M. J., Schlesinger, M. E., Biswas, A. K., and King, M. (2002). *Extractive Metallurgy of Copper* (4th ed.). Elsevier Science.

Davies, M.P. and Rice, S. (2001) An Alternative to Conventional Tailings Management – 'Dry Stack' Filtered Tailings. AMEC Earth and Environmental, Vancouver

Deng, X. J., Klein, B., Hallbom, D. J., de Wit, B., and Zhang, J. X. (2018). Influence of particle size on the basic and time-dependent rheological behaviors of cemented paste backfill. Journal of Materials Engineering and Performance, 27(7), 3478-3487

Deschamps, T., Benzaazoua, M., Bussière, B., Aubertin, M., and Belem, T. (2008). Microstructural and geochemical evolution of paste tailings in surface disposal conditions. *Minerals Engineering*, *21*(4), 341–353. https://doi.org/10.1016/j.mineng.2007.12.002

Dimitrova, R. S., and Yanful, E. K. (2012). Effect of drainage conditions, bed thickness, and age on the shear strength of mine tailings in a very low stress range. Canadian Geotechnical Journal, 49(3), 285–297. http://doi.org/10.1139/t11-098

Ding, Z., Yin, Z., Liu, L., and Chen, Q. (2007). Effect of grinding parameters on the rheology of pyrite–heptane slurry in a laboratory stirred media mill. *Minerals Engineering*, *20*(7), 701–709. https://doi.org/10.1016/j.mineng.2007.01.005

Dixon-Hardy, D., and Engels, J. (2007). Methods for the disposal and storage of mine tailings. *Land Contamination and Reclamation, 15*, 301-317. doi:10.2462/09670513.832.

Dong, Q., Liang, B., Jia, L., and Jiang, L. (2019). Effect of sulfide on the long-term strength of lead-zinc tailings cemented paste backfill. *Construction and Building Materials*, *200*, 436–446. https://doi.org/10.1016/j.conbuildmat.2018.12.069

Dopson, M., Sundkvist, J.-E., and Börje Lindström, E. (2006). Toxicity of metal extraction and flotation chemicals to Sulfolobus metallicus and chalcopyrite bioleaching. *Hydrometallurgy*,

81(3), 205–213. https://doi.org/10.1016/j.hydromet.2005.12.005

Double, D.D., 1983. New developments in understanding the chemistry of cement hydration. Philosophical Transactions of the Royal Society. London, A 310(1511): 53–66.

Douglas, E., and Malhotra, V. M. (1989). Ground granulated blast-furnace slag for cemented mine backfill: production and evaluation. *CIM bulletin*, *82*(929), 27-36.

DPI (2003) Management of Tailings Storage Facilities – Environmental Guidelines. Department of Primary Industries, Victoria – Minerals and Petroleum Division

Elmakki, R., Masalova, I., Haldenwang, R., Malkin, A., and Mbasha, W. (2016). Effect of limestone on the cement paste hydration in the presence of polycarboxylate superplasticizer. *Applied Rheology, 26*(2), 23–30.

El-Mosallamy, M., and Shehata, M. H. (2020). Sulphide oxidation mortar tests for evaluation of the oxidation potential of sulphide-bearing aggregate. *Construction and Building Materials*, *264*, 120627-. https://doi.org/10.1016/j.conbuildmat.2020.120627

Ercikdi, B., Cihangir, F., Kesimal, A., Deveci, H., and Alp, İ. (2009). Utilization of industrial waste products as pozzolanic material in cemented paste backfill of high sulphide mill tailings. *Journal of Hazardous Materials*, *168*(2), 848–856. https://doi.org/10.1016/j.jhazmat.2009.02.100

Esmaeely, S. N., and Nesic, S. (2017). Reduction Reactions on Iron Sulfides in Aqueous Acidic Solutions. *Journal of the Electrochemical Society*, *164*(12), C664–C670. https://doi.org/10.1149/2.1381712jes

Evans, S., and Raftery, E. (1982). Electron spectroscopic studies of galena and its oxidation by microwave-generated oxygen species and by air. *Journal of the Chemical Society, Faraday Transactions 1: Physical Chemistry in Condensed Phases*, *78*(12), 3545-. https://doi.org/10.1039/f19827803545

Fall, M., Adrien, D., Célestin, J. C., Pokharel, M., and Touré, M. (2009). Saturated hydraulic conductivity of cemented paste backfill. *Minerals Engineering*, *22*(15), 1307–1317. https://doi.org/10.1016/j.mineng.2009.08.002

Fall, M., and Pokharel, M. (2010). Coupled effects of sulphate and temperature on the strength development of cemented tailings backfills: Portland cement-paste backfill. *Cement and Concrete Composites*, *32*(10), 819–828. https://doi.org/10.1016/j.cemconcomp.2010.08.002

Fall, M., and Samb, S. S. (2006). Influence of curing temperature on strength, deformation behaviour and pore structure of cemented paste backfill at early ages. *Construction and Building Materials*. https://doi.org/10.1016/j.conbuildmat.2006.08.010

Fall, M., Belem, T., Samb, S., and Benzaazoua, M. (2007). Experimental Characterization of the stress-strain behaviour of cemented paste backfill in compression. *Journal of materials science*, *42*(11), 3914–3922. https://doi.org/10.1007/S10853-006-0403-2

Fall, M., Benzaazoua, M., and Ouellet, S. (2004). Effect of tailings properties on paste backfill performance. In Proceedings of the eighth international symposium on mining with backfill (Minefill 2004) (pp. 193–202). China.

Fall, M., Benzaazoua, M., and Ouellet, S. (2005). Experimental characterization of the influence of tailings fineness and density on the quality of cemented paste backfill. *Minerals Engineering*, *18*(1), 41–44. https://doi.org/10.1016/j.mineng.2004.05.012

Fall, M., Nasir, O., Cui, L., and Han, F. S. (2015). Coupled modeling of the strength development and distribution within cemented paste backfill Structure. In 49th US Rock Mechanics/Geomechanics Symposium. American Rock Mechanics Association

Fang, K., Cui, L., and Fall, M. (2020). A coupled chemo-elastic cohesive zone model for backfill-rock interface. *Computers and Geotechnics*, *125*, 103666-. https://doi.org/10.1016/j.compgeo.2020.103666

Fang, K., Zhang, J., Cui, L., Haruna, S., and Li, M. (2023). Cost optimization of cemented paste backfill: State-of-the-art review and future perspectives. *Minerals Engineering*, *204*, 108414-. https://doi.org/10.1016/j.mineng.2023.108414

Fontes, W. C., Mendes, J. C., Silva, S. N. D., and Peixoto, R. A. F. (2016). Mortars for laying and coating produced with iron ore tailings from tailing dams. *Construction and Building Materials*, *112*, 988–995. https://doi.org/10.1016/j.conbuildmat.2016.03.027

Fornasiero, D., Li, F., Ralston, J., and Smart, R. St. C. (1994). Oxidation of Galena Surfaces. *Journal of Colloid and Interface Science*, *164*(2), 333–344. https://doi.org/10.1006/jcis.1994.1175

Fourie, A. B., Blight, G. E., and Papageorgiou, G. (2001). Static liquefaction as a possible explanation for the Merriespruit tailings dam failure. *Canadian Geotechnical Journal*, *38*(4), 707–719. https://doi.org/10.1139/t00-112

Fourie, A.B. (2003) In Search of the Sustainable Tailings Dam: Do High-Density Thickened Tailings Provide the Solution? School of Civil and Environmental Engineering, University of the Witwatersrand, South Africa.

Godbout, M., Bussière, B., Aubertin, M., and Belem, T. (2007). Evolution of cemented past backfill saturated hydraulic conductivity at early curing time.

Gomes, R. B., De Tomi, G., and Assis, P. S. (2016). Iron ore tailings dry stacking in Pau Branco mine, Brazil. *Journal of Materials Research and Technology*, *5*(4), 339–344. https://doi.org/10.1016/j.jmrt.2016.03.008

Goto, S., and Roy, D. M. (1981). Diffusion of ions through hardened cement pastes. *Cement and Concrete Research*, *11*(5), 751–757. https://doi.org/10.1016/0008-8846(81)90033-8

Gou, M., Zhou, L. and Then, N. (2019). Utilization of tailings in cement and concrete: A review. *Science and Engineering of Composite Materials*, *26*(1), 449-464. https://doi.org/10.1515/secm-2019-0029

Goudoulas, T. B., Kastrinakis, E. G. and Nychas, S. G. 2003. Rheological aspects of dense lignite-water suspensions; time dependence. preshear and solids loading effects. Rheoogica Acta, 42: 73-85.

Grabinsky, M. W., and Bawden, W. F. (2007). In situ measurements for geomechanical design of cemented paste backfill systems. In *Proceedings of the 9th International Symposium in Mining with Backfill, Montréal, Que* (Vol. 29).

Grice, T. (1998). Underground mining with backfill. Proceedings of the 2nd Annual Summit-Mine Tailings Disposal Systems, 216, 234- 239.

Haiqiang, J., Fall, M., and Cui, L. (2016). Yield stress of cemented paste backfill in sub-zero environments: Experimental results. *Mineral Engineering, 92*, 141–150.

Han, D., and Ferron, R. D. (2016). Influence of high mixing intensity on rheology, hydration, and microstructure of fresh state cement paste. *Cement and Concrete Research, 84*, 95–106.

Haruna, S., and Fall, M. (2020). Time- and temperature-dependent rheological properties of cemented paste backfill that contains superplasticizer. *Powder Technology*, *360*, 731–740. https://doi.org/10.1016/j.powtec.2019.09.025

Hassani, F. and Archibald, J., 1998. Mine Backfill (CD-ROM), Canadian Institute of Mine, Metallurgy and Petroleum, 262 p

Hassani, F. P., Nokken, M. R., and Annor, A. B. (2007). Physical and mechanical behaviour of various combinations of minefill materials. *CIM Bull*, *2*(3), 72.

Hatje, V., Pedreira, R. M. A., de Rezende, C. E., Schettini, C. A. F., de Souza, G. C., Marin, D. C., and Hackspacher, P. C. (2017). The environmental impacts of one of the largest tailing dam failures worldwide. *Scientific Reports*, *7*(1), 10706–10713. https://doi.org/10.1038/s41598-017-11143-x

Hooton, Doug. (2011). Canadian use of ground granulated blast-furnace slag as a supplementary cementing material for enhanced performance of concrete. Canadian Journal of Civil Engineering. 27. 754-760. 10.1139/cjce-27-4-754.

Huynh, L., Beattie, D. A., Fornasiero, D. and Ralston, J. 2006. Effect of polyphosphate and naphthalene sulfonate formaldehyde condensate on the rheological properties of dewatered tailings and cemented paste backfill. Minerals Engineering, 19 (1): 28-36.

ICOLD and UNEP (2001) Bulletin 121: Tailings Dams – Risk of Dangerous Occurrences, Lessons Learnt from Practical Experiences. UNEP, DTIE and ICOLD, Paris

Impact Assessment Agency of Canada. (2021). Best Available Technologies Assessment for Tailings. Retrieved from https://iaac-aeic.gc.ca/050/documents/p54755/139035E.pdf

Jacobsen, S., Mork, J.H., Lee, S.F., Haugan, L., 2008. Pumping of concrete and mortar – State of the art. COIN Project report 5. COIN P2 Improved construction technology. SP 2.4 Workability. p. 46.

Jakubick, A., McKenna, G. and Robertson, A. (2003) Stabilisation of Tailings Deposits: International Experience. Mining and the Environment III, Sudbury, Ontario, Canada, 25– 28 May, 2003, pp. 1–9

Jambor, J and Ptacek, Carol and Blowes, D and Moncur, Michael. (2005). Acid drainage from the oxidation of iron sulfides and sphalerite.

James, M., Aubertin, M. and Bussière, B. 2013. On the use of waste rock inclusions to improve the performance of tailings impoundments. 18th International Conference on Soil Mechanics and Geotechnical Engineering, pp. 735-738.

Jeyakaran, T., Pornsiri, N., Saengsoy, W., and Tangtermsirikul, S. (2023). Test methods for performance-based evaluation of concrete containing iron sulfide-bearing aggregates: Development and application. *Results in Engineering*, *18*, 101068-. https://doi.org/10.1016/j.rineng.2023.101068

Jeyakaran, T., Pornsiri, N., Saengsoy, W., and Tangtermsirikul, S. (2023). Test methods for performance-based evaluation of concrete containing iron sulfide-bearing aggregates: Development and application. *Results in Engineering*, *18*, 101068-. https://doi.org/10.1016/j.rineng.2023.101068

Jiang, H. and Fall, M. (2017). Yield stress and strength of saline cemented tailings materials in sub-zero environments: slag-paste backfill. Journal of Sustainable Cement-Based Materials, 1-18.

Joshi, Y. M., and Petekidis, G. (2018). Yield stress fluids and ageing. *Rheologica Acta, 57*(6-7), 521–549.

Kalinnikov, V. T., Makarov, D. V., and Makarov, V. N. (2001). Oxidation Sequence of Sulfide Minerals in Operating and Out-of-Service Mine Waste Storage. *Theoretical Foundations of Chemical Engineering*, *35*(1), 63–68. https://doi.org/10.1023/A:1005272819672

Kartio, I. J., Laajalehto, K., Suoninen, E. J., Buckley, A. N., and Woods, R. (1998). The initial products of the anodic oxidation of galena in acidic solution and the influence of mineral stoichiometry. *Colloids and Surfaces. A, Physicochemical and Engineering Aspects*, *133*(3), 303–311. https://doi.org/10.1016/S0927-7757(97)00202-1

Kesimal, A., Ercikdi, B., and Yilmaz, E. (2003). The effect of desliming by sedimentation on paste backfill performance. *Minerals Engineering*, *16*(10), 1009–1011. https://doi.org/10.1016/S0892-6875(03)00267-X

Kesimal, A., Yilmaz, E., Ercikdi, B., Alp, I., and Deveci, H. (2005). Effect of properties of tailings and binder on the short-and long-term strength and stability of cemented paste backfill. Materials Letters, 59(28), 3703–3709. http://doi.org/10.1016/j.matlet.2005.06.042

Kheirkhah Gildeh, H., Halliday, A., Arenas, A., and Zhang, H. (2021). Tailings Dam Breach Analysis: A Review of Methods, Practices, and Uncertainties. *Mine Water and the Environment*, *40*(1), 128–150. https://doi.org/10.1007/s10230-020-00718-2

Kim, B. S., Hayes, R. A., Prestidge, C. A., Ralston, J., and Smart, R. St. C. (1995). Scanning Tunneling Microscopy Studies of Galena: The Mechanisms of Oxidation in Aqueous Solution. *Langmuir*, *11*(7), 2554–2562. https://doi.org/10.1021/la00007a039

Kiventerä, J., Perumal, P., Yliniemi, J., and Illikainen, M. (2020). Mine tailings as a raw material in alkali activation: A review. *International Journal of Minerals, Metallurgy and Materials*, *27*(8), 1009–1020. https://doi.org/10.1007/s12613-020-2129-6

Kjellsen, K. O., Detwiler, R. J., and Gjørv, O. E. (1991). Development of microstructures in plain cement pastes hydrated at different temperatures. *Cement and Concrete Research*, *21*(1), 179–189. https://doi.org/10.1016/0008-8846(91)90044-I

Klein, K., and Simon, D. (2006). Effect of specimen composition on the strength development in cemented paste backfill. *Canadian Geotechnical Journal*, *43*(3), 310–324. https://doi.org/10.1139/t06-005

Kleiv, R. A. (2021). A flotation-based approach to the quantification of pyrrhotite in concrete aggregates. *Results in Engineering*, *11*, 100243-. https://doi.org/10.1016/j.rineng.2021.100243

Kossoff, D., Dubbin, W. E., Alfredsson, M., Edwards, S. J., Macklin, M. G., and Hudson-Edwards, K. A. (2014). Mine tailings dams: Characteristics, failure, environmental impacts, and remediation. *Applied Geochemistry*, *51*, 229–245. https://doi.org/10.1016/j.apgeochem.2014.09.010

Kwak, M., James, D. F., and Klein, K. A. (2005). Flow behaviour of tailings paste for surface disposal. *International Journal of Mineral Processing, 77*(3), 139–153.

Laajalehto, K., Smart, R. St. C., Ralston, J., and Suoninen, E. (1993). STM and XPS investigation of reaction of galena in air. *Applied Surface Science*, *64*(1), 29–39. https://doi.org/10.1016/0169-4332(93)90019-8

Lamos, A. W., and Clark, I. H. (2021). The influence of material composition and sample geometry on the strength. *Innovations in Mining Backfill Technology*, *80*, 89.

Landriault, D., 2001. Chapter 69: Backfill in Underground Mining. In: Underground Mining Methods: Engineering Fundamentals and International Case Studies (eds W. A. Hustrulid and R. L. Bullock), 29-48. Society for Mining, Metallurgy and Exploration: Littleton, Colorado.

Landriault, D.A., Brown, R.E. and Counter, David. (2000). Paste backfill study for deep mining at Kidd Creek. 93. 156-161.

Landriault, D.A., Verburg, R., Cincilla, W. and Welch, D., 1997. Paste technology for underground backfill and surface tailings disposal applications. Short course notes, Canadian Institute of Mining and Metallurgy, Technical workshop-April 27, 1997, Vancouver, British Columbia, Canada, 120p

Lee, J., Ko, J., and Kim, Y. (2017). Rheology of fly ash mixed tailings slurries and applicability of prediction models. *Minerals, 7*(9), 165.

Legrand, C. 1972. Contribution à l'étude de la rhéologie du béton frais. Matériaux et constructions, 30(5): 379- 393.

Levens, R.L., Marcy A.D. and Boldt, C.M.K., 1996. Environmental Impacts of Cemented Mine Waste Backfill. RI 9599. United States Bureau of Mines, 23p.

Li, M., Moerman, A., 2002. Perspectives on the scientific and engineering principles underlying flow of mineral pastes. In: Proceedings of 34th Annual Meeting of the Canadian Mineral Processors. Ottawa, Canada.

Li, X., Du, J., Gao, L., He, S., Gan, L., Sun, C., and Shi, Y. (2017). Immobilization of phosphogypsum for cemented paste backfill and its environmental effect. *Journal of Cleaner Production, 156*, 137–146. https://doi.org/10.1016/j.jclepro.2017.04.046.

Liao, J., Ru, X., Xie, B., Zhang, W., Wu, H., Wu, C., & Wei, C. (2017). Multi-phase distribution and comprehensive ecological risk assessment of heavy metal pollutants in a river affected by acid mine drainage. *Ecotoxicology and Environmental Safety*, *141*, 75–84. https://doi.org/10.1016/j.ecoenv.2017.03.009

Liao, J., Wen, Z., Ru, X., Chen, J., Wu, H., and Wei, C. (2016). Distribution and migration of heavy metals in soil and crops affected by acid mine drainage: Public health implications in Guangdong Province, China. *Ecotoxicology and Environmental Safety*, *124*, 460–469. https://doi.org/10.1016/j.ecoenv.2015.11.023

Liddel, P. V., and Boger, D. V. (1996). Yield stress measurements with the vane. *Journal of Non-Newtonian Fluid Mechanics, 63*(2–3), 235-261. https://doi.org/10.1016/0377-0257(95)01421-7

Lin, F., and Meyer, C. (2009). Hydration kinetics modeling of Portland cement considering the effects of curing temperature and applied pressure. *Cement and Concrete Research*, *39*(4), 255–265. https://doi.org/10.1016/j.cemconres.2009.01.014

Lindsay, M. B. J., Moncur, M. C., Bain, J. G., Jambor, J. L., Ptacek, C. J., and Blowes, D. W. (2015). Geochemical and mineralogical aspects of sulfide mine tailings. *Applied Geochemistry*, *57*, 157–177. https://doi.org/10.1016/j.apgeochem.2015.01.009

Lottermoser, B. (2010). Mine Wastes: Characterization, Treatment and Environmental Impacts. Springer Berlin Heidelberg. http://doi.org/10.1007/978-3-642-12419-8

Lu, H., Qi, C., Chen, Q., Gan, D., Xue, Z., and Hu, Y. (2018). A new procedure for recycling waste tailings as cemented paste backfill to underground stopes and open pits. *Journal of Cleaner Production*, *188*, 601–612. https://doi.org/10.1016/j.jclepro.2018.04.041

Ma, B. G., Cai, L. X., Li, X. G., and Jian, S. W. (2016). Utilization of iron tailings as a substitute in autoclaved aerated concrete: Physico-mechanical and microstructure of hydration products. *Journal of Cleaner Production, 127*, 162–171. https://doi.org/10.1016/j.jclepro.2016.03.172.

Ma, X.-W., Chen, H.-X., Wang, P.-M., 2010. Effect of CuO on the formation of clinker minerals and the hydration properties. Cement Concr. Res. 40, 1681–1687. https:// doi.org/10.1016/j.cemconres.2010.08.009

Malkin, A., Kulichikhin, V., and Ilyin, S. (2017). A modern look on yield stress fluids. *Rheologica Acta, 56*(3), 177–188.

Malmström, M. E., and Collin, C. (2004). Sphalerite weathering kinetics: Effect of pH and particle size. In R. B. Wanty and R. R. Seal II (Eds.), Water-Rock Interaction (Vol. 2, pp. 849–852). Taylor and Francis, London.

Maltais, Y., And Marchand, J. (1997). Influence of Curing Temperature on Cement Hydration and Mechanical Strength Development of Fly Ash Mortars. *Cement And Concrete Research*, *27*(7), 1009–1020. Https://Doi.Org/10.1016/S0008-8846(97)00098-7

Martin, A. J., McNee, J. J., and Pedersen, T. F. (2001). The reactivity of sediments impacted by metal-mining in Lago Junin, Peru. *Journal of Geochemical Exploration*, *74*(1), 175–187. https://doi.org/10.1016/S0375-6742(01)00183-2

Martin, T.E., Davies, M.P., Rice, S., Higgs, T. and Lighthall, P.C. (2002) Stewardship of Tailings Facilities. Report commissioned by Mining, Minerals and Sustainable Development (MMSD) a project of the Institute for Environment and Development (IIED). No. 20

Mbasha, W., Masalova, I., Haldenwang, R., and Malkin, A. (2015). The yield stress of cement pastes as obtained by different rheological approaches. *Applied Rheology, 25*, article 53517.

McKibben, M. A., and Barnes, H. L. (1986). Oxidation of pyrite in low temperature acidic solutions: Rate laws and surface textures. *Geochimica et Cosmochimica Acta*, *50*(7), 1509–1520. https://doi.org/10.1016/0016-7037(86)90325-X

Medina, D., and Anderson, C. G. (2020). A Review of the Cyanidation Treatment of Copper-Gold Ores and Concentrates. *Metals (Basel)*, *10*(7), 897-. https://doi.org/10.3390/met10070897

Mehta, P. and Monteiro, P.J., 1993. Concrete Structures, Properties, and Materials (2nd ed.). Upper Saddle River, NJ: Prentice Hall

Mine Environmental Neutral Drainage (MEND) Project. (2017). Study of Tailings Management Technologies. MEND Report 2.50.1.

Mishra, D. P., and Das, S. K. (2010). A study of physico-chemical and mineralogical properties of Talcher coal fly ash for stowing in underground coal mines. *Materials Characterization*, *61*(11), 1252–1259. https://doi.org/10.1016/j.matchar.2010.08.008

Moses, C. O., Kirk Nordstrom, D., Herman, J. S., and Mills, A. L. (1987). Aqueous pyrite oxidation by dissolved oxygen and by ferric iron. *Geochimica et Cosmochimica Acta*, *51*(6), 1561–1571. https://doi.org/10.1016/0016-7037(87)90337-1

Nantel, J., and Lecuyer, N. (1983). Assessment of slag backfill properties for the Noranda Chadbourne project. CIM Bulletin, 76(849), 57–60. International Journal of Rock Mechanics and Mining Sciences and Geomechanics Abstracts, 20(5), 163–163. https://doi.org/10.1016/0148-9062(83)90279-6

Neville, A. M. (1995). *Properties of concrete* (Vol. 4, p. 1995). London: Longman.

Nordstrom, D. K. (1982). Aqueous Pyrite Oxidation and the Consequent Formation of Secondary Iron Minerals. In *Acid Sulfate Weathering* (pp. 37–56). Soil Science Society of America. https://doi.org/10.2136/sssaspecpub10.c3

Nordstrom, D. K., and Alpers, C. N. (1999). Negative pH, Efflorescent Mineralogy, and Consequences for Environmental Restoration at the Iron Mountain Superfund Site, California. *Proceedings of the National Academy of Sciences - PNAS*, *96*(7), 3455–3462. https://doi.org/10.1073/pnas.96.7.3455

Nouairi, J., Hajjaji, W., Costa, C. S., Senff, L., Patinha, C., Ferreira da Silva, E., Labrincha, J. A., Rocha, F., and Medhioub, M. (2018). Study of Zn-Pb ore tailings and their potential in cement technology. *Journal of African Earth Sciences (1994)*, *139*, 165–172. https://doi.org/10.1016/j.jafrearsci.2017.11.004

Nowak, P., and Laajalehto, K. (2000). Oxidation of galena surface – an XPS study of the formation of sulfoxy species. *Applied Surface Science*, *157*(3), 101–111. https://doi.org/10.1016/S0169-4332(99)00575-9

Oberle, B., Brereton, D., and Mihaylova, A. (2020). Towards Zero Harm: A Compendium of Papers Prepared for the Global Tailings Review. St Gallen, Switzerland: Global Tailings Review. https://globaltailingsreview.org/]

Onuaguluchi, O., Eren, O., ¨ 2012. Cement mixtures containing copper tailings as an additive: durability properties. Mater. Res. 15, 1029–1036. https://doi.org/ 10.1590/S1516-14392012005000129.

Ouattara, D., Mbonimpa, M., Yahia, A., and Belem, T. (2018). Assessment of rheological parameters of high density cemented paste backfill mixtures incorporating superplasticizers. *Construction and Building Materials, 190*, 294–307.

Ouattara, D., Yahia, A., Mbonimpa, M., and Belem, T. (2017). Effects of superplasticizer on rheological properties of cemented paste backfills. *International Journal of Mineral Processing*, *161*, 28–40. https://doi.org/10.1016/j.minpro.2017.02.003

Ouellet, J., Benzaazoua, M., and Servant, S. (1998). Mechanical, mineralogical and chemical characterization of a paste backfill. In *Tailings and mine waste'98* (pp. 139-146).

Ouellet, S., Bussière, B., Benzaazoua, M., Aubertin, M., Fall, M., Belem, T., 2003. Sulphide reactivity within cemented paste backfill: oxygen consumption test results. Proceedings of 56th Canadian Geotechnical Conference; September 28 to October 1, 2003 in Winnipeg, Manitoba, Canada, pp.176-183.

Ouellet, S., Bussière, B., Mbonimpa, M., Benzaazoua, M., and Aubertin, M. (2006). Reactivity and mineralogical evolution of an underground mine sulphidic cemented paste backfill. *Minerals Engineering*, *19*(5), 407–419. https://doi.org/10.1016/j.mineng.2005.10.006

Parbhakar-Fox, A., Lottermoser, B., and Bradshaw, D. (2013). Evaluating waste rock mineralogy and microtexture during kinetic testing for improved acid rock drainage prediction. *Minerals Engineering*, *52*, 111–124. https://doi.org/10.1016/j.mineng.2013.04.022

Park, I., Tabelin, C. B., Jeon, S., Li, X., Seno, K., Ito, M., and Hiroyoshi, N. (2019). A review of recent strategies for acid mine drainage prevention and mine tailings recycling. *Chemosphere (Oxford)*, *219*, 588–606. https://doi.org/10.1016/j.chemosphere.2018.11.053

Pokharel, M., and Fall, M. (2013). Combined influence of sulphate and temperature on the saturated hydraulic conductivity of hardened cemented paste backfill. Cement and Concrete Composites, 38, 21-28

Pokharel, M., and Fall, M. (2011). Coupled Thermochemical Effects on the Strength Development of Slag-Paste Backfill Materials. *Journal of Materials in Civil Engineering*, *23*(5), 511–525. https://doi.org/10.1061/(ASCE)MT.1943-5533.0000192

Pokharel, M., and Fall, M. (2013). Combined influence of sulphate and temperature on the saturated hydraulic conductivity of hardened cemented paste backfill. *Cement and Concrete Composites*, *38*, 21–28. https://doi.org/10.1016/j.cemconcomp.2013.03.015

Potvin, Y., Thomas, E., and Fourie, A. (2005). Handbook on mine fill. Nedlands, Western Australia: Australian Centre for Geomechanics. Retrieved from https://books.google.ca/books?id=oe3gAAAAMAAJ

Punmatharith, T., Rachakornkij, M., Imyim, A., and Wecharatana, M. (2010). Co-processing of grinding sludge as alternative raw material in Portland cement clinker production. *Journal of Applied Sciences, 10*(15), 1525–1535.

Rankine, R.M., Sivakugan, N. Geotechnical properties of cemented paste backfill from Cannington Mine, Australia. *Geotech Geol Eng* **25**, 383–393 (2007). https://doi.org/10.1007/s10706-006-9104-5

Rao, S. M., and Reddy, B. V. V. (2006). Characterization of Kolar gold field mine tailings for cyanide and acid drainage. *Geotechnical and Geological Engineering*, *24*(6), 1545–1559. https://doi.org/10.1007/s10706-005-3372-3

Rickard, D., and Luther, G. W. (2007). Chemistry of Iron Sulfides. *Chemical Reviews*, *107*(2), 514–562. https://doi.org/10.1021/cr0503658

Rimstidt, J. D., and Vaughan, D. J. (2003). Pyrite oxidation: a state-of-the-art assessment of the reaction mechanism. *Geochimica et Cosmochimica Acta*, *67*(5), 873–880. https://doi.org/10.1016/S0016-7037(02)01165-1

Rimstidt, J. D., Chermak, J. A., and Gagen, P. M. (1993). Rates of Reaction of Galena, Sphalerite, Chalcopyrite, and Arsenopyrite with Fe(III) in Acidic Solutions. In *Environmental geochemistry of sulfide oxidation*. American Chemical Society. https://doi.org/10.1021/bk-1994-0550.ch001

Roshani, A., and Fall, M. (2020). Flow ability of cemented pastefill material that contains nanosilica particles. *Powder Technology, 373*, 289–300.

Saengsoy, W., Yongchaitrakul, L., Sinlapasertsakulwong, P., and Tangtermsirikul, S. (2021). Identification of iron sulfide minerals in aggregates by accelerated mortar bar test. In Bridge Maintenance, Safety, Management, Life-Cycle Sustainability and Innovations (pp. 568-568). https://doi.org/10.1201/9780429279119-364

Sasaki, K., Tsunekawa, M., Ohtsuka, T., and Konno, H. (1997). Reply to the Comment by G. W. Luther III on "Confirmation of a sulfur-rich layer on pyrite after oxidative dissolution by Fe(III) ions around pH 2." *Geochimica et Cosmochimica Acta*, *61*(15), 3273–3274. https://doi.org/10.1016/S0016-7037(97)00145-2

Schippers, A., and Jørgensen, B. B. (2002). Biogeochemistry of pyrite and iron sulfide oxidation in marine sediments. *Geochimica et Cosmochimica Acta*, *66*(1), 85–92. https://doi.org/10.1016/S0016-7037(01)00745-1

Schoonen, M. A. A., Cohn, C. A., Roemer, E., Laffers, R., Simon, S. R., and O'Riordan, T. (2006). Mineral-induced formation of reactive oxygen species. *Reviews in Mineralogy and Geochemistry*, *64*(1), 179–221. https://doi.org/10.2138/rmg.2006.64.7

Schoonen, M., Harrington, A., Laffers, R., and Strongin, D. (2010). Role of hydrogen peroxide and hydroxyl radical in pyrite oxidation by molecular oxygen. *Geochimica et Cosmochimica Acta, 74*(17), 4971-4987. https://doi.org/10.1016/j.gca.2010.05.028.

Seal, R. R., and Hammarstrom, J. M. (2003). Geoenvironmental models of mineral deposits: Examples from massive sulphide and gold deposits. In J. L. Jambor, D. W. Blowes, and A. I. M. Ritchie (Eds.), Environmental Aspects of Mine Wastes (Vol. 31, pp. 1–50). Mineralogical Association of Canada, Short Course Series, Vancouver, British Columbia, Canada, Chapter 2.

Shapter, J. G., Brooker, M. H., and Skinner, W. M. (2000). Observation of the oxidation of galena using Raman spectroscopy. *International Journal of Mineral Processing*, *60*(3), 199–211. https://doi.org/10.1016/S0301-7516(00)00017-X

Sharma, S., and Kothiyal, N. C. (2015). Synergistic effect of zero-dimensional spherical carbon nanoparticles and one-dimensional carbon nanotubes on properties of cement-based ceramic matrix: Microstructural perspectives and crystallization investigations. *Composites Interfaces, 22*(9), 899–921. https://doi.org/10.1080/09276440.2015.1076281.

Shaughnessy, R. and Clark, P.E. 1988. The rheological behavior of fresh cement pastes. Cement Concrete Research, 18:327–341.

Sheshpari, M. (2015). A review of underground mine backfilling methods with emphasis on cemented paste backfill. Electron J Geotech Eng, 20, 5183-520

Simon, D., and Grabinsky, M. (2013). Apparent yield stress measurement in cemented paste backfill. *International Journal of Mining, Reclamation and Environment*, *27*(4), 231–256. https://doi.org/10.1080/17480930.2012.680754

Singer, P. C., and Stumm, W. (1970). Acidic Mine Drainage: The Rate-Determining Step. *Science (American Association for the Advancement of Science)*, *167*(3921), 1121–1123. https://doi.org/10.1126/science.167.3921.1121

Sivakugan, N., Rankine, R. M., Rankine, K. J., and Rankine, K. S. (2006). Geotechnical considerations in mine backfilling in Australia. *Journal of Cleaner Production*, *14*(12), 1168–1175. https://doi.org/10.1016/j.jclepro.2004.06.007

Smuda, J., Dold, B., Spangenberg, J.E., Pfeifer, H.-R., 2008. Geochemistry and stable isotope composition of fresh alkaline porphyry copper tailings: implications on sources and mobility of elements during transport and early stages of deposition. Chem. Geol. 256, 62–76. https://doi.org/10.1016/j.chemgeo.2008.08.001.

Sofra, F., and Boger, D. V. (2002). Environmental rheology for waste minimisation in the minerals industry. *Chemical Engineering Journal, 86*(3), 319–330.

Soroka, I., 1994. Concrete in hot environments. Taylor and Francis, New York.

Stone, D. (2014, May). The evolution of paste for backfill. In Mine Fill 2014: Proceedings of the Eleventh International Symposium on Mining with Backfill (pp. 31-38). Australian Centre for Geomechanics.

Swaddiwudhipong, S., Chen, D., Zhang, M.H., 2002. Simulation of the exothermic process of Portland cement. Advance in Cement Research, 14(2): 61-69.

Takahashi, K., Bier, T. A., and Westphal, T. (2011). Effects of mixing energy on technological properties and hydration kinetics of grouting mortars. *Cement and Concrete Research, 41*(11), 1167–1176.

Theriault, J., Frostiak, J. and Welch, D. (2003) Surface disposal of paste tailings at the Bulyanhulu Gold Mine, Tanzania. Mining and the Environment III Conference, Sudbury 2003 – Mining and the Environment, Sudbury, Ontario, Canada

Torres, E., Lozano, A., Macías, F., Gomez-Arias, A., Castillo, J., and Ayora, C. (2018). Passive elimination of sulfate and metals from acid mine drainage using combined limestone and barium carbonate systems. *Journal of Cleaner Production*, *182*, 114–123. https://doi.org/10.1016/j.jclepro.2018.01.224

U.S. Geological Survey, 2016, Mineral commodity summaries 2016: U.S. Geological Survey, 202 p., http://dx.doi.org/10.3133/70140094.

Uusitalo, R., Seppanen, P., and Nieminin, P. (1993). The use of blast furnace slag as a binder. In *Symposium Presented at the Fifth International Symposium on Mining with Backfill* (pp. 169-172).

Vargas, F., and Lopez, M. (2018). Development of a new supplementary cementitious material from the activation of copper tailings: Mechanical performance and analysis of factors. *Journal of Cleaner Production*, *182*, 427–436. https://doi.org/10.1016/j.jclepro.2018.01.223

Vaughan D J, 2005. Minerals/Sulphides. In Encyclopedia of geology. Amsterdam: Elsevier, 574–586.

Vaughan, D. J., and Corkhill, C. L. (2017). Mineralogy of sulfides. *Elements (Quebec)*, *13*(2), 81–87. https://doi.org/10.2113/gselements.13.2.81

Watson, AH, Corser, PG, Garces Pardo, EE, Lopez Christian, TE and Vandekeybus, J. (2010). 'A comparison of alternative tailings disposal methods -the promises and realities', in R Jewell and AB Fourie (eds), *Mine Waste 2010: Proceedings of the First International Seminar on the Reduction of Risk in the Management of Tailings and Mine Waste*, Australian Centre for Geomechanics, Perth, pp. 499-514, https://doi.org/10.36487/ACG_rep/1008_41_Watson

Weaver, W. S., and Luka, R. (1970). Laboratory studies of cement-stabilized mine tailings. *Canadian Mining and Metallurgical Bulletin*, *63*(701), 988.

Welch, D. (2003) Advantages of Tailings Thickening and Paste Technology, Responding to Change – Issues and Trends in Tailings Management. Golder Associates.

Wong, I. Y. H., and Wong, D. S. H. (2013). Special adjuncts to treatment. Retina (5th ed.).

Wu, A., Ruan, Z., Shao, Y., Wang, J., Yin, S., Wang, S., and Li, C. (2019). Friction Losses of Cemented Unclassified Iron Tailings Slurry Based on Full-Scale Pipe-Loop Test. Australian Centre for Geomechanics, Perth, Australia. (pp. 571–578).

Xiao, B., Fall, M., and Roshani, A. (2021). Towards understanding the rheological properties of slag-cemented paste backfill. *International Journal of Mining, Reclamation and Environment, 35*(4), 268–290.

Xiapeng, P., Fall, M., and Haruna, S. (2019). Sulphate-induced changes of rheological properties of cemented paste backfill. *Mineral Engineering, 141*, 105849. https://doi.org/10.1016/j.mineng.2019.105849.

Xu, D.-M., Zhan, C.-L., Liu, H.-X., and Lin, H.-Z. (2019). A critical review on environmental implications, recycling strategies, and ecological remediation for mine tailings. *Environmental Science and Pollution Research International*, *26*(35), 35657–35669. https://doi.org/10.1007/s11356-019-06555-3

Xu, W., Wen, X., Wei, J., Xu, P., Zhang, B., Yu, Q., and Ma, H. (2018). Feasibility of kaolin tailing sand to be as an environmentally friendly alternative to river sand in construction applications. *Journal of Cleaner Production*, *205*, 1114–1126. https://doi.org/10.1016/j.jclepro.2018.09.119

Yang, L., Wang, H., Li, H., and Zhou, X. (2019). Effect of High Mixing Intensity on Rheological Properties of Cemented Paste Backfill. *Minerals, 9*(4), 240.

Yang, L., Wang, H., Wu, A., Li, H., Arlin Bruno, T., Zhou, X., and Wang, X. (2020). Effect of mixing time on hydration kinetics and mechanical property of cemented paste backfill. *Construction and Building Materials, 247*, 118516. https://doi.org/10.1016/j.conbuildmat.2020.118516.

Yilmaz, E., Belem, T., and Benzaazoua, M. (2014). Effects of curing and stress conditions on hydromechanical, geotechnical and geochemical properties of cemented paste backfill. *Engineering Geology*, *168*, 23–37. https://doi.org/10.1016/j.enggeo.2013.10.024

Yilmaz, E., Belem, T., Bussière, B., and Benzaazoua, M. (2011). Relationships between microstructural properties and compressive strength of consolidated and unconsolidated cemented paste backfills. *Cement and Concrete Composites*, *33*(6), 702–715. https://doi.org/10.1016/j.cemconcomp.2011.03.013

Yilmaz, E., Benzaazoua, M., Belem, T., and Bussière, B. (2009). Effect of curing under pressure on compressive strength development of cemented paste backfill. *Minerals Engineering*, *22*(9), 772–785. https://doi.org/10.1016/j.mineng.2009.02.002

Zhang, G., Yan, Y., Hu, Z., and Xiao, B. (2017). Investigation on preparation of pyrite tailings-based mineral admixture with photocatalytic activity. *Construction and Building Materials*, *138*, 26–34. https://doi.org/10.1016/j.conbuildmat.2017.01.134

Zhou, Q., and Beaudoin, J. J. (2003). Effect of applied hydrostatic stress on the hydration of Portland cement and C3S. *Advances in Cement Research*, *15*(1), 9–16. https://doi.org/10.1680/adcr.2003.15.1.9

CHAPTER THREE.

TECHNICAL PAPER I: FLOW CHARACTERISTICS OF PASTE TAILINGS IN SURFACE DISPOSAL: THE ROLE OF PYRITE CONTENT

Published in Env Science and Pollution Research International, 32(11), 6446-6467

Oyewale Miracle, Mamadou Fall and Ghirian Alireza

Department of Civil Engineering, University of Ottawa
800 King Edward Ave, Ottawa, ON, K1N 6N5, Canada.

3.1 ABSTRACT

The flow characteristics of paste tailings (PT), including uncemented and lightly cemented paste tailings (UPT/LCPT), are critical for pipeline transport and surface paste disposal. These properties, particularly yield stress and viscosity, may be significantly affected by the presence of sulfide minerals like pyrite in tailings from hard rock mines. Pyrite's oxidative capacity alters the chemistry of mixtures, impacting their rheological behaviour. However, comprehensive studies on the effects of pyrite on UPT/LCPT rheology are lacking, despite their importance for effective transport and disposal. This study experimentally assesses the influence of varying pyrite concentrations (0%, 5%, 15%, and 45%) on the rheological properties of UPT and LCPT, prepared with two binder types (PCI and Slag) and analyzed at room temperature (20 °C) over curing times (0, 20, 60, and 120 min). Key assessments included yield stress, viscosity, electrical conductivity, pH, zeta potential, and microstructural analysis. Results show that pyrite content substantially affects

the rheological properties of UPT and LCPT. The rheological properties of UPT increased as pyrite concentration rose, with yield stress and viscosity rising in the order of 5%, 15%, and 45% pyrite content. In LCPT mixtures, yield stress increased steadily over time with increasing pyrite content, while viscosity increased with pyrite content but decreased over time. The results also show that pyrite content causes microstructural and chemical changes in fresh LCPT, particularly, changes related to interparticle forces and inhibition of cement hydration. These findings provide valuable insights for optimizing tailings management and advancing environmentally sustainable designs of LCPTs and UPTs.

Keywords Uncemented paste tailings · Cemented paste backfill · Pyrite · Tailings · Rheology · Mine

3.2 INTRODUCTION

Over the years, the global mining industry has witnessed a paradigm shift in its environmental responsibility and sustainability approaches. As the quest for a sustainable future continues, the mining sector is more aware of the need to implement innovative practices that minimize ecological footprints, particularly in areas related to mine waste management. One such groundbreaking advancement is the development of paste tailings (PT) (Fall et al. 2005; Nasir and Fall 2008), a technique that has been implemented to address the problems of voluminous mine waste quantities and also aligns with the overall goal of achieving environmental sustainability in the mining sector.

Paste tailings are tailings that have undergone significant dewatering, such that they do not have critical flow velocity during pumping, exhibit no segregation upon deposition, and produce minimal bleed water upon discharge from a pipe (Dixon-Hardy and Engels 2007). Compared to other conventional tailings management methods (e.g., slurry tailings), PTs are more advantageous in terms of mechanical, economic, and environmental aspects. They can be used for backfilling underground mines in the form of cemented paste backfill (CPB) and/or for surface paste disposal (SPD) in the form of uncemented (UPT) or lightly cemented (LCPT) paste tailings (Tariq and Ernest 2013; Cincilla et al. 1997; Robinsky 1999; Aubertin et al. 2003; Kesimal et al. 2004; Aldhafeeri and Fall 2016; Bull and Fall 2020).

In SPD, paste tailings undergo thickening and filtration processes to yield a filter cake, with a water content by weight ranging between 15 and 25% and approximately 80–85% by weight solids contents (Ichrak et al. 2016). This method helps with water recycling and efficient management of excess water during deposition (Ichrak et al. 2016), thus reducing seepage and evaporation losses from the tailings storage area. Ensuring sustainable water management practices in mining operations has become increasingly crucial. The potential to recover significant water quantities directly at the PT plant, facilitated by thickeners, mitigates the challenges linked with transporting

and storing water at either the tailings site or in reservoirs (Fourie 2003). This not only addresses environmental concerns, such as seepage and process water spillage but also greatly reduces the risk of water acting as a pathway for tailings flows, particularly in the event of embankment breaches. Moreover, utilizing PT for SPD minimizes the requirement for costly maintenance of impoundment dikes and dams, as well as post-closure site rehabilitation (Ichrak et al. 2016). Additionally, because of their substantially lower water content relative to conventional slurry tailings, surface PT structures show enhanced geomechanical stability under both static and dynamic loads compared to traditional slurry tailings. In other words, these surface PT structures are less susceptible to major geotechnical failures (e.g., static and dynamic liquefaction), thereby lessening the risks associated with catastrophic dam failures linked to surface slurry tailings facilities.

However, despite recognizing their improved geomechanical stability, significant concerns persist regarding the environmental impact and performance of these surface PT structures. Specifically, there are apprehensions regarding their potential to generate Acid Rock Drainage (ARD), release contaminants into the environment (leachability of contaminants from PT), and produce wind-blown tailings dust. For example, PT can contain a significant quantity of sulfide minerals. Iron sulfide minerals like pyrite (FeS_2) and pyrrhotite (Fe1-XS: x = 0–0.125) are one of the most hazardous types of sulfide minerals found in mine tailings (Dold 2014; Öhlander et al. 2012). When exposed to air, these sulfide minerals react with oxygen and undergo an oxidation process. This process reduces the pH of the surrounding environment through the dissolution of various heavy metals or metalloids, leading to the acidification of nearby waters (Ichrak et al. 2016; Marcus 1997). This phenomenon is commonly known as ARD. Therefore, if pyrite- bearing tailings are not managed appropriately during SPD, they are prone to generating ARD, which is characterized by high acidity with a low pH (< pH 6), elevated sulfate levels (> 1000 mg L^{-1}) and mine drainage-rich in metals, such as Cd, Co, Cr, Cu, Fe, Ni, Pb, and Zn (INAP 2009). This pyrite-containing

leachate may further spread to nearby groundwater and/or surface water, propagating into the surrounding biosphere, chemosphere, and hydrosphere. This may result in damage to plants, organisms, animals, and humans (Nason et al. 2013). To address these challenges and mitigate environmental risks, the introduction of small amounts of binder (e.g., up to 2% binder) into paste-tailing mixtures has been proposed and implemented to create lightly cemented PT (Deschamps et al. 2011). Incorporating a suitable binder serves to immobilize contaminants within the tailings, improve the mechanical stability of surface PT structures, reduce the potential acid generation, minimize the generation of airborne dust from the tailings, and significantly decrease the pore structure of the tailings, thereby limiting the release of substances from the tailings into the environment.

To gain deeper insights and advance PT technology, researchers have continually investigated the main performance characteristics of PT. Among these characteristics, rheological properties stand out as crucial factors governing the flowability or transportability of fresh PT. It is imperative for PT to possess satisfactory rheological properties to facilitate its transportation from the PT plant to the deposition site (Fall et al. 2010). These rheological properties, including yield stress (the lowest shear stress needed to start flow (Simon and Grabinsky 2013)) and viscosity (the measure of a fluid's resistance to shear deformation or its opposition to flow (Akbar et al. 2009)), could be strongly altered by the presence of sulfide minerals (e.g., pyrite, pyrrhotite) in the tailings and/or by the ability of the sulfide minerals to oxidize. Given that tailings generated from hard rock mines often contain significant amounts of sulfide minerals, particularly pyrite, understanding the impact of these minerals on the flow properties of PT, whether uncemented or lightly cemented, is crucial for designing paste tailings (PT) with optimal flowability. This knowledge is essential for the effective implementation of PT technology in SPD as inadequate flowability can result in pipeline clogging which has significant financial ramifications for the mine. Therefore, investigating the impact of sulfide minerals on PT rheology becomes imperative.

However, in the past decade, research studies on PTs there is a paucity of studies on the rheological characteristics of uncemented paste tailings (Kwak et al. 2005; Huynh et al. 2006), and no research has been conducted on the rheological behaviour of lightly cemented PT. Many studies have also focused on studying how numerous factors like chemical functional groups, pore volume, pore fluid pH, and solid particle surface potential affect the flow properties of paste tailings (Goudoulas et al. 2003; Huynh et al. 2006). Some of these investigations, including the work by Kwak et al. (2005), utilized vane geometry to assess how varying water content influences the rheological behavior of mine tailings, drawing com- comparisons with kaolin clay. They concluded that the flow behaviour or ability of PT is a function of its water content. Huynh et al. (2006), who examined the effect of polymer addition on the rheology of dewatered tailings, found that these polymers are effective in lowering the yield stress of concentrated plant tailings. The earlier studies on the rheological behaviour of PT have significantly enhanced our understanding of PT's flow properties.

Despite these significant findings, previous studies have overlooked investigating the impact of sulfide mineral content, notably pyrite, which is prevalent in hard rock mine tailings, on the rheological characteristics of uncemented or lightly cemented PT. This represents a critical gap in the literature that needs to be addressed. To fill this void, this study seeks to experimentally examine the impact of pyrite content of varying pyrite content, curing durations, and binder types on the rheological characteristics of lightly cemented (LCPT) and uncemented (UPT) paste tailings for SPD. (Koohestani et al. 2016; Yılmaz et al. 2014) have focused majorly on their mechanical (Yin et al. 2012; Cui and Fall 2016; Fahey et al. 2011) and environmental (Kwak et al. 2005; Aldhafeeri and Fall 2017; Adiguzel and Bascetin 2019; Xiapeng et al. 2019) properties or behaviour. Only limited studies examined factors influencing the flow behaviour or rheological characteristics of PT (Aldhafeeri and Fall 2017). Moreover, the existing research on the rheological characteristics of PT

largely focused on cemented paste tailings or cemented paste backfill (CPB) used for backfilling in underground mining operations (Ouattara et al. 2017; Bian et al. 2021); Xiapeng et al. 2019). These investigations have concluded that the rheological properties of CPB are time-dependent and influenced by various factors, including temperature, sulfate content, mixing duration, and fiber content. However, there is a paucity of studies on the rheological characteristics of uncemented paste tailings (Kwak et al. 2005; Huynh et al. 2006), and no research has been conducted on the rheological behaviour of lightly cemented PT. Many studies have also focused on studying how numerous factors like chemical functional groups, pore volume, pore fluid pH, and solid particle surface potential affect the flow properties of paste tailings (Goudoulas et al. 2003; Huynh et al. 2006). Some of these investigations, including the work by Kwak et al. (2005), utilized vane geometry to assess how varying water content influences the rheological behavior of mine tailings, drawing comparisons with kaolin clay. They concluded that the flow behavior or ability of PT is a function of its water content. Huynh et al. (2006), who examined the effect of polymer addition on the rheology of dewatered tailings, found that these polymers are effective in lowering the yield stress of concentrated plant tailings. The earlier studies on the rheological behaviour of PT have significantly enhanced our understanding of PT's flow properties.

Despite these significant findings, previous studies have overlooked investigating the impact of sulfide mineral content, notably pyrite, which is prevalent in hard rock mine tailings, on the rheological characteristics of uncemented or lightly cemented PT. This represents a critical gap in the literature that needs to be addressed. To fill this void, this study seeks to experimentally examine the impact of pyrite content of varying pyrite content, curing durations, and binder types on the rheological characteristics of lightly cemented (LCPT) and uncemented (UPT) paste tailings for SPD.

3.3 EXPERIMENTAL PROGRAM

The experimental plan aimed to investigate several key factors: (i) The effect of varying pyrite content (0%, 5%, 15%, 45%) on both the yield stress and viscosity of lightly cemented and uncemented PT. (ii) The influence of different binder types on the yield stress and viscosity of pyrite-containing PT. (iii) The time-dependent changes in yield stress and viscosity of lightly cemented and uncemented PT. (iv) The evolution of pH, zeta potential, microstructure, and electrical conductivity in both cemented and lightly uncemented pyrite-bearing PT.

3.3.1 MATERIALS USED

3.3.1.1 TAILINGS

In this study, high-purity synthetic silica tailings (ST), produced by U.S. Silica Co., were utilized. These STs, classified as medium tailings according to Landriault (1995), consist of 99.8% quartz, which is a dominant mineral commonly found in Canadian hardrock mines. STs were chosen as a replacement for natural tailings due to their particle size distribution (PSD) closely resembling the average grain size distribution of tailings from nine different Canadian mining sites, as depicted in Fig. 1, as well as due to the fact they are essentially made of quartz. Since STs are primarily made up of quartz, they serve as a non-reactive and non-acid-generating tailings material. This reduces the uncertainty associated with natural tailings, which often contain a variety of reactive chemical elements and sulfide minerals that can oxidize and produce sulfates when exposed to water and oxygen. Such chemical interactions could interfere with cement hydration and compromise the accuracy of the results (Fall et al. 2010). The physical and mineralogical char- characteristics of the STs are presented in Tables 1 and 2, respectively.

Table 1: Physical properties of ST.

ELEMENT	G_s(µm)	D_{10}(µm)	D_{30}(µm)	D_{50}(µm)	D_{60}(µm)
ST	2.7	1.9	9.0	22.5	31.5
Average of 9 types of tailings	-	1.8	9.1	20.0	30.8

Gs: specific gravity; Ss: specific surface area

Table 2: The mineral composition of ST

TAILINGS (wt.%)	MINERAL											
	Quartz	Albite	Dolomite	Calcite	Chlorite	Magnetite	Pyrite	Talc	Pyrrhotite	Spinel	Others	Total
ST	99.8	-	-	-	-	-	-	-	-	-	0.2	100

ST: Silica tailings; wt.: weight.

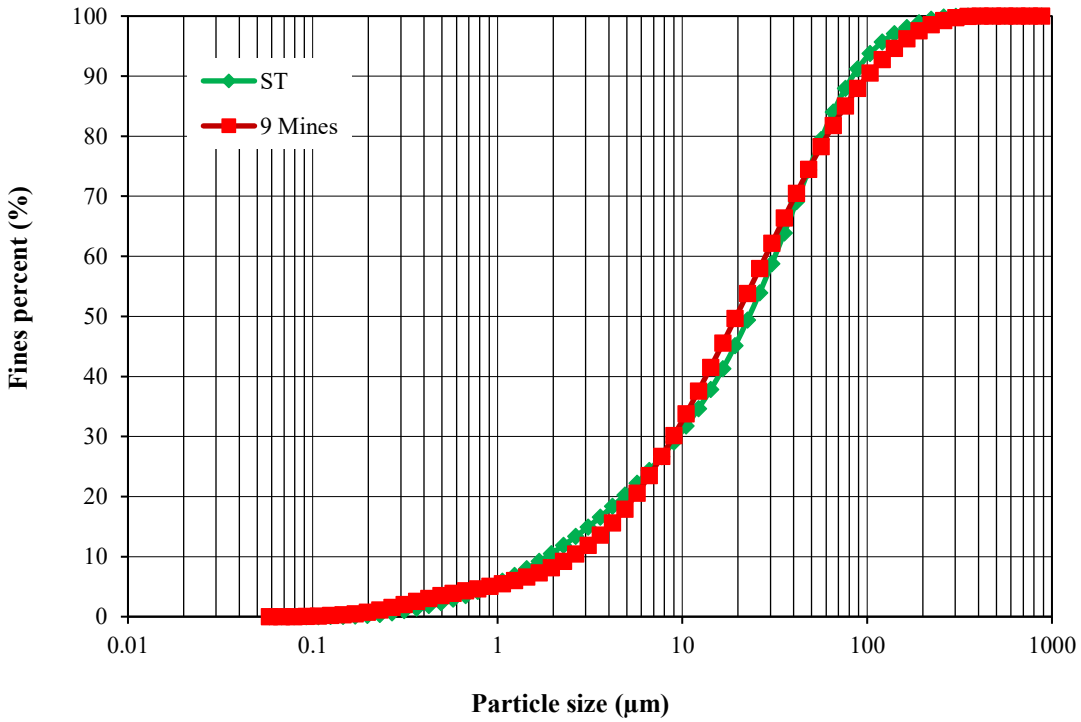

Figure 1 Particle size distribution of ST utilized in this study, along with the average particle size distribution of tailings from nine Canadian mines

3.3.1.2 BINDER

In this research, Type I Portland cement (PC), the most widely used binder in PT mixtures, was selected as the main binding material. Additionally, granulated ground blast furnace slag (SA) was included in some LCPT mixtures as a partial replacement for PC. The use of blended binders was motivated by economic considerations, as PC is relatively expensive. Furthermore, substituting part of the PC with SA helps reduce the carbon footprint of LCPT technology since the production of PC emits significantly more greenhouse gases compared to slag. These combinations of binders are referred to as SG for mixtures containing both PC and slag and PC-only for mixtures composed entirely of Portland cement. The blending ratio of PC and slag used in this study was 50:50 by weight. The physical and chemical characteristics of both PC and slag are provided in Table 3.

Table 3 Physical and chemical composition of PC and SG

	Na_2O	MgO	Al_2O_3	SiO_2	K_2O	CaO	TiO_2	MnO	Fe_2O_3	LOI	Relative density	Specific surface area (cm^2/g)
PCI	0.341	2.577	4.808	20.375	0.962	62.700	0.225	0.054	3.609	2.162	3.2	1300
Slag	0.284	11.782	10.595	35.572	0.478	39.212	0.467	0.298	0.621	0.388	2.8	2100

3.3.1.3 PYRITE AND MIXING WATER

In this study, pyrite powder (FeS2, Molecular Weight = 119.98) sourced from Washington Mills North Grafton, Inc. was utilized. The particle size of this pyrite powder is comparable to that of pyrite minerals typically present in natural tailings. The pyrite powder was combined with ST, PC, and SG to create three distinct types of pyrite-containing tailings mixtures (PT-ST, LCPT-ST-PC, and LCPT-ST-SG), with pyrite concentrations of 0%, 5%, 15%, and 45% by weight. The physical properties of the pyrite used are detailed in Table 4. Tap water was employed

for all the tailings and binder mixtures in this research. A consistent water-to-binder ratio of 32 was applied to prepare all samples.

Table 4: Physical and chemical properties of pyrite.

BULK DENSITY (g/cm^3)	DENSITY AT 20 °C (g/cm^3)	SP. GRAVITY	PH	MELTING POINT
2.35	4.7	4.6	4.0-6.0	1193

Sp: specific. gravity

3.3.2 SAMPLE PREPARATION AND MIXING RATIOS

The different cemented and uncemented mix samples (PT- ST, LCPT-ST-PC; LCPT-ST-SG) investigated in this study were prepared following the experimental plan outlined in Table 5. Silica tailings, pyrite, and binders were first weighed into a mechanical mixing bowl using a scientific weighing scale, then the powders were subsequently mixed for 5 min using a mechanical mixer at a constant mixing speed (Speed 2) under room temperature. Then the pre-measured quantity of tap water was added to the mechanical mixer containing the powders. The mixtures were subsequently blended for another 5 min to achieve a uniform consistency. Following the mixing procedure, the paste was poured into plastic cylindrical molds measuring 10 cm in diameter and 20 cm in height. The samples were then cured in line with the experimental schedule outlined in Table 5. The choice of plastic cylinder molds aimed to replicate the sizes of pipes used in on-field PT practice (Haiqiang et al. 2016). Other tests or experiments, including microstructural analysis, pH, zeta potential measurements, and monitoring of the electrical conductivity were also carried out on the mix samples at room temperature. For these analyses, moulds measuring 5 cm in diameter and 10 cm in height were utilized, and electrical conductivity was tracked over a period of 6 h.

Table 5 Experimental plan for rheological tests

SAMPLE NAME	TAILINGS TYPE	BINDER TYPE	BINDER CONTENT (vl%)	PYRITE CONTENT (w%)	VOL. W/VOL. B RATIO	CURING TIME (min)
			UNCEMENTED PASTE TAILINGS			
PT-ST-0	ST + PY	-	0	0	0	0
PT-ST-5	ST + PY	-	0	5	0	0
PT-ST-15	ST + PY	-	0	15	0	0
PT-ST-45	ST + PY	-	0	45	0	0
PT-PT-45	ST + PY	-	0	45	0	0
			LIGHTLY CEMENTED PASTE TAILINGS			
LCPT-ST-PC-0	ST + PY	PCI	1.0	0	32	0, 20, 60, 120
LCPT-ST-PC-5	ST + PY	PCI	1.0	5	32	0, 20, 60, 120
LCPT-ST-PC-15	ST + PY	PCI	1.0	15	32	0, 20, 60, 120
LCPT-ST-PC-45	ST + PY	PCI	1.0	45	32	0, 20, 60, 120
LCPT-PT-PC-45	ST + PY	PCI	1.0	45	32	0, 20, 60, 120
LCPT-ST-SG-0	ST + PY	PCI/SG(50/50)	1.0	0	32	0, 20, 60, 120
LCPT-ST-SG-45	ST + PY	PCI/SG(50/50)	1.0	45	32	0, 20, 60, 120

V%- Volume percentage; W%- Weight percentage; Vol.w/Vol.b- Volume of binder/Volume of water ratio; SG: slag; PY: pyrite; ST: silica tailings.

3.3.3 TEST PROCEDURES

3.3.3.1 VISCOSITY MEASUREMENT

Viscosity measurements for all sample mixtures were performed using a Brookfield digital viscometer (DV-E model) from Brookfield Engineering Laboratories Inc. This instrument determines the viscosity of fluids at specific shear rates by rotating a spindle at a constant speed, controlled by a calibrated spring. The device measures the resistance (viscous drag) of the fluid against the spindle using a rotary transducer, which generates a torque signal that is interpreted as spring deflection (Brookfield 2016). The selection of spindles depends on the viscosity range of the material being tested. In this study, an RV6 spindle was used in accordance with the operating guidelines. For each sample, the spindle was carefully submerged in the fluid to prevent the introduction of air bubbles. The viscometer was then activated, and readings were taken after the values had stabilized, with measurements recorded at a speed of 50 rpm for a duration of 1 min. Each experiment was conducted at least twice, with the average value considered for analysis.

3.3.3.2 YIELD STRESS

The yield stress measurements were conducted using the Wykeham-Farrance laboratory vane shear device. While this equipment is primarily designed for determining the shear strength of cohesive soils, it can also be adapted to measure the yield stress of non-Newtonian fluids (Keentok 1982; Nguyen and Boger 1985). The vane consists of four blades, each measuring 2.5 cm in diameter and 2.5 cm in height, and it was carefully placed into the center of the mixture samples. Before taking any measurements, the sample was allowed to rest for 30 s to minimize any disturbances caused by the vane insertion (Saebimoghaddam 2005). Afterwards, the motor was activated, rotating the vane steadily at a fixed speed of 0.18 rpm. The highest torque at which the material failed under shear was recorded, and the corresponding yield stress was calculated according to the guidelines specified in ASTM D4648/D4648M-16. To ensure the reliability of the results, each test was performed at least twice.

3.3.3.3 ELECTRICAL CONDUCTIVITY MONITORING

To further understand the reaction mechanisms driving changes in the rheological behaviour of LCPT samples, a TEROS-12 sensor, with a measurement precision of ± 5, was employed to monitor the electrical conductivity (EC) of each specimen (MMM Tech, n.d). The evolution of EC in the samples provides valuable information about ion movement, which results from chemical reactions and the water content within the LCPT. This property serves as an indicator for tracking the progress of cement hydration (Tamás et al. 1987; McCarter and Curran 1984; Aschan 1966) and for observing structural changes in hydrating cementitious materials (Courard et al. 2014). In this study, EC measurements were taken using the TEROS-12 sensor, which determines EC by passing an alternating electrical current between two electrodes and measuring the resulting resistance. The sensor was inserted into a plastic cylindrical container (10 cm in diameter and 20 cm in height)

holding the LCPT, with readings recorded every minute for a period of 6 h. All data was then collected using an Em50 data logger manufactured by Decagon Devices, Inc.

3.3.3.4 pH AND ZETA POTENTIAL MEASUREMENTS

The flow behavior of suspensions is heavily influenced by the surface chemistry of the particles, a fact established by various researchers, including Leong and Boger (1990), Bradley et al. (1991), and Johnson et al. (2000). To assess the surface chemical characteristics of particles in the samples for this research, pH and zeta potential measurements were taken from selected UPT and LCPT samples. The pH levels were recorded using an Oakton pH 6 + meter, which has an accuracy of ± 0.01 (Oakton, n.d). Each pH measurement was taken at least twice to ensure the precision of the readings, and the average values were reported. The zeta potential (ZP) was measured with a Malvern Zetasizer Nano series instrument, which determines the electrophoretic mobility of particles in suspension through phase analysis light scattering (PALS). The zeta potential of the particles is then calculated using the Henry equation (Clogston and Patri 2011). For each sample, the zeta potential measurement was repeated a minimum of three times to guarantee the reliability of the results.

3.3.3.5 MICROSTRUCTURAL ANALYSIS

To gain a deeper insight into the microstructural characteristics and the progression of binder hydration in the tested materials, as well as their influence on the rheological behaviour of the paste tailings, thermal gravimetric analysis (TG), differential thermal gravimetry (DTG), and x-ray diffraction (XRD) were performed on selected cement paste samples of LCPT. These analyses help to evaluate the microstructural attributes and transformations occurring within the LCPT. The samples were first prepared and cured for periods ranging from 20 to 60 min, after which they were

oven-dried at 45 °C for 4 days to remove free water. Once mass stabilization was achieved, the samples were ground into powder for microstructural testing.

3.4 RESULTS AND DISCUSSION

3.4.1 EFFECT OF PYRITE ON THE RHEOLOGICAL PROPERTIES OF UNCEMENTED PASTE TAILINGS

The variation of initial yield stress and viscosity in uncemented paste tailings (UPT) with different pyrite contents is presented in Figure 2. From the figure, it is evident that pyrite content significantly impacts both the yield stress and viscosity of UPT.

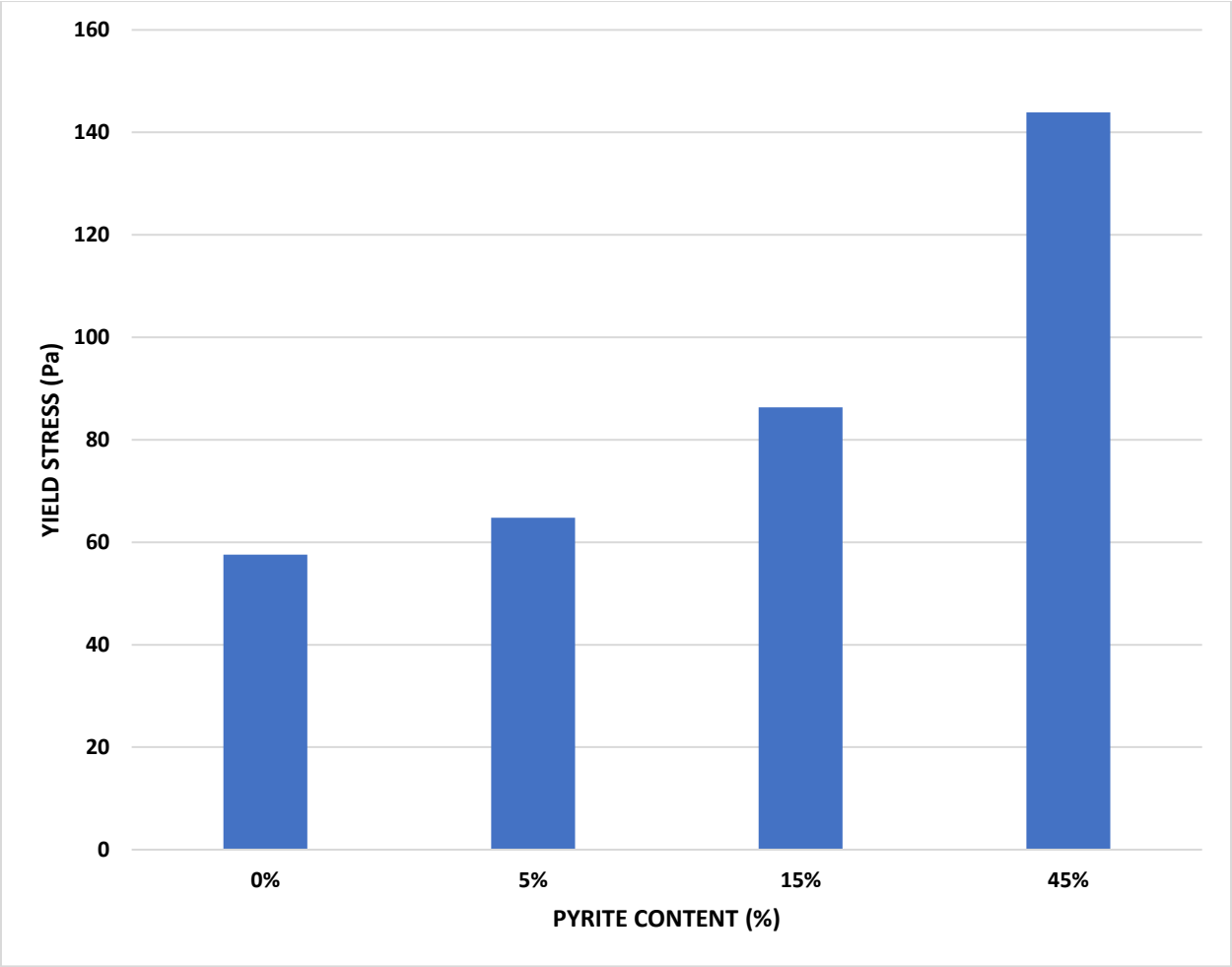

A) Yield stress.

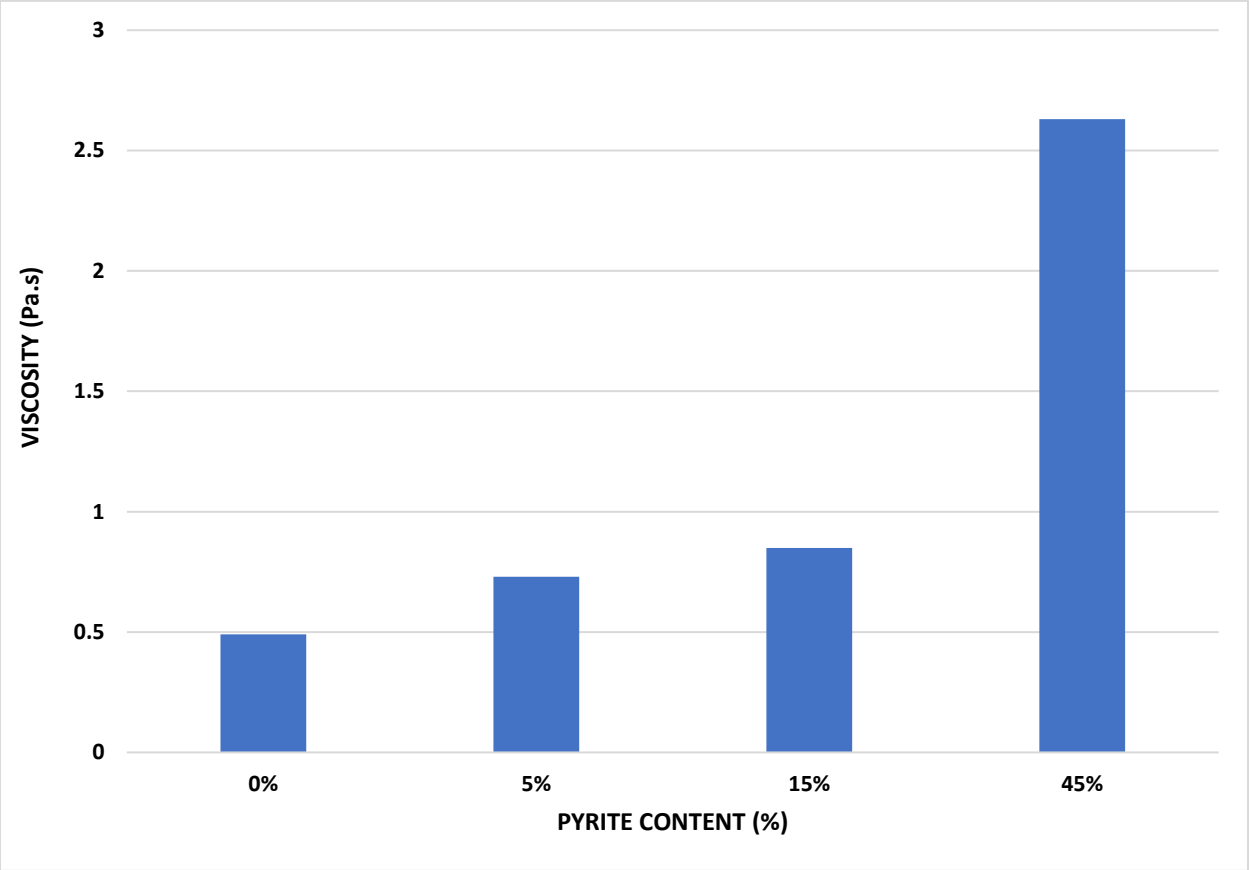

B) Viscosity

Figure 2: Impact of pyrite content on yield stress (a) and viscosity (b) of uncemented paste tailings (UPT).

According to Fig. 2, the yield stress of UPT simultaneously rises as the pyrite content increases (Fig. 2a). A comparable pattern is also noticed in the viscosity results (Fig. 2b), as viscosity is also seen to increase significantly as pyrite content increases. The rise in both yield stress and viscosity is seen to follow the order of 5% < 15% < 45% pyrite content. Hence, the samples containing 45% pyrite exhibited the most significant rise in yield stress and viscosity when compared to those with lower pyrite concentrations. The increase in yield stress and viscosity could be

attributed to several factors, including the particle packing and size distribution of pyrite within the paste mixture (Ding et al. 2007). Pyrite particles in this mixture are denser (specific gravity of pyrite = 4.6; Table 4) than other constituents of the mixture (specific gravity of the quartz = 2.7; Table 1), so an increase in pyrite content influences the overall arrangement of particles promoting a more tightly packed structure. As a result of this, the denser packing induced by increased pyrite content will elevate the resistance to flow within the paste mixture, thereby altering and increasing the yield stress (from 57.5 to 143.9 Pa) and viscosity (from 0.49 to 2.61 Pa.s) of the mixture. Furthermore, the size distribution of pyrite, particularly fine particles (which was used in this study), could be considered an additional factor responsible for the increased rheological properties (yield stress and viscosity). This is because finer particles can fill void spaces between larger particles in the mixture, thereby promoting a more closely packed system. This explanation is corroborated by Ding et al. (2007) research study, where the effect of solid concentration on the rheological behaviour of pyrite-heptane slurry was studied. The authors concluded that as the solid concentration of pyrite rises from 64 wt% to 79 wt%, the rheological behavior shifts from a Bingham characteristic to a pseudoplastic one with a higher yield stress. The authors further explained that at lower solid concentrations (below 64 wt%), the slurry exhibited a Bingham flow, possibly because the pyrite particles are widely spaced and not influenced by attractive forces like van der Waals forces, allowing them to move independently. While at higher solid concentration (75 wt%), the slurry had a higher yield stress and was more resistant to flow because the particles were more tightly packed. In addition, the authors also highlighted that as the pyrite particle size decreased to finer particles with increasing concentration, the slurry became more viscous.

Another critical factor contributing to the increase in yield stress and viscosity would be the chemical oxidation of the pyrite minerals. Pyrite oxidation creates acidic conditions and the formation of compounds such as sulfate ions (SO_4^{2-}) (Kumari et al. 2010). These conditions and

compounds can alter the chemical and physical properties of the UPT mixture (Ding and Pacek 2008; He et al. 2006; Li et al. 2006), thereby contributing to changes in pH, ionic strength, and overall reactivity of the paste mixture, as demonstrated by pH and zeta potential experimental results given in Figs. 3 and 4, respectively.

According to the time-dependent graphical illustration given in Fig. 3, it is evident that the pH value decreases in more acidic conditions as pyrite content increases. The UPT sample labeled PT-ST-45% is seen to be more acidic compared to other sample mixtures, this is because it contains the highest percentage of pyrite. Also, the graph indicates that the rate of pyrite oxidation is time-dependent, therefore as time progresses, the samples containing pyrite (e.g., the pH value of PT-ST-45% decreases from 2.99 to 2.62) undergo further oxidation, leading to more acidic conditions and a decrease in pH.

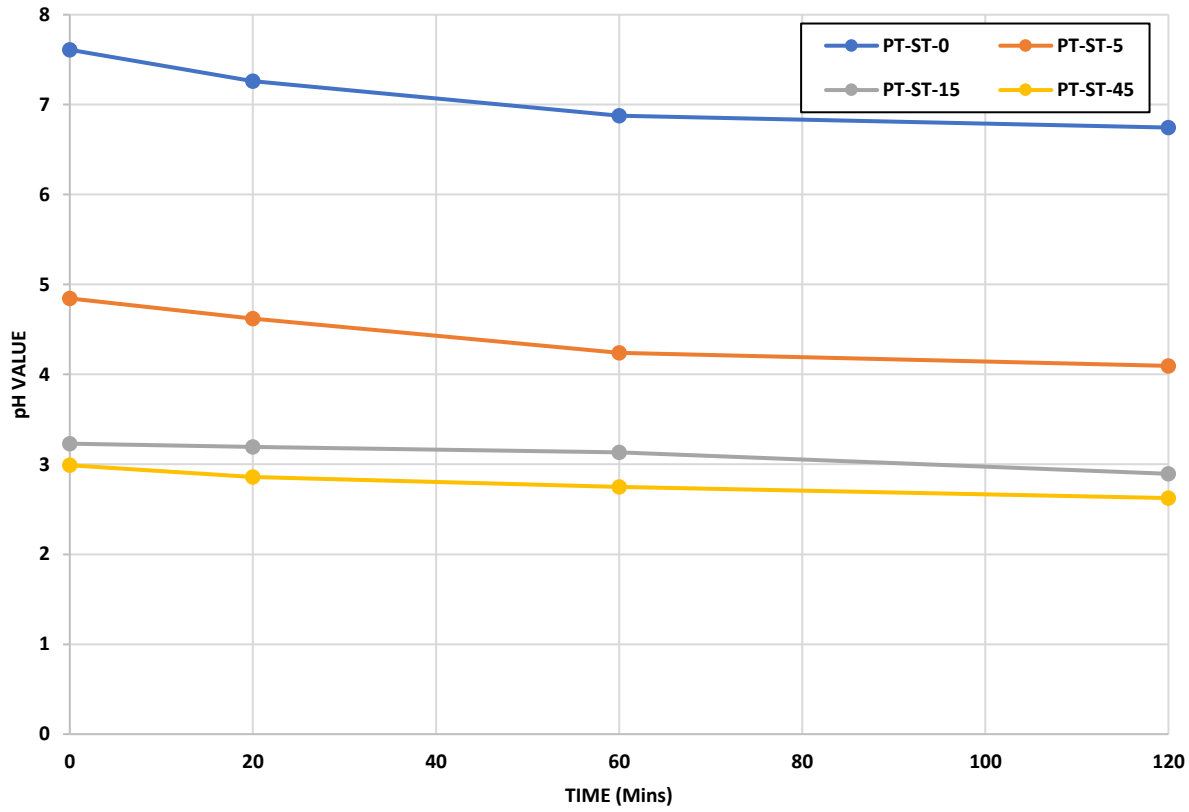

Figure 3: pH of uncemented paste tailings (UPT)

The zeta potential results, which reflect the level of particle surface charge (Huynh et al. 2006; Elakneswaran et al. 2009; Hunter 2013; Haiqiang et al. 2016), are shown in Fig. 4. Typically, a higher zeta potential indicates that more ions adhere to the particle surfaces. Additionally, zeta potential values are directly linked to the intensity of the electrostatic repulsive forces between particles. In particular, a strongly negative or positive zeta potential usually generates strong repulsive forces, potentially leading to a decrease in particle cohesion (Plank and Hirsch 2007; Zingg et al. 2008). The data presented in Fig. 4 indicate that the absolute zeta potential drops from 30 mV in samples without pyrite to 18.35 mV in samples containing 45% pyrite. This means that as the pyrite concentration increases, the absolute zeta potential decreases.

This is an indication that increased pyrite content leads to reduced repulsive forces between the UPT particles, which promotes possible flocculation, thereby increasing the viscosity (Divet and Randriambololona 1998; Zingg et al. 2008; Elakneswaran et al. 2009). Therefore, these alterations in pH and zeta potential can enhance cohesion and particle interactions, thereby leading to increased yield stress (Xiapeng et al. 2019; Nachbaur et al. 1998), which may also affect the fluidity of UPT, causing an increased viscosity.

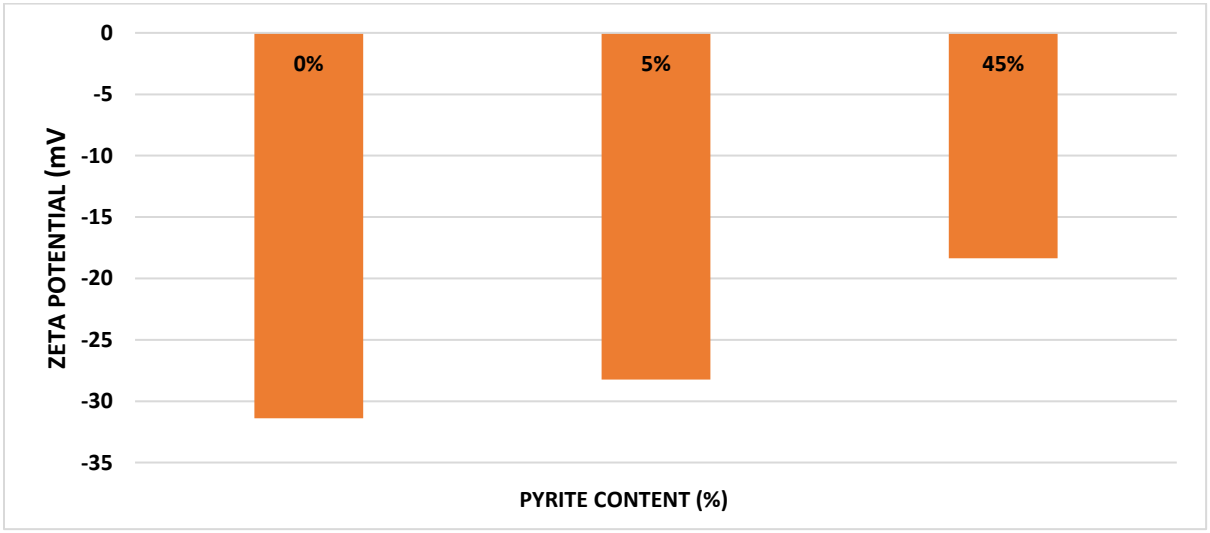

Figure 4: Zeta potential of UPT samples with different pyrite content

3.4.2 EFFECT OF PYRITE ON THE RHEOLOGICAL PROPERTIES OF LIGHTLY CEMENTED PASTE TAILINGS

To assess the effect of curing duration and pyrite contents on the yield stress of LCPT, a time-dependent graph was generated, plotting yield stress against curing times of 0, 20, 60, and 120 min, as illustrated in Fig. 5. The graph's results indicate that both the duration of curing and the pyrite content have a notable impact on the yield stress across all LCPT mixtures. Figure 5 demonstrates that the yield stress of LCPT samples increases consistently with longer curing times, regardless of the pyrite content. This rise over time is attributed to the formation of additional cement hydration products as curing progresses (Jiang and Fall 2017). Cement hydration progress is generally associated with longer curing time, leading to the generation of a greater volume of hydration products in LCPT. This would enhance the interparticle frictional resistance of the LCPT mixture, causing a corresponding rise in yield stress (Jiang and Fall 2017). In addition, hydration products like calcium silicate (C-S–H) enhance cohesion among particles, thereby leading to high-yield stress (Yin et al. 2012).

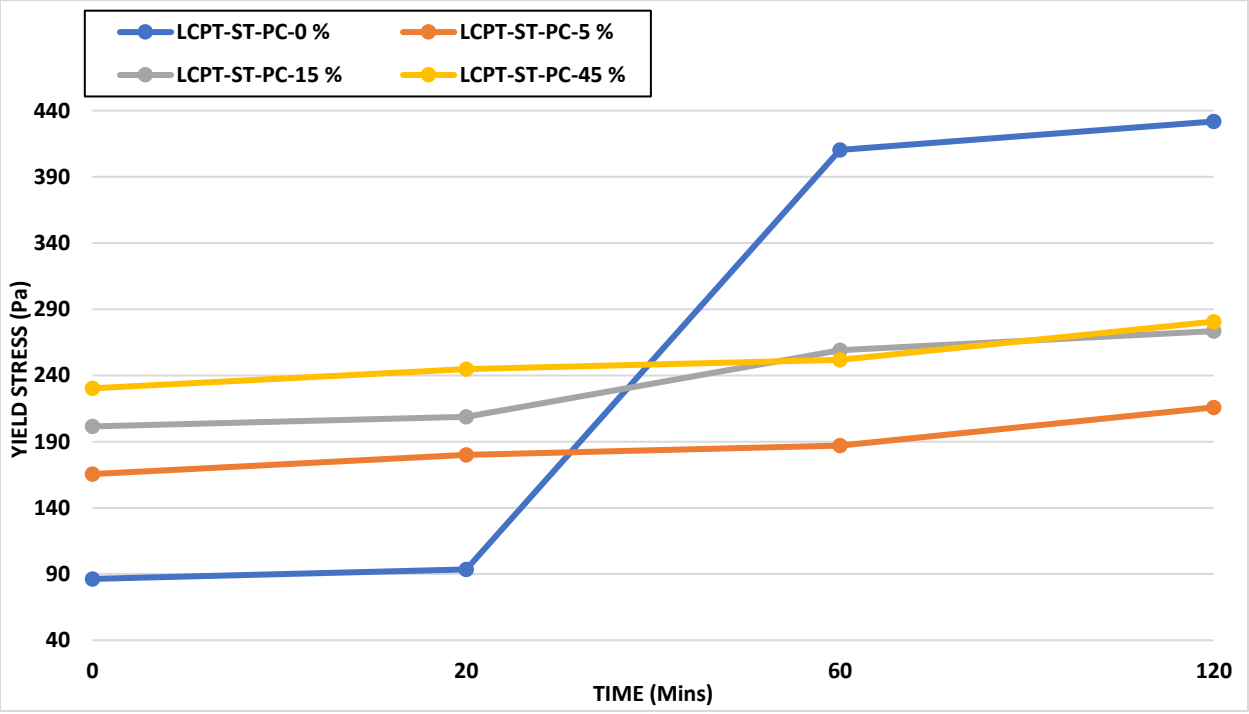

Figure 5: Time-dependent yield stress evolution of LCPT containing different pyrite content.

Furthermore, a portion of the available free water is utilized in the hydration reaction, causing a reduction in the thickness of the water film surrounding the solid particles. Consequently, this leads to an increase in the yield stress for samples with more hydration products (Zhou and Fall 2022). The increase in hydration products (e.g., C-S–H, ettringite, CH) over an extended curing period is validated by the findings from TG/ DTG analysis. Figure 6 illustrates the outcomes of DT/DTG analyses conducted on LCPT-5% at 20 and 60 min. The peak observed between 60 °C and 180 °C corresponds to the dehydration process of hydration compounds like C-S–H, carboaluminates, and ettringite, while the temperature peak around 400–480 °C indicates the dehydroxylation of CH (Rocha et al. 2015). A comparison of the plotted TG/DTG results cured for 20 and 60 min shows a more pronounced peak in the 60-min sample compared to the 20-min sample. This outcome indicates that a greater amount of hydration products forms in samples subjected to longer curing periods compared to those cured for a shorter duration.

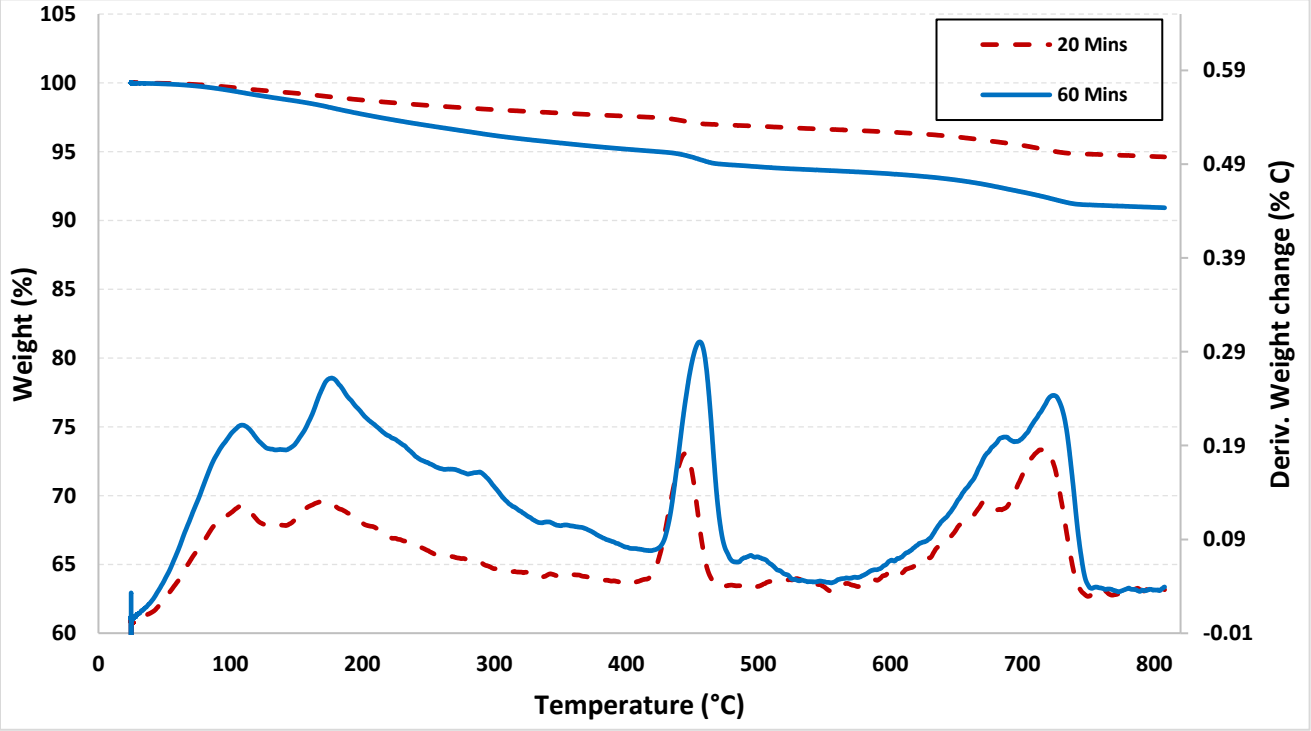

Figure 6: TG/DTG analysis of LCPT cured for 20 and 60 mins

Aside from curing time, Fig. 5 also suggests that the time-dependent increase in yield stress is also affected by the presence or absence of pyrite in the LCPT mixtures. The yield stress of the LCPT without any pyrite (LCPT-ST- PC-0%) was seen to increase drastically from 86 to 431 Pa within 2 h (from time = 0 to time = 2 h), which corresponds to an increase of about 500%. In contrast, all the samples containing pyrite (LCPT 5%, 15%, and 45%) recorded much lower final yield stress values compared to samples without pyrite. Particularly, the sample with the highest pyrite content (LCPT-45%) was seen to increase from 230 to 280 Pa within 2 h (from time = 0 to time = 2 h), which is about a 30% increase within the same time interval as samples without pyrite content (LCPT 0%). The low percentage increase in yield stress exhibited by pyrite-containing samples can be attributed to cement hydration inhibition caused by exposure to pyrite and its byproducts like sulfate. Earlier investigations (Lawrence 1990; Pokharel and Fall 2013) have shown that sulfate ions generated during the oxidation of pyrite can hinder the hydration process in cemented tailings mate- rials. This inhibition reduces the production of hydration products and is attributed to the formation of ettringite, a hydrous mineral resulting from the reaction between sulfate and tricalcium aluminate (C_3A). It is well-established that when C_3A is dissolved in solution, it readily reacts with sulfate ions to form ettringite. The ettringite then subsequently coats unhydrated cement particles' surfaces, blocking additional reactions (Pye and Schiavon 1989; Prince et al. 2003; Lawrence 1990; Zingg et al. 2009; Pokharel and Fall 2013). The formation of less hydration products leads to a decrease in interparticle frictional resistance and a less cohesive structure, consequently lowering the yield stresses of LCPT-containing pyrite. The formation of a greater volume of ettringite in samples with a higher pyrite content is confirmed by the results of XRD analyses carried out on 2 h cured LCPT cement pastes without pyrite content (Fig. 7a) and with pyrite content (Fig. 7b). The XRD results (Fig. 7a, b) reveal that the 20% pyrite sample contains more ettringite compared to the 5% pyrite, as shown by the higher intensity of the ettringite peak in the 20% pyrite. For example, the ettringite peaks observed

between 14–15 (2θ) recorded an intensity of 418 cps for the 20% sample while the 5% sample recorded an intensity of 319 cps. This was the same for peaks between 20–25 (2θ) and 40–45 (2θ). Furthermore, the XRD results show that the 20% pyrite sample contains more unreacted C_2S and C_3S than the 5% pyrite sample, correlating with the inhibition of cement hydration by the presence of more sulfate ions in the 20% pyrite sample.

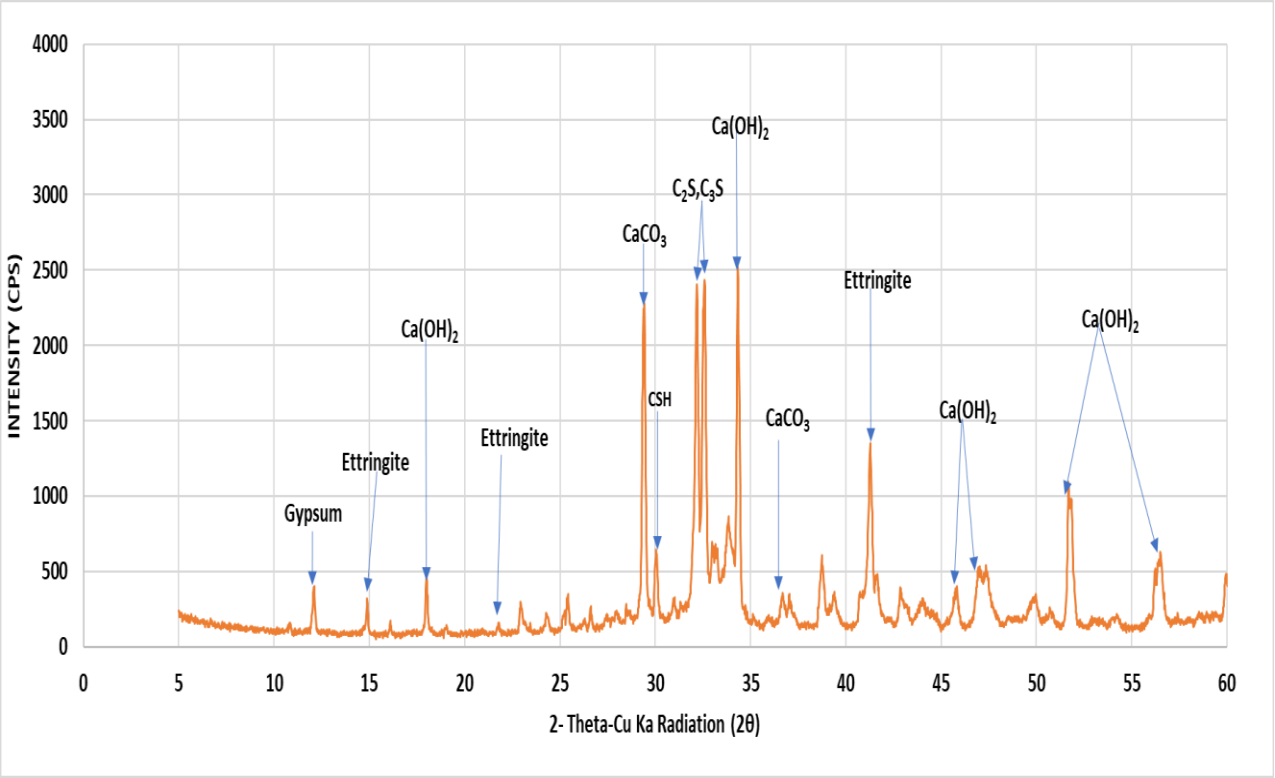

a) 5%

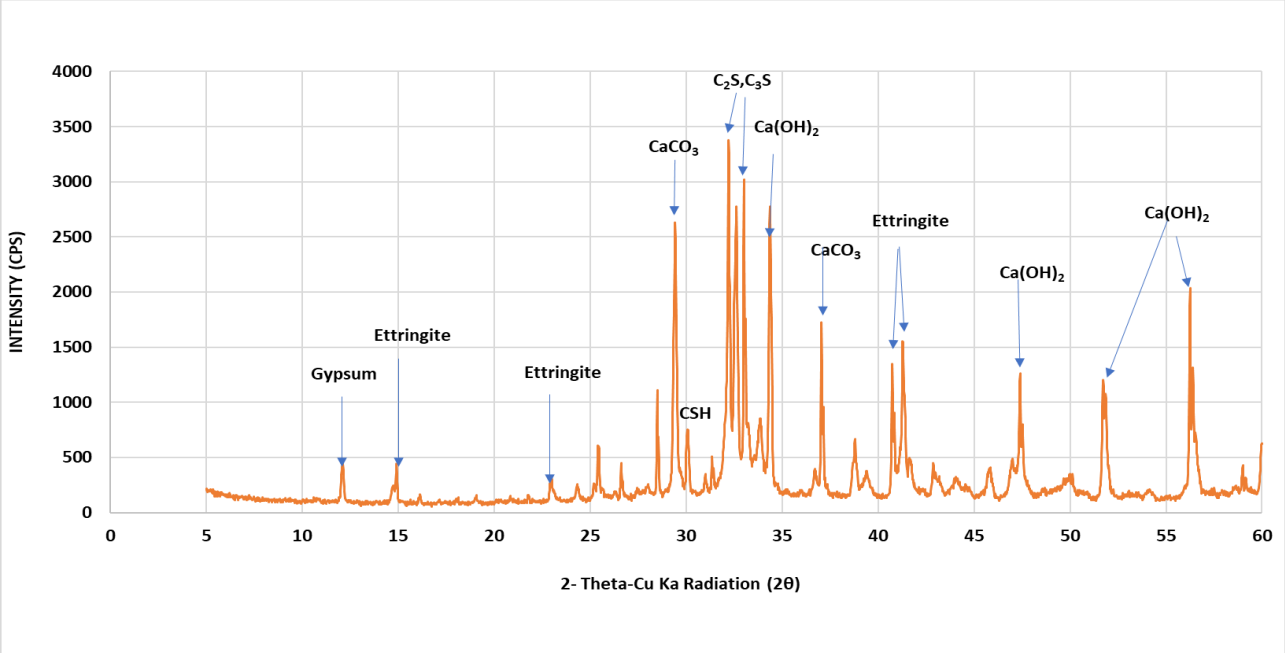

b) 20%

Figure 7: Plotted XRD patterns for LCPT with 20% and 5% pyrite contents.

The inhibition assertion previously explained using the XRD results is further validated experimentally by electrical conductivity (EC) monitoring results, presented in Fig. 8. Electrical conductivity reflects the level of ion concentration and the mobility of ions within the samples, and the ion concentration provides insight into the speed of the cement hydration process (Bian et al. 2021). Figure 8 shows the changes in the EC values with curing time for the LCPT samples without pyrite and with pyrite content of 15 and45% concentration. According to the results, the samples with pyrite results recorded the highest initial EC compared to samples without pyrite content. For example, the 45% sample's initial EC value was 4.53 mS/cm, the 15% sample recorded an initial EC value of 1.96 mS/cm, while the sample with no pyrite content recorded an initial EC value of 1.17 mS/cm. However, as time progressed the curves representing samples with pyrite maintained a similar trend of a drastic decline in EC value, while the EC curve of the sample with no pyrite content showed a rapid trend of increase in comparison to the two samples with pyrite. This rapid increase

reflects faster cement hydration in the pyrite-free sample. Thus, this result is in line with the above-mentioned inhibition due to the presence of ettringite. Ettringite is a hydration product formed during the early stages of cement hydration, especially in sulphate-rich environments. However, in the presence of pyrite, sulfate ions released from pyrite oxidation can react with calcium ions from cement hydration to form ettringite. The formation of ettringite consumes both sulfate ions and calcium ions, which are essential for the progression of cement hydration reactions. This inhibition slows down the hydration process, leading to a decrease in the rate of formation of hydration products and, as a result, a decrease in electrical conductivity over time compared to the control without pyrite. This confirms that the presence of pyrite in paste mixtures can delay/inhibit the hydration reaction.

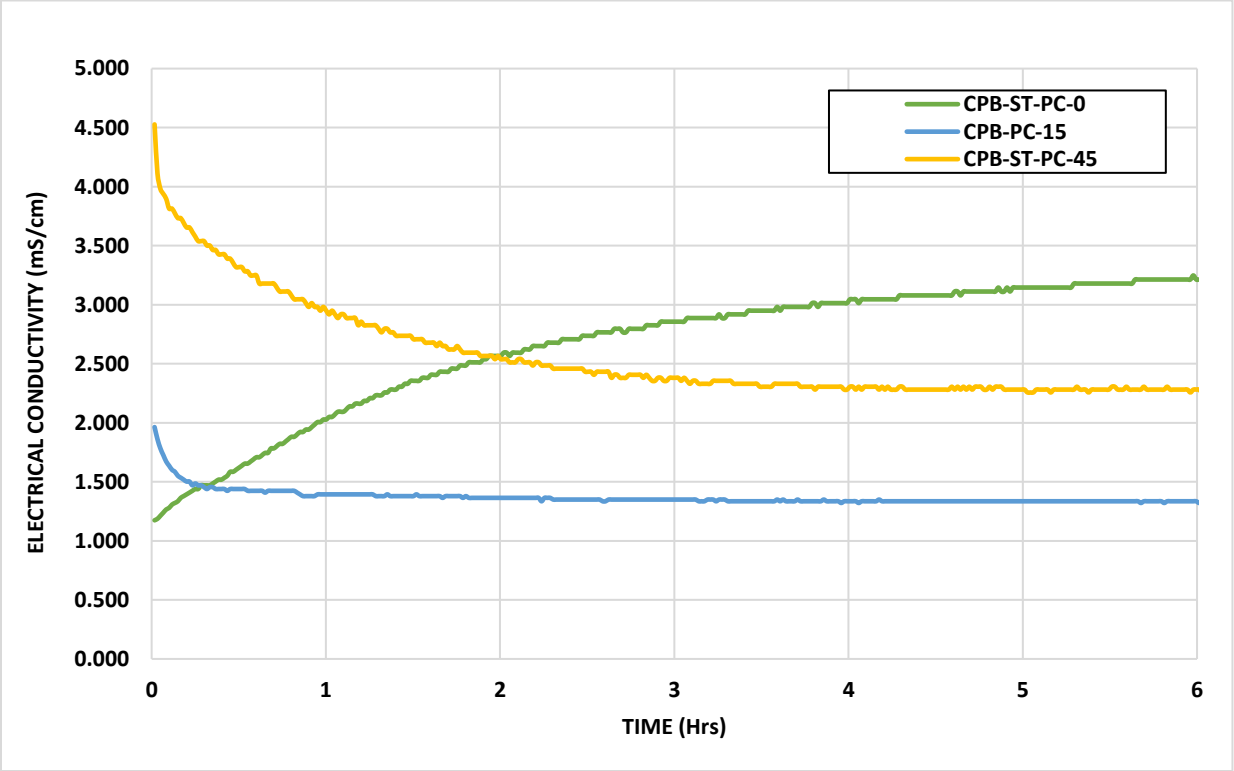

Figure 8: Development of electrical conductivity in LCPT with different pyrite contents.

Figure 9 illustrates the results of evaluating the effect of pyrite content on the time-dependent evolution of the viscosity of LCPT. It shows that both curing time and pyrite content

influence the viscosity of all LCPT samples. Two trends are observed in the evolution of viscosity: (i) viscosity increases with increasing pyrite content; (2) viscosity decreases as curing time increases. In the first trend, Fig. 9 shows that higher pyrite content results in higher viscosity of the samples. In other words, LCPT samples with the highest pyrite content (LCPT-ST-PC-45%) had the highest initial viscosity of 5.9 Pa.s, compared to other pyrite-containing LCPT mixtures (0%, 5%, and 15%). This pyrite-induced increment in viscosity can be attributed to increased solid concentration, leading to increased interparticle forces and subsequently higher viscosity. Indeed, as discussed earlier, higher pyrite content increases the packing density of the mixture, thereby increasing its solid concentration per unit volume, which causes an increase in viscosity (Ding et al. 2007).

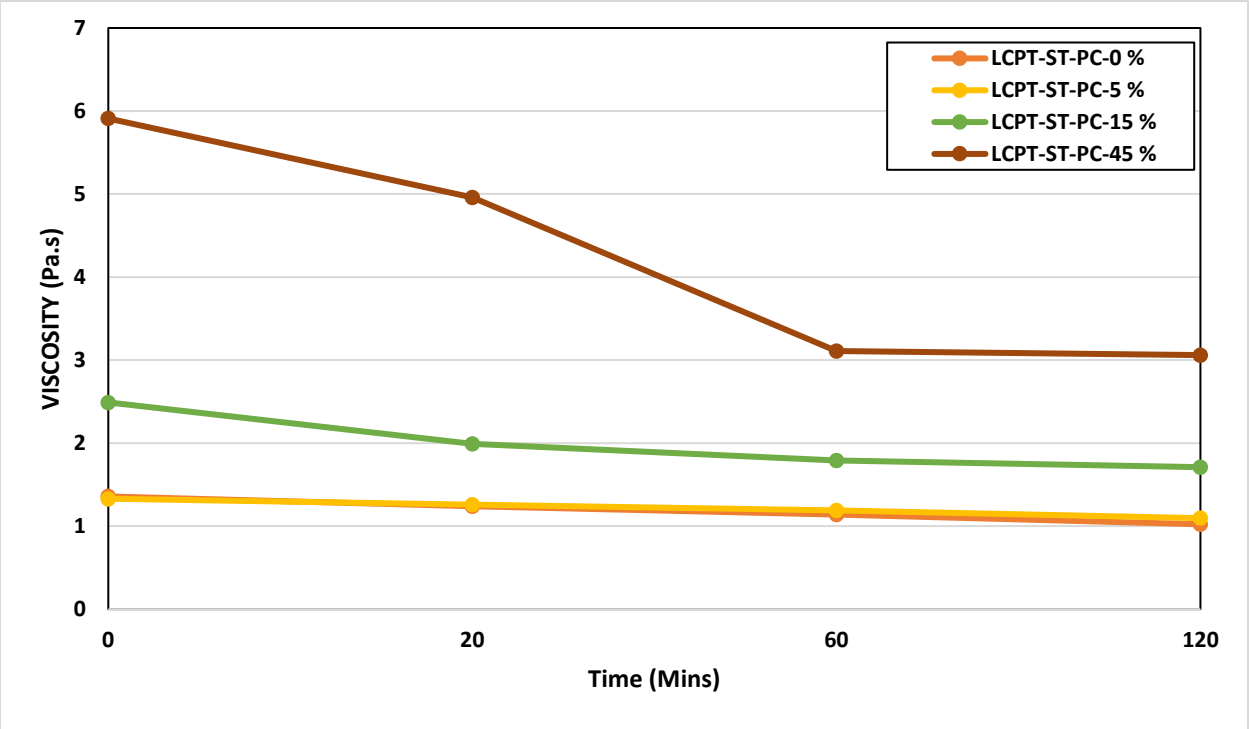

Figure 9: Time-dependent viscosity evolution of LCPT containing different pyrite content.

Furthermore, increased pyrite content causes changes in the surface chemistry of fresh LCPT due to the adsorption of sulfate ions (formed from the oxidation of pyrite) to LCPT cement particles and hydration products. These changes affect the attractive forces between particles, eventually

increasing the viscosity of LCPT (Elakneswaran et al. 2009; Haiqiang et al. 2016). This proposition is further supported through experimental zeta potential measurements given in Fig. 10. According to the zeta potential graph, the LCPT containing 45% pyrite content (LCPT-ST- PC 45%) has a zeta potential of – 18 mV as opposed to a zeta potential of about − 32 mV for the samples without pyrite (LCPT-ST-PC-0%). This lower absolute value of zeta potential suggests diminished particle repulsion, resulting in increased cohesion and thickening of LCPT with higher pyrite content, hence increased viscosity (Plank and Hirsch 2007; Zingg et al. 2008).

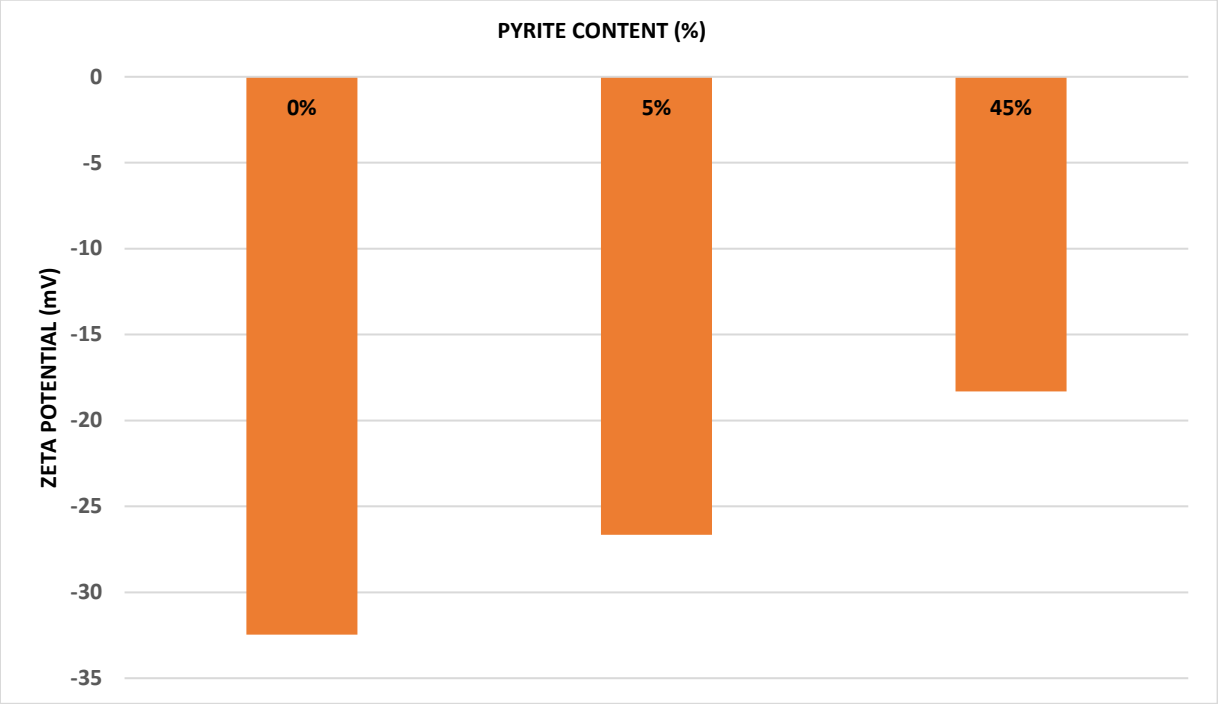

Figure 10: Zeta potential of LCPT samples with different pyrite content

The zeta potential results align well with the pH results given in Fig. 11. The pH of bulk solutions is a major factor that influences zeta potential. pH of a solution is known to facilitate/hinder the adsorption of ions to LCPT mixtures containing pyrite (Elakneswaran et al. 2009; Hunter 2013). Therefore, the changes in pH values with curing time indicate that higher pyrite contents result in a lower pH.

The zeta potential results are further supported by pH results given in Figure 3.11. because the pH of bulk solutions is a major factor that influences zeta potential. pH of a solution is known to facilitate/hinder the adsorption of ions to LCPT mixtures containing pyrite (Elakneswaran et al., 2009; Hunter, 2013). Therefore, the changes in pH values with curing time indicate that higher pyrite contents result in a lower pH.

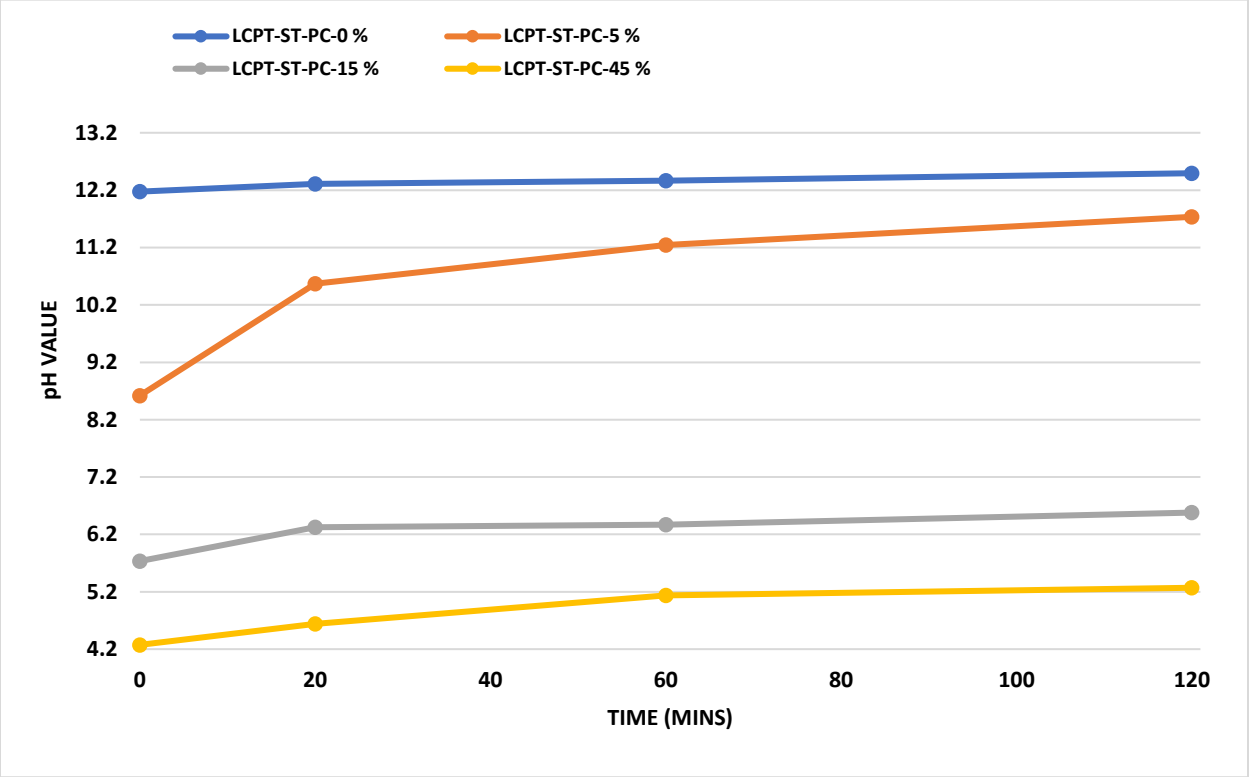

Figure 11: Time-dependent pH of LCPT samples with different pyrite contents

As shown in Fig. 9, the viscosity results are also seen to exhibit a second trend of decreasing with increasing curing time. This notable trend could be due to chemical reactions leading to ettringite formation and microstructural changes. As previously explained, the generation of ettringite retards the process of cement hydration, resulting in fewer cement hydration byproducts in samples containing pyrite. This reduction in cement hydration byproducts corresponds to a decrease in the solid volume ratio within the LCPT material. A lower solid volume ratio diminishes the likelihood of neighbouring particles colliding, consequently increasing the space between solid

particles, and reducing the attractive forces among them (Saleh Ahari et al. 2015). Essentially, particle interaction is reduced, leading to a less dense microstructure in the LCPT, which, in turn, lowers its viscosity as curing time progresses (Bian et al. 2021). This assertion is validated by the DT/DTG (Fig. 12) and XRD (Fig. 13) results, which show that the presence of pyrite content forms more ettringite in the LCPT matrix. Based on the DTG curve shown in Fig. 12, it is evident that the sample containing 50% pyrite exhibits a more pronounced peak in the 100–200 °C temperature range and a smaller peak in the 400–500 °C range. As previously mentioned, the weight loss within these temperature intervals is associated with the dehydration of hydration products, such as C-S–H gel and ettringite at the lower range, and calcium hydroxide (CH) at the higher range. The presence of pyrite leads to a rapid reaction between SO_4^{2-} ions and C3A, resulting in a significant amount of ettringite, which is reflected in the initial peak. As a result, the formation of ettringite hinders the typical hydration process responsible for generating CH, leading to a reduced second peak. Thus, it is evident that the samples with 50% pyrite contain fewer hydration products compared to the samples without pyrite, thereby supporting the assertion that pyrite inhibits binder hydration. In other words, these results validate the previous assertion that the formation of ettringite and less hydration products in samples with pyrite leads to less cohesion and interparticle forces which in turn leads to the noticed decrease in viscosity as curing time progresses.

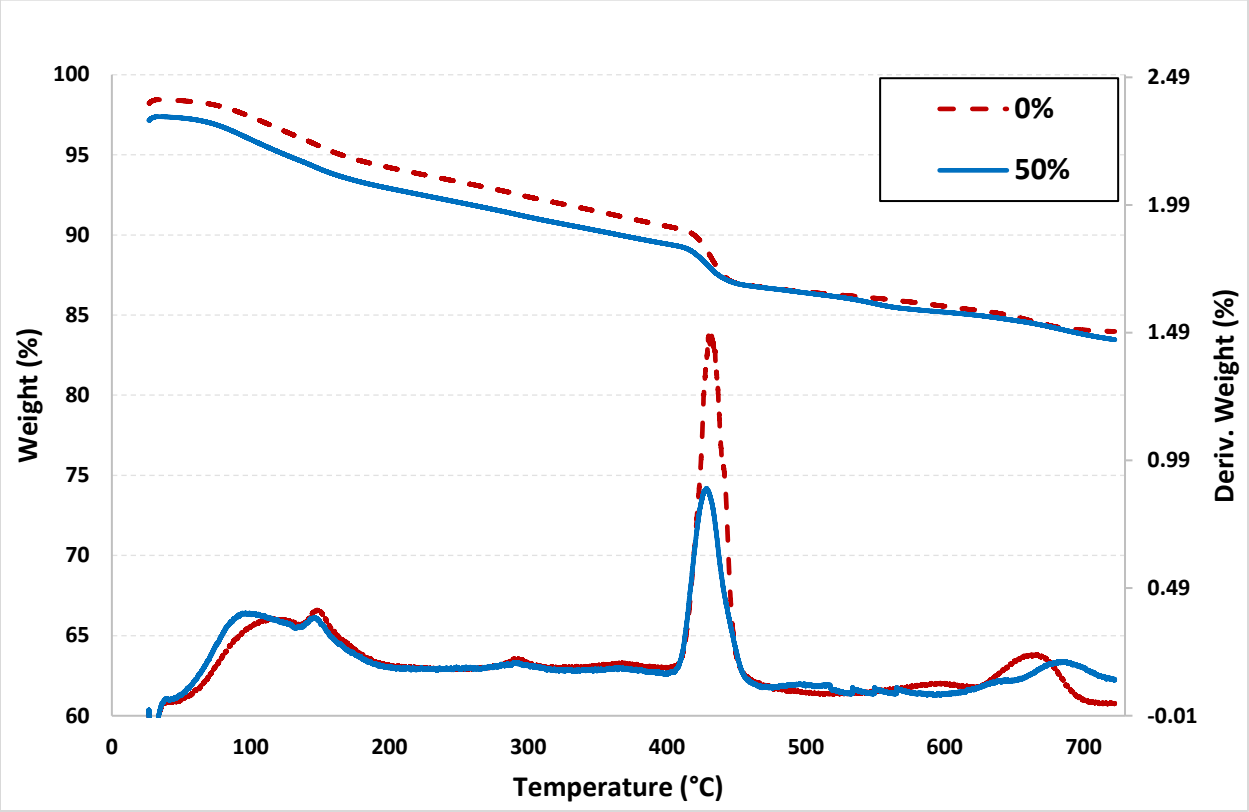

Figure 12: Plotted TG/DTG patterns of LCPT with different pyrite content cured for 2hr.

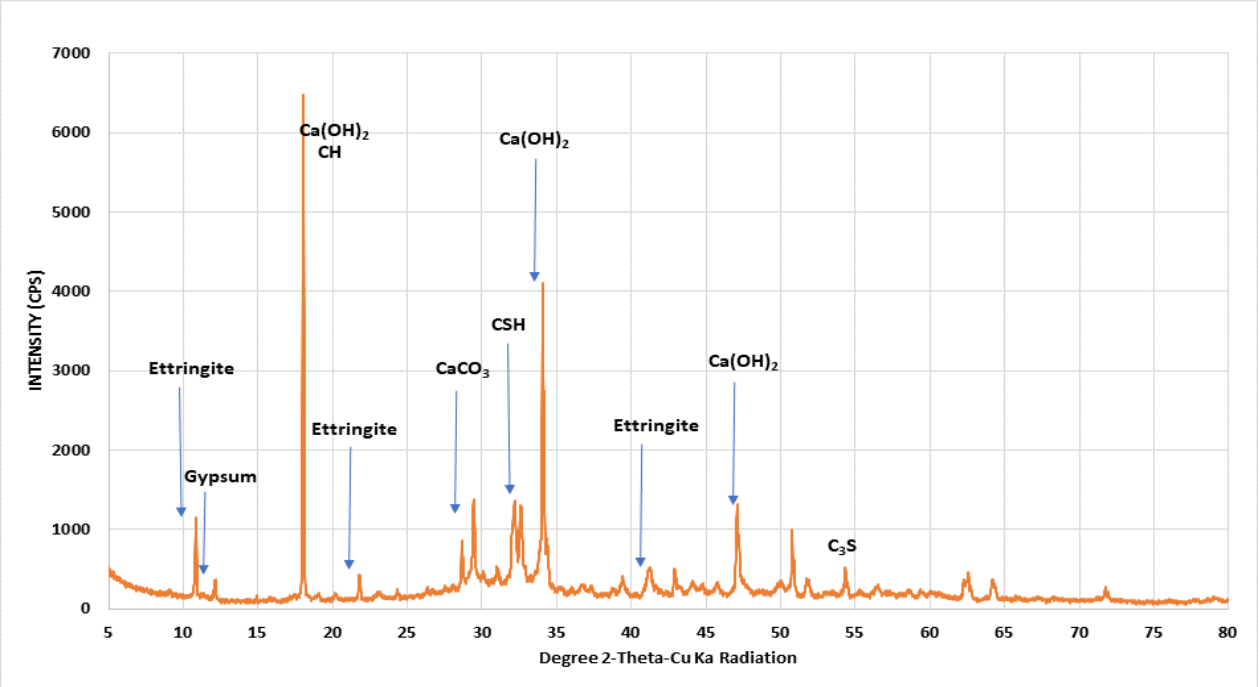

a). 0%

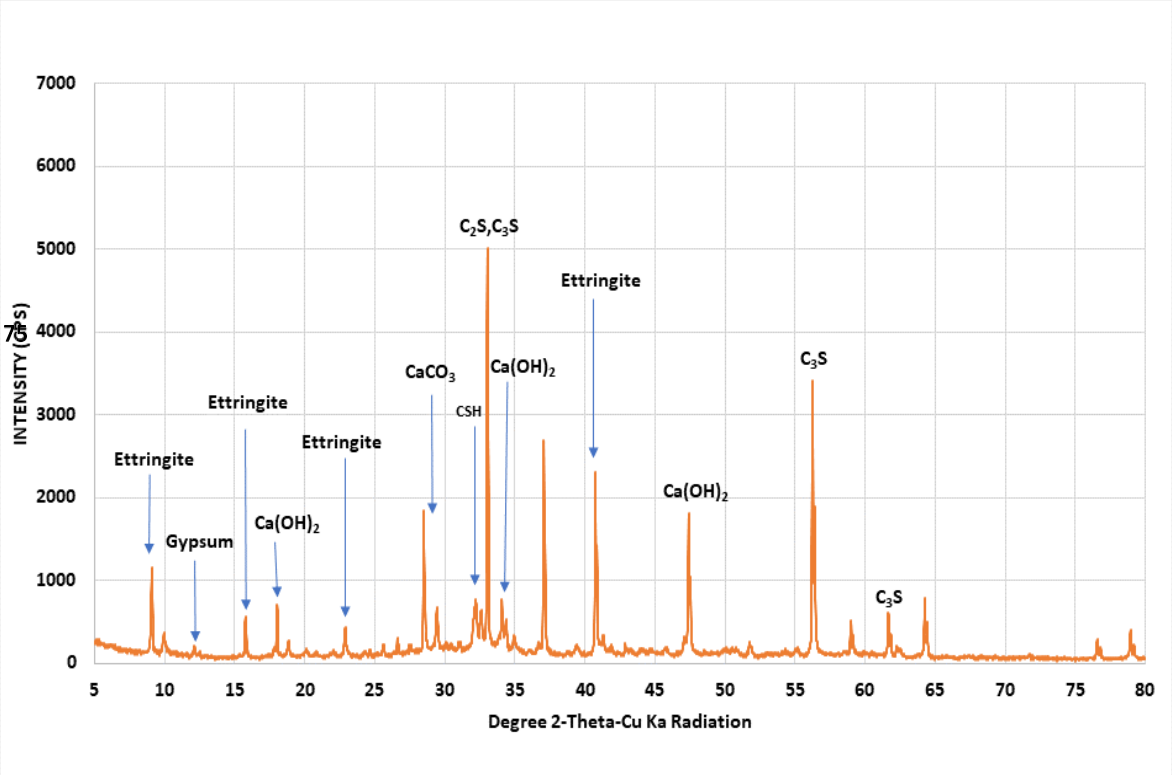

b) 50%

Figure 13: Plotted XRD patterns for LCPT with 0% and 50% pyrite contents.

3.4.3 COUPLED EFFECT OF BINDER TYPE AND PYRITE ON THE YIELD STRESS AND VISCOSITY OF LIGHTLY CEMENTED PASTE TAILINGS

Ordinary Portland cement is widely utilized as a binder in paste tailings technology because it is readily available in numerous parts of the world. However, Portland cement is not only costly, but its production contributes to a significant release of greenhouse gases. Portland cement production accounts for 5–8% of global man-made CO_2 emissions (Damtoft et al. 2008). Thus, to reduce the cost of cemented paste technology and improve the carbon footprint of mining operations, many mines aim to partially or totally replace Portland cement with a low-carbon binder. An

approach to this is to partially replace Portland cement with slag in LCPT. However, the coupled effect of the partial replacement of Portland with slag on the rheological properties of LCPT with pyrite is unknown. Thus, this section aims to study the coupled effect of binder type and pyrite on the rheological properties of LCPT. To investigate this, two binder types namely 100% PCI and a blended binder containing 50% PCI and 50% SLAG were used in the LCPT mixes with different pyrite contents (0% and 45%). Samples with 100% PCI included LCPT-ST-PC-0% and LCPT- ST-PC-45%, while samples with blended binders included LCPT-ST-SG-0% and LCPT-ST-SG-45%. The time-dependent yield stress and viscosity results are shown in Fig. 14. From this figure, it can be concluded that aside from pyrite content, the binder type also notably influences the yield stress and viscosity of LCPT mixtures for surface paste disposal. Both samples prepared with 100% PCI and blended binders are seen to increase in yield stress with increasing pyrite content as time progresses. The mechanisms responsible for the increase due to pyrite content were explained in the previous section. However, samples with blended binders were also seen to have lower yield stress compared to samples prepared with 100% PCI. More specifically, in the LCPT-ST-PC-45% sample mix prepared with 100% PCI, yield stress is seen to increase from 230 to 280 Pa, while LCPT-ST-SG-45%, which was prepared with blended binders and the same pyrite content as LCPT-ST- PC-45% had an increasing yield stress of 72 to 108 Pa. A similar trend is also noticed in viscosity results. Samples with blended binders containing Slag are seen to decrease in viscosity compared to samples with 100% PCI. For instance, LCPT-SG-45% is seen to have an initial viscosity of 2.54 Pa while LCPT-PC-45% reported an initial viscosity of 5.99 Pa.

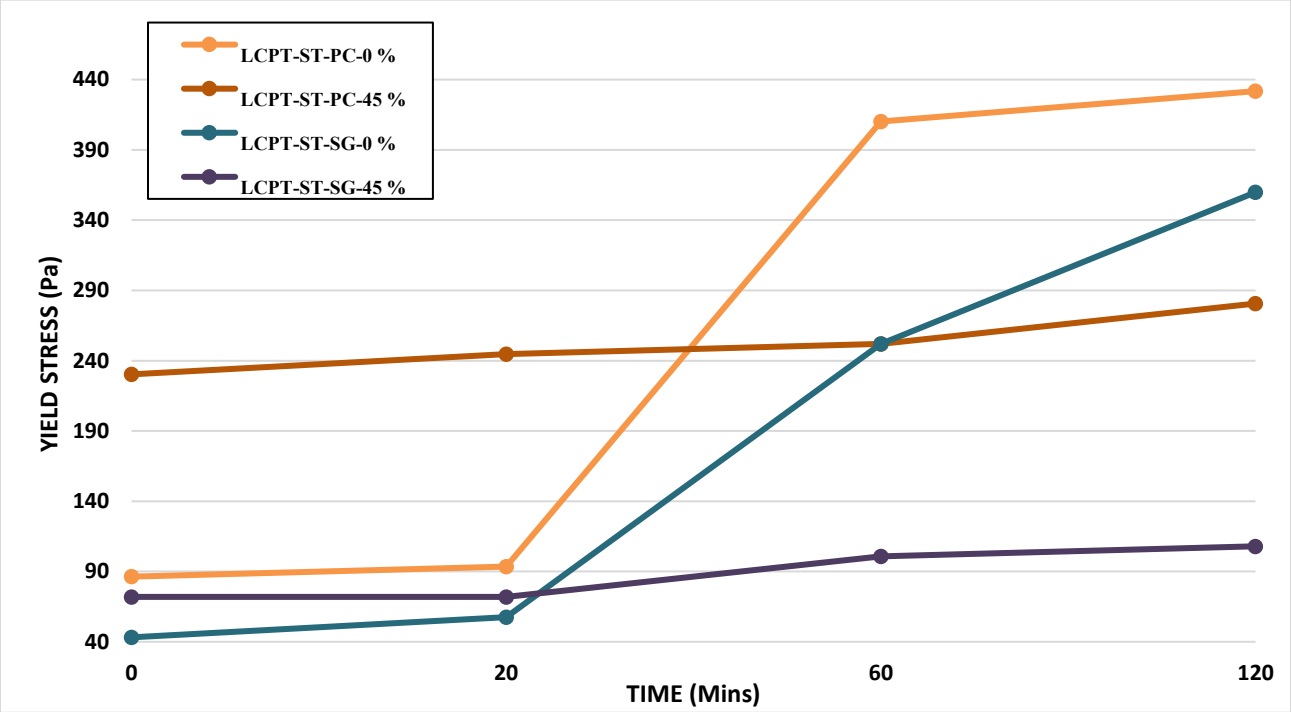

a) Yield stress

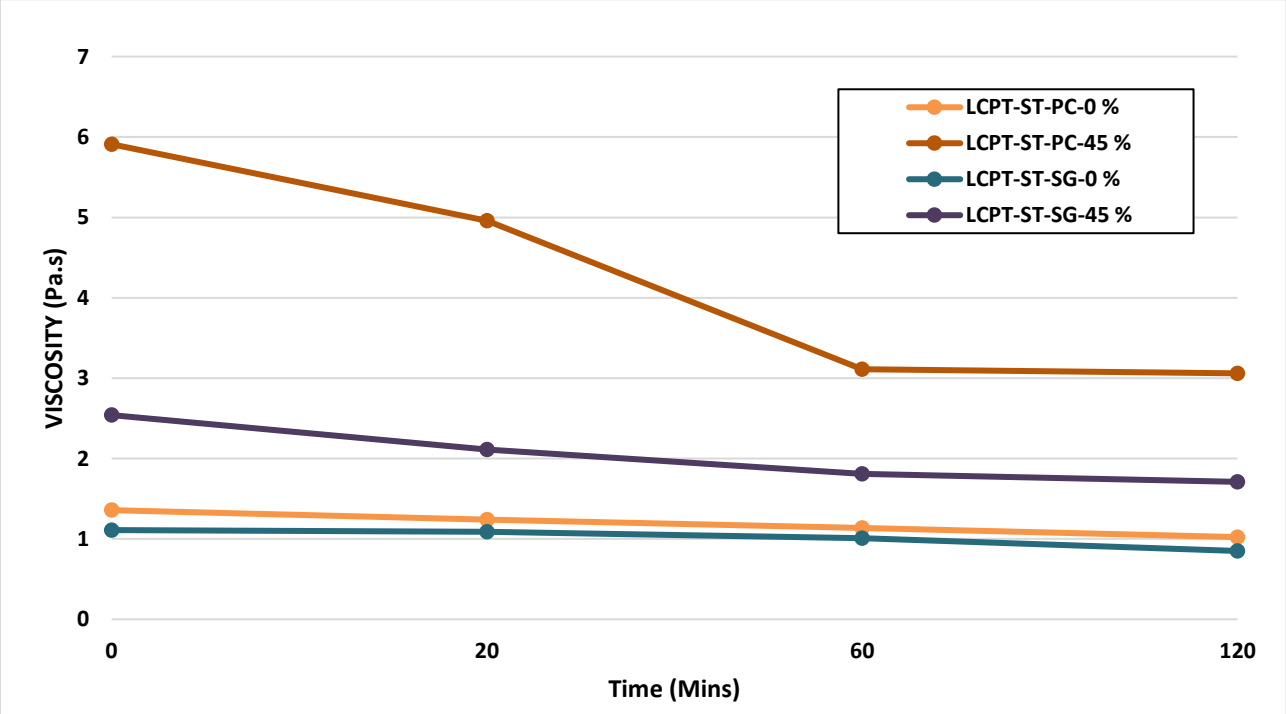

b) Viscosity

Figure 14: Effect of binder type on the yield stress and viscosity of LCPT with and without pyrite: a)Yield stress b)Viscosity

The primary reason for the reduced yield stress and viscosity in LCPT-containing blended binder is due to the pozzolanic nature of Slag. Slag is a pozzolanic binder, that needs to be activated by an activator to start generating hydration products. Hence, Slag is usually activated in an alkaline environment (e.g., calcium hydroxide) and cannot react with water alone (Pokharel and Fall 2011; Xue et al. 2018; Jiang et al. 2019). In the Portland cement-slag system of this study, Slag reacts pozzolanically with calcium hydroxide (CH), a product formed during the hydration of PCI. This leads to a delayed formation of hydration products in blended binder mixtures compared to mixtures with 100% PCI. In simpler terms, LCPTs with blended binders with slag will have fewer hydration products than those composed solely of Portland cement. As hydration products play a crucial role in binding tailings particles together, resulting in a denser matrix, the inter-particle frictional resistance and solid volume fraction in the 100%PCI-LCPT samples will be notably enhanced. Consequently, this increase in interparticle bonding enhances the stress and viscosity of the 100% PCI-LCPT samples (Xiao et al. 2020). This assertion is experimentally supported by DT/DTG and XRD results in Figs. 15 and 16. Figure 15 depicts TG/DTG diagrams for samples containing PCI/Slag (50/50) and 100%PCI. The initial peak around 80–110 °C signifies the dehydration reactions of specific hydrates such as C–S–H, carboaluminates, ettringites, and gypsum. Subsequently, a peak at 400–500 °C indicates the de-hydroxylation of calcium hydroxide, while a third peak between 650 °C and 750 °C corresponds to the decomposition of calcite. Comparing the TG/DTG graphs of these different binders reveals increased hydration product levels at early ages when 100% PCI serves as the binder. These findings align closely with XRD results (Fig. 16). These results indicate a higher content of hydration products (e.g., CH, C-S–H, ettringite) in the 100% PCI sample compared to the blended binder. Indeed, the intensity of the primary hydration products, such as CH, ettringite, and C-S–H, is greater in the 100% PCI binder. This suggests that the 100% PCI-LCPT samples contain more hydration products.

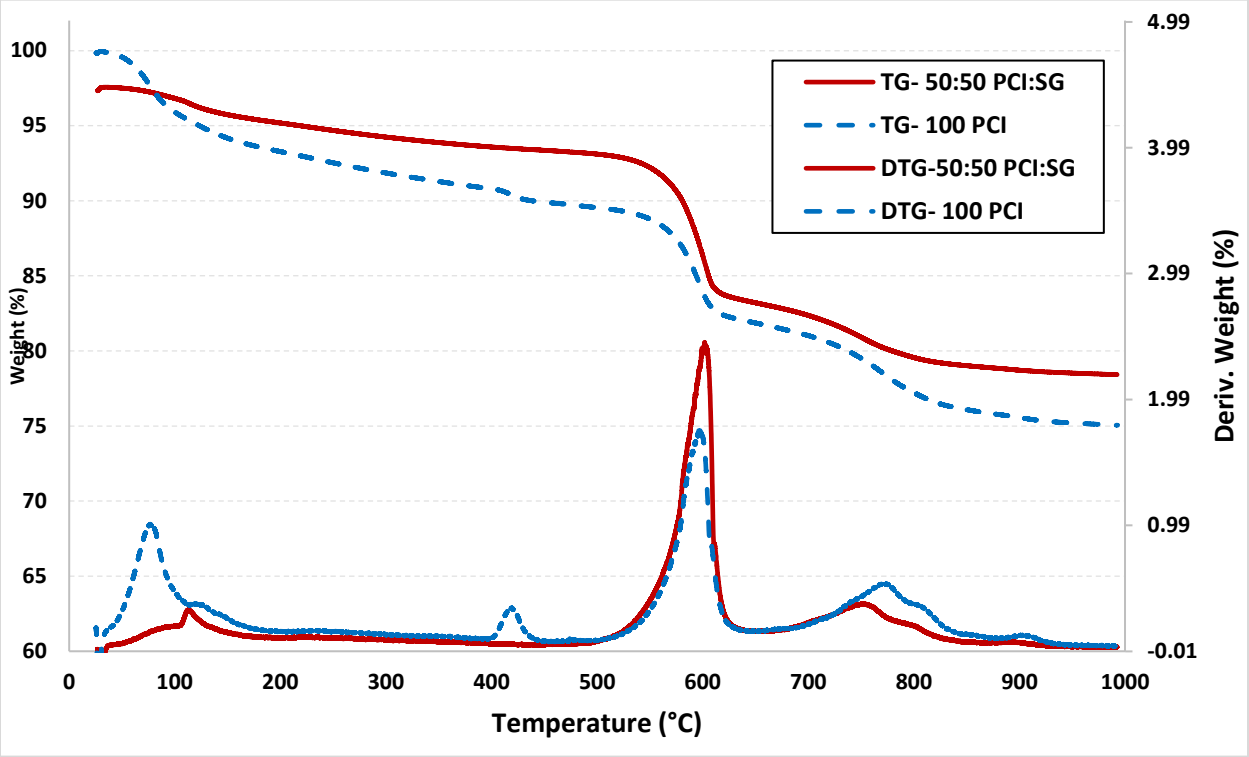

Figure 15: Plotted TG/DTG patterns of LCPT made of 100%PC (100 PCI) and PCI/Slag (50:50).

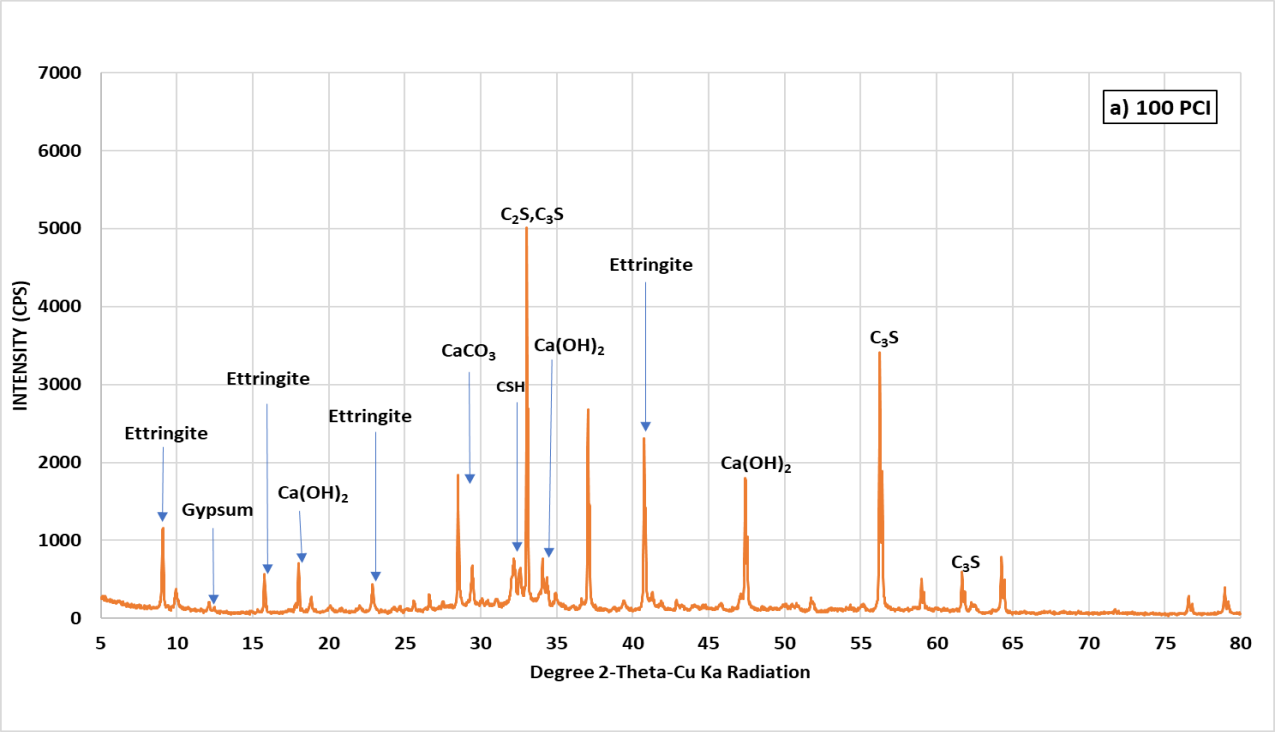

a). 100%PCI

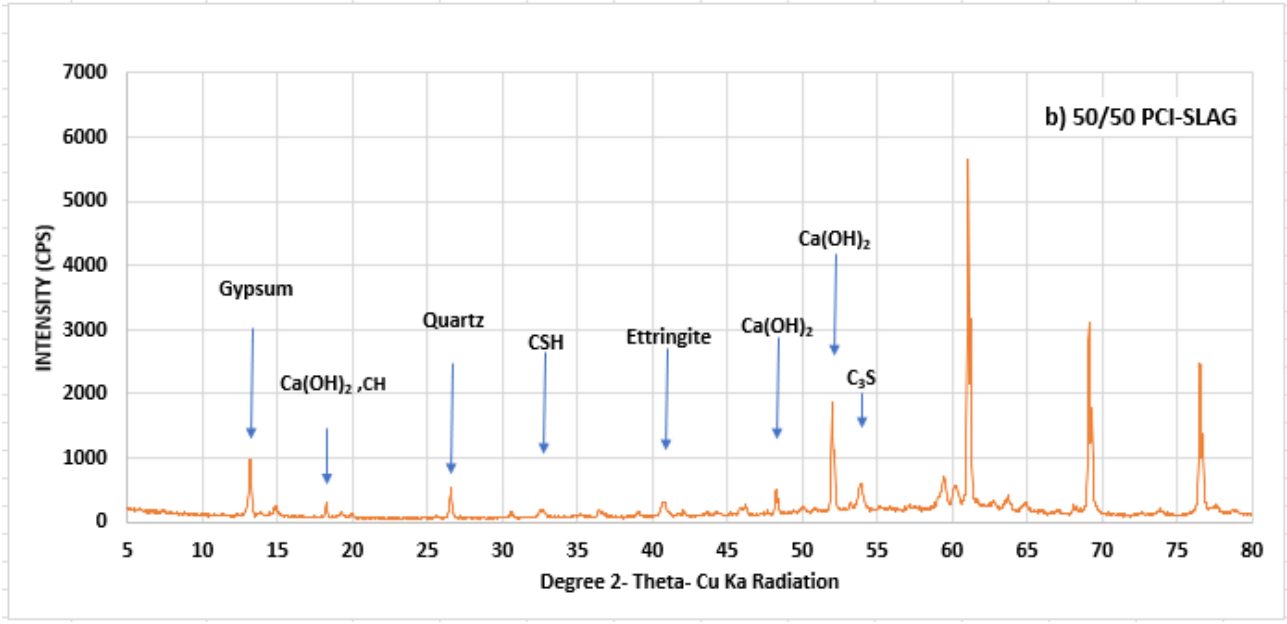

b). 50/50 PCI-SLAG

Figure 16: XRD results of LCPT made of 100% PC (100 PCI) and PCI/Slag (50:50) a) 100 PCI and b) PCI/Slag (50:50).

3.5 SUMMARY AND CONCLUSIONS

The time-dependent yield stress and viscosity of uncemented paste tailings (UPT) and lightly cemented paste tailings (LCPT) with different pyrite contents, cured over different times of 0, 20, 60, and 120 min under room temperature conditions, were studied in this paper. The following conclusions from this study are summarized below.

1. Pyrite minerals significantly influence the rheological properties of both LCPT and UPT. The effect of pyrite on rheological properties increases with increasing pyrite content. Hence, this factor should be taken into consideration in surface paste disposal to ensure the successful application of PT technology for pyrite-bearing tailings.

2. Rheological properties such as yield stress and viscosity of LCPT and UPT mixtures, with or without pyrite, are time-dependent. Yield stress generally increases over time as pyrite content increases, while viscosity increases with increasing pyrite content but decreases over time.

3. A higher concentration of pyrite solids can lead to several microstructural or chemical alterations in fresh LCPT, such as slowing down the cement hydration process or modifying the repulsive interactions between particles.

4. The experimental findings indicate that as curing time increases, pyrite can hinder the hydration process due to chemical interactions that result in the formation of ettringite crystals.

5. The experimental findings from this study indicate that the type of binder used, specifically Portland cement type I (PCI) and ground furnace slag (Slag), plays a crucial role in influencing the rheological characteristics of pyrite- containing LCPT. In particular, the samples composed entirely of PCI exhibited higher yield stress and viscosity than those in which 50% of the PCI was substituted with Slag.

This study concludes that pyrite content is a crucial factor to consider for the cost-effective and successful transportation and implementation of LCPTs and UPTs made of pyrite-bearing tailings. However, the scope of this research was limited to specific binder types and silica-based tailings, potentially excluding other combinations that might influence the rheological behaviour of LCPTs and UPTs. To build on these findings, future research should (i) explore the use of alternative binders or binder additives that enhance sustainability and reduce greenhouse gas emissions while maintaining optimal rheological properties, and (ii) expand the investigation to include a wider range of natural tailings with diverse chemical compositions to validate the results under varied field scenarios.

3.6 REFERENCES

Adiguzel, D., & Bascetin, A. (2019). The investigation of effect of particle size distribution on flow behavior of paste tailings. *Journal of Environmental Management*, *243*, 393–401. https://doi.org/10.1016/j.jenvman.2019.05.039

Akbar, E., Yaakob, Z., Kamarudin, S.K., Ismail, M., Salimon, J., (2009). Characteristic and composition of Jatropha curcas oil seed from Malaysia and its potential as biodiesel feedstock feedstock. Europ. J. Sci. Res. 29 (3), 396–403.

Aldhafeeri, Z., and Fall, M. (2016). Time and damage-induced changes in the chemical reactivity of cemented paste backfill. *Journal of Environmental Chemical Engineering*, *4*(4), 4038–4049. https://doi.org/10.1016/j.jece.2016.09.006

Aldhafeeri, Z., and Fall, M. (2017). Sulphate-induced changes in the reactivity of cemented tailings backfill. *International Journal of Mineral Processing*, *166*, 13–23. https://doi.org/10.1016/j.minpro.2017.06.007

Aschan, N. (1966). Determining the setting time of cement paste, mortar and concrete with a copper-lead electrode. *Magazine of Concrete Research*, *18*(56), 153–160. https://doi.org/10.1680/macr.1966.18.56.153

ASTMD4648/D4648M-16. (2016). Standard Test Methods for Laboratory Miniature Vane Shear Test for Saturated Fine-Grained Clayey Soil, ASTM International, 100 Barr Harbor Drive, PO Box C700, West Conshohocken, PA 19428-2959, United States.

Aubertin, M., Li, L., Arnoldi, S., Belem, T., Bussière, B., Benzaazoua, M., and Simon, R. (2003). Interaction between backfill and rock mass in narrow stopes. In: Proceedings of 12th Panamerican conference on soil mechanics and geotechnical engineering and 39th U.S. rock mechanics symposium. 22–26 June. Boston, Massachusetts, USA. Vol. 1. Verlag Glückauf GmbH, Essen, 1157–1164.

Benzaazoua, M., Belem, T., and Bussière, B. (2002). Chemical factors that influence the performance of mine sulphidic paste backfill. *Cement and Concrete Research*, *32*(7), 1133–1144. https://doi.org/10.1016/S0008-8846(02)00752-4

Benzaazoua, M., Fall, M., and Belem, T. (2004a). A contribution to understanding the hardening process of cemented pastefill. *Minerals Engineering*, *17*(2), 141–152. https://doi.org/10.1016/j.mineng.2003.10.022

Benzaazoua, M., Marion, P., Picquet, I., and Bussière, B. (2004b). The use of pastefill as a solidification and stabilization process for the control of acid mine drainage. *Minerals Engineering*, *17*(2), 233–243. https://doi.org/10.1016/j.mineng.2003.10.027

Bian, J., Fall, M., and Haruna, S. (2021). Sulfate-induced changes in rheological properties of fibre-reinforced cemented paste backfill. *Magazine of Concrete Research*, *73*(11), 574–583. https://doi.org/10.1680/jmacr.19.00311

Bradley, J. S., Millar, J. M., and Hill, E. W. (1991). Surface chemistry on colloidal metals: a high-resolution NMR study of carbon monoxide adsorbed on metallic palladium crystallites in colloidal suspension. *Journal of the American Chemical Society*, *113*(10), 4016–4017. https://doi.org/10.1021/ja00010a067

Brookfield, DV-E Digital Viscometer (2016): Operating Instructions. Middleboro, USA. Web, (n.d.) https://pim-resources.coleparmer.com/instruction-manual/ 98945-xx.pdf 2016.

Cadden, A., Newman, P., & Fordham, M. (2003). New developments in surface paste disposal of mine wastes. *Processing & Disposal of Mineral Industry Wastes*, *3*, 1-17.

Cincilla, W. A., Landriault, D. A., and Verburg, R. (1997). Application of paste technology to surface tailings disposal of mineral wastes. In: Proceedings of the 4th International Symposium on Tailings and Mine Waste '97, A. A. Balkema, Vail, Fort Collins, Colorado, USA, pp 343–356.

Clogston, J. D., and Patri, A. K. (2011). Zeta Potential Measurement. *Characterization of Nanoparticles Intended for Drug Delivery*, 63–70. https://doi.org/10.1007/978-1-60327-198-1_6

Cooke, R., Spearing, A. J., and Gericke, D. J. (1993). Influence of binder addition on the hydraulic transport of classified-tailings backfill. *International Journal of Rock Mechanics and Mining Sciences and Geomechanics Abstracts, 30*(6), 372–372. https://doi.org/10.1016/0148-9062(93)91543-R

Courard, L., Michel, F., Perkowicz, S., and Garbacz, A. (2014). Effects of limestone fillers on surface free energy and electrical conductivity of the interstitial solution of cement mixes. *Cement and Concrete Composites*, *45*, 111–116. https://doi.org/10.1016/j.cemconcomp.2013.09.014

Cui, L., and Fall, M. (2016). Mechanical and thermal properties of cemented tailings materials at early ages: Influence of initial temperature, curing stress and drainage conditions. *Construction & Building Materials*, *125*, 553–563. https://doi.org/10.1016/j.conbuildmat.2016.08.080

Deschamps, T., Benzaazoua, M., Bussière, B., and Aubertin, M. (2011). Laboratory study of surface paste disposal for sulfidic tailings: Physical model testing. *Minerals Engineering*, *24*(8), 794–806. https://doi.org/10.1016/j.mineng.2011.02.013

Ding, P., and Pacek, A. W. (2008). Effect of pH on deagglomeration and rheology/morphology of aqueous suspensions of goethite nanopowder. *Journal of Colloid and Interface Science*, *325*(1), 165–172. https://doi.org/10.1016/j.jcis.2008.04.077

Ding, Z., Yin, Z., Liu, L., and Chen, Q. (2007). Effect of grinding parameters on the rheology of pyrite–heptane slurry in a laboratory stirred media mill. *Minerals Engineering*, *20*(7), 701–709. https://doi.org/10.1016/j.mineng.2007.01.005

Divet, L., and Randriambololona, R. (1998). Delayed Ettringite Formation: The Effect of Temperature and Basicity on the Interaction of Sulphate and C-S-H Phase. *Cement and Concrete Research*, *28*(3), 357–363. https://doi.org/10.1016/S0008-8846(98)00006-4

Dixon-Hardy, D., and Engels, J. (2007). Methods for the disposal and storage of mine tailings. *Land Contamination and Reclamation, 15*, 301-317. doi:10.2462/09670513.832.

Dold, B. (2014). Evolution of Acid Mine Drainage Formation in Sulphidic Mine Tailings. *Minerals*, 4(3), 621–641. http://doi.org/10.3390/min4030621

Dzuy, N. Q., and Boger, D. V. (1985). Direct Yield Stress Measurement with the Vane Method. *Journal of Rheology (New York : 1978)*, *29*(3), 335–347. https://doi.org/10.1122/1.549794

Elakneswaran, Y., Nawa, T., and Kurumisawa, K. (2009). Zeta potential study of paste blends with slag. *Cement and Concrete Composites*, *31*(1), 72–76. https://doi.org/10.1016/j.cemconcomp.2008.09.007

Fahey, M., Helinski, M., & Fourie, A. (2011). Development of Specimen Curing Procedures that Account for the Influence of Effective Stress During Curing on the Strength of Cemented Mine Backfill. *Geotechnical and Geological Engineering*, *29*(5), 709–723. https://doi.org/10.1007/s10706-011-9412-2

Fall, M., Célestin, J. C., Pokharel, M., & Touré, M. (2010). A contribution to understanding the effects of curing temperature on the mechanical properties of mine cemented tailings backfill. *Engineering Geology*, *114*(3), 397–413. https://doi.org/10.1016/j.enggeo.2010.05.016

Fall, M., and Benzaazoua, M. (2005). Modeling the effect of sulphate on strength development of paste backfill and binder mixture optimization. *Cement and Concrete Research*, *35*(2), 301–314. https://doi.org/10.1016/j.cemconres.2004.05.020

Fall, M., Belem, T., Samb, S., Benzaazoua, M. (2007). Experimental characterization of the stress–strain behaviour of cemented paste backfill in compression. J. Mater. Sci. 42 (11):3914–3922. http://dx.doi.org/10.1007/s10853-006-0403-2.

Fall, M., Benzaazoua, M., and Saa, E. G. (2008). Mix proportioning of underground cemented tailings backfill. *Tunnelling and Underground Space Technology*, *23*(1), 80–90. https://doi.org/10.1016/j.tust.2006.08.005

Fall, M., Benzaazoua, M., and Ouellet, S. (2005). Experimental characterization of the influence of tailings fineness and density on the quality of cemented paste backfill. *Minerals Engineering*, 18(1), 41–44. https://doi.org/10.1016/j.mineng.2004.05.012

Fall, M., Wu, D., and Pokharel, M. (2014). Effect of deep mine temperature conditions on the heat development in cemented paste backfill and its properties. In M. Hudyma and Y. Potvin (Eds.), *Deep Mining 2014: Proceedings of the Seventh International Conference on Deep and High Stress Mining* (pp. 559-573). Australian Centre for Geomechanics, Perth. https://doi.org/10.36487/ACG_rep/1410_39_Fall

Fourie, A. (2003). Achieving a stable landform with mine tailings: opportunities offered by the Thickened Tailings technique. In I. Vanicek, R. Barvinek, J. Bohac, J. Jettmar, D. Jirasko, & J. Salak (Eds.), Geotechnical Problems with Man-made and Man Influenced Grounds (Prague, Chech Republic ed., Vol. 1, pp. 77-82). The Chech Geotechnical Society.

Ghirian, A., and Fall, M. (2015). Coupled Behavior of Cemented Paste Backfill at Early Ages. *Geotechnical and Geological Engineering*, *33*(5), 1141–1166. https://doi.org/10.1007/s10706-015-9892-6

Ghirian, A., and Fall, M. (2016). Strength evolution and deformation behaviour of cemented paste backfill at early ages: effect of curing stress, filling strategy and drainage. Int. J. Min. Sci. Technol. http://dx.doi.org/10.1016/j.ijmst.2016.05.039

Goudoulas, T. B., Kastrinakis, E. G., and Nychas, S. G. (2003). Rheological aspects of dense lignite-water suspensions; time dependence, preshear and solids loading effects. *Rheologica Acta*, *42*(1–2), 73–85. https://doi.org/10.1007/s00397-002-0257-8

Haiqiang, J., Fall, M., and Cui, L. (2016). Yield stress of cemented paste backfill in sub-zero environments: Experimental results. *Minerals Engineering*, *92*, 141–150. https://doi.org/10.1016/j.mineng.2016.03.014

Haiqiang, J., Fall, M., and Cui, L. (2016). Yield stress of cemented paste backfill in sub-zero environments: Experimental results. *Minerals Engineering*, *92*, 141–150. https://doi.org/10.1016/j.mineng.2016.03.014

He, M., Wang, Y., and Forssberg, E. (2004). Slurry rheology in wet ultrafine grinding of industrial minerals: a review. *Powder Technology*, *147*(1), 94–112. https://doi.org/10.1016/j.powtec.2004.09.032

He, M., Wang, Y., and Forssberg, E. (2006). Parameter studies on the rheology of limestone slurries. *International Journal of Mineral Processing*, *78*(2), 63–77. https://doi.org/10.1016/j.minpro.2005.07.006

Hunter, R. J. (2013). *Zeta potential in colloid science : principles and applications*. Academic Press.

Huynh, L., Beattie, D. A., Fornasiero, D., and Ralston, J. (2006). Effect of polyphosphate and naphthalene sulfonate formaldehyde condensate on the rheological properties of dewatered tailings and cemented paste backfill. *Minerals Engineering*, *19*(1), 28–36. https://doi.org/10.1016/j.mineng.2005.05.001

Huynh, L., Beattie, D. A., Fornasiero, D., and Ralston, J. (2006). Effect of polyphosphate and naphthalene sulfonate formaldehyde condensate on the rheological properties of dewatered tailings and cemented paste backfill. *Minerals Engineering*, *19*(1), 28–36. https://doi.org/10.1016/j.mineng.2005.05.001

Ichrak, H., Mostafa, B., Abdelkabir, M., and Bruno, B. (2016). Effect of cementitious amendment on the hydrogeological behavior of a surface paste tailings' disposal. *Innovative Infrastructure Solutions : The Official Journal of the Soil-Structure Interaction Group in Egypt (SSIGE)*, *1*(1). https://doi.org/10.1007/s41062-016-0019-6

INAP. (2009). Global Acid Rock Drainage (GARD) Guide. Retrieved from http://www.gardguide.com, Accessed June 2009.

Jiang, H., Qi, Z., Yilmaz, E., Han, J., Qiu, J.P., & Dong, C. (2019). Effectiveness of alkali-activated slag as alternative binder on workability and early age compressive strength of cemented paste backfills. *Construction and Building Materials, 218*, 689–700. doi:10.1016/j.conbuildmat.2019.05.162.

Johnson, S. B., Franks, G. V., Scales, P. J., Boger, D. V., and Healy, T. W. (2000). Surface chemistry–rheology relationships in concentrated mineral suspensions. *International Journal of Mineral Processing*, *58*(1), 267–304. https://doi.org/10.1016/S0301-7516(99)00041-1

Keentok, M. (1982). The measurement of the yield stress of liquids. *Rheologica Acta*, *21*(3), 325–332. https://doi.org/10.1007/BF01515720

Kesimal, A., Yilmaz, E., and Ercikdi, B. (2004). Evaluation of paste backfill mixtures consisting of sulphide-rich mill tailings and varying cement contents. *Cement and Concrete Research*, *34*(10), 1817–1822. https://doi.org/10.1016/j.cemconres.2004.01.018

Klein, K., and Simon, D. (2006). Effect of specimen composition on the strength development in cemented paste backfill. *Canadian Geotechnical Journal*, *43*(3), 310–324. https://doi.org/10.1139/t06-005

Kleinmann RLP, Crerar DA, Pacelli RR (1981) Biogeochemistry of acid mine drainage and a method to control acid formation. Min Eng 33(3):300–305

Koohestani, B., Belem, T., Koubaa, A., Bussière, B., 2016. Experimental investigation into the compressive strength development of cemented paste backfill containing nanosilica. Cem. Concr. Compos. 72:180–189. http://dx.doi.org/10.1016/j.cemconcomp. 2016.06.016

Kumari, S., Udayabhanu, G., Prasad, B., 2010. Studies on environmental impact of acid mine drainage generation and its treatment: an appraisal. Indian J. Environ. Prot. 30 (11), 953e967

Kwak, M., James, D. F., and Klein, K. A. (2005). Flow behaviour of tailings paste for surface disposal. *International Journal of Mineral Processing*, *77*(3), 139–153. https://doi.org/10.1016/j.minpro.2005.06.001

Landriault, D. (1995). Paste backfill Mix design for Canadian Underground Hard Rock Mining. In: Proceedings of the 97th Annual General Meeting of CIM. Rock Mechanics and Strata Control Session. Halifax, Nova Scotia, pp. 229–238.

Lawrence, C. D. (1990). Sulphate attack on concrete. *Magazine of Concrete Research*, *42*(153), 249–264. https://doi.org/10.1680/macr.1990.42.153.249

Leong, Y.-K., and Boger, D. V. (1990). Surface chemistry effects on concentrated suspension rheology. *Journal of Colloid and Interface Science*, *136*(1), 249–258. https://doi.org/10.1016/0021-9797(90)90095-6

Li, W., Zhang, Q., Gu, M., and Jin, Y. (2006). Effect of temperature on rheological behavior of silicon carbide aqueous suspension. *Ceramics International*, *32*(7), 761–765. https://doi.org/10.1016/j.ceramint.2005.05.017

Manmohan, D., and Mehta, P. (1981). Influence of Pozzolanic, Slag, and Chemical Admixtures on Pore Size Distribution and Permeability of Hardened Cement Pastes. In *Cement, concrete and aggregates* (Vol. 3, Issue 1, pp. 63–67). ASTM International. https://doi.org/10.1520/CCA10203J

Marcus JJ (1997) Mining environmental handbook: effect of mining on the environment and American Environmental Controls on Mining. Imperial College Press, London

McCarter, W. J., and Curran, P. N. (1984). Electrical response characteristics of setting cement paste. *Magazine of Concrete Research*, *36*(126), 42–49. https://doi.org/10.1680/macr.1984.36.126.42

MMM Tech. (n.d.). Teros 11-12 Manual (English). MMM Medcenter Einrichtungen GmbH. Retrieved fromhttps://mmm-tech.de/index.php/en/volumetric/teros-12

Møller, P. and Mewis, J. and Bonn, Daniel. (2006). Yield Stress and Thixotropy: On the Difficulty of Measuring Yield Stresses in Practice. Soft Matter. 2. 274-283. 10.1039/b517840a.

Nachbaur, L., Nkinamubanzi, P.-C., Nonat, A., and Mutin, J.-C. (1998). Electrokinetic Properties which Control the Coagulation of Silicate Cement Suspensions during Early Age Hydration. *Journal of Colloid and Interface Science*, *202*(2), 261–268. https://doi.org/10.1006/jcis.1998.5445

Nasir, O., and Fall, M. (2008). Shear behaviour of cemented pastefill-rock interfaces. *Engineering Geology*, 101(3), 146–153. https://doi.org/10.1016/j.enggeo.2008.04.010

Nason, Peter and Alakangas, Lena and Öhlander, Björn. (2013). Using sewage sludge as a sealing layer to remediate sulphidic mine tailings: A pilot-scale experiment, northern Sweden. Environmental Earth Sciences. 70. 10.1007/s12665-013-2369-0.

Oakton. (n.d.). Oakton pH 5+, pH 6+, Ion 6+ Instruction Manual. Novatech USA. Retrieved from https://www.novatechusa.com/pdf/Oakton%20pH%205+,%20pH%206+,%20Ion%206+%20Instruction%20Manual.pdf

Öhlander, B., Chatwin, T., and Alakangas, L. (2012). Management of Sulfide-Bearing Waste, a Challenge for the Mining Industry. Minerals (Basel), 2(1), 1–10. https://doi.org/10.3390/min2010001

Ouattara, D., Yahia, A., Mbonimpa, M., and Belem, T. (2017). Effects of superplasticizer on rheological properties of cemented paste backfills. *International Journal of Mineral Processing*, *161*, 28–40. https://doi.org/10.1016/j.minpro.2017.02.003

Plank, J., and Hirsch, C. (2007). Impact of zeta potential of early cement hydration phases on superplasticizer adsorption. *Cement and Concrete Research*, *37*(4), 537–542. https://doi.org/10.1016/j.cemconres.2007.01.007

Pokharel, M., and Fall, M. (2013). Combined influence of sulphate and temperature on the saturated hydraulic conductivity of hardened cemented paste backfill. *Cement and Concrete Composites*, *38*, 21–28. https://doi.org/10.1016/j.cemconcomp.2013.03.015

Prince, W., Espagne, M., and Aïtcin, P.-C. (2003). Ettringite formation: A crucial step in cement superplasticizer compatibility. *Cement and Concrete Research*, *33*(5), 635–641. https://doi.org/10.1016/S0008-8846(02)01042-6

Pye, K., Schiavon, N., 1989. Cause of sulphate attack on concrete, render and stone indicated by sulphur isotope ratios. Nature 342 (6250), 663–664.

Robinsky, E.I. 1999. Thickened Tailings Disposal in the Mining Industry. E.I. Robinsky Associates Ltd., Toronto, Canada.

Rocha, C.A.A., Cordeiro, G.C., Toledo Filho, R.D., Use of thermal analysis to determine the hydration products of oil well cement pastes containing NaCl and KCl. Journal of Thermal Analysis and Calorimetry, 2015, 122(3), 1279-1288.

Saebimoghaddam, A. (2005). Rheological yield stress measurement of mine paste fill material. ProQuest Dissertations Publishing.

Saleh Ahari R, Erdem TK and Ramyar K (2015) Time-dependent rheological characteristics of self-consolidating concrete containing various mineral admixtures. Construction and Building Materials88: 134–142.

Simon, D., and Grabinsky, M. (2013). Apparent yield stress measurement in cemented paste backfill. *International Journal of Mining, Reclamation and Environment*, *27*(4), 231–256. https://doi.org/10.1080/17480930.2012.680754

Singer PC, Stumm W (1970) Acidic mine drainage: the rate-determining step. Science 167:1121–1123

Tamás, F. D., Farkas, E., Vörös, M., and Roy, D. M. (1987). Low-frequency electrical conductivity of cement, clinker and clinker mineral pastes. *Cement and Concrete Research*, *17*(2), 340–348. https://doi.org/10.1016/0008-8846(87)90116-5

Tarì, G., Ferreira, J. M. F., and Fonseca, A. T. (1999). Influence of particle size and particle size distribution on drying-shrinkage behaviour of alumina slip cast bodies. *Ceramics International*, *25*(6), 577–580. https://doi.org/10.1016/S0272-8842(98)00068-6

Tariq, A, and Ernest, K. Y. (2013). A Review of Binders Used in Cemented Paste Tailings for Underground and Surface Disposal Practices. *Journal of Environmental Management*, 131, 138–149. https://doi.org/10.1016/j.jenvman.2013.09.039

Xiapeng, P., Fall, M., and Haruna, S. (2019). Sulphate induced changes of rheological properties of cemented paste backfill. *Minerals Engineering*, *141*, 105849-. https://doi.org/10.1016/j.mineng.2019.105849

Xue, G., Yilmaz, E., Song, W., & Cao, S. (2018). Compressive strength characteristics of cemented tailings backfill with alkali-activated slag. *Applied Sciences, 8*, 1537. doi:10.3390/app8091537.

Yilmaz, E., Benzaazoua, M., Belem, T., & Bussière, B. (2009). Effect of curing under pressure on compressive strength development of cemented paste backfill. *Minerals Engineering*, *22*(9), 772–785. https://doi.org/10.1016/j.mineng.2009.02.002

Yılmaz, T., Ercikdi, B., Karaman, K., Külekçi, G., (2014). Assessment of strength properties of cemented paste backfill by ultrasonic pulse velocity test. Ultrasonics http://dx.doi. org/10.1016/j.ultras.2014.02.012.

Yin, S., Wu, A., Hu, K., Wang, Y., and Zhang, Y. (2012). The effect of solid components on the rheological and mechanical properties of cemented paste backfill. *Minerals Engineering*, *35*, 61–66. https://doi.org/10.1016/j.mineng.2012.04.008.

Zhou, Y., Fall, M (2022). Flow ability of cemented paste backfill with chloride-free antifreeze additives in sub-zero environments. Cement and Concrete Composites 126:104359.

Zingg, A., Winnefeld, F., Holzer, L., Pakusch, J., Becker, S., and Gauckler, L. (2008). Adsorption of polyelectrolytes and its influence on the rheology, zeta potential, and microstructure of various cement and hydrate phases. *Journal of Colloid and Interface Science*, *323*(2), 301–312. https://doi.org/10.1016/j.jcis.2008.04.052

Zingg, A., Winnefeld, F., Holzer, L., Pakusch, J., Becker, S., Figi, R., and Gauckler, L. (2009). Interaction of polycarboxylate-based superplasticizers with cements containing different C3A amounts. *Cement and Concrete Composites*, *31*(3), 153–162. https://doi.org/10.1016/j.cemconcomp.2009.01.005

CHAPTER FOUR.

TECHNICAL PAPER II: RHEOLOGICAL CHARACTERISTICS OF CEMENTED PASTE TAILINGS FOR UNDERGROUND MINING OPERATIONS: VARIATIONS WITH PYRITE CONTENT.

Paper submitted for publication

Oyewale Miracle, Mamadou Fall and Ghirian Alireza

Department of Civil Engineering, University of Ottawa.
800 King Edward Ave, Ottawa, ON, K1N 6N5, Canada.

4.1 ABSTRACT

Iron sulphide minerals, particularly pyrite (FeS_2), found in mine waste pose significant challenges to the global mining industry due to their chemical reactivity and potential to cause acid rock drainage (ARD). Cemented paste backfill (CPB) has emerged as an innovative technique to mitigate these environmental issues while providing structural support in underground mining operations. However, the rheological behaviour of CPB containing pyrite-bearing tailings and the effects of utilizing blended binders remain insufficiently understood. This research investigates the evolution of yield stress and viscosity over time in CPB with varying pyrite content (0%, 5%, 15%, 45%) and different binder types (PCI (100), PCI/SLAG (50:50)). Samples were prepared and analyzed over curing times of 0, 20, 60, and 120 minutes. Additional tests, including electrical

conductivity, pH, zeta potential, thermal, and microstructural analyses, were performed to confirm the validity of the experimental results. The findings reveal that pyrite content significantly impacts the rheological properties of CPB, with both yield stress and viscosity increasing with increasing pyrite levels. Moreover, the results also show that incorporating pyrite-bearing tailings with blended binder reduced yield stress and viscosity compared to 100% PCI samples. These findings highlight that optimizing CPB flowability requires a careful analysis of pyrite content and binder type, which is vital for successful underground tailings management and mining operations.

Keywords: Cemented paste backfill, Pyrite, Tailings, Mine, Yield stress, Viscosity, Rheology.

4.2 INTRODUCTION

Iron sulphide minerals such as pyrite (FeS_2) exhibit high reactivity as accessory minerals in mining environments (Agboola et al., 2020). They often coexist with economically valuable minerals like gold, copper and lead (Deditius et al., 2011; Large et al., 2009; Hofstra and Cline, 2000; Reich et al., 2013), and their presence in ore deposits and subsequently in mine tailings remains a significant challenge for the global mining sector (Ohlander et al., 2012). This challenge arises from the ambiguities associated with the disposal of pyrite-containing tailings, especially when using conventional methods. Such methods generally increase the propensity of pyrite-bearing tailings to undergo oxidation as tailings are typically stored in open storage facilities without additional treatment or stabilization. This exposure facilitates extensive interaction of tailings with air and water, leading to oxidative reactions that can result in ARD. The resulting ARD poses severe environmental risks and incurs environmental liabilities for mining companies (Kumari et al., 2010).

The risks and consequences, as well as the negative public perception associated with the conventional disposal of pyrite-bearing tailings, have prompted the mining industry to adopt new techniques for the management of ARD (Alakangas et al., 2013; Fall et al., 2009). Amongst these techniques, cemented paste backfilling (CPB) stands out as the most advantageous technology for managing pyrite-bearing tailings. CPB is an innovative mine waste management technique that aims to mitigate geotechnical and environmental problems arising from mining operations. This is achieved by depositing mine wastes (tailings) into excavated mine cavities, thereby providing structural support for the roofs of underground stopes, while also simultaneously reducing voluminous mine wastes and acidic mine discharges (Fall et al., 2009; Qi et al., 2018; Ma et al., 2021, Cui and Fall., 2016). Furthermore, CPB can also enhance mineral recovery, boost mine production rates, eliminate the need for drainage construction and extend the overall service of the mine (Fall et al., 2008; Kesimal et al., 2005; Hassani and Archibald, 1998).

CPB is a cement-based mixture comprising 70-85% dewatered tailings by weight, a binding agent (usually ordinary Portland cement between 2% to 7% by total weight), and water (either fresh and/or mine processed) (Alakangas et al., 2013; Fall et al., 2008; Yilmaz, 2010). The components of CPB are usually prepared on the mine surface and transported to underground cavities either through gravity flow or by pumping. Consequently, the transportability/flowability of fresh CPB is a vital parameter and a key engineering design criterion for the successful implementation of cemented paste backfilling (Yilmaz, 2010; Hassani et al., 2001). However, its rheological properties, particularly when using pyrite-bearing tailings, are not well understood, as it is presumed that the incorporation of highly reactive pyrite tailings may introduce a new set of challenges that may alter the flow behaviour of CPB.

One primary challenge is the possibility that adding pyrite-bearing tailings to CPB mixtures might alter the flow behaviour of CPB, consequently leading to increased operational costs. This issue is particularly significant in underground tailings management, especially for mines operating at greater depths. Given the known fact that transporting CPB over long distances to reach deeper mine cavities inherently takes more time and considering that the integral components of CPB include water and binder, it is presumed that the presence of highly reactive pyrite-bearing tailings in CPB mixtures might affect the hydration reactions during long-distance transportation into mine cavities, thereby resulting into changes in CPB properties that may cause premature solidification and stiffening of CPB (Wu et al., 2013; Wang et al., 2016). Consequently, this might reduce the flowability of CPB, and cause blockage of pipe systems, ultimately increasing the operational costs of the cemented paste backfilling process. Despite the significance of understanding how pyrite content influences the flowability/transportability of CPB for underground paste tailings disposal, a comprehensive research study addressing this knowledge gap is currently lacking in literature.

Hence, there is a pressing need for further investigation into this area to facilitate more informed decision-making and optimize cemented paste backfilling practices in mining operations.

Another notable challenge presumed to emerge is the alteration of CPB properties due to the synergistic effect of incorporating pyrite-bearing tailings with partially blended PCI binders. Generally, Portland cement is the most commonly used binding material in CPB because of its availability, versality, ability to improve the compressive strength and structural integrity of the backfill materials. However, when used as the sole cementitious component, PCI contributes to over 70% of the overall CPB cost, thereby reducing the economic viability of the cemented paste backfilling method. Furthermore, the manufacturing process of PCI consumes a large amount of energy and is linked to substantial environmental pollution, leading to significantly high CO_2 emissions (Tayeh et al., 2020). Numerous studies have highlighted the unsustainable nature of relying solely on PCI, as each ton of production generates about 0.85 -1.12 tons of CO_2, thereby contributing to approximately 5-8% of global CO_2 emissions (Wang et al., 2016; Cao et al., 2018; Qiu et al., 2019). Hence, scientific findings have reported that using low-carbon and cost-effective binders like slag as partial substitutes for PCI can aid in reducing the carbon footprint associated with the use of PCI in CPB (Zhao et al., 2021). However, the potential flowability issues that may arise when utilizing pyrite tailings in CPB mixtures with these blended binders remain unknown. Consequently, there is a gap in existing literature that needs further investigation into this aspect to comprehensively understand the implications of using blended binders in conjunction with pyrite-bearing tailings in CPB.

The flow behaviour and transportability of CPB are determined by its rheological properties, particularly its yield stress and viscosity. In rheology, yield stress is the threshold shear stress required to induce the flow of fresh CPB (Simon and Grabinsky, 2013), while viscosity quantifies the material's resistance to shear deformation or its impediment to flow (Akbar et al.,

2009). Both parameters are important indicators of the cohesive forces between particles in fresh CPB, which serves as a critical factor for pump selection, as well as for evaluating flow stability and energy dissipation (Xiapeng et al., 2019).

Previous studies on CPB rheology (Dzuy and Boger, 1985; Penner and Lagaly, 2001; Park et al., 2005; Simon and Grabinsky, 2013; Haiqiang et al., 2016) have demonstrated that the yield stress and viscosity are influenced by several factors. These include curing temperature (Wu et al., 2013; Haiqiang et al., 2016), the presence of chemical additives (Simon and Grabinsky, 2013; Jiang et al., 2017), progression of binder hydration and its products, as well as the physical and chemical characteristics of the tailings (Huynh et al., 2006; Simon and Grabinsky, 2013; Wu et al., 2013; Hot et al., 2014). Unfortunately, there is still a lack of studies that have focused on understanding how the pyrite content in tailings alters/impacts the time-dependent rheology of paste tailings for underground tailings management or the complications in CPB operation that may arise when using blended binders in conjunction with high pyrite content tailings. This study, therefore, examines the effects of pyrite content and blended binders on the evolution of yield stress and viscosity in CPB for underground tailings management.

4.3 EXPERIMENTAL PROGRAM

4.3.1 MATERIALS USED

4.3.1.1 TAILINGS

Synthetic pure high-purity silica tailings (ST), composed of 99.8% quartz (a mineral predominant in tailings from hard rock mines in Canada) sourced from U.S. Silica Co., were used as the main PT components in this mixture. Compared to natural tailings (NT), ST are non-reactive and do not generate acid, providing better control over uncertainties associated with reactive elements present in NT. Figure 1 illustrates the grain size distribution of ST and compares it with the average grain size distribution of tailings from nine different Canadian mines. The physical and mineralogical characteristics of ST are given in Tables 1 and 2, respectively.

Table 1: Physical characteristics of Silica tailings utilized.

ELEMENT	G_s(µm)	D_{10}(µm)	D_{30}(µm)	D_{50}(µm)	D_{60}(µm)
ST	2.7	1.9	9.0	22.5	31.5
Average of 9 types of tailings	-	1.8	9.1	20.0	30.8

Gs: specific gravity; Ss: specific surface area

Table 2 Mineralogical composition of Silica tailings utilized.

TAILINGS (wt.%)	MINERAL											
	Quartz	Albite	Dolomite	Calcite	Chlorite	Magnetite	Pyrite	Talc	Pyrrhotite	Spinel	Others	Total
ST	99.8	-	-	-	-	-	-	-	-	-	0.2	100

ST: Silica tailings; wt.: weight.

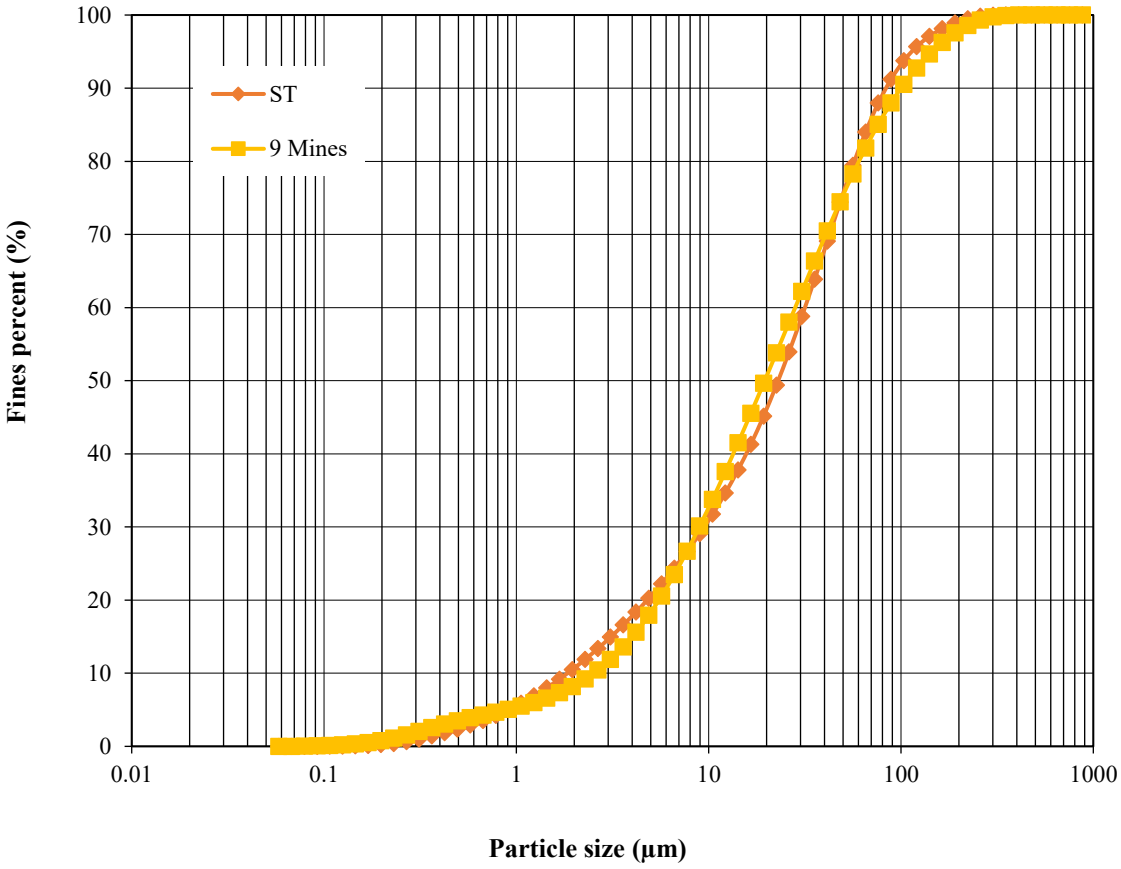

Figure 1: Grain size distribution of utilized Silica tailings compared to the average tailings from nine Canadian mines.

4.3.1.2 BINDER

This research utilized, Type I Portland cement (PCI), the most widely used binder in CPB mixtures, as the primary binding material. Granulated ground blast furnace slag (SG), a mineral byproduct, was included in selected CPB mixtures to partially replace PCI. The adoption of blended binders is considered as a more economical option due to the high cost of PCI. Moreover, substituting PCI with SG contributes to reducing the carbon footprint of the CPB technology. The ratio of PCI to SG in this investigation was 50/50 by weight. The physical and chemical composition of PCI and SG are outlined in Table 3.

Table 3 Physical and chemical composition of PCI and SG powders.

	Na_2O	MgO	Al_2O_3	SiO_2	K_2O	CaO	TiO_2	MnO	Fe_2O_3	LOI	Relative density	Specific surface area (cm^2/g)
PCI	0.341	2.577	4.808	20.375	0.962	62.700	0.225	0.054	3.609	2.162	3.2	1300
Slag	0.284	11.782	10.595	35.572	0.478	39.212	0.467	0.298	0.621	0.388	2.8	2100

4.3.1.3 PYRITE

Pyrite powder (FeS2, M.W. = 119.98) sourced from Washington Mills North Grafton, Inc. was utilized in this research. This pyrite powder has a particle size comparable to that of pyrite minerals typically present in natural tailings. The pyrite powder was combined with ST, PC, and SG to form pyrite-containing tailings mixtures (CPB-ST-PC and CPB-ST-SG) with pyrite content levels of 0, 5, 15, and 45 wt.%. The physical properties of the pyrite used in this research are detailed in Table 4.

Table 4: Physical and Chemical properties of pyrite.

BULK (g/cm^3)	DENSITY	DENSITY AT 20 °C (g/cm^3)	SP. GRAVITY	PH	MELTING POINT
2.35		4.7	4.6	4.0-6.0	1193

Sp: specific.

4.3.1.4 MIXING WATER

All tailings and binder mixtures in this study were prepared using tap water. A water-to-binder (w/b) ratio of 7.8 was utilized for the preparation of all specimens.

4.3.2 SPECIMEN PREPARATION AND MIX PROPORTIONS

The CPB samples analyzed in this research study (CPB-ST-PC and CPB-ST-SG) were prepared according to the procedure detailed in Table 5. Silica tailings, pyrite, and binders were precisely weighed and mixed for 5 mins using a mechanical mixer at a constant mixing speed at room temperature. The pre-measured amount of tap water was then introduced into the mixture, and the blending continued for an additional 5 minutes to ensure a uniform paste and transferred to plastic cylindrical moulds with a diameter of 10 cm and height of 20 cm and cured according to the plan in Table 5. In the present study, samples were cured for 0,20,60 and 120 mins.

Table 5: Experimental design for rheological tests for CPB samples

SAMPLE NAME	TAILINGS TYPE	BINDER TYPE	BINDER CONTENT (vl%)	PYRITE CONTENT (w%)	VOL. W/VOL. B RATIO	CURING TIME (min)
CPB-ST-PC-0	ST + PY	PCI	4.5	0	7.8	0, 20, 60, 120
CPB-ST-PC-5	ST + PY	PCI	4.5	5	7.8	0, 20, 60, 120
CPB-ST-PC-15	ST + PY	PCI	4.5	15	7.8	0, 20, 60, 120
CPB-ST-PC-45	ST + PY	PCI	4.5	45	7.8	0, 20, 60, 120
CPB-ST-SG-0	ST + PY	PCI/SG(50/50)	4.5	0	7.8	0, 20, 60, 120
CPB-ST-SG- 15	ST + PY	PCI/SG(50/50)	4.5	15	7.8	0, 20, 60, 120
CPB-ST-SG-45	ST + PY	PCI/SG(50/50)	4.5	45	7.8	0, 20, 60, 120

V%- Volume percentage; W%- Weight percentage; Vol.w/Vol.b- Volume of binder/Volume of water ratio; SG: slag; PY: pyrite; ST: silica tailings.

4.3.3 TEST METHODS

4.3.3.1 VISCOSITY TEST

Viscosity measurements for all samples were conducted using the Brookfield digital viscometer (DV-E model) manufactured by Brookfield Engineering Laboratories Inc. Each measurement was repeated at least in two trials, and the average was taken in this study.

4.3.3.2 YIELD STRESS

The Wykeham-Ferrance laboratory vane shear apparatus was used to assess the yield stress of each mixture following the guidelines outlined in the ASTM D4648/D4648M-16. This instrument determines the fluid's viscosity at specific shear rates by rotating a spindle at a constant speed with the help of a calibrated spring. Viscosity is measured by detecting the resistance of the fluid against the spindle using a rotary transducer, which generates a torque signal that is interpreted as a spring deflection (Brookfield, 2016). The selection of spindles depends on the viscosity range of the sample being tested. In this study, an RV6 spindle was used as recommended in the manual. To prevent air entrapment, the spindle was carefully placed into the sample. The viscometer was then activated, and the reading was allowed to stabilize before recording at a fixed speed of 50 rpm for one minute. Each test was repeated at least twice to ensure repeatability of results.

4.3.3.3 ELECTRICAL CONDUCTIVITY MONITORING

To better understand the mechanisms driving changes in the rheological behaviour of the samples, a TEROS-12 sensor, with a measurement precision of ±5, was utilized to measure the electrical conductivity (EC) of each mix sample (MMM Tech, n.d). The variation in EC serves as an indicator of ion mobility resulting from chemical reactions and water content within the CPB. This parameter is valuable for evaluating the progress of cement hydration (Tamás et al., 1987; McCarter and Curran, 1984; Aschan, 1966) and monitoring structural changes in hydrating cementitious systems (Courard et al., 2014). For EC measurement, the TEROS-12 sensor, designed to apply an alternating electrical current across its two electrodes and determine resistance, was placed inside a cylindrical plastic container (10 cm in diameter and 20 cm in height) filled with CPB. Readings were recorded every minute for a total duration of 6 hours.All measurement data were collected and stored using the Em50 data logger manufactured by Decagon Devices, Inc.

4.3.3.4 pH AND ZETA POTENTIAL MEASUREMENTS

The surface chemical characteristics of particles play a crucial role in determining the rheological behaviour of suspensions (e.g., Leong and Boger 1990, Bradley et al. 1991, and Johnson et al. 2000). In this research, the pH and zeta potential (ZP) of CPB samples were analyzed to determine the surface chemical properties of the particles. The pH levels were measured using an Oakton pH 6+ meter, with a measurement accuracy of ±0.01 (Oakton, n.d). To ensure data reliability, at least two measurements were taken, and the average values were reported. Zeta potential analysis was performed using the Malvern Zetasizer Nano series, which determines electrophoretic mobility in suspensions via phase analysis light scattering (PALS). The zeta potential values were calculated based on the Henry equation (Clogston and Patri, 2011). For accuracy, each ZP test was conducted at least three times per sample, and the average results were documented.

4.3.3.5 MICROSTRUCTURAL ANALYSIS

To gain deeper insights into the microstructural characteristics and binder hydration progress of the tested materials, as well as their influence on the rheological behaviour of the studied paste tailings, thermal gravimetry (TG), differential thermal gravimetry (DTG), and x-ray diffraction (XRD) analyses were conducted on the CPB cement paste samples. These methods assess microstructural attributes and transformations within the CPB. The samples were first prepared and cured for 20-60 minutes, after which they were oven-dried at 45 °C for four days to remove any free water. Once the mass stabilized, the samples were ground into a fine powder for microstructural evaluation.

4.4 RESULTS AND DISCUSSION

4.4.1 EFFECT OF PYRITE CONTENT ON THE RHEOLOGICAL PROPERTIES OF CPB

To assess how the pyrite content in tailings influences the flowability and transportability of CPB, the progression of yield stress and viscosity over time were analyzed, with the findings illustrated in Figures 2a and 2b.

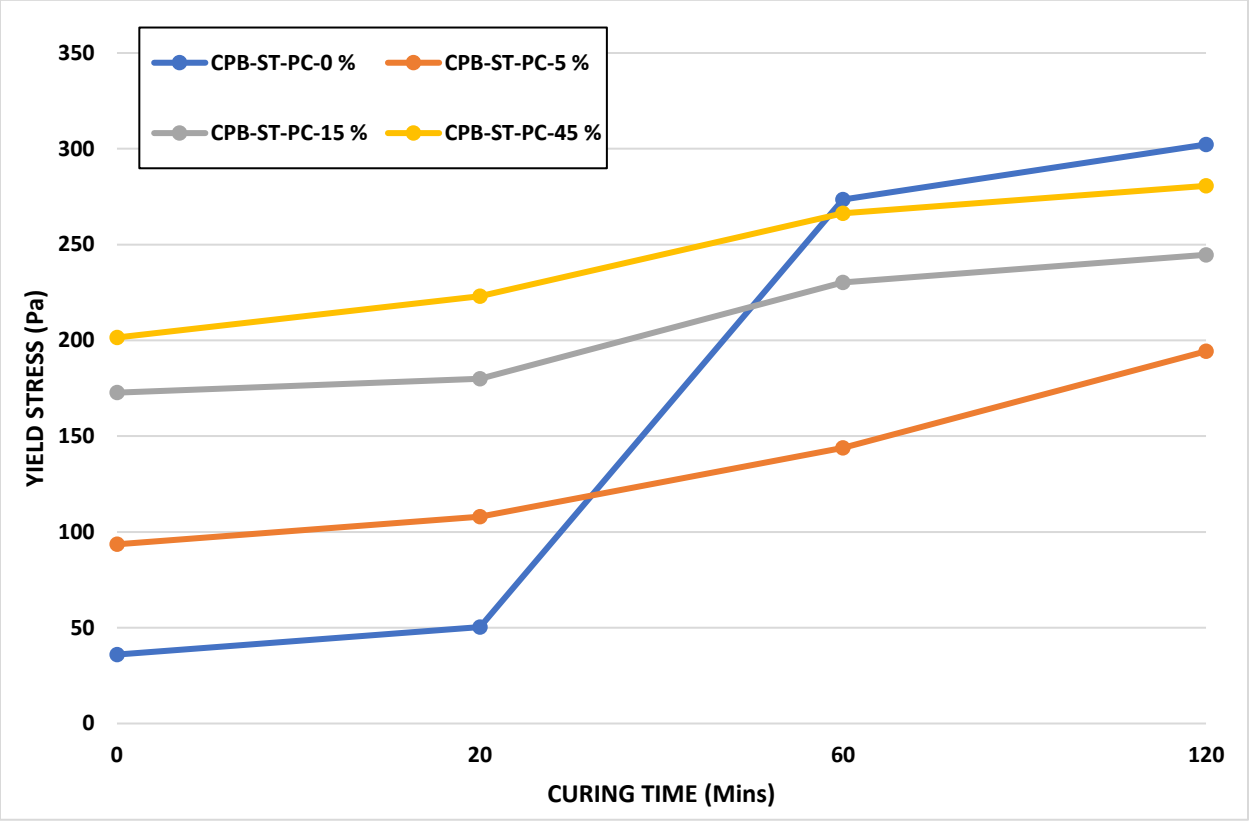

a) Yield stress

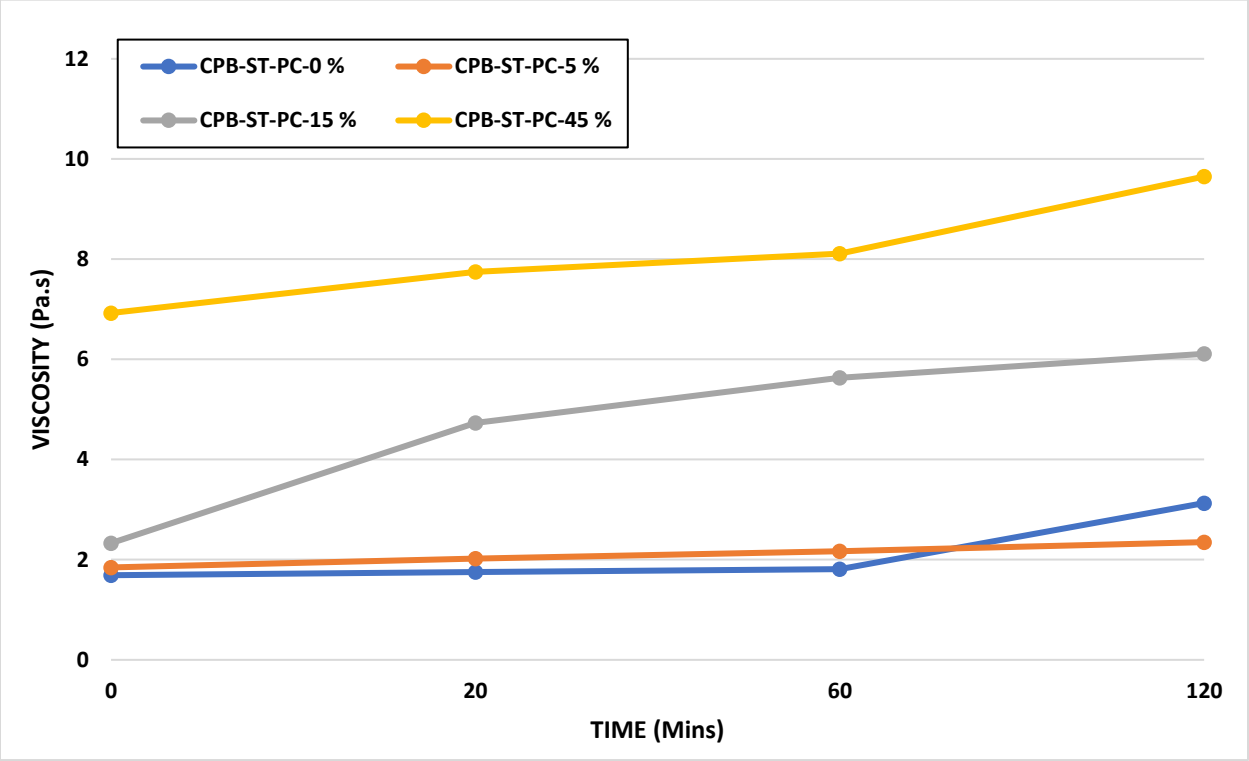

b) Viscosity

Figure 2: Time-dependent evolution of yield stress (2a) and viscosity (2b) of CPB mixtures with different pyrite contents.

These figures show there was a significant uptrend in both yield stress (Fig. 2a) and viscosity (Fig. 2b) in all CPB mixtures as the curing time progressed, regardless of the presence or absence of pyrite. Figure 2 also shows that the pyrite content significantly altered the flow properties of CPB, irrespective of CPB age. The CPB mixtures without pyrite content (CPB-ST-PC-0%) had a much lower initial yield stress of 35.9 Pa compared to other samples (Fig. 2a). However, as the pyrite content gradually increased from 5% to 45%, the initial yield stress was seen to increase from 93.5 Pa (CPB-ST-PC-5%, i.e. CPB with 5% pyrite content) to 201.4 Pa (CPB-ST-PC-45%, CPB with 45% pyrite content), and this trend was seen to increase as curing time increased in all mixtures.

More specifically, at a curing time of 120 minutes, the yield stress of CPB-ST-PC-5% had a final yield stress of 201Pa, while the yield stress of CPB-ST-PC-45% was at 280.6 Pa. The viscosity results are also similar to yield stress results, as viscosity was seen to also increase with increasing pyrite content (Figure 2b). The sample without pyrite (CPB-ST-PC-0%) was seen to have the lowest initial viscosity of 1.69 Pa.s, while the samples with the highest pyrite content (CPB-ST-PC-45%) had the highest initial viscosity of 6.9 Pa. Similar to yield stress results, viscosity was also seen to increase as time progressed. Hence, the results suggest two key conclusions: 1) the rheological properties of CPB increase with increasing pyrite content, and 2) the rheological properties of CPB increase as time progresses. The mechanisms responsible for these changes are discussed below.

1) The rheological parameters of CPB increase with increasing pyrite content.

The observed increase in both yield stress and viscosity with increasing pyrite content in the CPBs can be ascribed to the unique characteristics of pyrite minerals to alter/modify the material properties of CPB. Pyrite, being a sulphide mineral is composed of iron and sulphur, hence, it possesses distinct physical and chemical properties that can impact the overall composition of CPB thereby causing changes in its rheological behaviour. One such physical property is the physical nature of pyrite to be denser (specific gravity of pyrite = 4.6; Table 4) than other components of the CPB mixture (specific gravity of the quartz = 2.7; Table 1). So, the introduction of highly dense pyrite is likely to modify the arrangement of particles in the mixture and encourage a more tightly packed structure. Therefore, as pyrite is incorporated into the CPB mix and its content increases from 5% to 45%, it contributes to a more complex and interconnected network within the CPB, leading to higher overall density and specific gravity, which causes higher resistance to deformation (yield stress) and increase in internal friction (viscosity).

In addition to the previously discussed physical properties, another factor that contributes to the elevated change in rheological behaviour caused by an increase in pyrite content can be attributed to alterations in the chemical properties of CPB due to pyrite's ability to undergo oxidative reactions. When pyrite undergoes oxidation, it produces various by-products, including sulfuric acid (H_2SO_4). These chemical transformations lead to acid generation, which contributes to a decrease in pH within CPB. Decreased pH levels can affect the charged state of particles and their interactions, which may influence the material's viscosity and flow behaviour. Furthermore, the generation of sulfuric acid may also influence the surface charge of particles in the material. These changes in surface charge can alter the electrostatic interactions between particles, thereby affecting their dispersion and aggregation, resulting in elevated levels of yield stress and viscosity. This assertion is further proven experimentally through pH and Zeta potential test results depicted in Figures 3 and 4, respectively.

Based on the results given in Figure 3, a significant shift towards a more acidic condition with increasing pyrite content is noticed. Specifically, as evidenced in Figure 3, the sample without pyrite (CPB-ST-PC-0) is seen to record an initial pH of 11.56; however, with the gradual increase in pyrite content from 5% to 45%, the pH level is seen to decrease drastically in the pyrite containing samples. Specifically, CPB-ST-PC-5% exhibits an initial pH of 11.29, CPB-ST-PC-15% displays an initial pH of 9.63, and CPB-ST-PC-45% shows the most substantial decrease with an initial pH of 5.86.

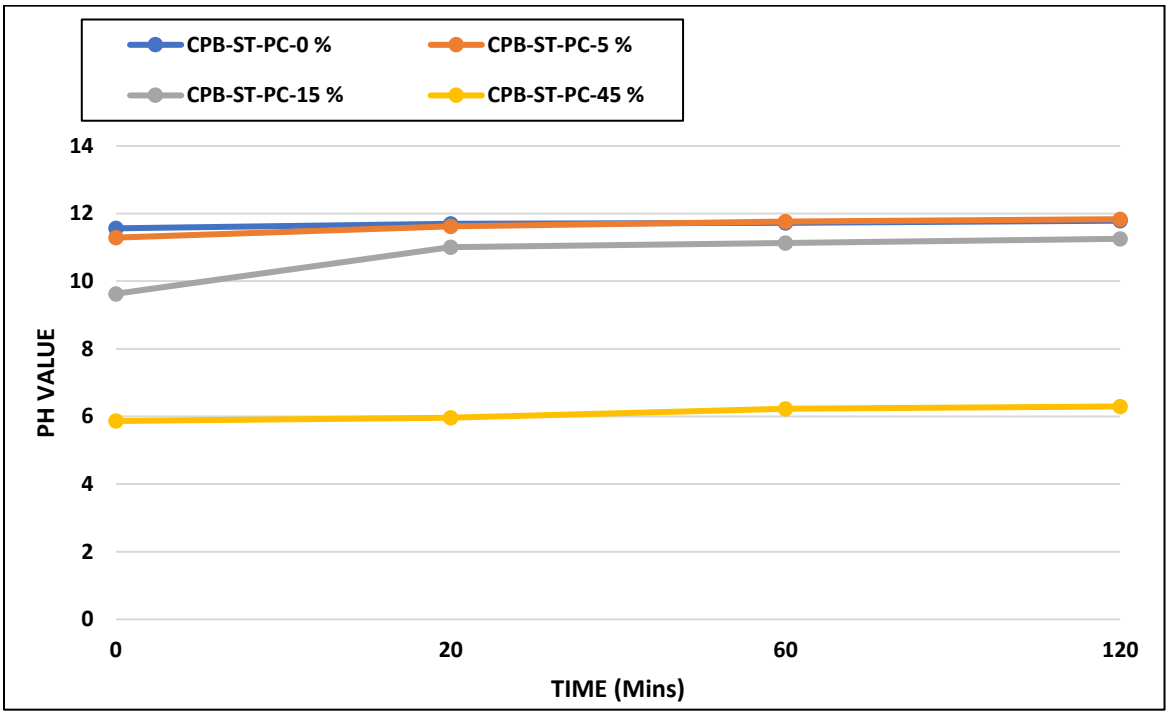

Figure 3: pH of CPB samples with different pyrite content

The pH results given in Figure 3 agree with the results of zeta potential tests shown in Figure 4. Zeta potential serves as a quantitative measure of particle surface charge, with higher values indicating greater ion concentration on particle surfaces (Huynh et al., 2006; Elakneswaran et al., 2009; Hunter, 2013; Haiqiang et al., 2016). This parameter is closely linked with the strength of electrostatic repulsive forces, where a high negative or positive zeta potential leads to particle repulsion, thus reducing their cohesion (Plank and Hirsch, 2007; Zingg et al., 2008). Based on the results in Figure 4, zeta potential absolute values decreased from 28.4 mV in the sample with no pyrite (CPB-ST-PC-0%) to 24.9 mV in the sample with the highest pyrite content (CPB-ST-PC-45%). These results indicate that increased pyrite content decreases the repulsive forces between particles in CPB. Consequently, this causes particles to aggregate, leading to an increase in viscosity (Divet and Randriambololona 1998, Zingg et al. 2008, Elakneswaran et al. 2009). Hence, the changes

in pH and zeta potential can enhance cohesion and particle interactions, potentially leading to higher yield stress (Xiapeng et al., 2019; Nachbaur et al., 1998).

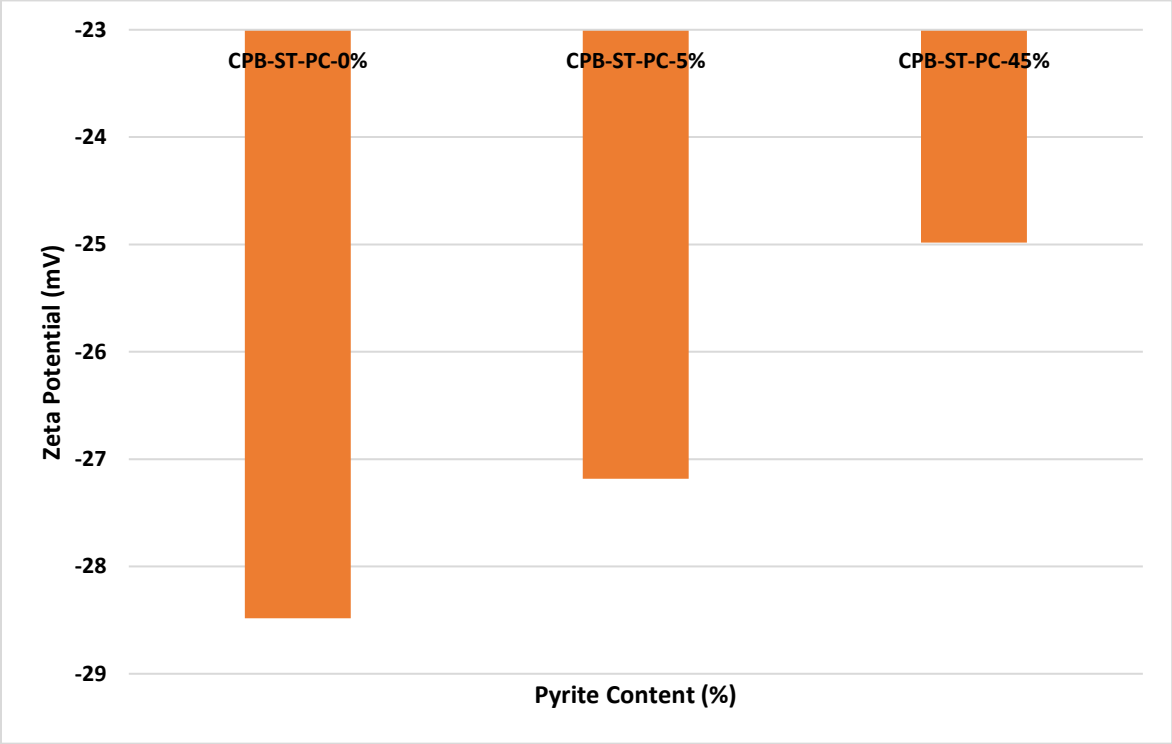

Figure 4: Zeta potential of UPT samples with different pyrite content

2) The rheological parameters of CPB increases as time progresses.

Another trend deduced from the yield stress and viscosity results given in Figure 2 is that rheological properties of each CPB mixture increases as curing time progresses irrespective of the presence or absence of pyrite. This observed trend is attributed to the advancement of the hydration of cement, leading to the formation of hydration products (Haiqiang et al., 2017). Generally, when water is added to cementitious materials, a chemical reaction known as hydration occurs. The cement particles then react with water to form various hydrates, including calcium silicate hydrate (C-S-H) gel (known to contribute to the strengthening of CPB), ettringite and calcium hydroxide (Klein and Simon, 2006; Yin et al., 2012). As hydration progresses, additional hydration by-products are

produced, and the formation of these hydration products increases the interparticle forces within the paste as well as the adhesion between particles. This in turn leads to an increase in the yield stress and viscosity of CPB in samples with and without pyrite materials.

However, in the samples with pyrite content, there's a notable impact of pyrite on the time-dependent yield stress and viscosity development. The samples with pyrite show a consistent trend of lower final yield stress value compared with samples without pyrite content. For example, the sample with 0% pyrite recorded a final yield stress value of 302 Pa while the final yield stress value noticed in samples with pyrite content include 280 Pa (for the 45% pyrite sample), 244 Pa (for the 15% pyrite sample) and 194 Pa (for the 5% pyrite sample). The lower final yield stress value in pyrite-containing samples is due to the delay and inhibition of the cement hydration reaction caused by pyrite.

This inhibition, which produces fewer hydration products, is caused by the formation of ettringite, a hydrated mineral formed through the reaction between sulfate and tricalcium aluminate (C_3A). C_3A exhibits a rapid reaction with sulfate ions, leading to the creation of ettringite when dissolved in a solution. Subsequently, ettringite envelops the surfaces of unhydrated cement particles, thereby impeding further reactions (Pye and Schiavon, 1989; Prince et al., 2003; Lawrence, 1990; Fall and Benzaazoua, 2005; Zingg et al., 2009; Pokharel and Fall, 2013). The presence of pyrite leads to fewer formation of cement hydration products, such as C–S–H gel and CH, which reduces particle cohesion and subsequently lowers the final yield stress of the CPB. This trend is reflected in the EC measurements in Figure 5, where the EC of CPB without pyrite reaches a maximum of 4.67 mS/cm at 4 hours, but the EC of CPB with pyrite fails to reach its peak even after 5 hours. This shows that the sample without pyrite reaches its peak in a shorter time compared to pyrite-containing, which confirms that the presence of pyrite can delay the progression of the hydration reaction. Figure 5 also shows that EC values decrease with increasing pyrite content, which

also confirms that pyrite can reduce the intensity of the hydration reaction. Hence, it is evident that pyrite content contributes to the inhibition of the hydration of cement.

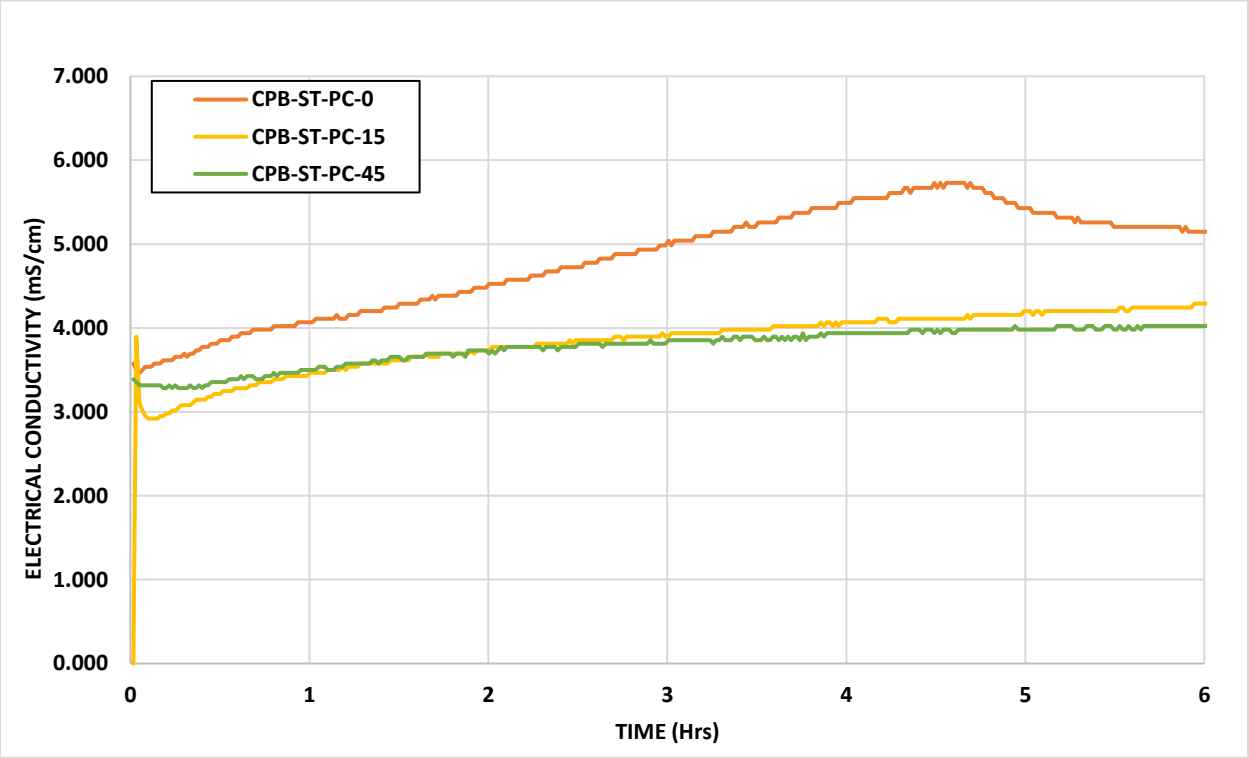

Figure 5: Electrical conductivity progression in CPB with different quantities of pyrite.

The formation of fewer hydration products due to ettringite formation as curing time progressed is further supported by TG/DTG (Figure 6) and XRD results (Figure 7) conducted on cement pastes containing different pyrite content (0 and 50%). Figure 6 reveals that the maximum weight loss occurring at temperatures between 400–450°C is greater in the sample without pyrite (0%) than in those containing 50% pyrite. This suggests a diminished production of Calcium Hydroxide (CH) in cement pastes with higher pyrite content. Furthermore, the X-ray diffraction (XRD) analysis shown in Figure 7 corroborates this observation. The comparison between XRD results for cement pastes with 0 and 50%, cured for 2 hours, indicates that elevated pyrite concentrations over time impede the formation of hydration products. Specifically, the intensity of

the CH peak is higher in the pyrite-free cement paste, whereas the ettringite peak intensity is greater in the sample with 50% pyrite. Thus, both TG/DTG and XRD results underscore the inhibitory effect of high pyrite amounts on hydration product formation.

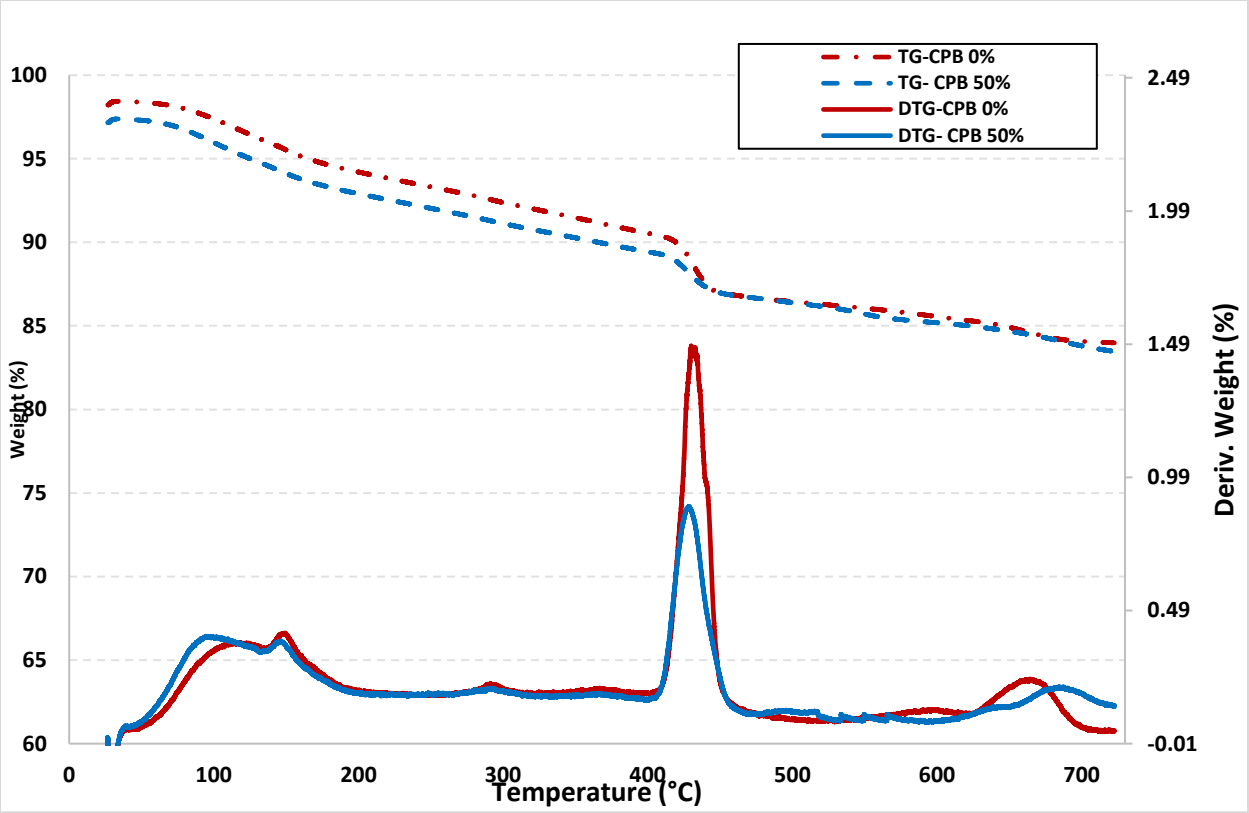

Figure 6: Plotted TG/DTG patterns of CPB with different pyrite content cured for 2hr.

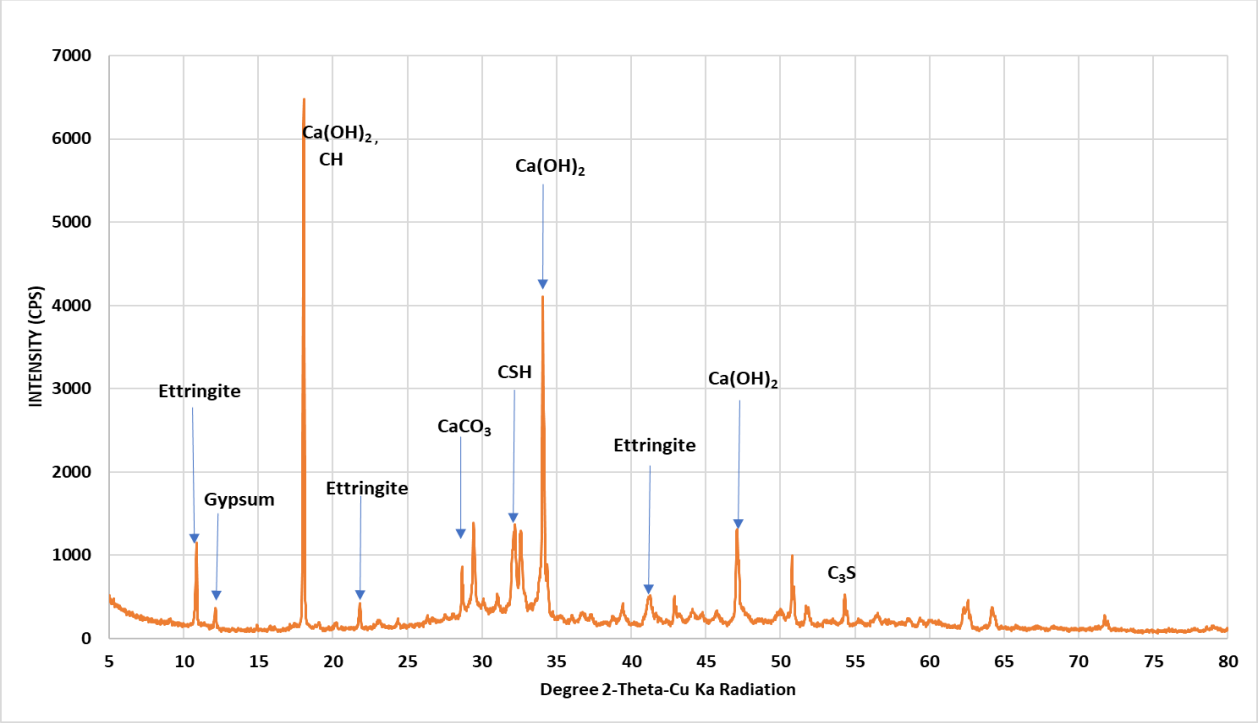

a). 0%

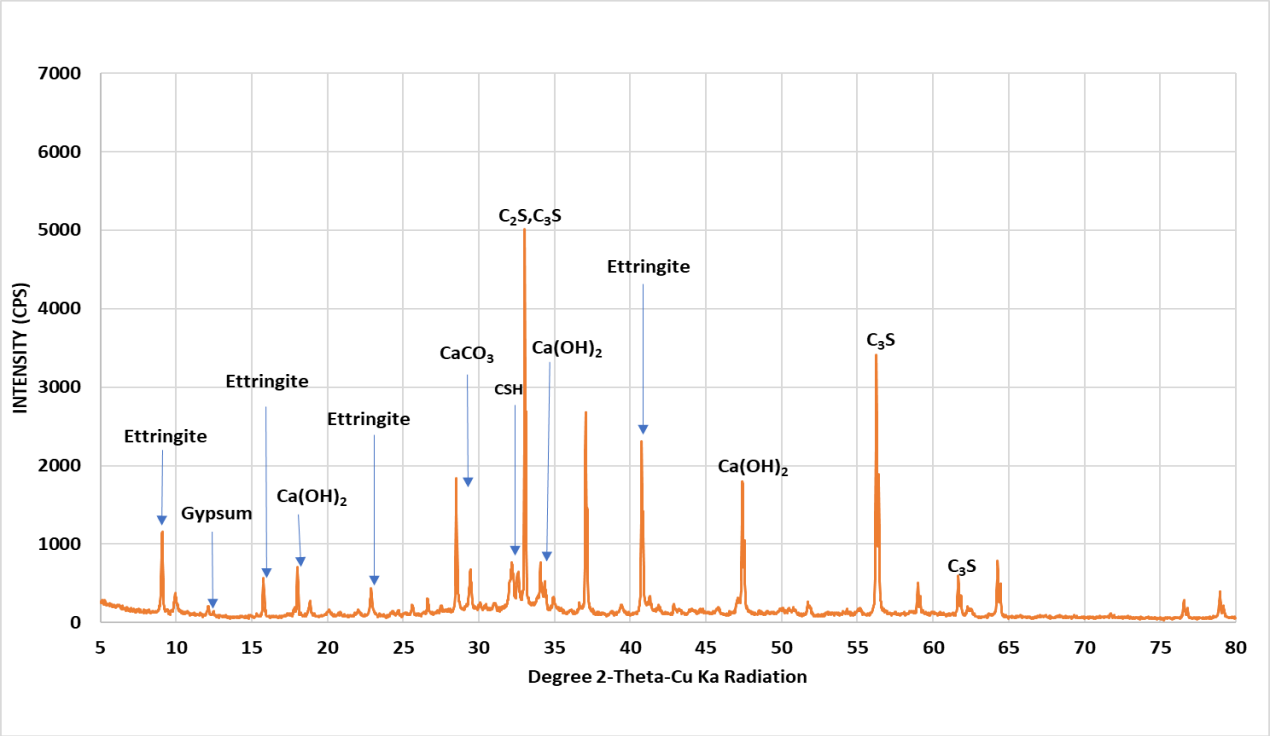

b). 50%

Figure 7: Plotted XRD patterns for CPB with 0% and 50% pyrite contents.

4.4.2 EFFECT OF BINDER TYPE ON THE RHEOLOGICAL PROPERTIES OF PYRITE-BEARING CPB

Figure 8 shows the synergistic effect of binder type (100% PCI, PCI/Slag (50/50)) and pyrite-bearing tailings on the time-dependent evolution of yield stress (Figure 8a) and viscosity (Figure 8b) of the CPB mixtures. To examine this, two binder types with different ratios, namely, 100% PCI and a blended binder containing 50% PCI and 50% SLAG were used in the CPB mix. Samples with 100% PCI included CPB-ST-PC-0% and CPB-ST-PC-45%, while samples with blended binders included CPB-ST-SG-0% and CPB-ST-SG-45%. According to the results, both pyrite content and binder type are seen to significantly affect the rheological behaviour of CPB mixtures. The mechanisms responsible for the increase due to increasing pyrite content have been explained in previous sections. However, samples with PCI partially replaced with slag (PCI/Slag (50/50)) are seen to exhibit a much lower yield stress than samples with 100% PCI. This trend is evident when juxtaposing all 100% PCI (CPB-ST-PC-0%, and CPB-ST-PC-45%), with PCI/SLAG (50/50) samples (CPB-ST-SG-0% and CPB-ST-SG-45%). More specifically, in the CPB-ST-PC-45% sample, initial yield stress at time = 0 mins was recorded at 201 Pa, and as time and cement hydration progressed, final yield stress at time = 120 mins was reported to be at 280 Pa. However, in the PCI/Slag (50/50) samples, a drastic decrease in yield stress was recorded compared to trends recorded in the 100% PCI samples. CPB-ST-SG-45% was initially reported at 79 Pa and finally at 178 Pa at 0 and 120 mins, respectively. Viscosity results also showed similar trends to yield stress results as all PCI/SLAG (50/50) samples were seen to experience at least a 2X decrease in viscosity compared to samples with 100%PCI. Specifically, the CPB-ST-PC-45% sample had an initial and final viscosity of 6.9 and 9.6 Pa.s, while the corresponding slag-containing sample (CPB-ST-SG-45%) had an initial and final viscosity of 3.3 and 4.9 Pa.s, respectively.

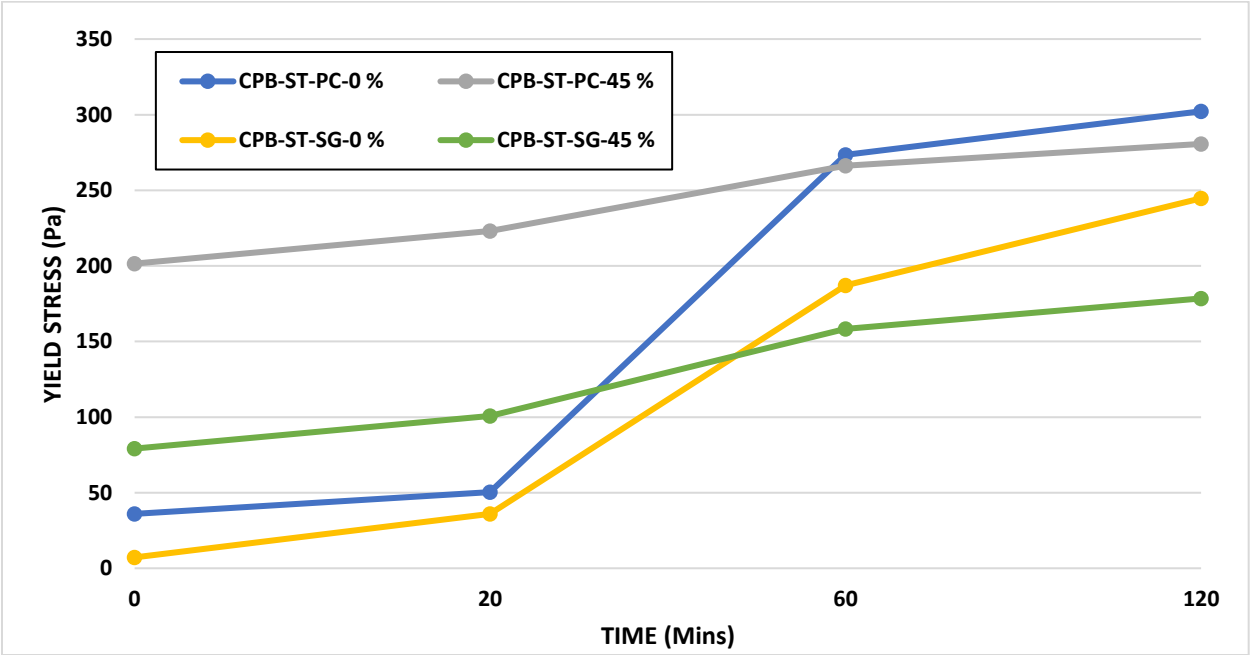

a) Yield stress

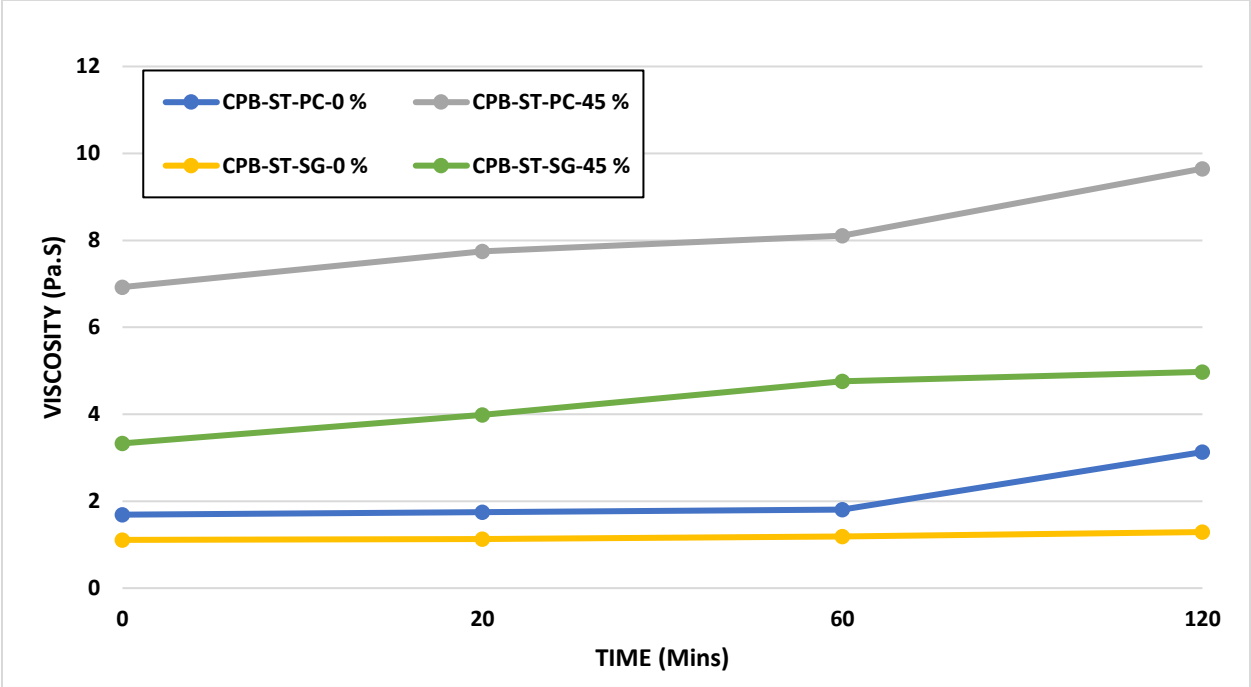

b) Viscosity

Figure 8: Time-dependent evolution of yield stress (8a) and viscosity (8b) of CPB mixtures containing different pyrite contents and types of binder.

The phenomenon responsible for these drastic decrements in the rheological properties of PCI/SLAG (50/50) samples compared to 100% PCI samples can be principally related to the pozzolanic nature of the slag binders. Slag, which is a residual product of the iron-smelting process, is known to impede the reaction kinetics of cement hydration at early ages, especially when hydrated with only water compared to PCI binders. Therefore, hydrating slag with water alone would generally delay the hydration process and formation of hydration products. Hence, to achieve faster rates of reaction, slag needs to be activated with an activator like, alkalis, or lime or Portlandite (CH) produced by the hydration of PCI (Xiao et al., 2021; Pokharel and Fall, 2011; Xue et al., 2018; Jiang et al., 2019). Therefore, the delayed hydration process caused by slag in PCI/SLAG (50/50) samples would lead to the formation of fewer hydration products, and since hydration products are critical in the binding process in CPB mixtures, PCI/SLAG (50/50) samples would generally exhibit a lower density compared to 100% PCI which has higher hydration products. Consequently, this results in the lower yield stress and viscosity values depicted in Figures 8a and 8b, respectively. This explanation is further supported by TG/DTG and XRD results illustrated in Figures 9 and 10, respectively. Figure 9 illustrates TG/DTG diagrams for specimens comprising PCI/Slag (50/50) and 100%PCI. The initial peak observed around 80-110°C indicates dehydration reactions involving specific hydrates like C–S–H, carboaluminates, ettringites, and gypsum. Subsequently, a peak appearing at 400–500°C signifies the dehydroxylation of calcium hydroxide, while a third peak between 650°C and 750°C corresponds to calcite decomposition. A comparison of TG/DTG graphs for these various binders reveals heightened levels of hydration products at early stages when 100% PCI serves as the binder. These observations closely correspond with XRD results (Figure 10), which demonstrate a higher hydrate content in samples composed solely of PCI compared to other binder compositions. Specifically, Figure 10 shows that the C-S-H and CH intensities in the 100% PCI

sample are greater than those in the PCI/Slag (50/50) sample, suggesting a higher formation of hydration products in the specimens composed of 100% PCI.

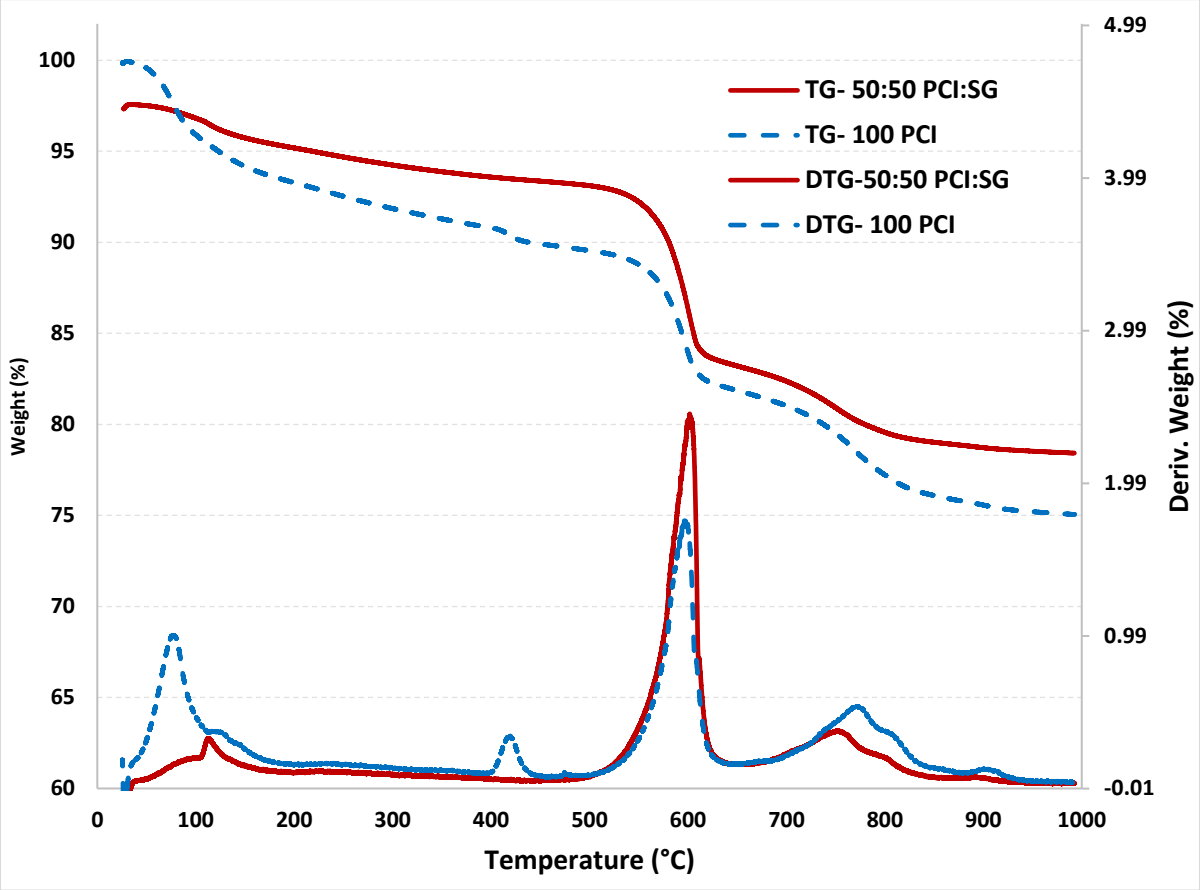

Figure 9: Plotted TG/DTG patterns of LCPT made of 100%PC (100 PCI) and PCI/Slag (50:50).

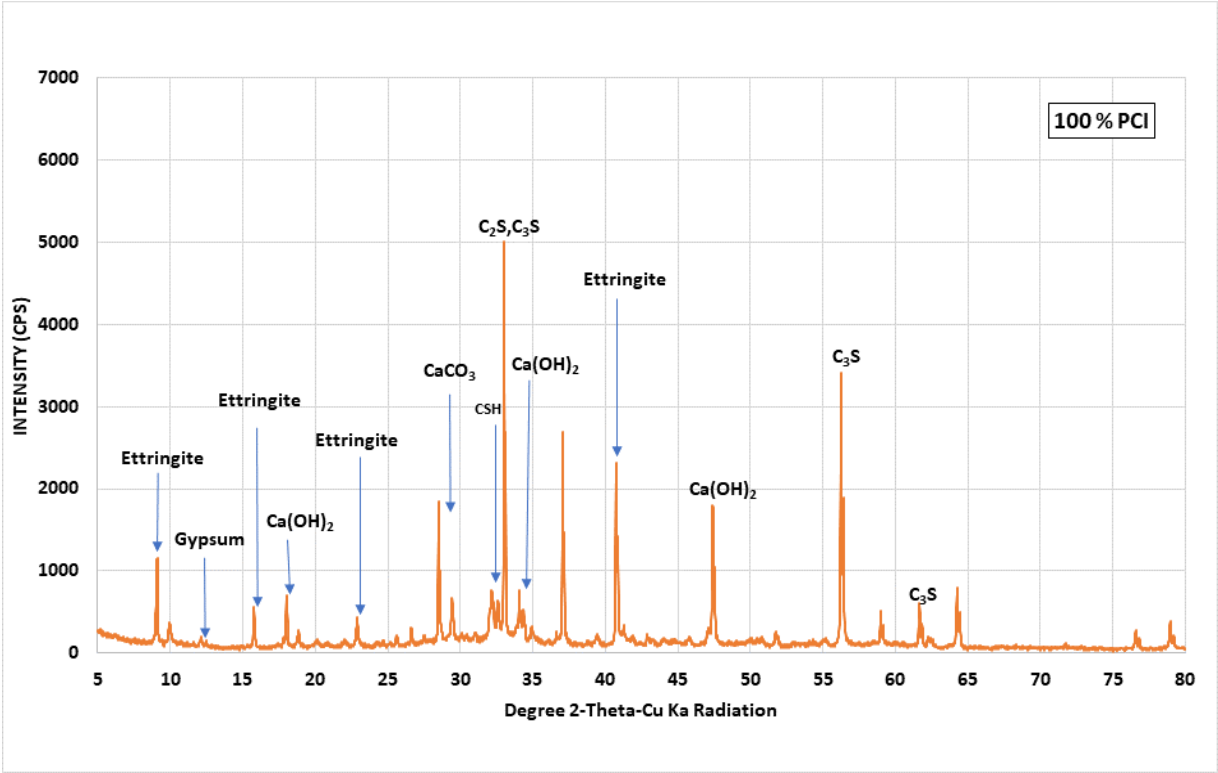

a). 100% PCI

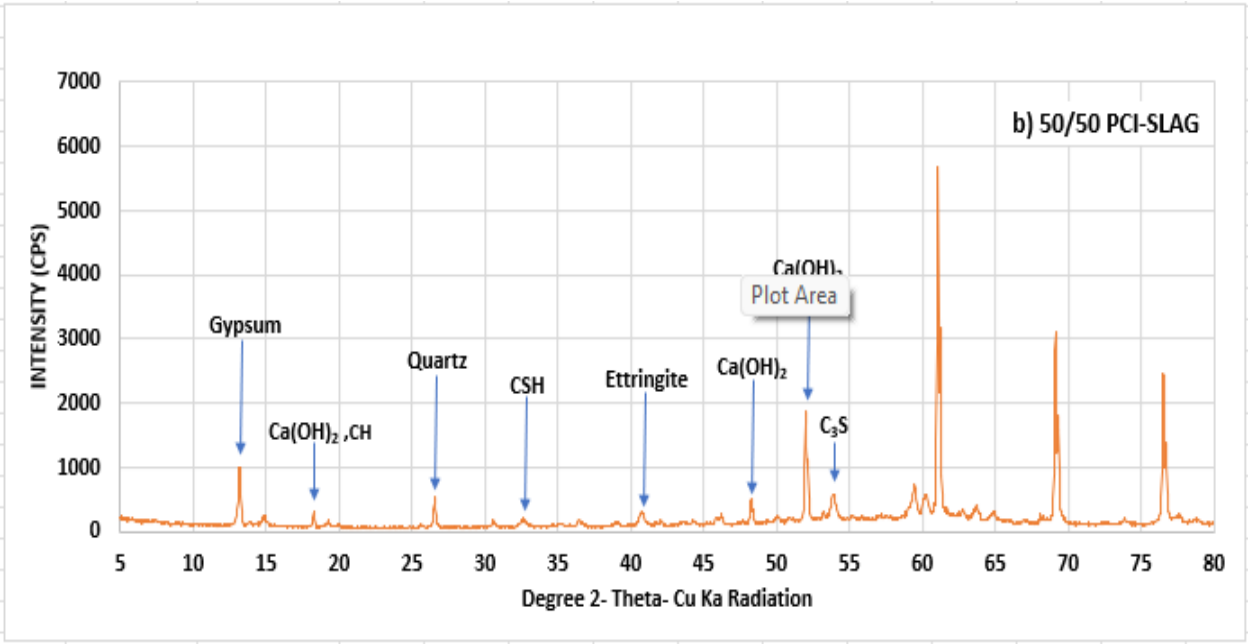

b). 50/50 PCI-SLAG

Figure 10: XRD results of LCPT made of a)100%PC (100 PCI) and b) PCI/Slag (50:50).

Another factor contributing to the noted decrease in rheological properties in the PCI/SLAG (50/50) samples can be changes in electrostatic forces and van der Waals forces in the samples containing slag caused by the introduction of slag into CPB mixtures. According to previous studies (e.g., Elakneswaran et al., 2009; Haiqiang et al., 2016), the introduction of slag will introduce new chemical components to the CPB-SLAG system. Thus, contributing to changes in the chemical composition, surface charge and physical characteristics that can influence electrostatic and van der Waals. This assertion is validated using zeta potential results given in Figure 11. It is evident that CPB with 100% PCI binder (CPB-ST-PC 45%) records a zeta potential of -24.9 mV, while the samples incorporating blended binders (CPB-ST-SG-45%) record a zeta potential value of approximately -25.8 mV. Higher absolute values of zeta potential mean stronger repulsive forces, which would result in lower yield stress and viscosity (Haiqiang et al. 2016). This outcome validates that the introduction of blended binders to CPB mixtures affects surface charges, consequently leading to a reduction in yield stress and viscosity.

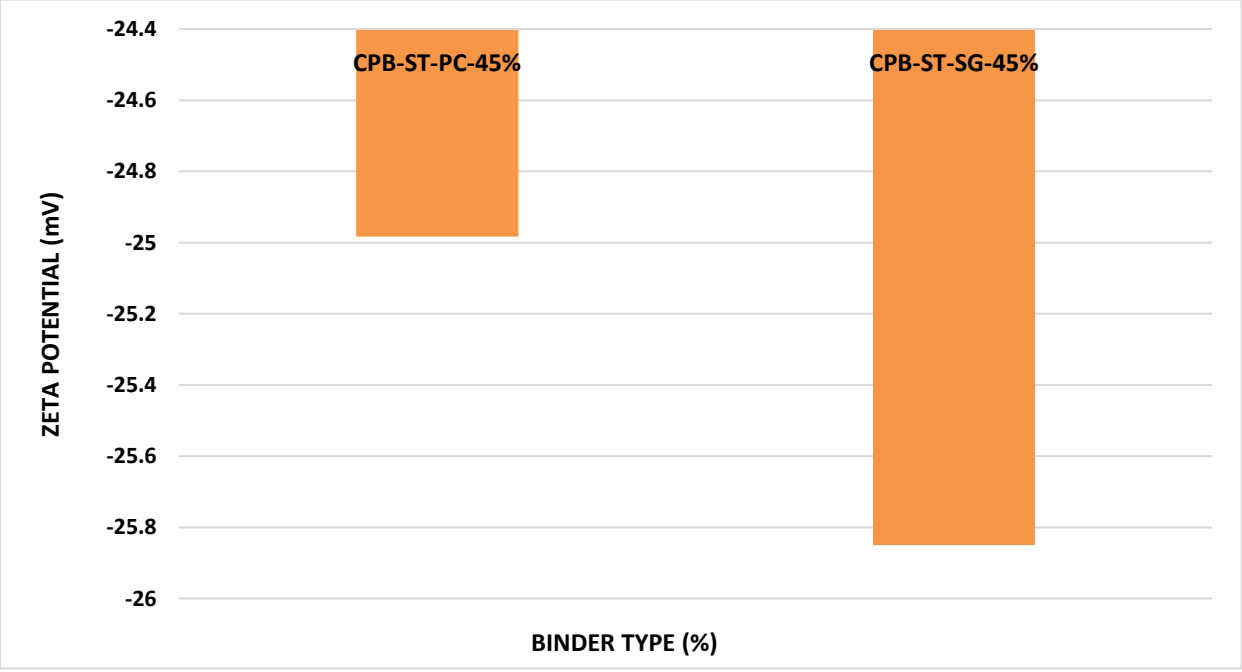

Figure 11: Zeta potential of CPB samples with different binder types at 45% pyrite content.

4.5 SUMMARY AND CONCLUSION

This research experimentally examined the effect of pyrite content as well as the partial replacement of PCI binders on the time-dependent yield stress and viscosity of CPB for successful underground tailings management and mining operations. The experiments focused on varying pyrite content (0%, 5%, 15%, and 45%) and binder types (pure Portland cement and a blend with slag) in the CPB mixtures. Based on the findings of this experimental study, the following conclusions can be inferred:

1. The tailings pyrite content has a notable effect on the flowability of CPB mixtures as both yield stress and viscosity of CPB mixtures were seen to increase drastically as pyrite content increased. This behaviour is attributed to the high density and chemical reactivity of pyrite, which promotes a denser particle packing and induces chemical reactions that alter the flow behaviour of the CPB mixtures.
2. Regardless of the presence or absence of pyrite, CPB flow ability is time-dependent, and the binder used, and its hydration products play a crucial part in the flow ability of CPB. This trend is due to the ongoing hydration processes in the cementitious materials, which produce hydration products that enhance interparticle cohesion and overall mixture stability. However, the presence of pyrite slows down the hydration process, leading to lower final yield stress and viscosity compared to pyrite-free mixtures.
3. The substitution of PCI with 50% slag in CPB samples containing pyrite produces a synergistic effect that significantly lowers the viscosity and yield stress compared to when 100% PCI is used. This reduction is primarily due to the delayed hydration kinetics of slag compared to PCI, resulting in fewer hydration products and, consequently, lower density and flow resistance in the CPB. Additionally, the incorporation of slag introduces changes in electrostatic forces within the mixture, further contributing to reduced rheological

parameters. Hence, the incorporation of slag in pyrite-containing CPB mixtures may be a cost-effective option.

4. The study's auxiliary tests, including pH, zeta potential, electrical conductivity, thermal analysis (TG/DTG), and x-ray diffraction (XRD), confirm that increasing pyrite content induces notable microstructural and chemical changes in the CPB. These changes include a decrease in pH, alterations in surface charge, and the formation of fewer hydration products, all of which affect the rheological behavior of the mixtures.

In conclusion, understanding the impact of pyrite content and binder type on the rheological properties of CPB is crucial for optimizing its performance in underground mining operations. The outcomes of this study provide valuable insights for engineers to enhance the flowability and stability of pyrite-bearing CPB mixtures, ensuring more efficient and cost-effective pyrite-bearing tailings management.

4.6 REFERENCES

Agboola, O., Babatunde, D. E., Isaac Fayomi, O. S., Sadiku, E. R., Popoola, P., Moropeng, L., Yahaya, A., & Mamudu, O. A. (2020). A review on the impact of mining operation: Monitoring, assessment and management. *Results in Engineering*, *8*, 100181-. https://doi.org/10.1016/j.rineng.2020.100181

Akbar, E., Yaakob, Z., Kamarudin, S.K., Ismail, M., Salimon, J., 2009. Characteristic and composition of Jatropha curcas oil seed from Malaysia and its potential as biodiesel feedstock feedstock. Europ. J. Sci. Res. 29 (3), 396–403.

Alakangas, L., Dagli, D., Knutsson, S., 2013. Literature Review on Potential Geochemical and Geotechnical Effects of Adopting Paste Technology under Cold Climate Conditions. Division of Geosciences and Environmental Engineering, Division of Mining and Geotechnical Engineering, Luleå University of Technology.

Alakangas, L., Dagli, D., Knutsson, S., 2013. Literature Review on Potential Geochemical and Geotechnical Effects of Adopting Paste Technology under Cold Climate Conditions. Division of Geosciences and Environmental Engineering, Division of Mining and Geotechnical Engineering, Luleå University of Technology.

Aschan, N. (1966). Determining the setting time of cement paste, mortar and concrete with a copper-lead electrode. *Magazine of Concrete Research*, *18*(56), 153–160. https://doi.org/10.1680/macr.1966.18.56.153

ASTMD4648/D4648M-16. (2016). Standard Test Methods for Laboratory Miniature Vane Shear Test for Saturated Fine-Grained Clayey Soil, ASTM International, 100 Barr Harbor Drive, PO Box C700, West Conshohocken, PA 19428-2959, United States.

Bassam A. Tayeh, Mohammed W. Hasaniyah, Abdullah M. Zeyad, Mohanad M. Awad, Abdulaziz Alaskar, Abdeliazim Mustafa Mohamed, & Rayed Alyousef. (2020). Durability and mechanical properties of seashell partially-replaced cement. *Journal of Building Engineering*, *31*, 101328-. https://doi.org/10.1016/j.jobe.2020.101328

Bradley, J. S., Millar, J. M., and Hill, E. W. (1991). Surface chemistry on colloidal metals: a high-resolution NMR study of carbon monoxide adsorbed on metallic palladium crystallites in colloidal suspension. *Journal of the American Chemical Society*, *113*(10), 4016–4017. https://doi.org/10.1021/ja00010a067

Brookfield, DV-E Digital Viscometer (2016): Operating Instructions. Middleboro, USA. Web, (n.d.) https://pim-resources.coleparmer.com/instruction-manual/ 98945-xx.pdf 2016.

Cao, V. D., Pilehvar, S., Salas-Bringas, C., Szczotok, A. M., Do, N. B. D., Le, H. T., Carmona, M., Rodriguez, J. F., & Kjøniksen, A.-L. (2018). Influence of Microcapsule Size and Shell Polarity on the Time-Dependent Viscosity of Geopolymer Paste. *Industrial & Engineering Chemistry Research*, *57*(29), 9457–9464. https://doi.org/10.1021/acs.iecr.8b01961

Clogston, J. D., and Patri, A. K. (2011). Zeta Potential Measurement. *Characterization of Nanoparticles Intended for Drug Delivery*, 63–70. https://doi.org/10.1007/978-1-60327-198-1_6

Courard, L., Michel, F., Perkowicz, S., and Garbacz, A. (2014). Effects of limestone fillers on surface free energy and electrical conductivity of the interstitial solution of cement mixes. *Cement and Concrete Composites*, *45*, 111–116. https://doi.org/10.1016/j.cemconcomp.2013.09.014

Cui, L., & Fall, M. (2017). Multiphysics Model for Consolidation Behavior of Cemented Paste Backfill. *International Journal of Geomechanics*, *17*(3). https://doi.org/10.1061/(ASCE)GM.1943-5622.0000743

Deditius, A. P., Reich, M., Kesler, S. E., Utsunomiya, S., Chryssoulis, S. L., Walshe, J., & Ewing, R. C. (2014). The coupled geochemistry of Au and As in pyrite from hydrothermal ore deposits. *Geochimica et Cosmochimica Acta*, *140*, 644–670. https://doi.org/10.1016/j.gca.2014.05.045

Diekmeyer, P. (2009). A supersized combo. CIM Magazine, 4(2), 54–57. ISSN 1718-4177.

Ding, Z., Yin, Z., Liu, L., and Chen, Q. (2007). Effect of grinding parameters on the rheology of pyrite–heptane slurry in a laboratory stirred media mill. *Minerals Engineering*, *20*(7), 701–709. https://doi.org/10.1016/j.mineng.2007.01.005

Dzuy, N. Q., and Boger, D. V. (1985). Direct Yield Stress Measurement with the Vane Method. *Journal of Rheology (New York : 1978)*, *29*(3), 335–347. https://doi.org/10.1122/1.549794

Dzuy, N.Q., Boger, D.V., 1985. Direct yield stress measurement with the vane method. J. Rheol. 29 (3), 335–347.

Fall, M., Adrien, D., Célestin, J. C., Pokharel, M., & Touré, M. (2009). Saturated hydraulic conductivity of cemented paste backfill. *Minerals Engineering*, *22*(15), 1307–1317. https://doi.org/10.1016/j.mineng.2009.08.002

Fall, M., Adrien, D., Celestin, J.C., Pokharel, M., Tour e, M., 2009. Saturated hydraulic conductivity of cemented paste backfill. Min. Eng. 22, 1307e1317. http:// dx.doi.org/10.1016/j.mineng.2009.08.002

Fall, M., Belem, T., Samb, S., and Benzaazoua, M. (2007). Experimental Characterization Of The Stress-Strain Behaviour Of Cemented Paste Backfill In Compression. *Journal Of Materials Science*, *42*(11), 3914–3922. Https://Doi.Org/10.1007/S10853-006-0403-2

Fall, M., Benzaazoua, M., & Saa, E. G. (2008). Mix proportioning of underground cemented tailings backfill. *Tunnelling and Underground Space Technology*, *23*(1), 80–90. https://doi.org/10.1016/j.tust.2006.08.005

Fall, M., Célestin, J. C., Pokharel, M., & Touré, M. (2010). A contribution to understanding the effects of curing temperature on the mechanical properties of mine cemented tailings backfill. *Engineering Geology*, *114*(3), 397–413. https://doi.org/10.1016/j.enggeo.2010.05.016

Ghirian, A., and Fall, M. (2015). Coupled Behavior of Cemented Paste Backfill at Early Ages. *Geotechnical and Geological Engineering*, *33*(5), 1141–1166. https://doi.org/10.1007/s10706-015-9892-6

Goldfarb, R.J., Baker, T., Dube, B., Groves, D.I., Hart, C.J.R., Gosselin, P., 2005. Distribution, character and genesis of gold deposits in metamorphic terranes. In: Econ. Geol. 100th Anniver., pp. 407–450.

Haiqiang, J., Fall, M., and Cui, L. (2016). Yield stress of cemented paste backfill in sub-zero environments: Experimental results. *Minerals Engineering*, *92*, 141–150. https://doi.org/10.1016/j.mineng.2016.03.014

Hassani, F. and Archibald, J.F. (1998). Mine Backfill, [CD-ROM]. Canadian Institute of Mining, Metallurgy and Petroleum (CIM), Montréal, Quebec, Canada.

Hassani, F., Ouellet, J., & Hossein, M. (2001). Strength development in underground high sulphate paste backfill operation. Canadian Institute of Mining, Metallurgy and Petroleum Bulletin, 94(1050), 57–62.

Hofstra, A. H., & Cline, J. S. (2000). Characteristics and models for Carlin-type gold deposits.

Hot, J., Bessaies-Bey, H., Brumaud, C., Duc, M., Castella, C., & Roussel, N. (2014). Adsorbing polymers and viscosity of cement pastes. *Cement and Concrete Research*, *63*, 12–19. https://doi.org/10.1016/j.cemconres.2014.04.005

Huynh, L., Beattie, D. A., Fornasiero, D., and Ralston, J. (2006). Effect of polyphosphate and naphthalene sulfonate formaldehyde condensate on the rheological properties of dewatered tailings and cemented paste backfill. *Minerals Engineering*, *19*(1), 28–36. https://doi.org/10.1016/j.mineng.2005.05.001

Jeyakaran, T., Pornsiri, N., Saengsoy, W., & Tangtermsirikul, S. (2023). Test methods for performance-based evaluation of concrete containing iron sulfide-bearing aggregates: Development and application. *Results in Engineering*, *18*, 101068-. https://doi.org/10.1016/j.rineng.2023.101068

Johnson, D. B., and Hallberg, K. B. (2005). Acid mine drainage remediation options: a review: Bioremediation of Acid Mine Drainage: The Wheal Jane Mine Wetlands Project. *The Science of the Total Environment*, *338*(1–2), 3–14.

Johnson, S. B., Franks, G. V., Scales, P. J., Boger, D. V., and Healy, T. W. (2000). Surface chemistry–rheology relationships in concentrated mineral suspensions. *International Journal of Mineral Processing*, *58*(1), 267–304. https://doi.org/10.1016/S0301-7516(99)00041-1

Keentok, M. (1982). The measurement of the yield stress of liquids. *Rheologica Acta*, *21*(3), 325–332. https://doi.org/10.1007/BF01515720

Kesimal, A., Yilmaz, E., Ercikdi, B., Alp, I., & Deveci, H. (2005). Effect of properties of tailings and binder on the short-and long-term strength and stability of cemented paste backfill. *Materials Letters*, *59*(28), 3703–3709. https://doi.org/10.1016/j.matlet.2005.06.042

Kumari, S., Udayabhanu, G., Prasad, B., 2010. Studies on environmental impact of acid mine drainage generation and its treatment: an appraisal. Indian J. Environ. Prot. 30 (11), 953e967.

Landriault, D. (1995). Paste backfill Mix design for Canadian Underground Hard Rock Mining. In: Proceedings of the 97th Annual General Meeting of CIM. Rock Mechanics and Strata Control Session. Halifax, Nova Scotia, pp. 229–238.

Large, R. R., Danyushevsky, L., Hollit, C., Maslennikov, V., Meffre, S., Gilbert, S., Bull, S., Scott, R., Emsbo, P., Thomas, H., Singh, B., & Foster, J. (2009). Gold and trace element zonation in pyrite using a laser imaging technique; implications for the timing of gold in orogenic and carlin-style sediment-hosted deposits. *Economic Geology and the Bulletin of the Society of Economic Geologists*, *104*(5), 635–668. https://doi.org/10.2113/gsecongeo.104.5.635

Leong, Y.-K., and Boger, D. V. (1990). Surface chemistry effects on concentrated suspension rheology. *Journal of Colloid and Interface Science*, *136*(1), 249–258. https://doi.org/10.1016/0021-9797(90)90095-6

Ma, D., Zhang, J., Duan, H., Huang, Y., Li, M., Sun, Q., & Zhou, N. (2021). Reutilization of gangue wastes in underground backfilling mining: Overburden aquifer protection. *Chemosphere (Oxford)*, *264*(Pt 1), 128400-. https://doi.org/10.1016/j.chemosphere.2020.128400

Martin, T. E., and Davies, M. P. (2000). Trends in the stewardship of tailings dams. In *Tailings and Mine Waste 2000* (1st ed., pp. 393–407). Routledge. https://doi.org/10.1201/9781003078579-51.

Marvila, M. T., Alexandre, J., Azevedo, A. R. G., Zanelato, E. B., Xavier, G. C., & Monteiro, S. N. (2019). Study on the replacement of the hydrated lime by kaolinitic clay in mortars. *Advances in Applied Ceramics*, *118*(7), 373–380. https://doi.org/10.1080/17436753.2019.1595266

McCarter, W. J., and Curran, P. N. (1984). Electrical response characteristics of setting cement paste. *Magazine of Concrete Research*, *36*(126), 42–49. https://doi.org/10.1680/macr.1984.36.126.42

Mercier-Langevin, F. (2010). LaRonde Extension mine design at three kilometres. In M. Van Sint Jan & Y. Potvin (Eds.), *Deep Mining 2010: Proceedings of the Fifth International Seminar on Deep and High Stress Mining* (pp. 3-16). Australian Centre for Geomechanics.

Oakton. (n.d.). Oakton pH 5+, pH 6+, Ion 6+ Instruction Manual. Novatech USA. Retrieved from https://www.novatechusa.com/pdf/Oakton%20pH%205+,%20pH%206+,%20Ion%206+%20Instruction%20Manual.pdf

Öhlander, B., Chatwin, T., & Alakangas, L. (2012). Management of Sulfide-Bearing Waste, a Challenge for the Mining Industry. *Minerals (Basel)*, *2*(1), 1–10. https://doi.org/10.3390/min2010001

Oyewale, M., Fall, M., & Ghirian, A. (2025). Flow characteristics of paste tailings in surface disposal: the role of pyrite content. *Environmental Science and Pollution Research International*, *32*(11), 6446–6467. https://doi.org/10.1007/s11356-025-36051-w

Park, C. K., Noh, M. H., & Park, T. H. (2005). Rheological properties of cementitious materials containing mineral admixtures. *Cement and Concrete Research*, *35*(5), 842–849. https://doi.org/10.1016/j.cemconres.2004.11.002

Penner, D., & Lagaly, G. (2001). Influence of anions on the rheological properties of clay mineral dispersions. *Applied Clay Science*, *19*(1), 131–142. https://doi.org/10.1016/S0169-1317(01)00052-7

Qi, C., Chen, Q., Fourie, A., Zhao, J., & Zhang, Q. (2018). Pressure drop in pipe flow of cemented paste backfill: Experimental and modeling study. *Powder Technology*, *333*, 9–18. https://doi.org/10.1016/j.powtec.2018.03.070

Qiu, J., Zhao, Y., Xing, J., & Sun, X. (2019). Fly Ash/Blast Furnace Slag-Based Geopolymer as a Potential Binder for Mine Backfilling: Effect of Binder Type and Activator Concentration. *Advances in Materials Science and Engineering*, *2019*, 1–12. https://doi.org/10.1155/2019/2028109

Reich, M., Deditius, A., Chryssoulis, S., Li, J.-W., Ma, C.-Q., Parada, M. A., Barra, F., & Mittermayr, F. (2013). Pyrite as a record of hydrothermal fluid evolution in a porphyry copper system: A SIMS/EMPA trace element study. *Geochimica et Cosmochimica Acta*, *104*, 42–62. https://doi.org/10.1016/j.gca.2012.11.006

Reich, M., Kesler, S. E., Utsunomiya, S., Palenik, C. S., Chryssoulis, S. L., & Ewing, R. C. (2005). Solubility of gold in arsenian pyrite. *Geochimica et Cosmochimica Acta*, *69*(11), 2781–2796. https://doi.org/10.1016/j.gca.2005.01.011

Saebimoghaddam, A. (2005). *Rheological yield stress measurement of mine paste fill material*. ProQuest Dissertations Publishing.

Simon, D., & Grabinsky, M. (2013). Apparent yield stress measurement in cemented paste backfill. *International Journal of Mining, Reclamation and Environment*, *27*(4), 231–256. https://doi.org/10.1080/17480930.2012.680754

Tamás, F. D., Farkas, E., Vörös, M., and Roy, D. M. (1987). Low-frequency electrical conductivity of cement, clinker and clinker mineral pastes. *Cement and Concrete Research*, *17*(2), 340–348. https://doi.org/10.1016/0008-8846(87)90116-5

Verkerk, C. G., & Marcus, R. D. (1988). The pumping characteristics and rheology of paste fills. *Backfill in South African Mines*, *1988*, 221-233

Wang, Y., Fall, M., & Wu, A. (2016). Initial temperature-dependence of strength development and self-desiccation in cemented paste backfill that contains sodium silicate. *Cement & Concrete Composites*, *67*, 101–110. https://doi.org/10.1016/j.cemconcomp.2016.01.005

Wu, D., Fall, M., & Cai, S. J. (2013). Coupling temperature, cement hydration and rheological behaviour of fresh cemented paste backfill. *Minerals Engineering*, *42*, 76–87. https://doi.org/10.1016/j.mineng.2012.11.011

Xiapeng, P., Fall, M., & Haruna, S. (2019). Sulphate-induced changes of rheological properties of cemented paste backfill. *Minerals Engineering*, *141*, 105849-. https://doi.org/10.1016/j.mineng.2019.105849

Yilmaz, E. (2010). Investigating the consolidation behavior, hydro-mechanical, and micro-structural properties of cemented paste backfills using the versatile CUAPS apparatus (Doctoral dissertation, Université du Québec en Abitibi-Témiscamingue (UQAT), Québec, Canada).

Yilmaz, E., 2010. Investigating the Hydrogeotechnical and Microstructural Properties of Cemented Paste Backfills Using the Versatile CUAPS Apparatus (Ph.D. Thesis). Universite du Qu ebec en Abitibi-T emiscamingue (UQAT).

Zhao, Y., Qiu, J., Zhang, S., Guo, Z., Wu, P., Sun, X., & Gu, X. (2021). Low carbon binder modified by calcined quarry dust for cemented paste backfill and the associated environmental assessments. *Journal of Environmental Management*, *300*, 113760–113760. https://doi.org/10.1016/j.jenvman.2021.113760

Ziegler, M., Reiter, K., Heidbach, O., Zang, A., Kwiatek, G., Stromeyer, D., Dahm, T., Dresen, G., & Hofmann, G. (2015). Mining-Induced Stress Transfer and Its Relation to a Mw 1.9 Seismic Event in an Ultra-deep South African Gold Mine. *Pure and Applied Geophysics*, *172*(10), 2557–2570. https://doi.org/10.1007/s00024-015-1033-x

CHAPTER FIVE.

TECHNICAL PAPER III: EFFECT OF PYRITE CONTENT ON THE PERMEABILITY PROPERTIES OF PASTE TAILINGS FOR SURFACE DISPOSAL.

Paper submitted for publication

Oyewale Miracle, Mamadou Fall and Ghirian Alireza

Department of Civil Engineering, University of Ottawa.
800 King Edward Ave, Ottawa, ON, K1N 6N5, Canada.

5.1 ABSTRACT

The safe disposal of tailings remains one of the most pressing environmental and geotechnical challenges in mining. Surface paste disposal systems are increasingly adopted for their financial feasibility and alignment with environmental sustainability objectives. However, significant knowledge gaps persist regarding system permeability especially when using pyrite bearing uncemented paste tailings (UPT) and lightly cemented paste tailings (LCPT). Permeability is a key environmental performance parameter and understanding how pyrite oxidation, its sulphate by-products, and binder composition govern permeability and microstructural evolution is critical for the effective design of paste systems to ensure long-term durability and minimize environmental risks. This study examines the effects of pyrite content (0-45%), initial sulphate concentration (0-25,000 ppm), and binder type (1 wt.% Portland cement, PC, and a slag–Portland cement blend, SG) on UPT and LCPT cured for 150 days at room temperature under sealed and air-dried conditions. Microstructural and physical

changes were evaluated using X-ray diffraction (XRD), mercury intrusion porosimetry (MIP), and physical property measurements (void ratio and dry density). Results show that in UPT samples, permeability increased gradually with higher pyrite content, accompanied by elevated void ratios and reduced dry densities, reflecting particle loosening and the development of open pore networks. In LCPT, permeability remained low at ≤15% pyrite due to matrix densification from cement hydration but increased sharply at 45% pyrite as sulphate ions from pyrite oxidation reacted with cement phases to form expansive minerals (ettringite, gypsum), leading to pore coarsening. Air-drying exacerbated this effect by accelerating pyrite oxidation and sulphate generation. Elevated sulphate concentrations further amplified permeability, particularly under oxygen exposure. Binder composition also played a decisive role: SG-LCPT, while exhibiting higher baseline permeability, showed superior resistance to pyrite- and sulphate-induced degradation. In contrast, PC-LCPT experienced more severe permeability loss at high pyrite and sulphate levels, attributed to its higher tricalcium aluminate content and greater portlandite availability.

Keywords: Paste tailings; mine; sustainability; permeability; pyrite; acid mine drainage; hydraulic conductivity.

5.2 INTRODUCTION

The mining industry is the cornerstone of many national economies due to the substantial financial revenues generated through the extraction and exportation of valuable resources like crude oil, gold, diamonds and iron. In resource-rich countries like Canada, Russia, and Australia, the industry's value chain extends beyond exportation, as mineral resources are also leveraged to create employment opportunities, improve trade balance, and attract significant foreign investment, which in turn fosters international trade relationships that are vital for bolstering national economies and the well-being of their populations (Fall et 2009; Yang et al., 2023).

The growing demand for socio-economic development in these resource-rich nations and globally has caused a global increase in the number of operating mines as the production chains for resources necessary for economic development are majorly dependent on mining, which in many cases poses significant threats to environmental and public health (Watari et al., 2023; Aguilar-Garrido et al., 2023). These challenges range from the production of unsustainable amounts of mine waste (e.g., waste rock and tailings) to more destructive challenges caused by vectors such as sulphide minerals in mine tailings (Aguilar-Garrido et al., 2023; Grande et al., 2018). Sulphide minerals are a group of potentially toxic accessory minerals that generally coexist with other high-valued minerals targeted by mining (Vaughan and Lennie, 1991; Gerasimov et al., 2019; Jacobs et al., 2014). The exposure of these sulphides, particularly pyrite mineral (FeS_2), is known to cause Acid Rock Drainage (ARD), a process where sulphide minerals in waste rock react with air and water to produce sulfuric acid, which can further leach into surrounding aquatic and terrestrial environments. Consequently, this harms inhabiting organisms, makes water resources unsafe for use, and threatens human health (Dhir, 2018; Hogsden and Harding, 2012; Evans et al., 2015). Although ARD can occur naturally, this phenomenon is more prevalent across mining sites due to increased exposure of

sulphide minerals during mining operations (Simate and Ndlovu, 2014; Jennings et al., 2008). Relevant statistics by Xu et al. (2020) highlighted that there are approximately 20,000 - 50,000 existing mines around the world producing ARD, and about 19,300 km^2 of freshwater and 720 km^2 of lakes and reservoirs have been contaminated with high acidity from ARD. Furthermore, the cost of treating ARD from mines is estimated to be about $10 billion in North America, $0.2–$5 billion in Canada, and $650 million/year in Australia (RoyChowdhury et al., 2019).

In light of the above, the mining industry is focused on addressing these challenges by developing innovative waste management strategies that are both environmentally friendly and cost-effective. In this context, recycling and reusing mine waste through a concept called paste tailing (PT) technology is gaining popularity amongst resource-rich countries (Fall et al., 2008; Fall et al., 2009) as this technology not only aligns with the concept of circular mining but also prioritizes environmental stewardship, ensures long-term sustainability and compliance with modern regulatory standards. Paste tailings are dense, viscous mixtures of tailings and water that have been sufficiently dewatered to a degree that is less fluid compared to slurries (Verburg, 1997). This dewatering process transforms the tailings state from a low-viscosity fluid to a paste, which accelerates consolidation and enhances the stability of the deposited stack (Brackebusch and Shillabeer, 1998). In mine waste management, PT can be applied in surface paste disposal (SPD) in the form of uncemented paste tailings (UPT) or lightly cemented paste tailings (LCPT). LCPT and UPT are similar in terms of composition and preparation as they are both produced by mixing tailings with a solid percentage between 70%-85% and water, however, LCPT mixtures contain minute quantities of binder (e.g., up to 2%) (Deschamps et al., 2011). The application of PT for SPD offers both environmental and operational benefits. For instance, PT technology minimizes leachate generation from tailings due to the availability of minimal amounts of free water in deposited stacks, which reduces/eliminates the potential impacts on receiving waters and biological receptors (Verburg,

1997). Moreover, the densely packed nature of PT stacks further restricts the infiltration of rainwater and snowmelt, thus decreasing seepage volume and the potential for ARD (Verburg, 1997). Another benefit of PT technology is its ability to improve efficiency by eradicating the cost of extensive water management systems targeted at managing generated leachate (Ichrak et al., 2016). Furthermore, the use of PT technology in arid regions is very advantageous as it aligns well with the region's limited water resources and helps to conserve valuable water resources (Verburg, 1997).

While recognizing paste tailings (PT) technology as a promising strategy for mine waste management, it is important to note that the science of PT is still not fully understood, especially the complexities that may arise in paste geochemistry when using sulphidic tailings. To explain better, in sulphidic PT, the primary source of sulphates is derived internally from tailings containing 2-60% sulphides, with pyrite being the most abundant sulphide found in these tailings (Fall and Benzaazoua, 2005; Tariq and Nehdi, 2007). It is believed that the chemical reactivity of pyrite in these paste mixtures may play a significant role in altering its permeability properties since pyrite is prone to oxidation, especially in the presence of oxygen and moisture. Hence, there are uncertainties surrounding the ability of internal pyrite to change the pore structure of PT and potentially increase the permeability of paste mixtures, leading to risks of ARD during surface paste disposal.

Furthermore, previous researchers (e.g., Quellet et al., 1998; Fall and Benzaazoua, 2005, Benzaazoua et al., 2002; Benzaazoua et al., 1995; Bernier et al., 1999; Hassani et al., 2001) have reported the potential of sulphates within sulphidic PT to cause "internal sulphate attack", which in turn affects the overall strength and stability properties of PT. More specifically, Quellet et al. (1998) highlighted that sulphates produced from pyrite oxidation in basic pH environment can react with free calcium ions released from the dissolution of unstable portlandite ($Ca(OH)_2$) to produce secondary gypsum ($CaSO_4 \cdot 2H_2O$) and highly expansive

ettringite ($3CaSO_4 \cdot 3CaO \cdot Al_2O_3 \cdot 32H_2O$). These expansive products can further create internal stresses (Tariq and Nehdi, 2007) leading to drastic deterioration of the cemented matrix leading to potential risks of ARD (Benzaazoua et al., 1995; Hassani et al., 2001; Fall and Benzaazoua, 2005). While this phenomenon is more pronounced in PT with low cement content and high sulphate concentration (Quellet et al., 1998), research is yet to report how the oxidation of pyrite-bearing tailings, in addition to the detrimental effects of 'initial sulphate attack", affects other important factors like permeation of UPT and LCPT for SPD.

Permeability is a major parameter that controls PT's environmental performance and durability (Fall et al., 2009). Hence, the leachability and susceptibility of PTs to cause ARD are key design criteria for the environmental design of PTs. The susceptibility is largely determined by the reactivity (oxidation potential) of the tailings they contain. Subsequently, this reactivity depends not only on the types and amounts of sulphide minerals in the PT but also on the permeability properties, which dictate how easily fluids like oxygen and water can penetrate and flow through the PTs (Fall et al., 2009). These permeability properties can be evaluated by the knowledge of the hydraulic conductivity of the PTs (Fall et al., 2009). Hydraulic conductivity measures how easily a fluid (e.g., water) can flow through the pores or cracks within a porous medium, such as the PT in this study (Pokharel and Fall, 2013). It also provides relevant information about the pore structure, the connectivity of the pores, and the extent to which cracks facilitate fluid transfer (e.g., oxygen and water) between paste tailings (PTs) and the surrounding environment (Fall et al., 2009).

Over the past decades, only a few noteworthy research studies (Abdul-Hussain et al., 2011; Fall et al., 2009; Goubout et al., 2007; Pokharel and Fall, 2013; Veensta et al., 2014; Cihangir and Akyol et al., 2018) have aimed to understand the hydraulic conductivity of PTs, however, these studies have majorly focused on paste backfill (cemented paste backfill (CPB)) applications for underground paste disposal. Additionally, the variations in hydraulic

conductivity CPB research have been centered on various factors such as tailings fineness (Fall et al., 2009; Ke et al., 2016), binder content (Abdul-Hussain and Fall., 2011; Abdul-Hussain et al., 2011), binder types (Fall et al., 2009; Abdul-Hussain et al., 2011; Goubout et al., 2007), curing time, curing temperature (Abdul-Hussain et al., 2011; Yilmaz et al.,2010), and sulphate content (Abdul-Hussain et al., 2011). Nonetheless, none of these studies have investigated the influence of varying pyrite contents on the permeability characteristics of uncemented (UPT) and lightly cemented paste tailings (LCPT) intended for surface paste disposal (SPD). Moreover, the impact of pyrite oxidation and initial sulphate content on the hydraulic behaviour of PTs under field-representative conditions remains unexplored. Addressing these knowledge gaps is essential for optimizing paste tailings technology and ensuring its long-term sustainability in mine waste management. Therefore, the objective of this study is to experimentally investigate the effects of pyrite content, pyrite oxidation, and the resulting sulphate concentrations on the permeability (saturated hydraulic conductivity) of UPT and LCPT for SPD under various field scenarios (E.g differing oxygen exposure/drying conditions). These controlled conditions allow for a systematic evaluation of how oxidation and sulphate content influence the hydraulic behaviour of PTs.

5.3 EXPERIMENTAL PROGRAM

5.3.1 MATERIALS

5.3.1.1 TAILINGS

High-purity silica tailings (ST), consisting of 99.8% quartz (SiO_2) by weight, were utilized as the primary material in this study. Quartz is a chemically inert and non-acid-generating mineral commonly found in hard rock mines across Canada, making ST a suitable and consistent alternative to natural tailings (NT). The selection of ST was intended to minimize variability and eliminate the chemical reactivity commonly associated with NT, whose reactive components can interfere with cement hydration processes and compromise the reproducibility of experimental results. In contrast, ST allow for a more controlled assessment of the influence of pyrite on the permeability properties of CPB. A detailed particle size analysis showed that the PSD of ST closely mirrors the average distribution observed in nine NT samples from Canadian mining operations (Figure 1). Specifically, about 43% of ST particles are finer than 20µm, classifying them as medium tailings, in accordance with Landriault's (1995) definition, which designates medium tailings as containing 35%–60% of particles smaller than 20µm. This classification also meets the recommended requirement that CPB materials contain a minimum of 15% by mass of fines below 20µm. The physical and chemical properties of ST are provided in Tables 1 and 2, respectively.

Table 1: Summary of physical attributes for the ST utilized and the average measurements from nine NT sources in Canada.

ELEMENT	G_s	D_{10}(µm)	D_{30}(µm)	D_{50}(µm)	D_{60}(µm)
ST	2.7	1.9	9.0	22.5	31.5
An average of 9 types of tailings	-	1.8	9.1	20.0	30.8

Gs: specific gravity

Table 2: Mineralogical profile of the ST used in this study

TAILINGS (wt.%)	MINERAL											
	Quartz	Albite	Dolomite	Calcite	Chlorite	Magnetite	Pyrite	Talc	Pyrrhotite	Spinel	Others	Total
ST	99.8	-	-	-	-	-	-	-	-	-	0.2	100

ST: Silica tailings; wt.: weight.

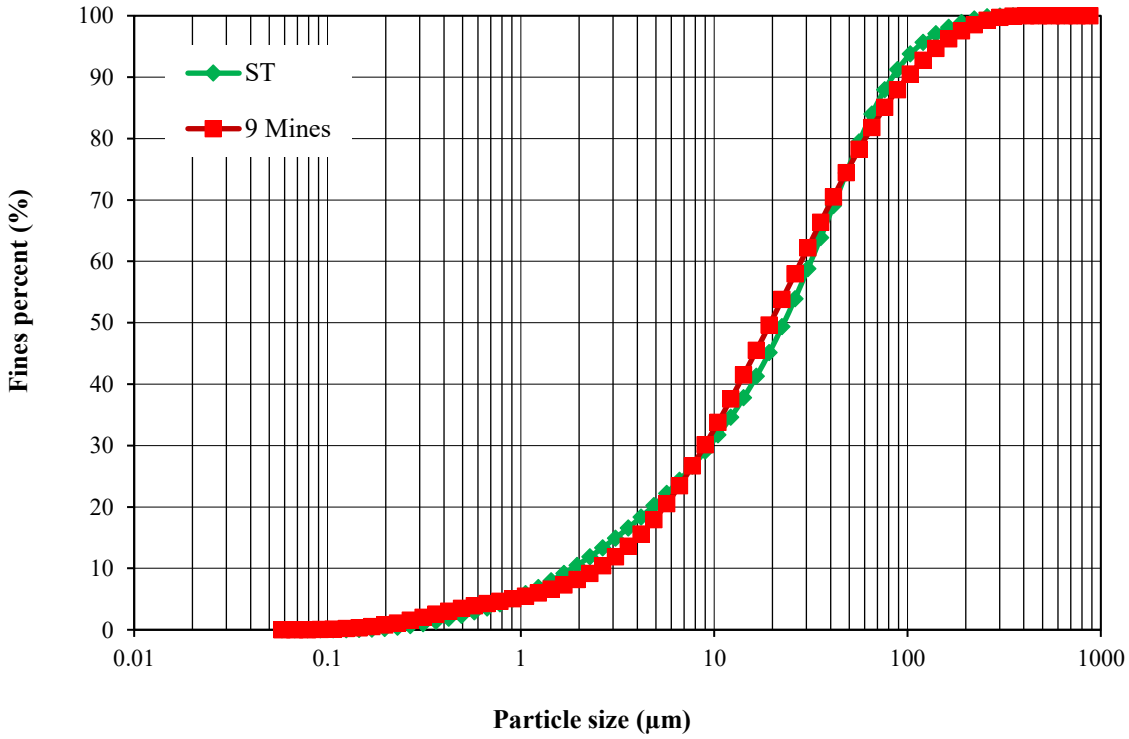

Figure 1: **Comparative grain size profiles of ST and nine Canadian natural tailings.**

5.3.1.2 BINDER

Type I Portland cement (PC), a conventional and widely adopted hydraulic binder in paste tailings (PT) mixtures, was used as the primary binding agent. To enhance sustainability and reduce material costs, granulated ground blast furnace slag (SA), a latent hydraulic mineral admixture, was incorporated in selected paste tailings mixtures to partially replace PC. The use of blended binders comprising Portland cement (PC) and slag (SA) provides both economic and environmental benefits, as PC production is associated with high costs and

significant greenhouse gas (GHG) emissions, whereas slag, an industrial by-product, offers a substantially lower carbon footprint. Two binder types were formulated: PC-only (100% Portland cement) and SG (a 50:50 weight ratio of PC to SA). These combinations were selected to evaluate the influence of binder composition on PT performance. The physical and chemical properties of both PC and SA are summarized in Table 3.

Table 3: Physicochemical Properties of Portland Cement and Slag in Binder Formulations

	Na_2O	MgO	Al_2O_3	SiO_2	K_2O	CaO	TiO_2	MnO	Fe_2O_3	LOI	Relative density	Specific surface area (cm^2/g)
PCI	0.341	2.577	4.808	20.375	0.962	62.700	0.225	0.054	3.609	2.162	3.2	1300
Slag	0.284	11.782	10.59	35.572	0.478	39.212	0.467	0.298	0.621	0.388	2.8	2100

5.3.1.3 PYRITE

A commercial-grade pyrite powder (FeS_2; molecular weight 119.98 g/mol) sourced from Washington Mills North Grafton, Inc. was utilized in this study. The particle size distribution of this pyrite closely matches that of pyrite minerals typically present in natural tailings. This pyrite powder was incorporated into blends with silica tailings (ST), Portland cement (PC), and slag (SG) to formulate three distinct pyrite-bearing tailings mixtures: UPT, PC-LCPT, and SG-LCPT. These mixtures were prepared with varying pyrite concentrations of 0, 5, 15, and 45 wt%, covering the typical range of pyrite contents observed in practice. The physical properties of the pyrite powder employed are detailed in Table 4.

Table 4: Physical properties of pyrite.

BULK DENSITY (g/cm^3)	DENSITY AT 20 °C (g/cm^3)	SP. GRAVITY	PH	MELTING POINT
2.35	4.7	4.6	4.0-6.0	1193

Sp: specific.

5.3.1.4 MIXING WATER AND SULPHATE CONCENTRATION

Distilled water was used for all tailings and binder mixtures in this study, with a constant water-to-binder (w/b) ratio of 32. To replicate sulphate-rich conditions often encountered in paste tailings environments, ferrous sulphate heptahydrate ($FeSO_4 \cdot 7H_2O$; molecular weight 278.01 g/mol) was selected as the representative sulphate source. In practice, sulphate ions in paste tailings typically originate from the oxidation of sulphide minerals, particularly pyrite. It is therefore important to examine how varying amounts of sulphate ions, initially present in tailings as a result of pyrite oxidation, influence the permeability of UPT and LCPT. Ferrous sulphate was chosen because it is the predominant sulphate compound in paste tailings and cemented tailings backfills, owing to the abundance of iron and sulphate ions in mine water. Measured amounts of $FeSO_4 \cdot 7H_2O$ were dissolved in specific volumes of tap water to produce blending solutions with controlled sulphate concentrations of 0, 5,000, 15,000, and 25,000 ppm. These predefined sulphate levels were then used to assess the influence of initial sulphate content on the permeability behaviour of the tailings mixtures.

5.3.2 SPECIMEN PREPARATION AND MIX PROPORTIONS

The different lightly cemented and uncemented mix samples investigated in this study were prepared following the experimental plan outlined in Table 5. Silica tailings, pyrite, and binders were first weighed into a mechanical mixing bowl using a scientific weighing scale, and then the powders were subsequently mixed for 5 min. using a mechanical mixer (Kitchen Aid mixer) at a constant mixing speed (Speed 2) under room temperature. Then the pre-measured quantity of tap water was added to the mechanical mixer containing the powders. The samples were then further mixed for an additional 5 minutes to obtain a homogeneous paste. After the mixing process, the paste mixtures were transferred into plastic cylinder moulds with a diameter of 5 cm and a height of 10 cm and cured according to the experimental

plan provided in Table 5. The choice of plastic cylinder moulds aimed to replicate the sizes of pipes used in on-field PT practice (Haiqiang et al., 2016).

Table 5: Experimental plan for hydraulic conductivity tests.

SAMPLE NAME	TAILINGS TYPE	BINDER TYPE	BINDER CONTENT (Vol%)	PYRITE CONTENT (wt.%)	SULPHATE CONTENT (ppm)	CURING TIME (days)
Effect of pyrite content on hydraulic conductivity of UPT						
UPT-0%	ST	-	0	0	0	150
UPT-5%	ST+PY	-	0	5	0	150
UPT-15%	ST+PY	-	0	15	0	150
UPT-45%	ST+PY	-	0	45	0	150
Effect of pyrite content and binder type on hydraulic conductivity of LCPT cured without air drying						
PC-LCPT-0%	ST	PCI (100%)	1.0	0	0	150
PC-LCPT-5%	ST+PY	PCI (100%)	1.0	5	0	150
PC-LCPT-15%	ST+PY	PCI (100%)	1.0	15	0	150
PC-LCPT-45%	ST+PY	PCI (100%)	1.0	45	0	150
SG-LCPT-0%	ST	PCI/SG (50/50)	1.0	0	0	150
SG-LCPT-45%	ST+PY	PCI/SG (50/50)	1.0	45	0	150
Effect of pyrite content and binder type on hydraulic conductivity of LCPT cured with air drying						
PC-LCPT-0%	ST	PCI (100%)	1.0	0	0	150
PC-LCPT-5%	ST+PY	PCI (100%)	1.0	5	0	150
PC-LCPT-15%	ST+PY	PCI (100%)	1.0	15	0	150
PC-LCPT-45%	ST+PY	PCI (100%)	1.0	45	0	150
SG-LCPT-0%	ST	PCI/SG (50/50)	1.0	0	0	150
SG-LCPT-45%	ST+PY	PCI/SG (50/50)	1.0	45	0	150
Effect of sulphate concentration and pyrite content on the hydraulic conductivity of LCPT cured without air drying						
PC-LCPT-0-0ppm	ST	PCI (100%)	1.0	0	0	150
PC-LCPT-0-5000ppm	ST	PCI (100%)	1.0	0	5000	150
PC-LCPT-0-25000ppm	ST	PCI (100%)	1.0	0	25000	150
PC-LCPT-15-0ppm	ST+PY	PCI (100%)	1.0	15	0	150
PC-LCPT-15-5000ppm	ST+PY	PCI (100%)	1.0	15	5000	150
PC-LCPT-15-25000ppm	ST+PY	PCI (100%)	1.0	15	25000	150
SG-LCPT-0-0ppm	ST	PCI/SG (50/50)	1.0	0	0	150
SG-LCPT-0-25000ppm	ST	PCI/SG (50/50)	1.0	0	25000	150
SG-LCPT-15-0ppm	ST+PY	PCI/SG (50/50)	1.0	15	0	150
SG-LCPT-15-25000ppm	ST+PY	PCI/SG (50/50)	1.0	15	25000	150

Effect of sulphate concentration and pyrite content on the hydraulic conductivity of LCPT cured with air drying						
PC-LCPT-0-0ppm	ST	PCI (100%)	1.0	0	0	150
PC-LCPT-0-5000ppm	ST	PCI (100%)	1.0	0	5000	150
PC-LCPT-0-25000ppm	ST	PCI (100%)	1.0	0	25000	150
PC-LCPT-15-0ppm	ST+PY	PCI (100%)	1.0	15	0	150
PC-LCPT-15-5000ppm	ST+PY	PCI (100%)	1.0	15	5000	150
PC-LCPT-15-25000ppm	ST+PY	PCI (100%)	1.0	15	25000	150
SG-LCPT-0-0ppm	ST	PCI/SG (50/50)	1.0	0	0	150
SG-LCPT-0-25000ppm	ST	PCI/SG (50/50)	1.0	0	25000	150
SG-LCPT-15-0ppm	ST+PY	PCI/SG (50/50)	1.0	15	0	150
SG-LCPT-15-25000ppm	ST+PY	PCI/SG (50/50)	1.0	15	25000	150

PC/PCI: Portland cement type I; SG: Blast furnace slag; ST: silica tailings; PY: Pyrite; UPT: Uncemented paste tailings; LCPT: Lightly cemented paste tailings.

ppm: parts per million; Vol: Volumetric percentage; Wt.%: Weight percentage: PCI (100%): Sample with 100% PCI; PCI/SG (50/50): Sample with 50% PCI and SG With air drying: water evaporation is allowed during sample curing; Without air drying: water evaporation is not allowed during sample curing

5.3.3 CURING CONDITIONS

To replicate realistic field conditions, two distinct curing scenarios were adopted: *without air drying* and *with air drying*.

(a) Without Air Drying: In this scenario, cylindrical moulds containing the paste tailings mixtures were sealed to prevent contact with air during the curing process. This scenario represents conditions where thin layers of paste tailings are deposited rapidly, or where climatic conditions are unfavourable for evaporation. In the first case, successive layers are placed in quick succession, so freshly deposited material is rapidly covered by subsequent layers and has little direct air exposure. In the second case, cold, humid, or rainy climates, particularly under snow cover or persistent cloudiness, minimize surface water loss, thereby reducing evaporation and restricting oxygen ingress. Consequently, oxidative reactions during curing are substantially suppressed under such conditions.

(b) With Air Drying: In this case, the tops of the cylindrical moulds were left open to air during curing, allowing for atmospheric exposure. This condition simulates field scenarios where surface-deposited paste tailings experience slower deposition rates and favourable climatic conditions for water evaporation. The influx of oxygen promotes the oxidation of sulphide minerals in the tailings, leading to sulphate generation and potentially affecting the chemical and physical behaviour of the cured material.

Together, these two curing scenarios represent contrasting field conditions. The *without air-drying* case limits oxidation, whereas the *with air-drying* case accelerates it by increasing oxygen exposure and evaporation.

5.3.4 TEST METHODS

5.3.4.1 HYDRAULIC CONDUCTIVITY TEST

The saturated hydraulic conductivity (permeability) of the cured PT samples was

evaluated using a Tri-Flex 2 flexible wall permeameter, following the ASTM D5084-00 standard for saturated soils. This method allows for precise measurement of hydraulic conductivity under controlled laboratory conditions. The constant head test procedure was adopted, applying a consistent pressure gradient of 10 psi (69 kPa) between the inflow and outflow burettes to drive water through the sample. Before testing, samples were saturated using a backpressure technique to eliminate entrapped air and ensure full saturation, which is critical for accurate permeability measurement. Back pressure was maintained until steady-state flow was observed, indicating that saturation had been achieved. The flexible wall setup also prevents side leakage, ensuring water flows only through the sample. Each test was conducted in duplicate to confirm the repeatability and reliability of the data. This method was selected due to its ability to simulate in-situ stress conditions and provide high-accuracy measurements of saturated hydraulic conductivity in fine-grained and cemented materials.

5.3.4.2 MICROSTRUCTURAL AND PHYSICAL PROPERTY ANALYSIS

The microstructural characteristics (such as pore structure and binder hydration products) and physical properties (including void ratio, porosity, and density) of selected PT samples were thoroughly analyzed. These tests aimed to assess the structural evolution and internal changes in the lightly cemented paste tailings (LCPT) over time. Prior to microstructural testing, the samples were oven-dried at 45 °C for 5 days to eliminate moisture variability. Mercury intrusion porosimetry (MIP) was conducted to evaluate the pore size distribution and total porosity of the hardened paste. Mineralogical assessments were performed using X-ray diffraction (XRD) to identify hydration products. The gravimetric water content (wc%) and bulk density of the samples were determined in accordance with ASTM standards D2216-10 and D7263-09, respectively. From these measurements, the void ratio (e) and porosity (n) were calculated for each test sample.

5.4 RESULTS AND DISCUSSION

5.4.1 PERMEABILITY OF UNCEMENTED AND LIGHTLY CEMENTED PASTE TAILINGS WITH PYRITE UNDER NON–AIR-DRIED CONDITIONS

Figure 2(a) shows the influence of pyrite content on the coefficient of permeability (k, cm/s) of uncemented paste tailings (UPT) and lightly cemented paste tailings with Portland cement (PC-LCPT) cured without air drying. The results indicate that increasing pyrite content affects the permeability of both UPT and PC-LCPT. For UPT, permeability increases steadily from approximately 3.4×10^{-5} cm/s at 0% pyrite to 4.8×10^{-5} cm/s at 45% pyrite. This represents only a modest increase (a factor of 1.4), i.e., less than one order of magnitude. In contrast, PC-LCPT samples exhibit consistently low permeability ($<2.0 \times 10^{-6}$ cm/s) up to 15% pyrite, highlighting the effectiveness of cement hydration products in refining pore structure and restricting fluid flow. However, at 45% pyrite, permeability rises sharply to 1.5×10^{-5} cm/s, representing nearly an order of magnitude increase compared with the pyrite-free PC-LCPT. This finding suggests that high pyrite contents cause more severe permeability deterioration in PC-LCPT than in UPT.

Figure 2(b) compares the effects of pyrite content on the permeability of LCPT prepared with PC (PC-LCPT) and slag (SG-LCPT). Across all pyrite levels, SG-LCPT samples exhibit higher baseline permeability than PC-LCPT. For instance, at 0% pyrite, permeability is 1.3×10^{-5} cm/s for SG-LCPT versus 1.6×10^{-6} cm/s for PC-LCPT. When pyrite content increases to 45%, permeability rises to 3.1×10^{-5} cm/s for SG-LCPT and 1.5×10^{-5} cm/s for PC-LCPT. Although SG-LCPT maintains higher absolute permeability, PC-LCPT undergoes a far greater relative increase: at 45% pyrite, its permeability is about ten times higher than at 0% pyrite, compared with only a 2.4-fold increase for SG-LCPT. Thus, while slag addition initially results in higher permeability, SG-LCPT is less sensitive to pyrite-induced deterioration than PC-LCPT.

Overall, these results demonstrate that UPT systems are more susceptible to pyrite-induced increases in permeability than LCPT. Between binder types, SG-LCPT generally shows greater resistance than PC-LCPT to permeability degradation at elevated pyrite contents, underscoring the influence of binder composition on the durability and environmental performance of paste tailings.

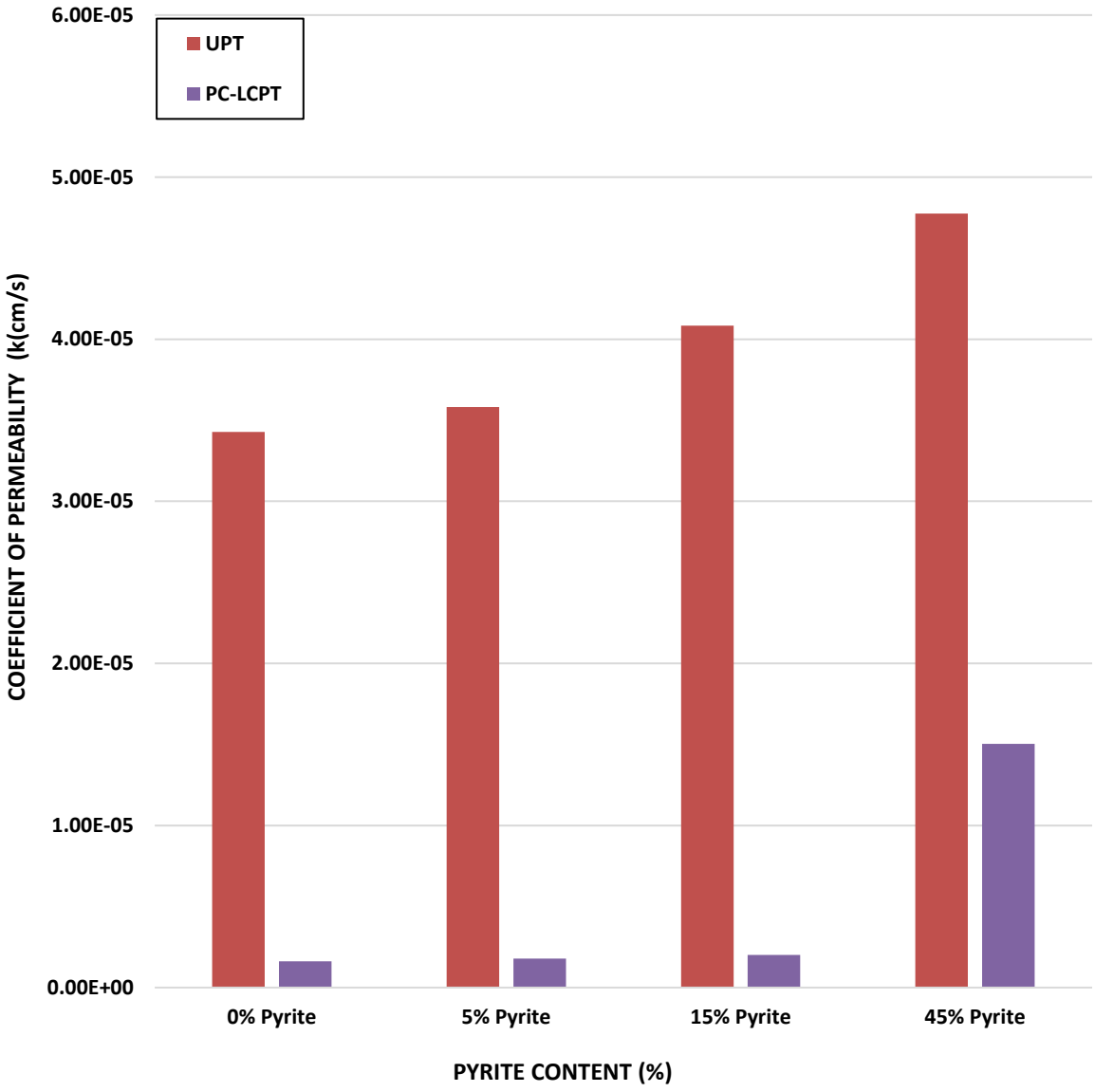

(a)

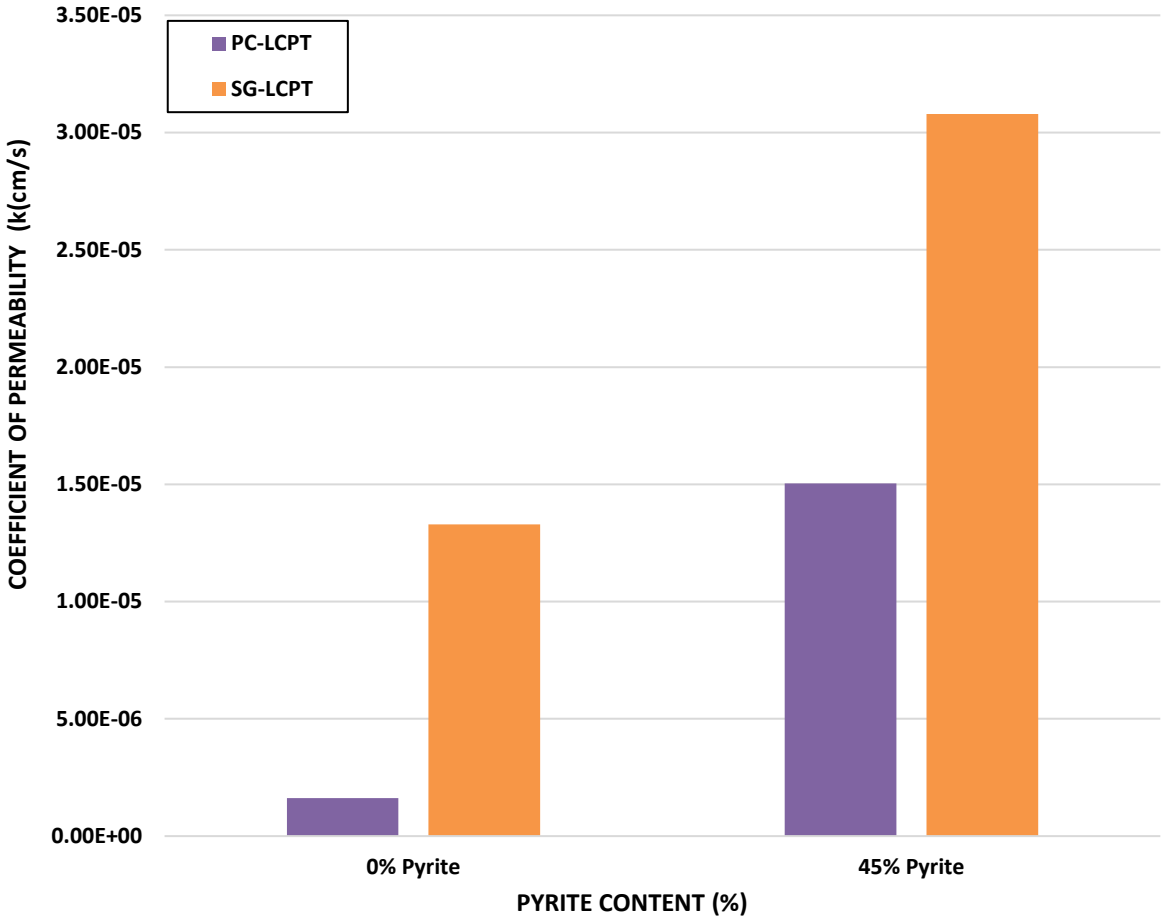

(b)

Figure 2: Effect of pyrite content on the permeability of (a) uncemented paste tailings (UPT) and lightly cemented paste tailings (PC-LCPT), and (b) paste tailings stabilized with different binder types (PC-LCPT and SG-LCPT) cured for 150days.

The permeability trends observed can be attributed to significant microstructural modifications within the PT matrix, as confirmed by the experimental characterization of physical properties-specifically, void ratio and dry density (Figures 3a and 3b). For UPT, the void ratio increased markedly from 0.69 at 0% pyrite to 1.64 at 45% pyrite, reflecting greater interparticle spacing and a more open pore network that facilitates fluid flow (Sicakova and Kovac, 2020; Sonebi et al., 2016; Luck et al., 2006; Timlin et al., 1999; Adajar, 2014; Wise, 1992). Correspondingly, dry density decreased from 1.46 g/cm³ to 1.17 g/cm³, indicating that lower density promotes higher permeability by enhancing pore interconnectivity and loosening

particle arrangements, thereby generating additional pathways for fluid migration (Sicakova and Kovac, 2020; Javed et al., 2025). These structural changes directly explain the steady increase in permeability observed in UPT.

In PC-LCPT, the significantly lower permeability compared with UPT, particularly at 0–15% pyrite, is attributed to cementitious bonding. At lower pyrite levels, cement hydration produces phases such as portlandite ($Ca(OH)_2$) and Calcium Silicate Hydrate (C-S-H), which densify the matrix by filling voids and binding tailings particles, thereby restricting fluid flow (Li and Fall, 2018; Marchon and Flatt, 2016). This agrees with Faraji and Fall (2025), who reported that hydration products in cement–tailings blends reduce permeability by filling pores and enhancing particle interlocking. However, as pyrite content increased from 0% to 45%, the void ratio rose from 0.66 to 1.41, while dry density decreased from 1.49 g/cm³ to 1.23 g/cm³. These changes suggest that pyrite interferes with cement-induced densification, weakening particle bonding and increasing pore connectivity. This disruption can be explained by the sulphate ions generated from pyrite oxidation in LCPT systems. Sulphate ions react with cement components (e.g., C_3A) and hydration products (e.g., CH), leading to the formation of expansive minerals such as ettringite and gypsum. The associated expansion pressures can generate cracks within the LCPT matrix, thereby elevating permeability (Fall and Benzaazoua, 2005). This interpretation aligns with Schmidt et al. (2011), who demonstrated that iron sulphide degradation in cement matrices induces internal cracking, and Rodrigues et al. (2012), who reported that oxidation of pyrite-bearing aggregates produces expansive secondary minerals (gypsum, thaumasite), which disrupt matrix compactness and increase permeability.

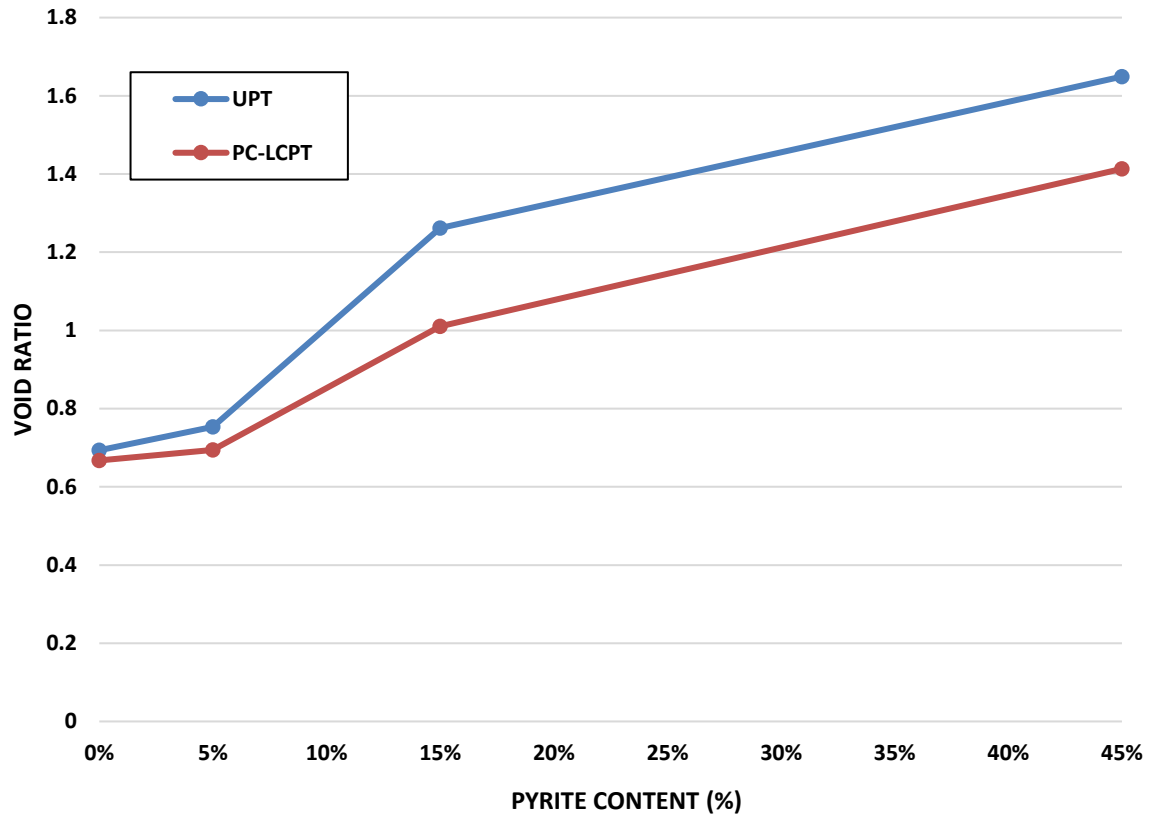

(a)

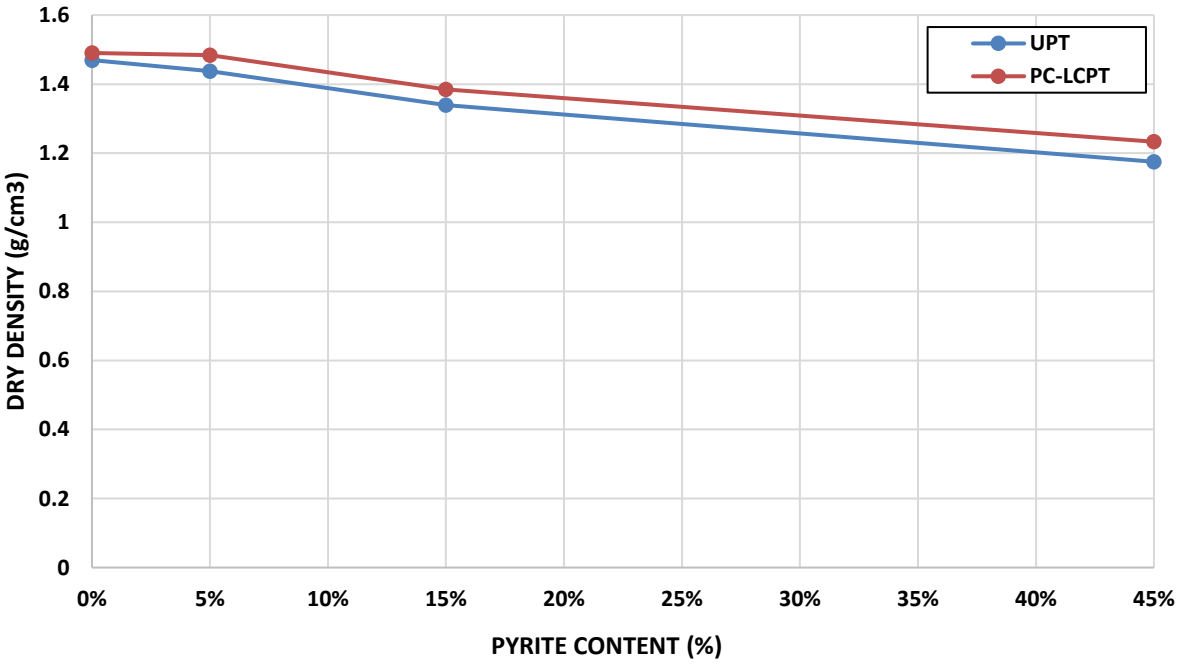

(b)

Figure 3: Changes in physical properties of 150-day cured uncemented paste tailings (UPT) and lightly cemented paste tailings (PC-LCPT), with increasing pyrite content: (a) void ratio, and (b) dry density.

Furthermore, the disruptive interaction between pyrite and the cement matrix is experimentally supported by the X-ray diffraction (XRD) results of LCPT samples with 0% and 45% pyrite, presented in Figure 4. The mineralogical transformations observed confirm the influence of sulphate ions released from pyrite oxidation. In the 0% pyrite sample (Figure 4a), the diffraction pattern is dominated by strong portlandite ($Ca(OH)_2$) peaks, with the most intense peak reaching 12,934 cps. Well-defined calcite ($CaCO_3$) signals are also present, suggesting mild carbonation of portlandite (Savija and Lukovic, 2016). Only trace amounts of gypsum are detected, likely originating from the initial cement (Frigione, 1983) rather than secondary sulphate reactions, while quartz peaks reflect inert tailings minerals. Importantly, no residual unhydrated clinker phases (e.g., C_2S or C_3S) are detected, indicating a well-hydrated cement matrix. The strong portlandite peak highlights the robust formation of hydration products that densify the pore structure and enhance binding. The absence of ettringite or other sulphate-bearing phases further confirms the lack of significant sulphate reactions in this system. By contrast, the 45% pyrite sample (Figure 4b) shows a markedly different mineralogical profile. Portlandite is still present but with a much weaker peak (2760 cps), indicating its partial consumption in secondary reactions (reactions of sulphate ions with portlandite to produce gypsum). Strong ettringite peaks and clear gypsum signals are observed, both of which are products of reactions between sulphate ions from pyrite oxidation and the calcium and aluminates in cement (Bérard et al., 1975; Chinchón et al., 1995; Casanova et al., 1997). Additionally, unhydrated clinker minerals such as C_2S and C_3S appear, suggesting that the high-sulphate environment inhibited normal cement hydration (Pokharel and Fall, 2013). This shift from a matrix dominated by portlandite and calcite to one enriched in ettringite and gypsum reflects a chemically weakened system vulnerable to cracking. The expansive growth of ettringite and gypsum not only consumes key hydration products but also generates internal stresses that fracture the matrix and open new pathways for fluid migration (Pokharel and Fall,

2013). These mineralogical changes are fully consistent with the permeability trends reported in Figure 2.

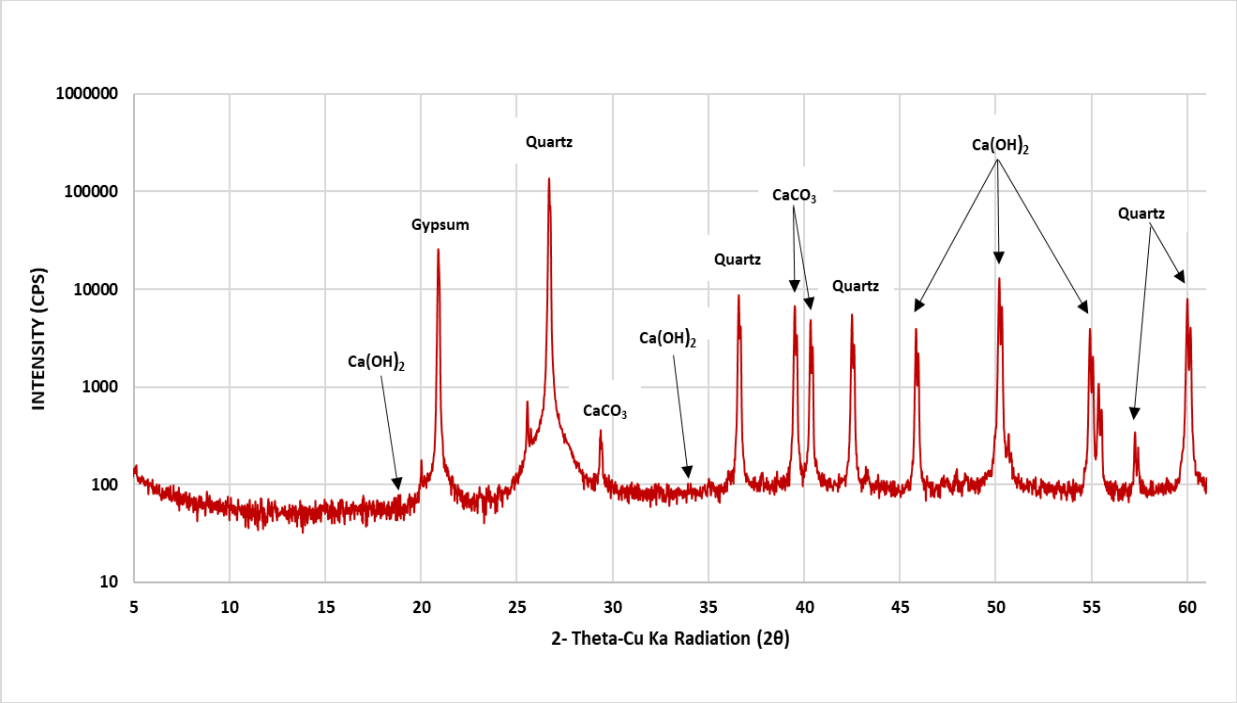

a)

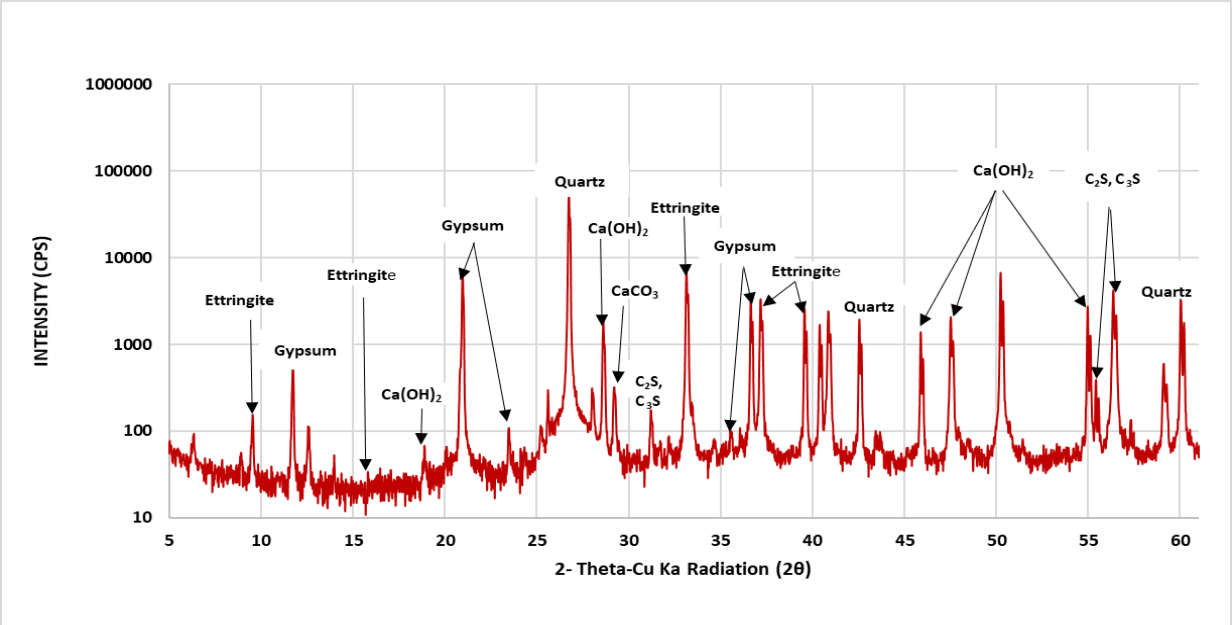

b)

Figure 4: X-ray diffraction (XRD) patterns of paste tailings lightly cemented with Portland cement (PC-LCPT) at (a) 0% and (b) 45% pyrite content after a 150-day curing period.

The higher permeability values observed for SG-LCPT compared to PC-LCPT can be attributed to the limited formation of secondary hydration products (secondary C–S–H) from slag hydration, which results in a coarser pore structure. The partial (50%) replacement of cement with slag reduces the amounts of C_2S and C_3S available for hydration, thereby lowering the production of C–S–H and CH at later ages. In contrast, PC-LCPT retains higher clinker content and continuously generates more hydration products, leading to finer pores and denser structures. This interpretation is consistent with the physical properties presented in Figure 5, where SG-LCPT already shows a higher void ratio (1.11) and lower dry density (1.36 g/cm³) at 0% pyrite compared to PC-LCPT. At 45% pyrite, these differences are more pronounced, with SG-LCPT reaching a void ratio of 1.64 and a dry density of 1.09 g/cm³.

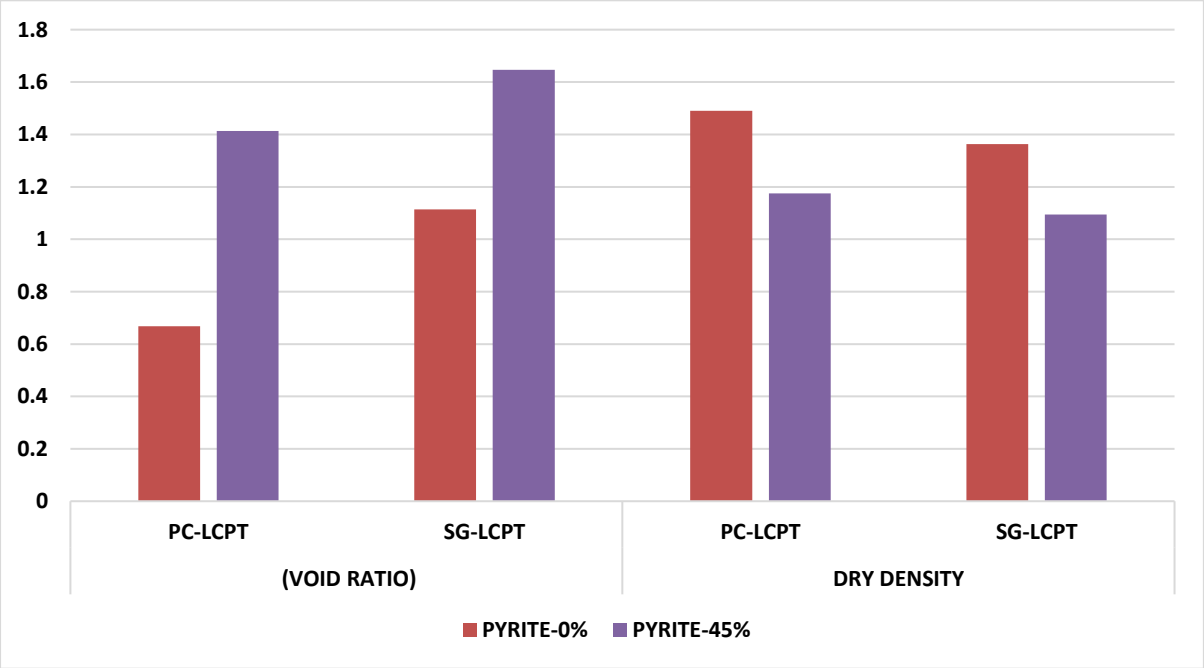

Figure 5: **Void ratio and dry density of PC-LCPT and SG-LCPT at 0% and 45% pyrite content after 150 curing days.**

Mercury intrusion porosimetry (MIP) results (Figure 6) further confirm these differences. At 0% pyrite (Figure 6a), PC-LCPT exhibits a sharp, unimodal pore size distribution centered around 1.3 μm with a maximum incremental porosity of 1.58%,

reflecting a compact, refined pore network (Aldhafeeri and Fall, 2016). By contrast, SG-LCPT at 0% pyrite shows a broader distribution spanning 0.7–3.5 μm, with lower peak porosity (1.2%), indicative of a more heterogeneous and coarser pore system due to reduced hydration product formation. At 45% pyrite (Figure 6b), both LCPT systems display increased threshold pore sizes, rising from 1.3 to 1.6 μm (23% increase) in PC-LCPT and from 1.8 to 2.1 μm (16% increase) in SG-LCPT. This confirms that pyrite oxidation promotes pore coarsening and enhances fluid transport. However, the sharper increase in PC-LCPT demonstrates its higher sensitivity to pyrite-induced permeability degradation compared with SG-LCPT.

The mechanistic explanation lies in binder composition. With 50% slag replacement, the blended binder contains less C_3A than pure Portland cement, limiting the extent of ettringite formation from sulphate attack (Fall and Pokharel, 2013). Additionally, the pozzolanic reaction of slag consumes portlandite (CH), thereby reducing gypsum formation. Consequently, pyrite-bearing SG-LCPT produces smaller amounts of expansive minerals (ettringite, gypsum) than pyrite-bearing PC-LCPT. Lower quantities of these expansive phases mean less internal stress and cracking, thus mitigating pore coarsening in SG-LCPT.

This explanation is supported by XRD results (Figures 4 and 7). At 0% pyrite, both PC-LCPT and SG-LCPT diffractograms are dominated by portlandite, gypsum, calcite, and quartz, with no detectable ettringite or unhydrated clinker phases, indicating stable hydration and well-developed matrices. At 45% pyrite, however, both systems show strong ettringite and gypsum peaks and the appearance of unhydrated C_2S and C_3S, confirming that sulphate ions from pyrite oxidation interfere with binder hydration (Pokharel and Fall, 2013; Rodrigues et al., 2012). Notably, PC-LCPT exhibits more intense ettringite and gypsum peaks than SG-LCPT, consistent with its greater permeability deterioration.

Overall, the results demonstrate that pyrite destabilizes the cement matrix by generating sulphate ions, which promote the formation of expansive minerals and hinder

complete hydration. This leads to microstructural degradation and higher permeability. Comparatively, SG-LCPT shows greater resistance than PC-LCPT, in line with prior studies reporting that slag-blended cements are more resistant to sulphate attack than pure Portland cement. From an environmental and geotechnical perspective, these findings highlight the importance of binder selection in the long-term performance of surface paste disposal (SPD) systems. While both PC- and SG-based LCPT are vulnerable to pyrite oxidation, SG-LCPT provides comparatively greater durability by limiting permeability increases and minimizing sulphate-induced cracking. This enhanced resistance has direct implications for reducing contaminant migration, improving structural stability, and ensuring the long-term environmental safety of mine tailings storage facilities.

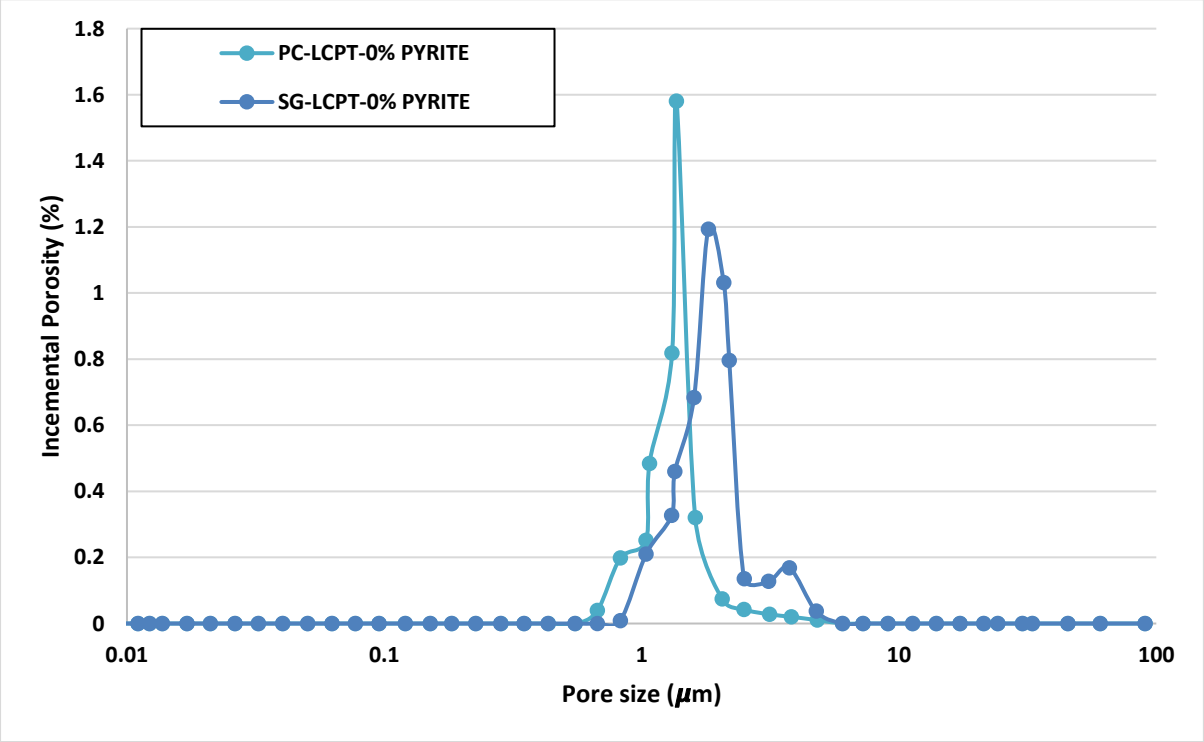

a)

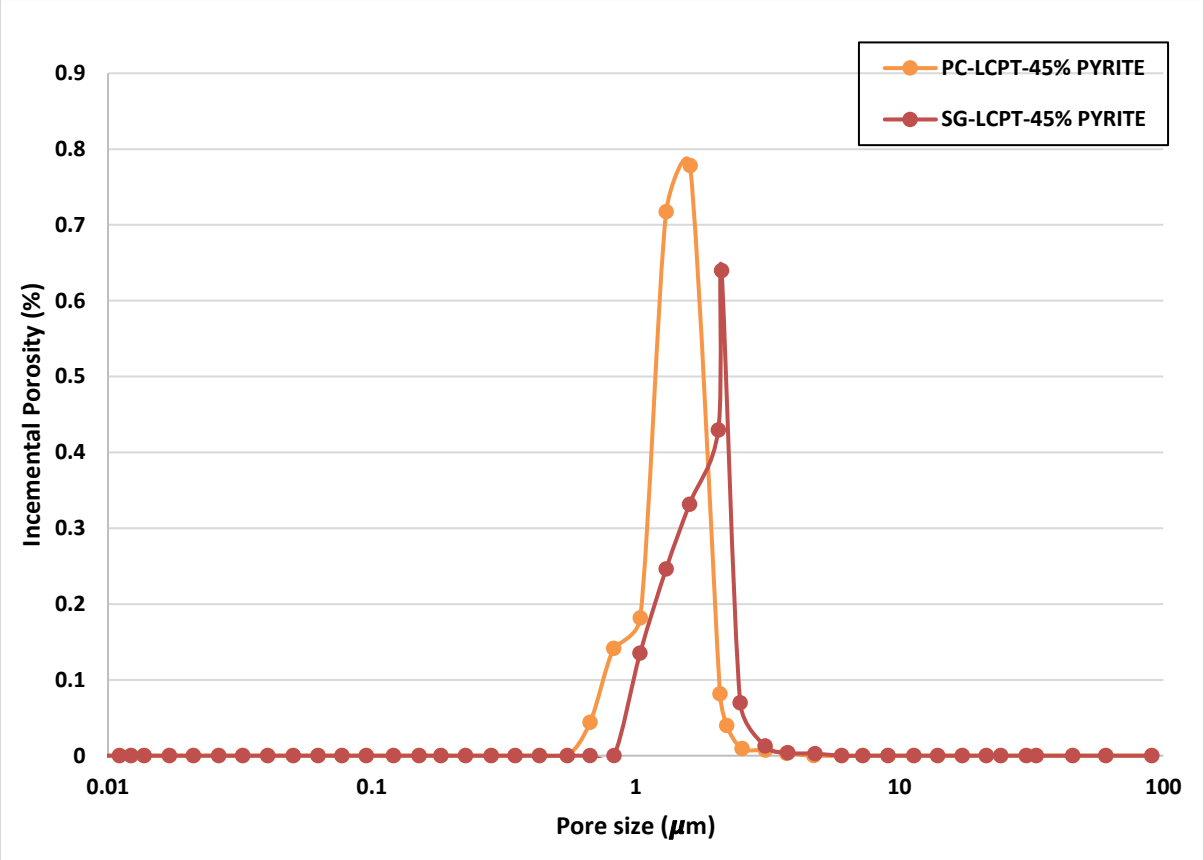

b)

Figure 6: MIP graphs showing Incremental pore size distributions of 150 days cured PC-LCPT and a SG-LCPT under sealed curing conditions: (a) at 0% pyrite content and (b) at 45% pyrite content.

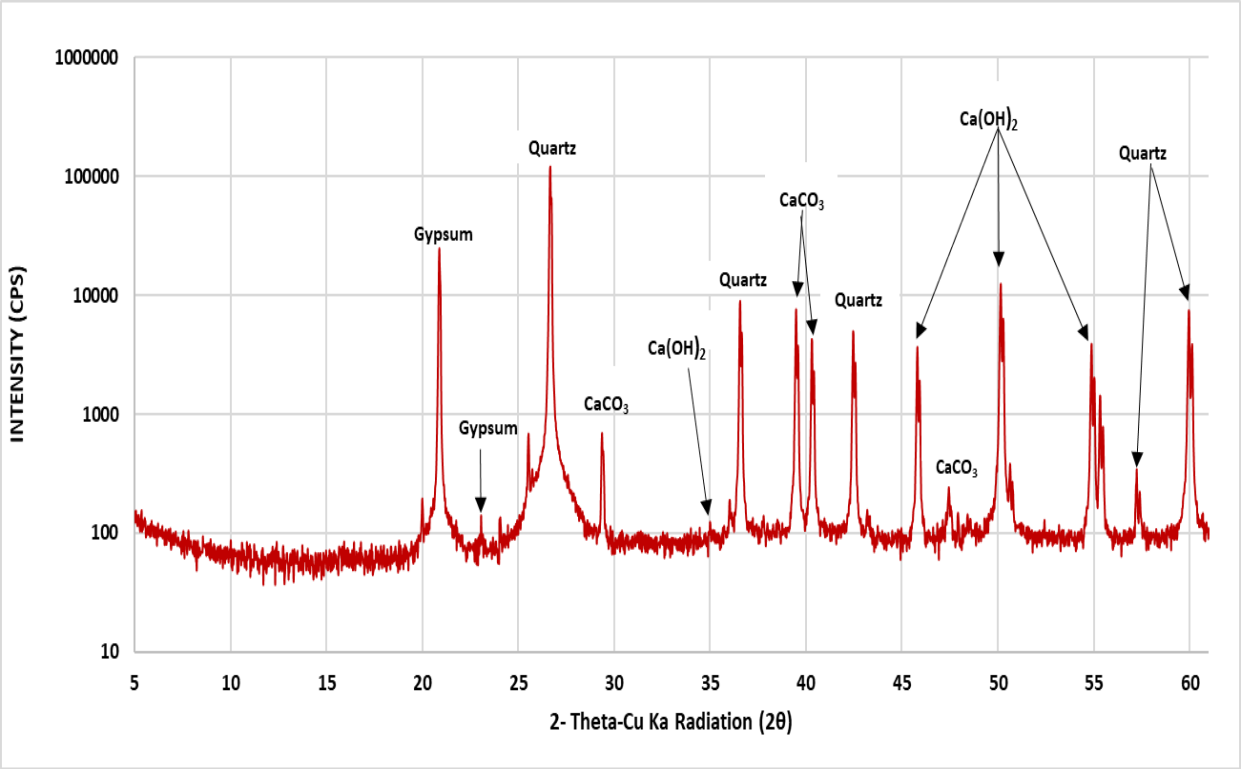

a)

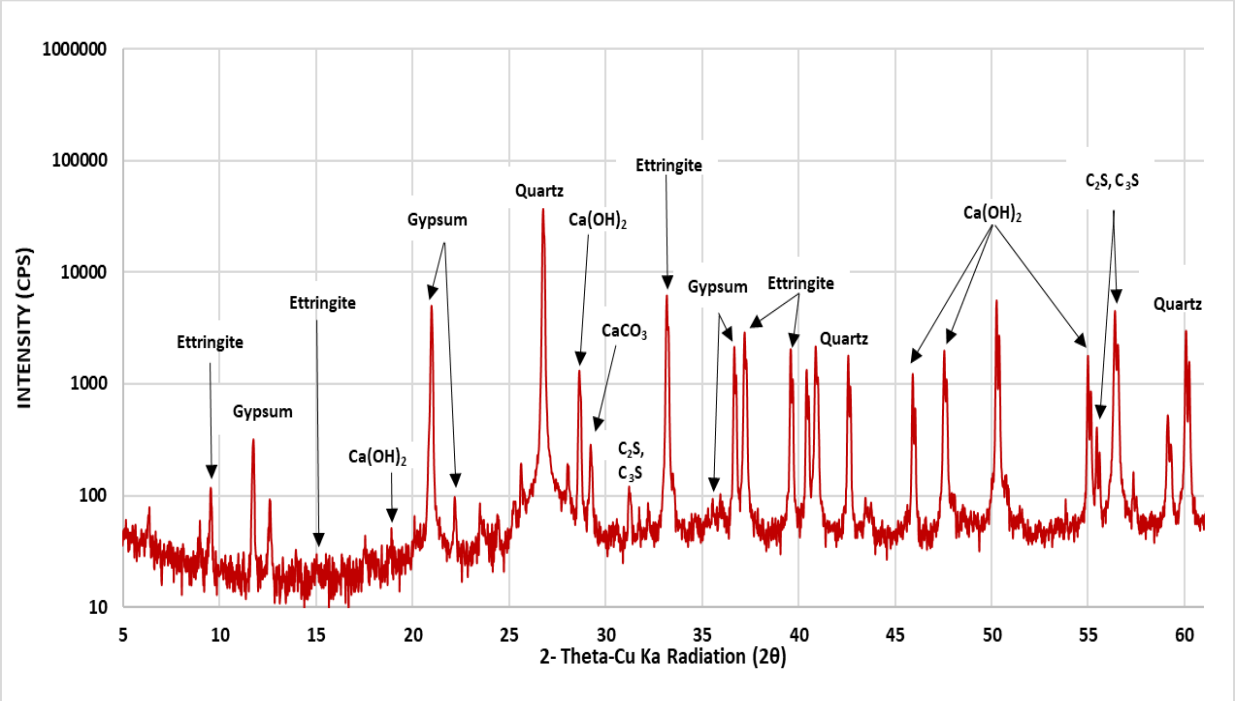

b)

Figure 7: **X-ray diffraction (XRD) patterns of paste tailings lightly cemented with a 50/50 blend of Portland cement and slag at (a) 0% and (b) 45% pyrite content after a 150-day curing period.**

5.4.2 EFFECT OF PYRITE CONTENT ON THE PERMEABILITY OF LIGHTLY CEMENTED PASTE TAILINGS SUBJECTED TO AIR DRYING

In practice, paste tailings are deposited in thin layers, and the interval between successive layers varies depending on mining operations and site conditions. When these intervals are long, and deposition occurs in climates that promote strong evaporation, surface drying can occur, exposing the paste tailings to oxygen. To replicate this scenario, the permeability of LCPT with varying pyrite contents subjected to air drying was investigated, and the results are presented in Figure 8. Figure 8 shows the combined influence of pyrite content (0%, 5%, 15%, and 45%), curing environment (sealed versus air-dried), and permeability of PC-LCPT. At low pyrite levels (0-15%), air drying has little effect. Permeability increases only slightly, from 1.97×10^{-6} to 2.44×10^{-6} cm/s under air drying and from 1.62×10^{-6} to 2.02×10^{-6} cm/s under sealed curing. These minor changes suggest that the cementitious matrix remains intact and that microstructural alterations are insufficient to significantly affect fluid flow.

At 45% pyrite, however, a more pronounced increase in permeability is observed under air drying. The coefficient of permeability rises to 1.9×10^{-5} cm/s, which is about 30% higher than the 1.5×10^{-5} cm/s recorded under sealed curing. This increase is attributed to accelerated pyrite oxidation under oxygen exposure, which produces more sulphate ions than in sealed conditions. The sulphate ions react with cement components (C_3A) and hydration products (CH), forming expansive secondary minerals such as ettringite and gypsum, while simultaneously inhibiting ongoing cement hydration. These processes disrupt the matrix, increase pore connectivity, and weaken the binder's ability to refine the pore structure, thereby inducing microcracking and reducing cohesion (Schmidt et al., 2011; Czerewko et al., 2003; Lee et al., 2005; Pokharel et al., 2013). Such degradation highlights the elevated risk of acid generation or contaminant migration and reduced long-term stability in field scenarios where

LCPT layers are exposed to drying and oxygen ingress.

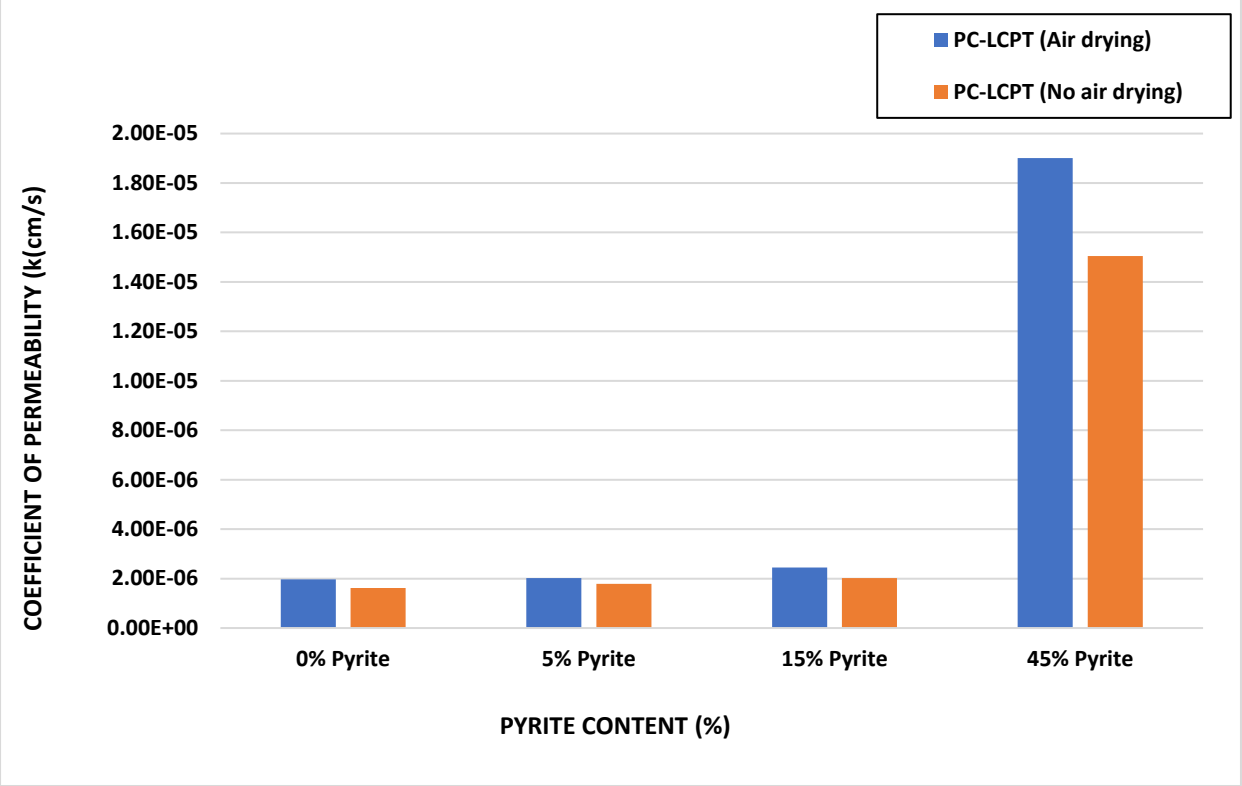

Figure 8: Effect of pyrite content and air drying on the permeability of PC-LCPT under air-drying and sealed conditions after 150 curing days.

To validate these mechanisms, XRD analyses were conducted on sealed and air-dried LCPT samples with 0% and 45% pyrite (Figure 9). At 0% pyrite, diffraction patterns under both curing conditions are dominated by strong portlandite peaks, confirming a well-hydrated matrix. Minor gypsum, likely residual from the original cement where it is added to control C_3A hydration (Frigione, 1983), was detected, along with monosulfoaluminate from early C_3A sulphate reactions (Pinter and Gosselin, 2018). Quartz peaks correspond to inert tailings minerals, while calcite reflects carbonation of portlandite (Savija and Lukovic, 2016). Compared with sealed specimens, air-dried samples show slightly lower portlandite intensity and marginally higher calcite, consistent with mild carbonation. Overall, this assemblage

reflects a stable, well-hydrated matrix with minimal sulphate generation and is consistent with the low permeability recorded under both curing conditions.

At 45% pyrite, the XRD patterns reveal a marked mineralogical shift: portlandite peaks are reduced, while gypsum and ettringite peaks intensify, indicating active sulphate reactions. Residual C_2S and C_3S are also detected, pointing to incomplete cement hydration (Pokharel and Fall, 2013). These effects are most pronounced in air-dried samples, where oxygen availability accelerates pyrite oxidation and sulphate production (Aldhafeeri et al. 2016), driving expansive ettringite formation. Similar findings have been reported by Rodrigues et al. (2012), Barnett et al. (2002), Macphee and Barnett (2004), and Aldhafeeri et al. (2016). The accumulation of expansive minerals consumes hydration products, induces internal stresses, and causes microcracking, thereby increasing pore connectivity and weakening the matrix. These transformations are consistent with the sharp rise in permeability observed in pyrite-bearing samples: 1.9×10^{-5} cm/s under air drying and 1.5×10^{-5} cm/s under sealed curing, the latter demonstrating that internal oxidation can still occur even without direct air exposure.

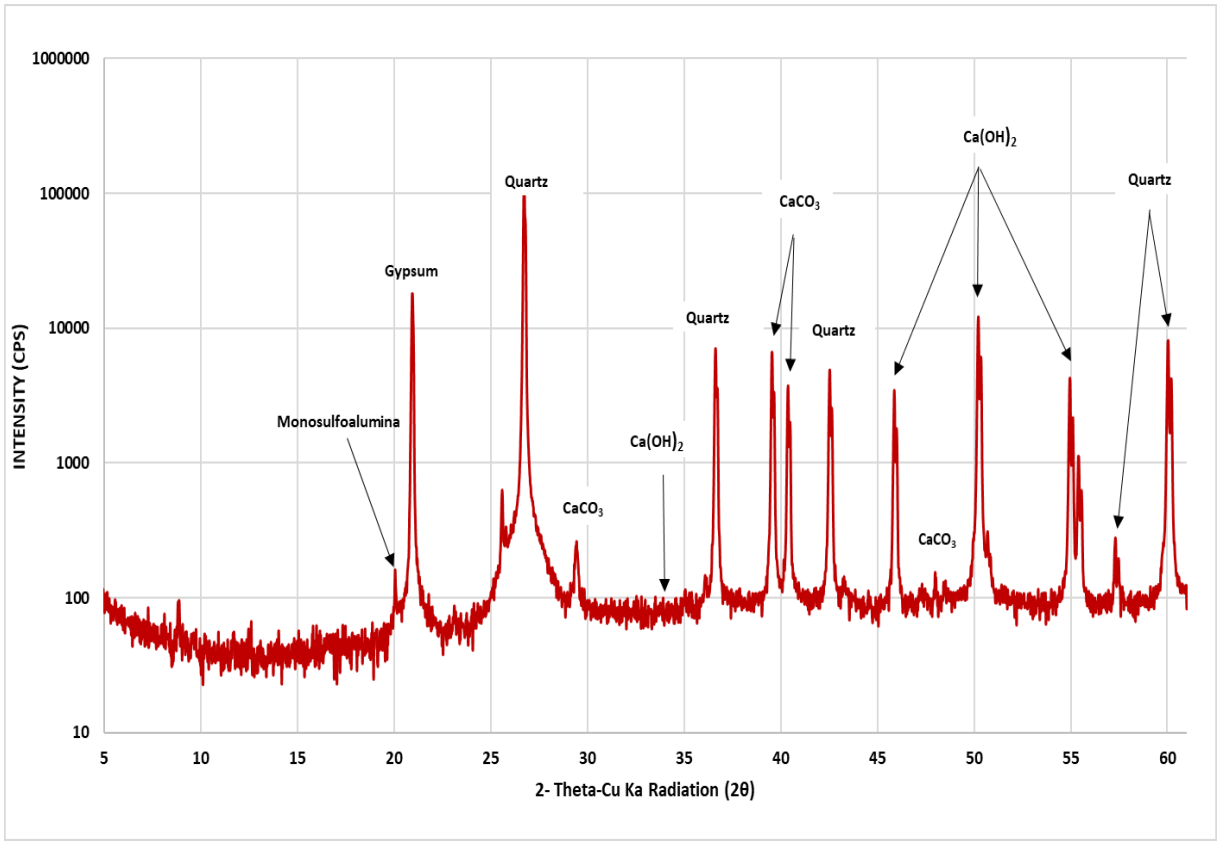
1000000
100000
10000
1000
100
10
INTENSITY (CPS)
5
10
15
20
25
30
35
40
45
50
55
60
2- Theta-Cu Ka Radiation (2θ)
Monosulfoalumina
Gypsum
Quartz
CaCO3
Ca(OH)2
Quartz
CaCO3
Quartz
Ca(OH)2
CaCO3
Quartz

a)

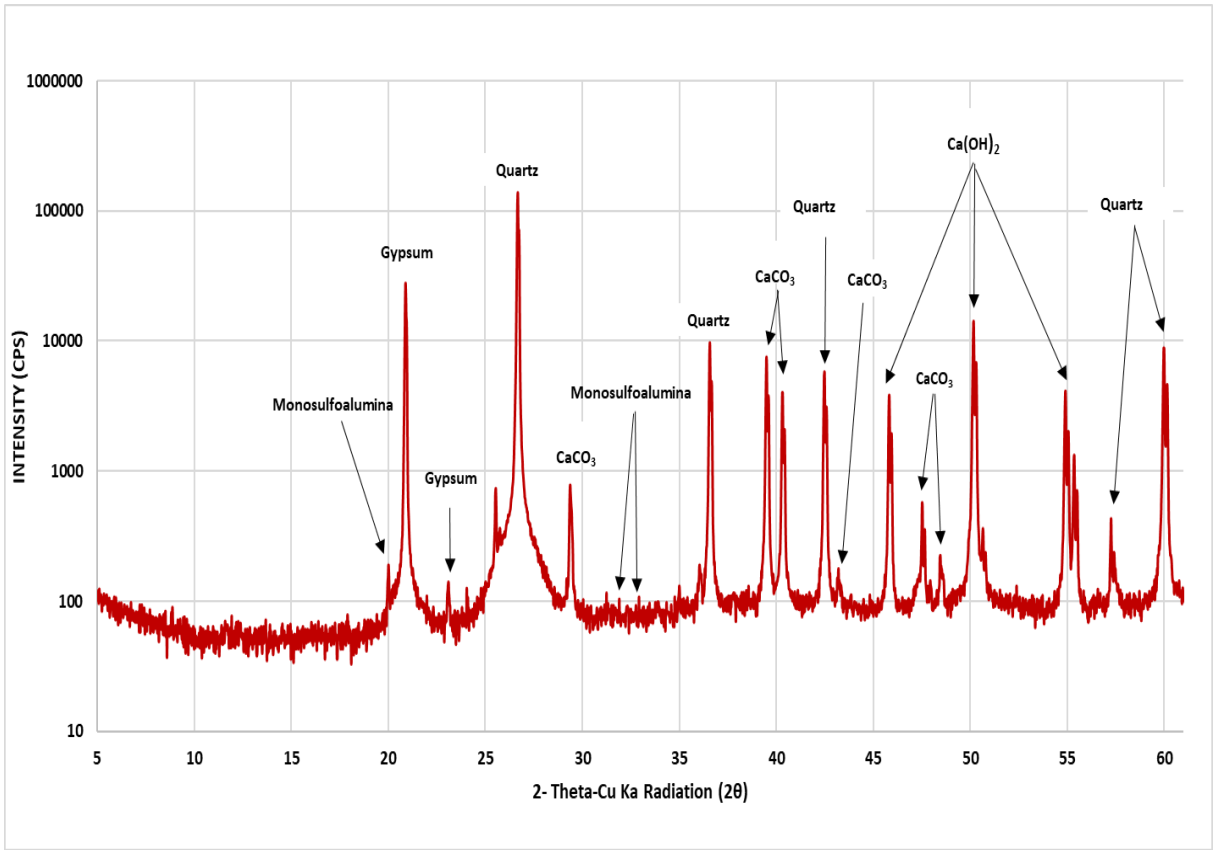
1000000
100000
10000
1000
100
10
INTENSITY (CPS)
5
10
15
20
25
30
35
40
45
50
55
60
2- Theta-Cu Ka Radiation (2θ)
Monosulfoalumina
Gypsum
Quartz
CaCO3
Monosulfoalumina
Quartz
CaCO3
Quartz
CaCO3
Ca(OH)2
CaCO3
Quartz

b)

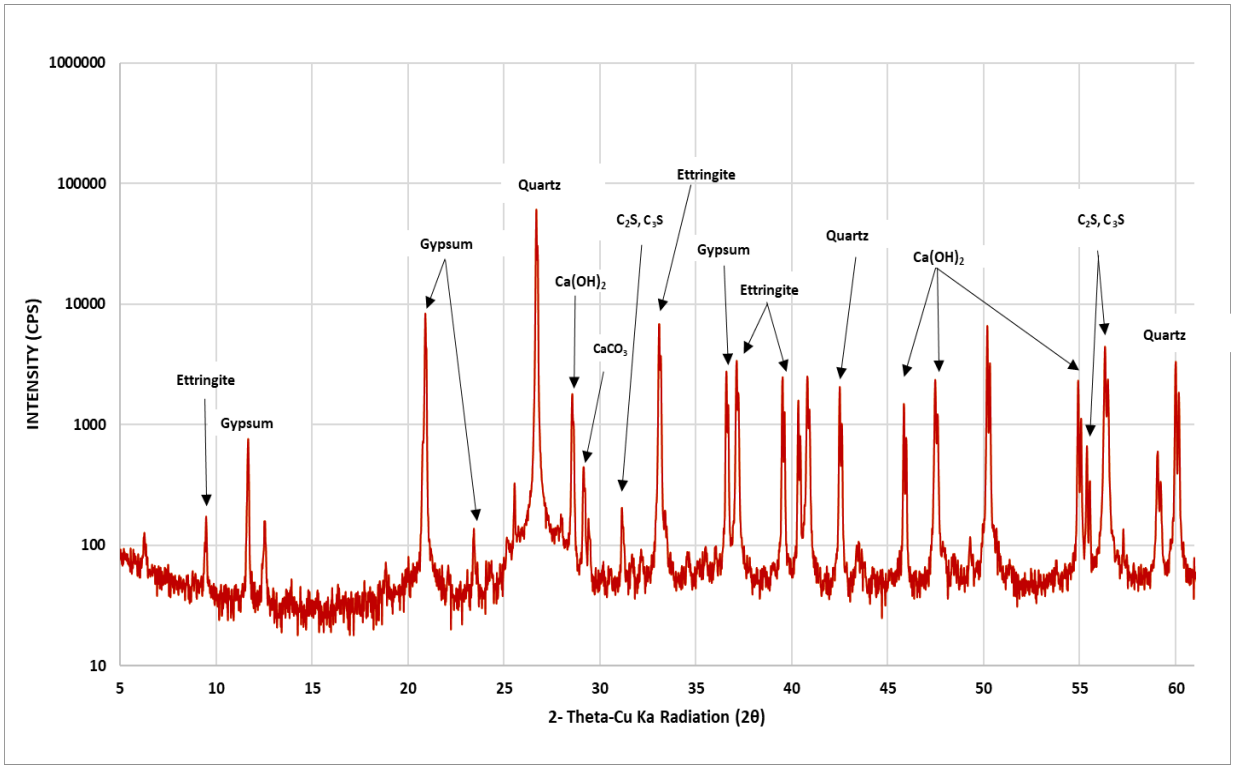

c)

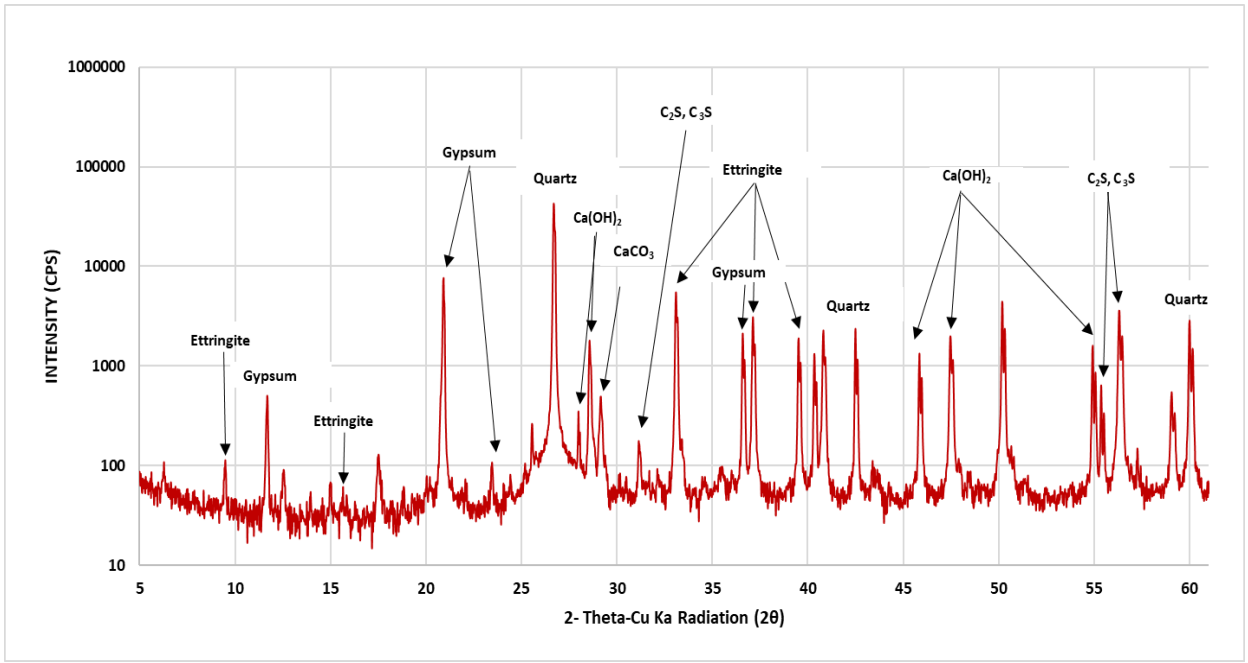

d)

Figure 9: X-ray diffraction (XRD) patterns of (a) PC-LCPT-0%pyrite (no air-drying), (b) PC-LCPT-0%pyrite (air-drying), (c) PC-LCPT-45%pyrite (no air-drying) (d) PC-LCPT-45%pyrite (air-drying).

The MIP results (Figure 10) and physical properties (Figure 11) provide quantitative confirmation of the XRD interpretations. At 0% pyrite, the sealed sample displays a sharp, narrow peak around 1.1 μm with a maximum incremental porosity of 1.6%, reflecting a refined, compact microstructure dominated by gel and small capillary pores (Figure 10a). By contrast, the air-dried sample shows a broader distribution with a smaller peak (0.23%) shifted toward larger pore sizes (2 μm), indicating coarser pores and reduced refinement. At 45% pyrite, air-dried PC-LCPT samples exhibit both higher peak porosity and a shift toward larger pore sizes relative to sealed samples. This pore coarsening is consistent with pyrite oxidation and expansive mineral formation under oxygen exposure. Sealed samples, while also affected, retain finer pores and lower connectivity, indicating comparatively better resistance to fluid transport. An additional factor contributing to pore coarsening in air-dried LCPT is shrinkage-induced microcracking caused by moisture loss, which further disrupts the cementitious matrix and increases permeability.

The bulk physical properties corroborate these observations (Figure 11). Void ratio increases progressively with pyrite content, with a more pronounced effect under air-dried conditions. At 45% pyrite, the void ratio reaches 1.56 in air-dried samples compared with 1.41 in sealed samples, reflecting enhanced porosity due to expansive mineral formation. Correspondingly, dry density decreases with increasing pyrite content, falling below 1.2 g/cm^3 at 45% pyrite for both curing conditions, with the lowest values observed under air drying. This reduction reflects the replacement of dense hydration products such as $Ca(OH)_2$ with lower-density sulphate minerals and overall matrix breakdown. Together, the increases in void ratio and decreases in dry density reinforce the mineralogical and pore structure findings, affirming that pyrite oxidation, particularly under air exposure, compromises the physical stability and permeability resistance of the LCPT matrix.

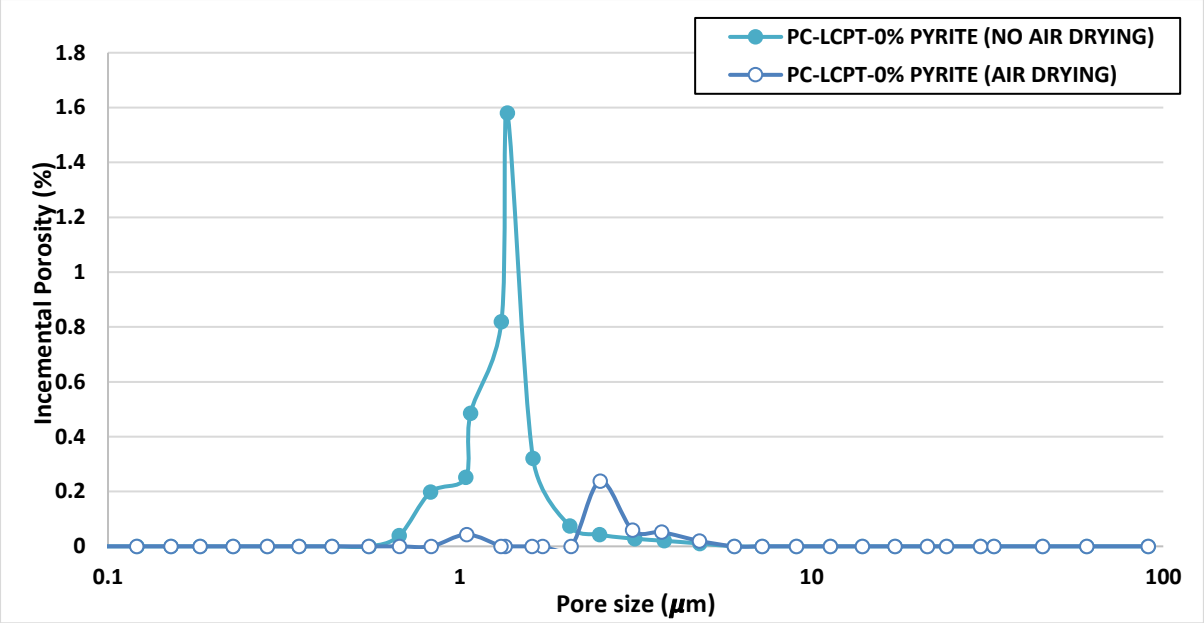

a)

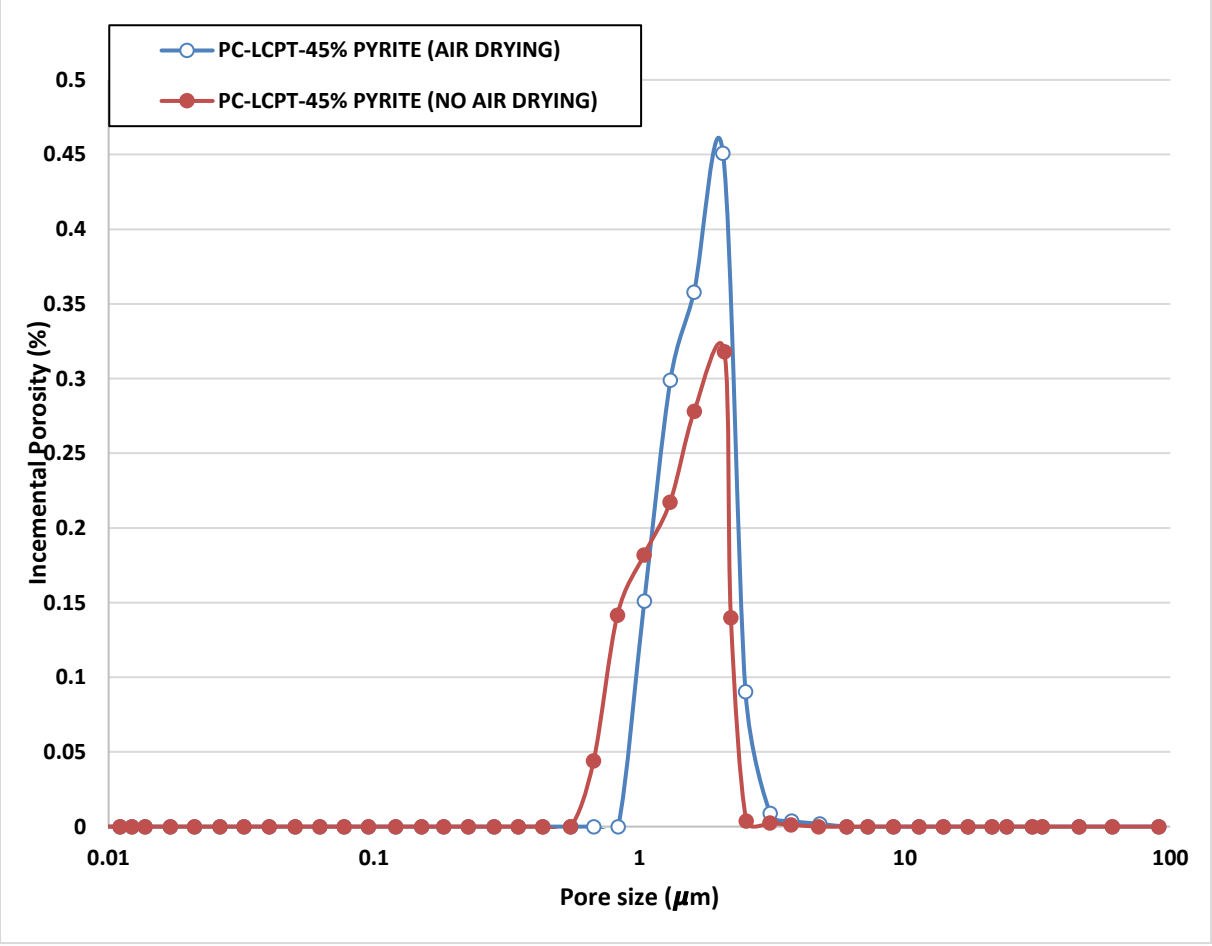

b)

Figure 10: MIP graphs showing Incremental pore size distributions of 150-day cured PC-LCPT under air-dried and sealed conditions at (a) at 0% pyrite (b) 45% pyrite.

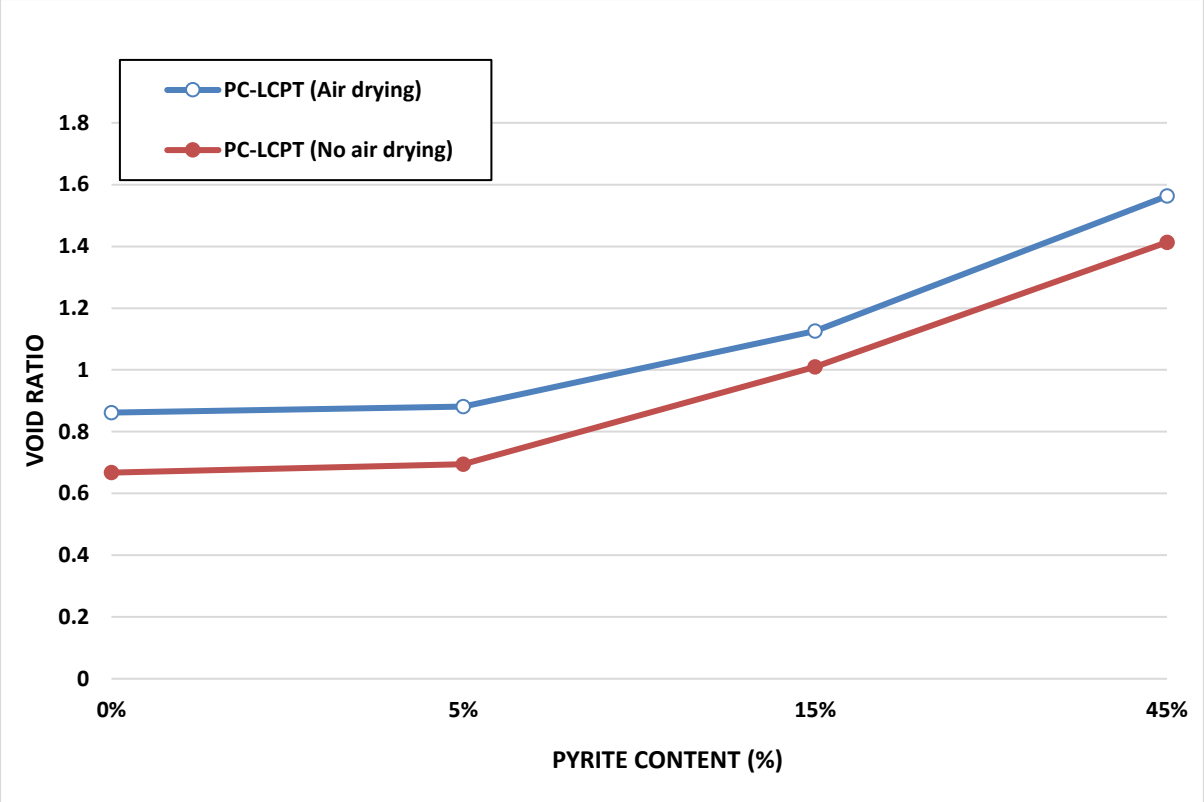

a)

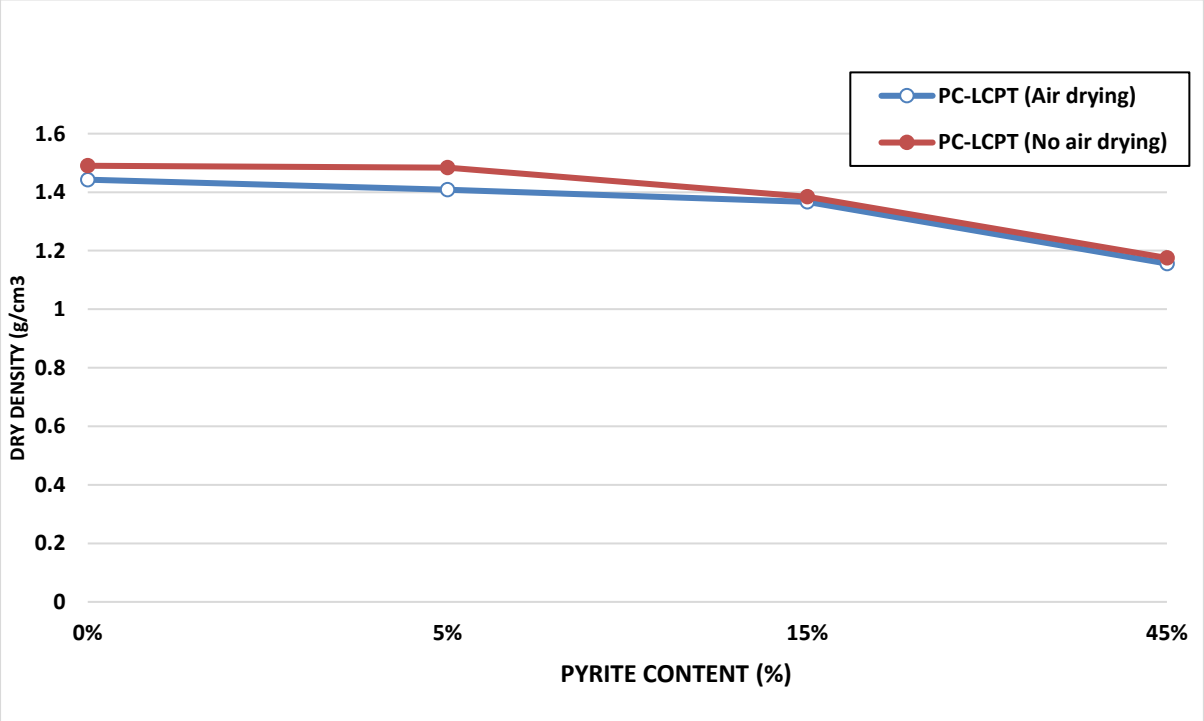

b)

Figure 11: Effect of increasing pyrite content and pyrite oxidation on the physical properties of lightly cemented paste tailings (PC-LCPT): (a) void ratio, and (b) dry density.

Given the common practice of using pozzolanic alternatives to Portland cement (PC) in the mining industry, this study compared the performance of a 1 wt.% 50:50 slag/PC blend (SG-LCPT) with that of 1 wt.% 100% PC (PC-LCPT), as shown in Figure 12. The results demonstrate that both pyrite content and air drying significantly influenced permeability, with clear differences between the binder systems. At 0% pyrite, PC-LCPT exhibited low permeability - approximately 1.97×10^{-6} cm/s under air drying and 1.62×10^{-6} cm/s under sealed curing - indicating that Portland cement effectively reduces pore connectivity, with only minor influence from potential microstructural damage such as shrinkage-induced microcracking during air drying. By contrast, SG-LCPT at 0% pyrite showed substantially higher baseline permeability, about 1.63×10^{-5} cm/s with air drying and 1.32×10^{-5} cm/s under sealed conditions, confirming that the slag-based binder is less efficient in refining pore connectivity in paste tailing systems. The mechanisms underlying this higher baseline permeability of SG-LCPT have been detailed earlier and are consistent with previous findings (Gruyaert et al., 2010; Gruyaert et al., 2012; Gruyaert et al., 2013). When pyrite content increased to 45%, permeability rose markedly in both binder systems, particularly under air-dried conditions where pyrite oxidation is most pronounced. For PC-LCPT, permeability increased to 1.90×10^{-5} cm/s under air drying and 1.50×10^{-5} cm/s under sealed curing, representing an approximate 30% rise. The relative increase was smaller in SG-LCPT, which reached 3.40×10^{-5} cm/s when air-dried and 3.07×10^{-5} cm/s in the sealed condition, corresponding to a 12% increase. These results indicate that PC-LCPT is more sensitive to sulphate attack induced by pyrite oxidation, consistent with the formation of expansive secondary minerals such as ettringite and gypsum, as demonstrated previously. The precipitation of these minerals generates internal stresses, induces microcracking, enlarges pore networks, and enhances fluid transport, ultimately compromising the structural integrity and long-term durability of the cemented matrix.

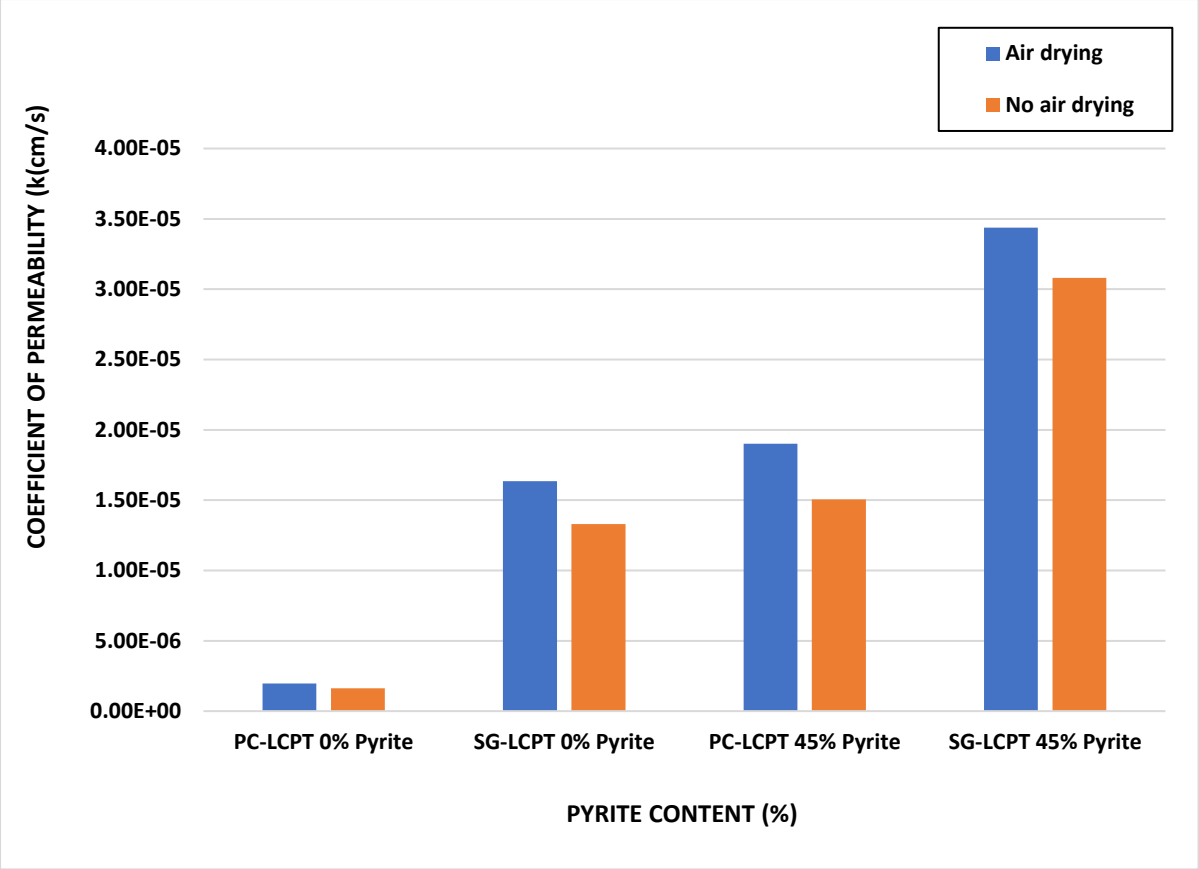

Figure 12: Effect of pyrite oxidation on the permeability of LCPT stabilized with different binder types (PC-LCPT and SG-LCPT) at 150 days curing time

5.4.3 EFFECT OF INITIAL SULPHATE CONTENTS ON THE PERMEABILITY OF LIGHTLY CEMENTED PASTE TAILINGS.

In practice, sulphide minerals contained in tailings may partially oxidize before their use in paste tailings or cemented paste backfill mixtures. This occurs most commonly when tailings are stored in surface impoundments, stockpiles, or dry stacks, where exposure to oxygen and moisture promotes oxidation. Such pre-oxidation releases sulphate ions into the pore water of the tailings, raising the initial sulphate concentration of the mixture and potentially influencing its hydraulic performance.

To investigate the combined effects of initial sulphate concentration, pyrite content, and oxygen exposure, this study assessed the permeability of LCPT prepared with 0% and 15%

pyrite and subjected to sulphate concentrations of 0, 5,000, and 25,000 ppm.

The results, presented in Figure 13, show that increasing sulphate content generally leads to higher permeability, with the effect becoming more pronounced at elevated concentrations and in the presence of pyrite. Under sealed curing, permeability in PC-LCPT without pyrite increased moderately from 1.6×10^{-6} cm/s at 0 ppm to 3.1×10^{-6} cm/s at 25,000 ppm. By comparison, SG-LCPT exhibited a significantly higher baseline permeability of 1.6×10^{-5} cm/s, reflecting its lower clinker content (Gruyaert et al., 2010; Gruyaert et al., 2012; Gruyaert et al., 2013) and less compact microstructure, as discussed earlier. The inclusion of pyrite amplified these effects, particularly at high sulphate levels, since pyrite oxidation generated additional sulphate internally, further fueling expansive mineral formation. Sulphate ions react with tricalcium aluminate (C_3A) and calcium hydroxide (CH) to form ettringite and gypsum (Pokharel and Fall, 2013). At high concentrations, excessive ettringite and gypsum formation induces matrix expansion and microcracking, which enlarge pores and disrupt structural integrity (Pokharel and Fall, 2013; Fall et al., 2009; Pokharel, 2008; Ouellet et al., 2006; Benzaazoua et al., 2002, 1999). This mechanism is particularly severe under air-drying conditions, where oxygen ingress accelerates pyrite oxidation and sulphate generation. As a result, permeability rises sharply rises, for example, in PC-LCPT with 25,000 ppm sulphate and pyrite, permeability reached 4.42×10^{-5} cm/s, while SG-LCPT recorded the highest value of 4.46×10^{-5} cm/s. These findings confirm that high sulphate concentrations, especially when combined with pyrite and oxygen exposure, compromise the cemented matrix and significantly increase permeability.

These permeability trends are corroborated by the void ratio and dry density results presented in Figure 14. Increasing initial sulphate content, particularly at 25,000 ppm, consistently elevated the void ratio and reduced the dry density in both PC-LCPT (Figure 14a) and SG-LCPT (Figure 14b), with stronger effects under air-drying and in pyrite-bearing systems. The

changes were more pronounced in SG-LCPT, reflecting greater pore coarsening and reduced compactness. These patterns are explained by sulphate reactions with cement phases, which form expansive minerals such as ettringite and gypsum. While limited amounts of these minerals may locally refine the pore structure, excessive precipitation at high sulphate levels generates expansion, cracking, and interconnected voids. Pyrite oxidation further intensifies this degradation by producing additional sulphate under oxygen exposure, accelerating matrix breakdown. The concurrent rise in void ratio and decline in dry density therefore reinforce the permeability data, confirming that both initial sulphate content and pyrite oxidation act synergistically to undermine the structural stability and hydraulic resistance of LCPT systems.

These findings underscore that pre-oxidized, sulphate-rich tailings pose a heightened risk to the performance of cemented paste tailings systems used in surface disposal. Elevated initial sulphate contents, particularly when combined with pyrite oxidation and oxygen exposure, accelerate microstructural degradation, leading to increased permeability, solute (e.g. oxygen) migration pathways, and loss of long-term integrity. From a field perspective, careful management of tailings storage and binder selection is therefore critical to ensure the environmental safety and durability of paste tailings disposal facilities.

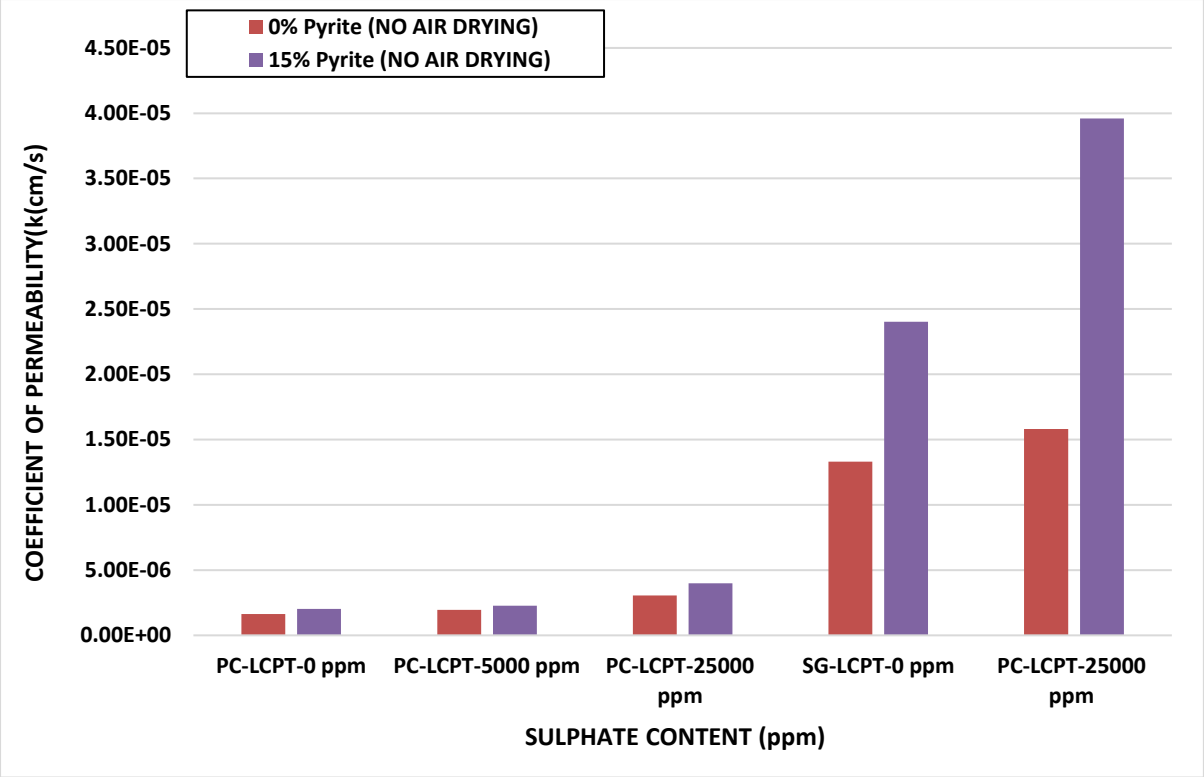

a)

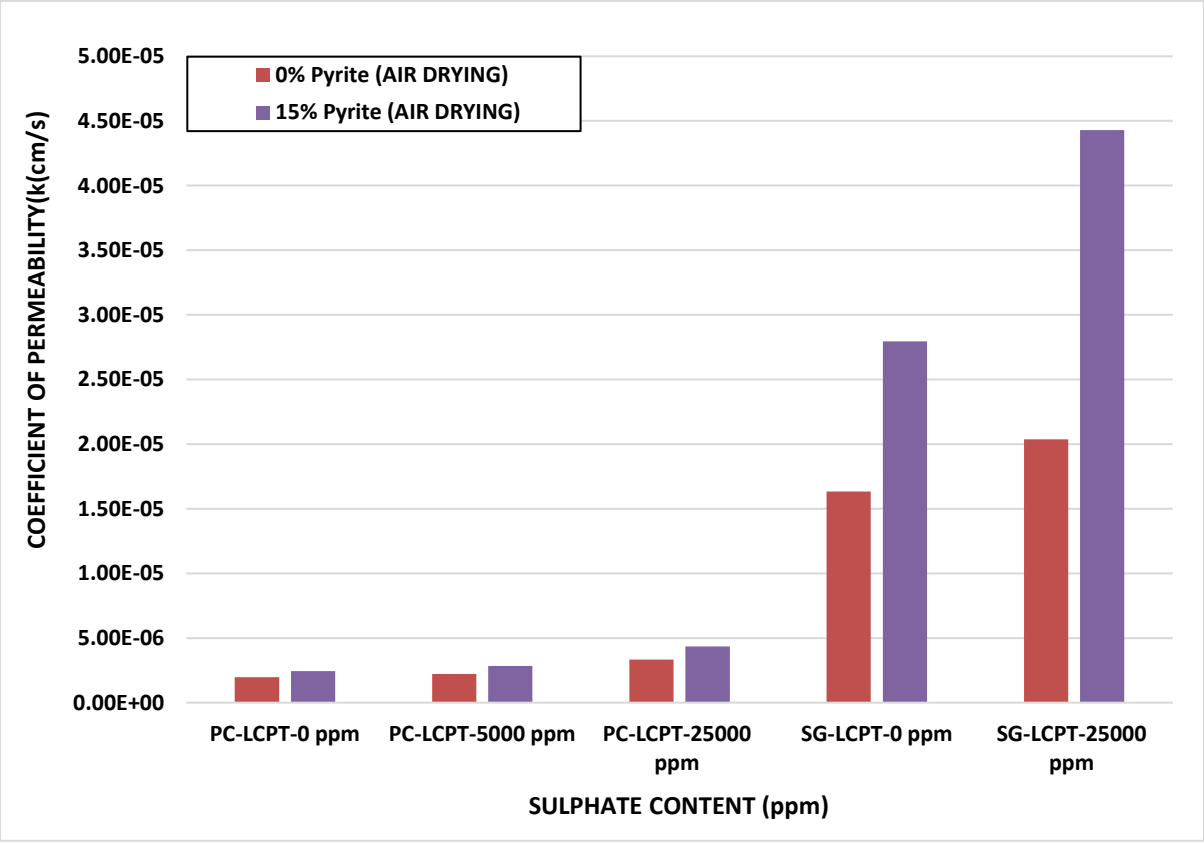

b)

Figure 13: Effect of initial sulphate, pyrite content and oxidation on the permeability of lightly cemented paste tailings exposed to a) No-air drying and b) Air-drying conditions.

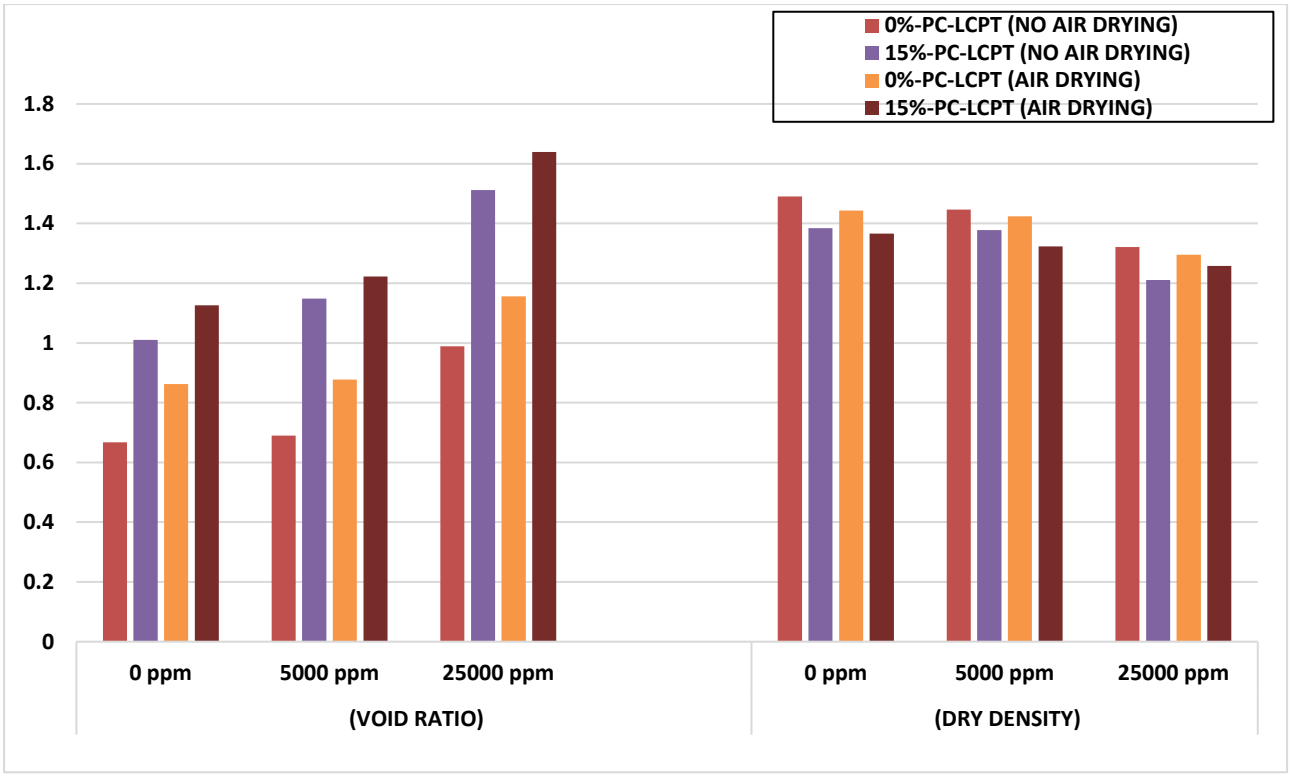

a

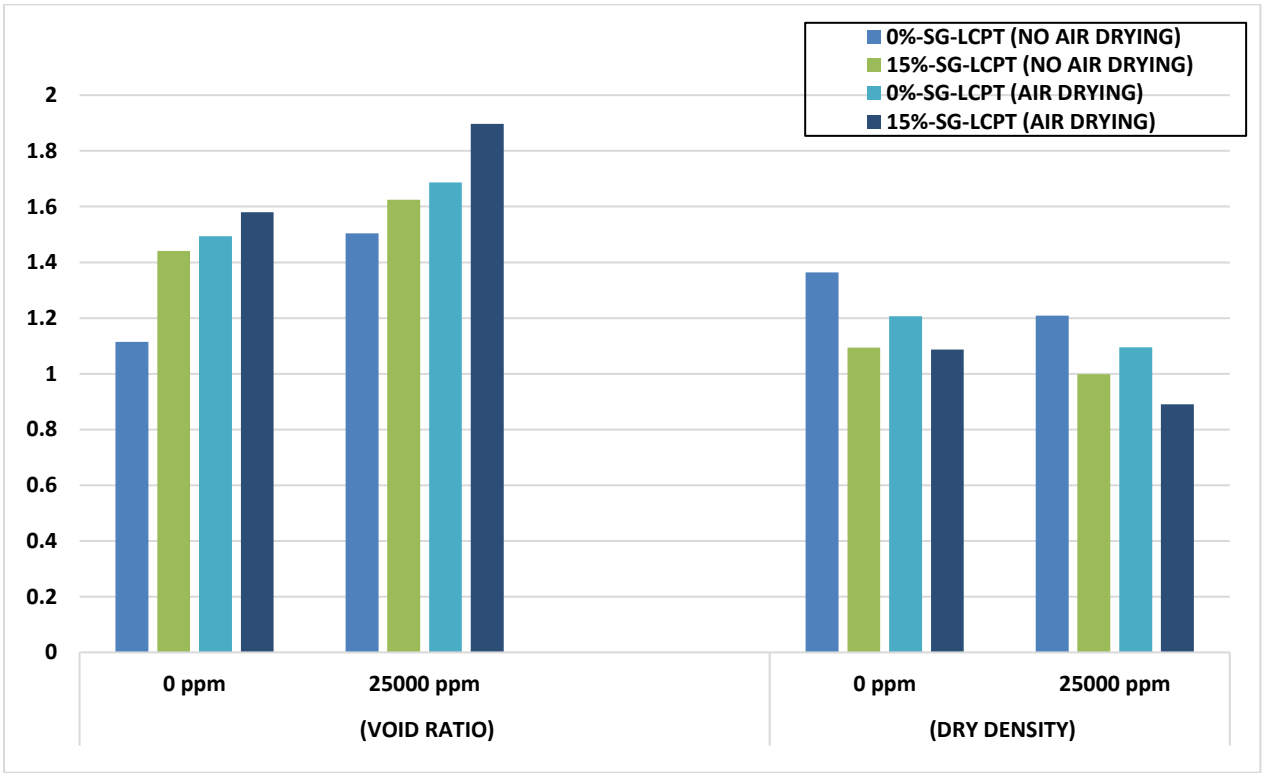

b)

Figure 14: Effect of initial sulphate content and pyrite content on the Void ratio and dry density of a) PC-LCPT samples b) SG-LCPT

5.5 SUMMARY AND CONCLUSIONS

This study systematically investigated the effects of pyrite content, pyrite oxidation, initial sulphate concentration, and binder type on the permeability and microstructural evolution of uncemented paste tailings (UPT) and lightly cemented paste tailings (LCPT) under field-representative curing conditions. The following conclusions can be drawn:

- Permeability of UPT increased steadily with higher pyrite content, driven by rising void ratios that created a looser, more open pore network.
- At low pyrite contents (≤15%), permeability remained low due to pore refinement and densification from cement hydration. At 45% pyrite, permeability rose sharply as sulphate ions released from pyrite oxidation reacted with portlandite and aluminous phases to form expansive minerals (ettringite, gypsum). These reactions consumed hydration products, induced internal stresses, caused microcracking, and coarsened the pore structure. Even under sealed conditions, limited internal oxidation was sufficient to compromise matrix integrity, showing that pyrite-bearing LCPT remains vulnerable without direct oxygen exposure.
- Increasing sulphate concentration consistently elevated permeability by promoting the formation of expansive minerals and weakening the matrix structure. When combined with pyrite, the sulphate released internally during pyrite oxidation further amplified permeability increases. This combined effect confirms sulphate as a critical factor undermining the stability of LCPT systems.
- Mineralogical, pore structure, and physical property analyses consistently confirmed matrix weakening under sulphate and pyrite-rich conditions. Portlandite depletion, elevated sulphate-bearing phases, and residual unhydrated clinker were accompanied by a shift from fine pores to larger connected voids. Void ratios increased and dry densities declined, reflecting a less compacted and weaker cemented matrix.

- Binder type had a decisive effect. Portland cement (PC)-LCPT initially showed lower permeability and finer pore structures, but was highly sensitive to pyrite- and sulphate-induced degradation due to its higher C_3A and portlandite contents. Slag-blended LCPT (SG-LCPT) exhibited higher baseline permeability but demonstrated greater resistance to sulphate attack and pyrite-induced deterioration, reflecting reduced C_3A availability and the pozzolanic consumption of portlandite, which limit expansive mineral formation.

This study demonstrates that permeability and, by extension, the durability and environmental performance of surface paste disposal systems (UPT and LCPT) are strongly governed by pyrite content, sulphate concentration, and binder composition. High pyrite and sulphate levels significantly accelerate permeability, solute migration pathways, and long-term structural degradation. While both binder systems are vulnerable, SG-LCPT shows comparatively greater durability under sulphate- and pyrite-rich conditions. From a field perspective, these findings highlight the need for careful paste tailings storage management, binder selection, and oxidation control to minimize acid mine drainage generation, ensure environmental safety, and improve the long-term durability of surface paste disposal facilities. Future research should extend these findings by coupling chemical reactivity, hydraulic performance with large-scale contaminant transport modelling and in-situ monitoring to better evaluate the environmental risks and long-term sustainability of surface paste tailings technologies.

5.0 REFERENCES

Abdul-Hussain, N., & Fall, M. (2011). Unsaturated hydraulic properties of cemented tailings backfill that contains sodium silicate. Engineering Geology, 123(4), 288–301. https://doi.org/10.1016/j.enggeo.2011.07.011.

Abdul-Hussain, A., Fall, M., & Su, G. (2011). Evolution of hydraulic and mechanical properties of gelfill. In Proceedings of the 14th PanAmerican Conference on Soil Mechanics and Geotechnical Engineering (PCSMGE), the 64th Canadian Geotechnical Conference (CGC), Toronto, Canada, 2–6 October 2011.

Aguilar-Garrido, A., Paniagua-López, M., Sierra-Aragón, M., Martínez Garzón, F. J., & Martín-Peinado, F. J. (2023). Remediation potential of mining, agro-industrial, and urban wastes against acid mine drainage. *Scientific Reports, 13(1), 12120. https://doi.org/10.1038/s41598-023-39266-4.

Aldhafeeri, Z., & Fall, M. (2016). Time and damage induced changes in the chemical reactivity of cemented paste backfill. Journal of Environmental Chemical Engineering, 4(4), 4038–4049. https://doi.org/10.1016/j.jece.2016.09.006

Benzaazoua, M., Belem, T., & Bussière, B. (2002). Chemical factors that influence the performance of mine sulphidic paste backfill. Cement and Concrete Research, 32(7), 1133–1144. https://doi.org/10.1016/S0008-8846(02)00752-4.

Benzaazoua, M., Ouellet, J., Servant, S., Newman, P., & Verburg, R. (1999). Cementitious backfill with high sulfur content: Physical, chemical, and mineralogical characterization. Cement and Concrete Research, 29(5), 719–725. https://doi.org/10.1016/S0008-8846(99)00023-X.

Bernier, R. L., Li, M. G., & Moerman, A. (1999). Effects of tailings and binder geochemistry on the physical strength of paste backfill. In Proceedings of Sudbury ’99, Mining and the Environment II (Vol. 3, pp. 1113–1118).

Bérard, J., Roux, R., & Durand, M. (1975). Performance of concrete containing a variety of black shale. Canadian Journal of Civil Engineering, 2(1), 58–65. https://doi.org/10.1139/l75-006.

Brackebusch, F., & Shillabeer, J. (1998). Use of paste for tailings disposal. In M. Bloss (Ed.), Minefill ’98: Proceedings of the Sixth International Symposium on Mining with Backfill (pp. 53–58). The Australasian Institute of Mining and Metallurgy.

Casanova, I., Aguado, A., & Agulló, L. (1997). Aggregate expansivity due to sulfide oxidation - II. Physico-chemical modeling of sulfate attack. Cement and Concrete Research, 27(11), 1627–1632. https://doi.org/10.1016/S0008-8846(97)00148-8.

Chinchón, J. S., Ayora, C., Aguado, A., & Guirado, F. (1995). Influence of weathering of iron sulfides contained in aggregates on concrete durability. Cement and Concrete Research, 25*(6),1264–1272. https://doi.org/10.1016/0008-8846(95)00119-W.

Cihangir, F., & Akyol, Y. (2018). Mechanical, hydrological and microstructural assessment of the durability of cemented paste backfill containing alkali-activated slag. International Journal of Mining, Reclamation and Environment, 32(2), 123–143. https://doi.org/10.1080/17480930.2016.1242183.

Czerewko, M. A., Cripps, J. C., Reid, J. M., & Duffell, C. G. (2003). Sulfur species in geological materials: Sources and quantification. Cement & Concrete Composites, 25*(7), 657–671. [https://doi.org/10.1016/S0958-9465(02)00066-5.

Deschamps, T., Benzaazoua, M., Bussière, B., & Aubertin, M. (2011). Laboratory study of surface paste disposal for sulfidic tailings: Physical model testing. *Minerals Engineering*, *24*(8), 794–806. https://doi.org/10.1016/j.mineng.2011.02.013

Dhir, B. (2018). Chapter 4 - Biotechnological Tools for Remediation of Acid Mine Drainage (Removal of Metals From Wastewater and Leachate). In *Bio-Geotechnologies for Mine Site Rehabilitation* (pp. 67–82). Elsevier Inc. https://doi.org/10.1016/B978-0-12-812986-9.00004-X

Evans, D. M., Zipper, C. E., Hester, E. T., & Schoenholtz, S. H. (2015). Hydrologic Effects of Surface Coal Mining in Appalachia (U.S.). *Journal of the American Water Resources Association*, *51*(5), 1436–1452. https://doi.org/10.1111/1752-1688.12322

Fall, M., Adrien, D., Célestin, J. C., Pokharel, M., & Touré, M. (2009). Saturated hydraulic conductivity of cemented paste backfill. Minerals Engineering, 22(15), 1307–1317. https://doi.org/10.1016/j.mineng.2009.08.002.

Fall, M., Benzaazoua, M., & Saa, E. G. (2008). Mix proportioning of underground cemented tailings backfill. Tunnelling and Underground Space Technology, 23(1), 80–90. https://doi.org/10.1016/j.tust.2006.08.005.

Fall, M., & Benzaazoua, M. (2005). Modeling the effect of sulphate on strength development of paste backfill and binder mixture optimization. Cement and Concrete Research, 35*(2), 301–314. https://doi.org/10.1016/j.cemconres.2004.05.020

Fall, M., Célestin, J. C., Pokharel, M., & Touré, M. (2010). A contribution to understanding the effects of curing temperature on the mechanical properties of mine cemented tailings backfill. Engineering Geology, 114(3), 397–413. https://doi.org/10.1016/j.enggeo.2010.05.016

Faraji, Z., & Fall, M. (2025). Saturated hydraulic conductivity of uncemented and lightly cemented high-density tailings for surface disposal. Environmental Earth Sciences, 84(1), Article 10. ://doi.org/10.1007/s12665-024-12019-w

Gerasimov, A., Kotova, E., & Ustinov, I. (2019). Applied mineralogy of anthropogenic accessory minerals. In S. Glagolev (Ed.), 14th International Congress for Applied Mineralogy (ICAM2019) (pp. 105–112). Springer. https://doi.org/10.1007/978-3-030-22974-0_16

Godbout, J., Bussière, B., & Belem, T. (2007). Evolution of cemented paste backfill saturated hydraulic conductivity at early curing time. In Proceedings of the 60th Canadian Geotechnical Society Conference (OttawaGeo 2007), Ottawa, Canada, 21–24 October 2007.

Grande, J. A., Santisteban, M., de la Torre, M. L., Fortes, J. C., de Miguel, E., Curiel, J., Dávila, J. M., & Biosca, B. (2018). The paradigm of circular mining in the world: The Iberian Pyrite Belt as a potential scenario of interaction. Environmental Earth Sciences, 77(10), 1–6. https://doi.org/10.1007/s12665-018-7577-1.

Gruyaert, E., Van den Heede, P., & De Belie, N. (2013). Carbonation of slag concrete: Effect of the cement replacement level and curing on the carbonation coefficient – Effect of carbonation on the pore structure. Cement & Concrete Composites, 35(1), 39–48. https://doi.org/10.1016/j.cemconcomp.2012.08.024

Gruyaert, E., Van den Heede, P., Maes, M., & De Belie, N. (2012). Investigation of the influence of blast-furnace slag on the resistance of concrete against organic acid or sulphate attack by means of accelerated degradation tests. Cement and Concrete Research, 42(1), 173–185.https://doi.org/10.1016/j.cemconres.2011.09.009

Hassani, F., Ouellet, J., & Hossein, M. (2001). Strength development in underground high-sulphate paste backfill operation. *CIM Bulletin, 94*, 57–62.

Hogsden, K. L., & Harding, J. S. (2012). Consequences of acid mine drainage for the structure and function of benthic stream communities: A review. Freshwater Science, 31(1), 108–120. https://doi.org/10.1899/11-091.1.

Ichrak, H., Mostafa, B., Abdelkabir, M., & Bruno, B. (2016). Effect of cementitious amendment on the hydrogeological behavior of a surface paste tailings' disposal. *Innovative Infrastructure Solutions : The Official Journal of the Soil-Structure Interaction Group in Egypt (SSIGE)*, *1*(1), Article 19. https://doi.org/10.1007/s41062-016-0019-6

Jacobs, J. A., Lehr, J. H., & Testa, S. M. (2014). Acid mine drainage, rock drainage, and acid sulfate soils: Causes, assessment, prediction, prevention, and remediation. (1st ed.). Wiley. https://doi.org/10.1002/9781118749197.

Javed, I., Ekinci, A., & Akintug, B. (2025). Utilization of artificially cemented sand for porous pavement applications and analysis of runoff control. Turkish Journal of Civil Engineering, 36. https://doi.org/10.18400/tjce.1603567

Ke, Y., Belem, T., & Benzaazoua, M. (2015). Effect of sulphate ions on the saturated hydraulic conductivity of cemented paste backfill. Cement and Concrete Composites, 62, 101–110. [https://doi.org/10.1016/j.cemconcomp.2015.06.005.

Landriault, D., & Anderson, J. (1998). Paste backfill for surface disposal. In Minefill '98: Proceedings of the Sixth International Symposium on Mining with Backfill (pp. 73–78). The Australasian Institute of Mining and Metallurgy.

Lee, I. K., & Coop, M. R. (1995). The intrinsic behaviour of a decomposed granite soil. *Géotechnique*, *45*(1), 117–130. https://doi.org/10.1680/geot.1995.45.1.117

Li, L., Aubertin, M., & Belem, T. (2005). The effect of tailings fineness and binder hydration on the mechanical strength of cemented paste backfill. Minerals Engineering, 18(6), 593–601.https://doi.org/10.1016/j.mineng.2004.10.004.

Li, W., & Fall, M. (2018). Strength and self-desiccation of slag-cemented paste backfill at early ages: Link to initial sulphate concentration. *Cement & Concrete Composites*, *89*, 160–168. https://doi.org/10.1016/j.cemconcomp.2017.09.019

Luck, G., & Richards, T. (2002). Surface paste disposal at Bulyanhulu gold mine, Tanzania. In Proceedings of the 105th Annual General Meeting of the Canadian Institute of Mining, Metallurgy and Petroleum (CIM), Vancouver, Canada.

Marchon, D., Sulser, U., Eberhardt, A., & Flatt, R. J. (2016). Molecular design of comb-shaped polycarboxylate dispersants for environmentally friendly concrete. Soft Matter, 12(3), 725–734. https://doi.org/10.1039/C5SM01913J.

Ouellet, S., Bussière, B., Mbonimpa, M., Benzaazoua, M., & Aubertin, M. (2006). Reactivity and mineralogical evolution of an underground mine sulphidic cemented paste backfill. Minerals Engineering, 19(5), 407–419. https://doi.org/10.1016/j.mineng.2005.10.006

Potvin, Y., Thomas, E. G., Fourie, A. B., & Australian Centre for Geomechanics. (2005). Handbook on mine fill. Australian Centre for Geomechanics.

Qi, C., Fourie, A., & Chen, Q. (2020). Cemented paste backfill for mineral tailings management: Review and future perspectives. Minerals Engineering, 148, 106222. https://doi.org/10.1016/j.mineng.2020.106222.

Qiu, J., Fall, M., & Yilmaz, E. (2019). Influence of curing time on the mechanical, microstructural and durability properties of cemented paste backfill containing nano-silica. Construction and Building Materials, 212, 18–28. https://doi.org/10.1016/j.conbuildmat.2019.03.309

Reddy, K. J., Wang, L., & Gloss, S. P. (1994). Solubility and mobility of copper, zinc and lead in acidic environments. Soil Science Society of America Journal, 58(6), 1753–1760. https://doi.org/10.2136/sssaj1994.03615995005800060012x

Richardson, I. G. (2008). The calcium silicate hydrates. Cement and Concrete Research, 38(2), 137–158. https://doi.org/10.1016/j.cemconres.2007.11.005

Savija, B., & Lukovic, M. (2016). Carbonation of cement paste: Understanding, challenges, and opportunities. Construction and Building Materials, 117, 285–301. https://doi.org/10.1016/j.conbuildmat.2016.04.138.

Sicakova, Alena & Kovac, Marek. (2020). Relationships between Functional Properties of Pervious Concrete. Sustainability. 12. 6318. 10.3390/su12166318.

Sivakugan, N., Rankine, R. M., Rankine, K. J., & Rankine, R. M. (2006). Geotechnical considerations in mine backfilling in Australia. Journal of Cleaner Production, 14(12–13), 1168–1175. https://doi.org/10.1016/j.jclepro.2004.09.008

Watari, T., Nansai, K., Nakajima, K., & Nakano, K. (2021). Toward global metal sustainability: Knowledge gaps and research needs. Resources, Conservation and Recycling, 168, 105248. https://doi.org/10.1016/j.resconrec.2021.105248

Xu, W., Fall, M., & Wu, A. (2020). Time and temperature effects on the strength and microstructure of cemented paste backfill. International Journal of Mining, Reclamation and Environment, 34(6), 398–419. https://doi.org/10.1080/17480930.2019.1654465

Yang, L., Fall, M., & Cui, L. (2022). Effects of temperature on hydration products, microstructure and strength development of cemented paste backfill. Cement and Concrete Composites, 134, 104754. https://doi.org/10.1016/j.cemconcomp.2022.104754

CHAPTER SIX.

TECHNICAL PAPER IV: EFFECT OF PYRITE CONTENT ON THE PERMEABILITY PROPERTIES OF PASTE TAILINGS FOR UNDERGROUND DISPOSAL.

Paper submitted for publication

Oyewale Miracle, Mamadou Fall and Ghirian Alireza

Department of Civil Engineering, University of Ottawa.
800 King Edward Ave, Ottawa, ON, K1N 6N5, Canada.

6.1 ABSTRACT

The long-term stability of sulphide-bearing cemented paste backfill (CPB) is a critical factor in sustainable mine waste management. Understanding how pyrite oxidation, sulphate generation, and binder composition influence hydraulic behaviour is essential for optimizing backfill performance. This study investigates the permeability response of pyrite-bearing CPB prepared with two binder systems-Portland cement (PC) and Slag–Portland cement blend (SG) cured for 150 days under sealed and air-dried conditions. The effects of pyrite content (0-45%) and initial sulphate concentration (0-25,000 ppm) on the microstructural and hydraulic characteristics were evaluated through X-ray diffraction (XRD) analysis, scanning electron microscopy (SEM) and physical property measurements (void ratio and dry density). Results revealed that permeability increased with increasing pyrite and sulphate levels due to the

formation of expansive secondary minerals such as ettringite and gypsum, which weakened matrix integrity and increased pore connectivity. Slag-based systems exhibited higher permeability than Portland cement mixtures, attributed to incomplete hydration and enhanced susceptibility to sulphate attack. Air exposure further intensified pyrite oxidation, leading to additional sulphate generation, microcracking, and structural loosening. Overall, the findings highlight that pyrite oxidation, binder type, and curing condition have a significant influence on the hydraulic behaviour of CPB. These results underscore the importance of selecting appropriate binders and implementing effective oxidation control measures to ensure durable and environmentally stable backfill structures.

6.2 INTRODUCTION

Cemented paste backfill (CPB) technology is an advanced mine waste management technique that represents a transformative step towards greener and more effective sustainable mining practices. Through a design concept of repurposing voluminous mine tailings into underground mining voids, CPB technology has revolutionized tailings disposal by transforming tailings into valuable resources for structural reinforcements of mined-out underground groves (Fall and Benzaazoua, 2005; Kesimal et al., 2003; Yilmaz et al., 2009; Fall and Pokharel et al., 2010; Mahlaba et al., 2011). This technology not only enhances the stability of underground mines but also simultaneously addresses the environmental and safety hazards associated with traditional tailings disposal, such as geotechnical failures, environmental pollution and acid mine drainage (Wu et al., 2024; Qi and Fourie, 2019; Cacciuttolo Vargas & Marinovic Pulido (2022).

The design and preparation of CPB are carefully engineered to optimize specific factors and properties, such as composition, cost, rheology, permeability, and mechanical strength. Typically, CPB is a composite mixture consisting of dewatered tailings (which make up approximately 70-85 wt% solids), freshwater or mine-processed water to ensure proper consistency and a hydraulic binder of 2-7% of the total weight for strength and stability (Fall and Pokharel, 2010; Fall et al., 2009; Abdul-Hussain and Fall, 2011). These components are thoroughly mixed on the mine surface, and the resulting slurries/paste are transported via gravity-fed or pump-assisted pipelines into previously excavated underground voids (Fall et al., 2008; Argane et al., 2015; Yilmaz and Fall, 2017). Over time, the paste undergoes a cement-hydration process, resulting in a stable and solidified backfill that must withstand certain stresses to ensure its successful application (Sheshpari, 2015). Therefore, the successful performance of CPBs is dependent on an in-depth understanding of the complex interplay between the design properties of the final paste backfill. Specifically, CPBs must exhibit

sufficient strength to provide structural support, while maintaining adequate flowability for transport (Sheshpari, 2015). Hydraulic conductivity is another critical factor as it must allow controlled drainage without compromising barricade integrity or the function of free-draining permeable retaining structures, such as bulkheads, or impermeable retaining walls (Fall et al., 2009; Abdul-Hussain & Fall, 2012; Ghirian & Fall, 2013, 2014). Equally important is the environmental performance and long-term durability of CPBs, which are largely dictated by their permeability characteristics.

Researchers and engineers have studied these interactions over time through laboratory and field investigations, focusing on the mechanical, rheological, environmental performance and durability properties of CPBs. Significant contributions to the study of mechanical properties are found in the documented works by Fall et al. (2008), Kesimal et al. (2005), Fall et al. (2010), and Ghiran and Fall (2014). These include investigations into strength development mechanisms (Nasir and Fall, 2010) and failure behaviour under uniaxial (Yilmaz et al., 2014) and triaxial compression (Klein and Simon, 2006; Fall et al., 2007). In the area of rheology, notable works include Oyewale et al. (2025), Aldhafeeri and Fall (2017), Ouattara et al. (2017), Bian et al. (2021) and Xiapeng et al. (2019). Environmental performance studies have been explored by Haruna and Fall (2022), Fall et al. (2009), Pokharel and Fall (2013) and Godbout (2005). While progress in CPB research is evident, the environmental implications of incorporating pyrite-bearing tailings remain insufficiently investigated (Martins et al., 2021,2024). In particular, the role of sulphide oxidation and its by-products in influencing long-term durability and environmental performance of CPBs for underground mining applications remains a critical gap in current knowledge. This is because, regardless of the potential for CPB technology to neutralize the chemical reactivity of tailings through the addition of alkaline materials like cement (Ercikdi et al., 2017), complexities might arise when pyrite-bearing tailings are used. These issues stem from the highly reactive nature of pyrite and

its ability to undergo chemical oxidation when exposed to water and oxygen, which further generates sulfuric acid, leading to ARD.

The presence of pyrite minerals in these CPB systems can lead to sulphate-induced deterioration known as “Internal sulphate attack” (Benzaazoua et al., 1998; Fall and Benzaazoua, 2005; Tariq and Nehdi, 2007). This phenomenon is triggered when pyrite minerals react with cementitious agents, such as cement, causing the dissolution of calcium hydroxide (Portlandite, Ca(OH)2), followed by the subsequent formation of highly expansive ettringite or gypsum. As these expansive phases absorb water and increase in volume, they generate internal stresses that cause internal swelling, cracking, and strength degradation of the CPB. Internal stresses can further compromise other CPB properties, such as its permeability properties. While no research study has investigated how pyrite-induced internal stresses affect the permeability properties of paste backfill, it is suspected that incorporating highly reactive pyrite tailings in CPB systems might cause more aggressive sulphate attacks leading to accelerated ARD formation and more severe environmental risks (Benzaazoua et al., 1998; Tariq and Nehdi, 2007). Therefore, research must also focus on studying the environmental behaviour of pyrite-laden tailings, particularly the ambiguities that may negatively affect the permeability properties of pyrite-containing paste backfills for underground tailings disposal.

The environmental behaviour of CPBs, such as their susceptibility to cause ARD and leaching potential, is an important design criterion for ensuring optimal performance after emplacement in underground stopes (Sheshpari, 2015). This susceptibility is a function of the chemical reactivity of the composition of tailings used in the CPB mixture and is controlled not only by the type and concentration of sulphide minerals present in the CPB matrix, but also by the easy permeation of fluids such as oxygen and water through the paste backfill (Sheshpari, 2015;Levens et al., 1996; Haruna and Fall, 2022; Fall et al, 2009; Wu et al., 2013). In essence, the chemical reactivity is largely dependent on the permeability properties of CPB,

which can be evaluated through hydraulic conductivity studies. Additionally, hydraulic conductivity is a crucial parameter for determining the flow rate of groundwater through the CPB matrix as the groundwater table returns to its natural level after mine closure. Consequently, it determines the leaching potential and transport of pyrite-polluted water from the CPB matrix into the surrounding groundwater systems (Bull and Fall, 2020; Fall et al., 2009; Haruna and Fall, 2022).

Several studies have successfully examined the factors influencing the permeability behaviour of cemented paste backfill (CPB). Most of these investigations have shown that parameters such as tailings particle size and gradation (Ke et al., 2016), binder type and content (Abdul-Hussain and Fall, 2011; Godbout et al., 2013), curing time and temperature (Yilmaz et al.,2010), and sulphate concentration (Abdul-Hussain and Fall, 2011) have a strong impact on its hydraulic performance. However, none of these studies has explored the influence of pyrite-bearing tailings on the hydraulic conductivity of CPB, particularly how pyrite oxidation and subsequent sulphate formation affect its microstructure and long-term permeability behaviour. Therefore, this study addresses this critical knowledge gap through controlled experimental investigations designed to enhance understanding of the hydraulic response, stability, and environmental performance of pyrite-laden CPBs.

6.3 EXPERIMENTAL PROGRAM

6.3.1 MATERIALS USED

6.3.1.1 TAILINGS

In this study, high-purity silica tailings (ST) containing 99.8% quartz (SiO_2) by weight were selected as the primary material. Quartz is an inert, non-acid-generating mineral that is widely present in hard rock mining deposits across Canada, making ST a reliable and uniform substitute for natural tailings (NT). The choice of ST was made to reduce variability and avoid the chemical reactivity often associated with NT, where reactive minerals can disrupt cement hydration and reduce the consistency of experimental outcomes. By contrast, the use of ST enables a more controlled evaluation of pyrite's role in influencing the permeability of CPB. Particle size distribution (PSD) analysis revealed that ST closely resemble the average gradation of nine NT samples collected from Canadian mining sites (Figure 1). Approximately 43% of ST particles are finer than 20 μm, placing them within the medium-tailings category as defined by Landriault (1995), which specifies 35%–60% of particles below 20 μm. This proportion also satisfies the requirement that CPB mixtures contain at least 15% fines smaller than 20 μm by mass. The detailed physical and chemical characteristics of ST are summarized in Tables 1 and 2.

Table 1: Summary of the physical characteristics of silica tailings (ST) and average values from nine Canadian natural tailings (NT) sources.

ELEMENT	G_s	D_{10}(μm)	D_{30}(μm)	D_{50}(μm)	D_{60}(μm)
ST	2.7	1.9	9.0	22.5	31.5
An average of 9 types of tailings	-	1.8	9.1	20.0	30.8

Gs: specific gravity

Table 2: Mineralogical composition of the tailings materials selected for experimental investigations.

TAILINGS (wt.%)	MINERAL											
	Quartz	Albite	Dolomite	Calcite	Chlorite	Magnetite	Pyrite	Talc	Pyrrhotite	Spinel	Others	Total
ST	99.8	-	-	-	-	-	-	-	-	-	0.2	100

ST: Silica tailings; wt.: weight.

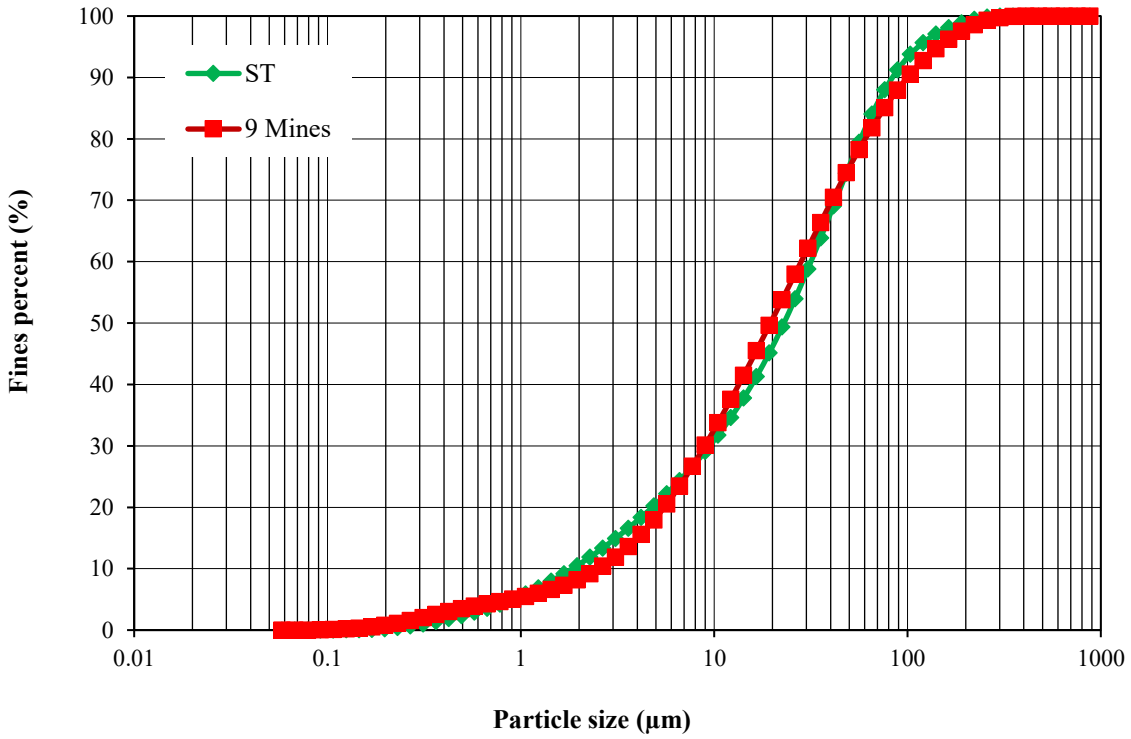

Figure 1. Grain size distribution of the tailings used and the average grain size distribution of tailings from nine mines in Canada.

6.3.1.2 BINDER

In this research, Type I Portland cement (PC) - the most commonly applied binder in paste tailings (PT) mixtures - served as the principal binding material. To enhance certain mixtures, a supplementary cementitious material, ground granulated blast furnace slag (SG),

was incorporated in selected cemented paste backfill (CPB) blends as a partial replacement for PC. The choice behind using blended binders stemmed from both economic and environmental considerations: Portland cement is relatively expensive, and its manufacturing process is highly energy-intensive, releasing significant amounts of greenhouse gases. By contrast, substituting part of the PC with SG not only lowers material costs but also reduces the overall carbon footprint of the mixture. For simplicity, mixtures containing both PC and SG are labelled "SG," while those composed entirely of PC are denoted as "PC only." In this study, the two binders were combined in equal proportions (50:50 by weight). A summary of the physical and chemical characteristics of PC and SG is provided in Table 3.3.

Table 3: Material characterization of PC and SG

	Na_2O	MgO	Al_2O_3	SiO_2	K_2O	CaO	TiO_2	MnO	Fe_2O_3	LOI	Relative density	Specific surface area (cm^2/g)
PCI	0.341	2.577	4.808	20.375	0.962	62.700	0.225	0.054	3.609	2.162	3.2	1300
Slag	0.284	11.782	10.59	35.572	0.478	39.212	0.467	0.298	0.621	0.388	2.8	2100

6.3.1.3 PYRITE

Commercial pyrite powder (FeS_2, M.W. = 119.98) supplied by Washington Mills North Grafton, Inc. was used. The grain size of this product is comparable to that of pyrite typically occurring in natural tailings. Pyrite was blended with ST, PC, and SG to produce CPB-ST-PC and CPB-ST-SG mixtures containing 0, 5, 15, and 45 wt.% pyrite. The physical properties of the pyrite are listed in Table 4.

6.3.1.4 MIXING WATER AND SULPHATE CONCENTRATION

Distilled water was used to prepare all tailings–binder mixtures, with a constant water-to-binder (w/b) ratio of 7.8. To simulate sulphate-rich conditions typical of paste tailings,

ferrous sulphate heptahydrate ($FeSO_4 \cdot 7H_2O$; M.W. = 278.01 g/mol) was adopted as the sulphate source. In mine environments, sulphate ions mainly arise from pyrite (FeS_2) oxidation, making their influence on paste tailings permeability important to evaluate. Ferrous sulphate was selected because it is a common sulphate phase in mine drainage and cemented backfill. Accurately weighed amounts of $FeSO_4 \cdot 7H_2O$ were dissolved in distilled water to yield mixing solutions with sulphate concentrations of 0, 5,000, and 25,000 ppm, which were then used to assess the effect of initial sulphate content on permeability.

Table 4: Material properties of pyrite

BULK DENSITY (g/cm^3)	DENSITY AT 20 °C (g/cm^3)	SP. GRAVITY	PH	MELTING POINT
2.35	4.7	4.6	4.0-6.0	~ 1,193

Sp: specific.

6.3.2 SPECIMEN PREPARATION AND MIX PROPORTIONS

The cemented mixtures examined in this study were prepared in accordance with the experimental program summarized in Table 5. Silica tailings, pyrite, and binders were accurately weighed using a laboratory balance and placed in a mechanical mixing bowl. The dry powders were blended for 5 minutes with a KitchenAid mixer operating at a constant speed setting (Speed 2) under ambient laboratory conditions. Subsequently, the premeasured volume of tap water was added, and mixing continued for another 5 minutes to produce a uniform paste. The resulting mixtures were cast into plastic cylindrical moulds (5 cm diameter × 10 cm height) and cured following the procedure outlined in Table 5. The use of plastic moulds was intended to approximate the dimensions of pipes commonly employed in field-scale PT operations (Haiqiang et al., 2016).

Table 5: Experimental plan for hydraulic conductivity tests.

SAMPLE NAME	TAILINGS TYPE	BINDER TYPE	BINDER CONTENT (Vol%)	PYRITE CONTENT (wt.%)	SULPHATE CONTENT (ppm)	CURING TIME (days)
Effect of pyrite content and binder type on hydraulic conductivity of CPB cured without air drying						
PC-CPB-0%	ST	PCI (100%)	4.5	0	0	150
PC-CPB-5%	ST+PY	PCI (100%)	4.5	5	0	150
PC-CPB-15%	ST+PY	PCI (100%)	4.5	15	0	150
PC-CPB-45%	ST+PY	PCI (100%)	4.5	45	0	150
SG-CPB-0%	ST	PCI/SG (50/50)	4.5	0	0	150
SG-CPB-45%	ST+PY	PCI/SG (50/50)	4.5	45	0	150
Effect of pyrite content and binder type on hydraulic conductivity of CPB cured with air drying						
PC-CPB-0%	ST	PCI (100%)	4.5	0	0	150
PC-CPB-5%	ST+PY	PCI (100%)	4.5	5	0	150
PC-CPB-15%	ST+PY	PCI (100%)	4.5	15	0	150
PC-CPB-45%	ST+PY	PCI (100%)	4.5	45	0	150
SG-CPB-0%	ST	PCI/SG (50/50)	4.5	0	0	150
SG-CPB-45%	ST+PY	PCI/SG (50/50)	4.5	45	0	150
Effect of sulphate concentration and pyrite content on the hydraulic conductivity of CPB cured without air drying						
PC-CPB-0-0ppm	ST	PCI (100%)	4.5	0	0	150
PC-CPB-0-5000ppm	ST	PCI (100%)	4.5	0	5000	150
PC-CPB-0-25000ppm	ST	PCI (100%)	4.5	0	25000	150
PC-CPB-15-0ppm	ST+PY	PCI (100%)	4.5	15	0	150
PC-CPB-15-5000ppm	ST+PY	PCI (100%)	4.5	15	5000	150
PC-CPB-15-25000ppm	ST+PY	PCI (100%)	4.5	15	25000	150
SG-CPB-0-0ppm	ST	PCI/SG (50/50)	4.5	0	0	150
SG-CPB-0-25000ppm	ST	PCI/SG (50/50)	4.5	0	25000	150
SG-CPB-15-0ppm	ST+PY	PCI/SG (50/50)	4.5	15	0	150
SG-CPB-15-25000ppm	ST+PY	PCI/SG (50/50)	4.5	15	25000	150
Effect of sulphate concentration and pyrite content on the hydraulic conductivity of CPB cured with air drying						
PC-CPB-0-0ppm	ST	PCI (100%)	4.5	0	0	150
PC-CPB-0-5000ppm	ST	PCI (100%)	4.5	0	5000	150
PC-CPB-0-25000ppm	ST	PCI (100%)	4.5	0	25000	150
PC-CPB-15-0ppm	ST+PY	PCI (100%)	4.5	15	0	150
PC-CPB-15-5000ppm	ST+PY	PCI (100%)	4.5	15	5000	150

PC-CPB-15-25000ppm	ST+PY	PCI (100%)	4.5	15	25000	150
SG-CPB-0-0ppm	ST	PCI/SG (50/50)	4.5	0	0	150
SG-CPB-0-25000ppm	ST	PCI/SG (50/50)	4.5	0	25000	150
SG-CPB-15-0ppm	ST+PY	PCI/SG (50/50)	4.5	15	0	150
SG-CPB-15-25000ppm	ST+PY	PCI/SG (50/50)	4.5	15	25000	150

PC/PCI: Portland cement type I; SG: Blast furnace slag; ST: silica tailings; PY: Pyrite; ppm: parts per million; Vol: Volumetric percentage; Wt.%: Weight percentage: PCI (100%): Sample with 100% PCI; PCI/SG (50/50): Sample with 50% PCI and SG. With air drying: water evaporation is allowed during sample curing; Without air drying: water evaporation is not allowed during sample curing.

6.3.3 CURING CONDITIONS

To simulate practical field scenarios, two contrasting curing regimes were adopted: *curing without air exposure* and *curing with air exposure*.

(a) ***Without Air Drying:*** In this condition, cylindrical moulds containing the paste tailings mixtures were sealed to prevent contact with the atmosphere during curing. This setup simulates deep underground conditions with limited oxidation. Under such conditions, moisture retention is high, and oxygen ingress is minimal, thereby reducing the extent of sulphide oxidation during curing.

(b) With Air Drying: In this condition, the tops of the cylindrical moulds were sealed for the first 60 days to ensure proper hydration, then exposed to air for the remaining curing period (60–150 days). This setup simulates ventilated or oxygen-rich mine zones, where oxygen diffusion promotes pyrite oxidation and sulphate generation. The resulting reactions enable evaluation of how oxidation processes influence the microstructure, permeability, and long-term durability of the CPB.

6.3.4 TEST METHODS

6.3.4.1 HYDRAULIC CONDUCTIVITY TEST

The saturated hydraulic conductivity of the cured paste tailings specimens was determined using a Tri-Flex 2 flexible-wall permeameter in accordance with ASTM D5084-00, which specifies procedures for measuring the permeability of saturated soils. The constant-head approach was employed, whereby a stable pressure gradient of 10 psi (69 kPa) was imposed between the inflow and outflow burettes to drive water through the specimen. Prior to testing, backpressure saturation was applied to remove entrapped air and achieve full specimen saturation, a prerequisite for reliable hydraulic conductivity measurements.

Saturation was confirmed once a steady-state flow was established. The flexible-wall configuration further ensured that flow was confined to the specimen by eliminating side leakage. Each measurement was repeated twice to verify consistency and reproducibility. This testing method was selected because it closely replicates in-situ stress conditions while providing accurate determinations of hydraulic conductivity in fine-grained and cemented materials.

6.3.4.2 MICROSTRUCTURAL ANALYSIS

The microstructural features (e.g., pore network and hydration products) and physical parameters (void ratio, porosity, and density) of selected paste tailings specimens were systematically examined to track the internal evolution of cemented paste tailings (CPB) over time. Prior to testing, samples were oven-dried at 45 °C for five days to minimize moisture-related variability. Scanning electron microscopy (SEM) was conducted to observe the morphology and microstructural development of hydration products and to provide visual evidence of pore structure evolution. X-ray diffraction (XRD) was additionally conducted to identify cement hydration phases. Gravimetric water content (w%) and bulk density were measured following ASTM D2216-10 and ASTM D7263-09, respectively. Based on these data, void ratio (e) and porosity (n) were subsequently calculated for each specimen.

6.4 RESULTS AND DISCUSSION

6.4.1 PERMEABILITY RESPONSE OF PYRITE-BEARING CEMENTED PASTE TAILINGS UNDER NON–AIR-DRIED CONDITIONS.

The effect of pyrite content and binder type on the coefficient of permeability (k) of CPB samples cured under sealed (no air-drying) conditions is illustrated in Figure 2. According to the graphs, a distinct upward trend in permeability is observed with increasing pyrite content in both figures, and this incremental pattern is also noticed irrespective of the binder type. These results indicate that sulphide-bearing tailings significantly affect the hydraulic performance of the backfill. For the PC-CPB samples (Figure 2a), the permeability increased from approximately 8.6×10^{-7} cm/s at 0 % pyrite to 2.5×10^{-6} cm/s at 45 % pyrite, which is nearly a threefold increase. This indicates that as the concentration of pyrite in the tailings increases, the hydraulic sealing capacity of the backfill significantly decreases, thereby allowing easier movement of water or pore fluid through the backfill matrix.

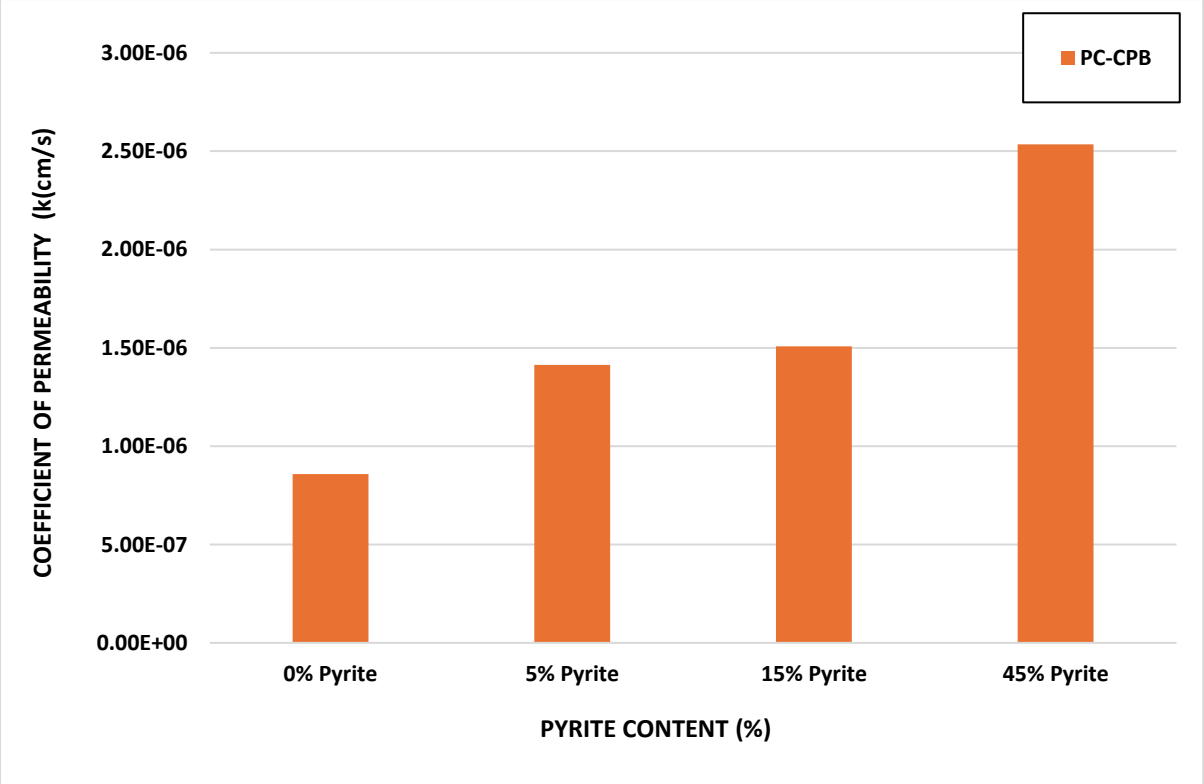

a)

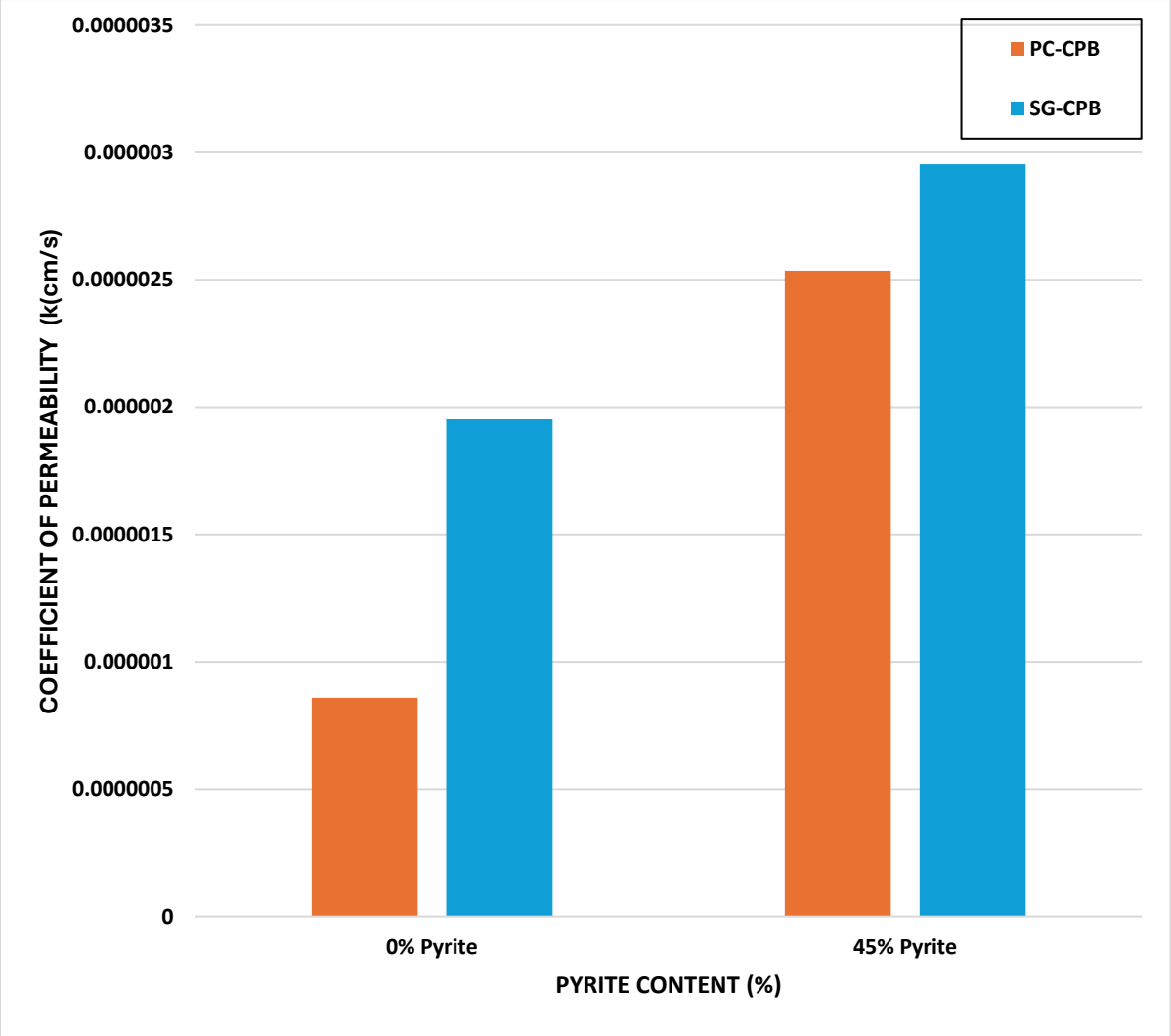

b)

Figure 2: Effect of pyrite content on the permeability of **(a)** Cemented paste backfill (CPB) with PC and **(b)** paste tailings stabilized with different binder types (PC-CPB and SG-CPB) cured for 150days.

Regardless of the sealed conditions, the observed increase in permeability in Figure 2(a) can be attributed to limited oxygen entrapped within the paste or introduced during mixing, which may have initiated partial oxidation of pyrite (FeS_2). The oxidation process may have generated ferrous and ferric sulphates along with sulphuric acid, consequently altering the pore structure and enhancing fluid transport pathways within the matrix. This interpretation

aligns with Moses et al. (1987), who demonstrated that pyrite oxidation can proceed in both aerobic and anaerobic systems through direct oxidation by Fe (III), confirming that complete oxygen exclusion does not halt pyrite oxidation. The products of this oxidation process can react with cement compounds (C_3A) and hydrates, particularly calcium hydroxide, leading to the formation of secondary expansive or soluble minerals such as gypsum, ettringite, and iron hydroxides (Schmidt et al., 2011; Rodrigues et al., 2012). The formation and subsequent dissolution of these phases may create micro-voids, cracks, and interconnected pore channels within the hardened matrix, facilitating the passage of fluids (Tariq and Nehdi, 2007; Fall et al. 2009). These interpretations are supported by XRD results (Figure 3), which confirm the formation of secondary sulphate minerals indicative of pyrite oxidation. For the PC-CPB sample containing 0% pyrite, the dominant crystalline phases identified were portlandite ($Ca(OH)_2$) and quartz, indicating normal hydration of Portland cement, which progressively fills and seals the capillary pores, maintaining a dense and stable matrix (Li and Fall, 2018; Marchon et al., 2016). The quartz peaks originate from the silica-rich tailings used in the mix. In contrast, the PC-CPB sample with 45% pyrite shows distinct secondary sulphate phases such as ettringite and intensified gypsum peaks, along with noticeably reduced portlandite intensity. These mineralogical transformations confirm that pyrite oxidation released sulphate ions, which reacted with available calcium hydroxide to form expansive ettringite, thereby disrupting the matrix integrity and enhancing pore connectivity (Edwards et al., 1999; Casanova et al., 1997; Lee et al., 2005), ultimately accounting for the higher permeability observed in the 45% pyrite sample. Moreover, the reduced intensity of portlandite peaks further supports this reaction pathway, implying consumption of $Ca(OH)_2$ during secondary sulphate formation. These claims and explanations are further supported by physical tests (Figure 4) that studied the physical structure compaction of the samples. According to the graph, the void ratio of the PC-CPB samples increased while the dry density decreased with

increasing pyrite content, indicating greater porosity and reduced matrix compactness as the sulphide content rose (Sicakova and Kovac, 2020).

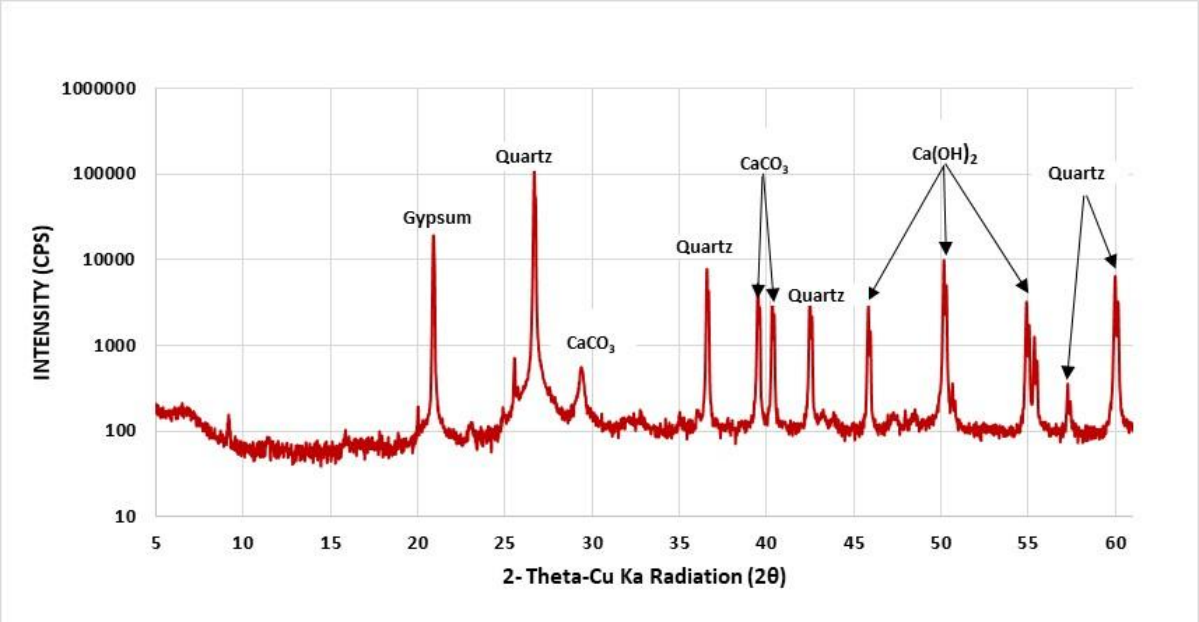

a)

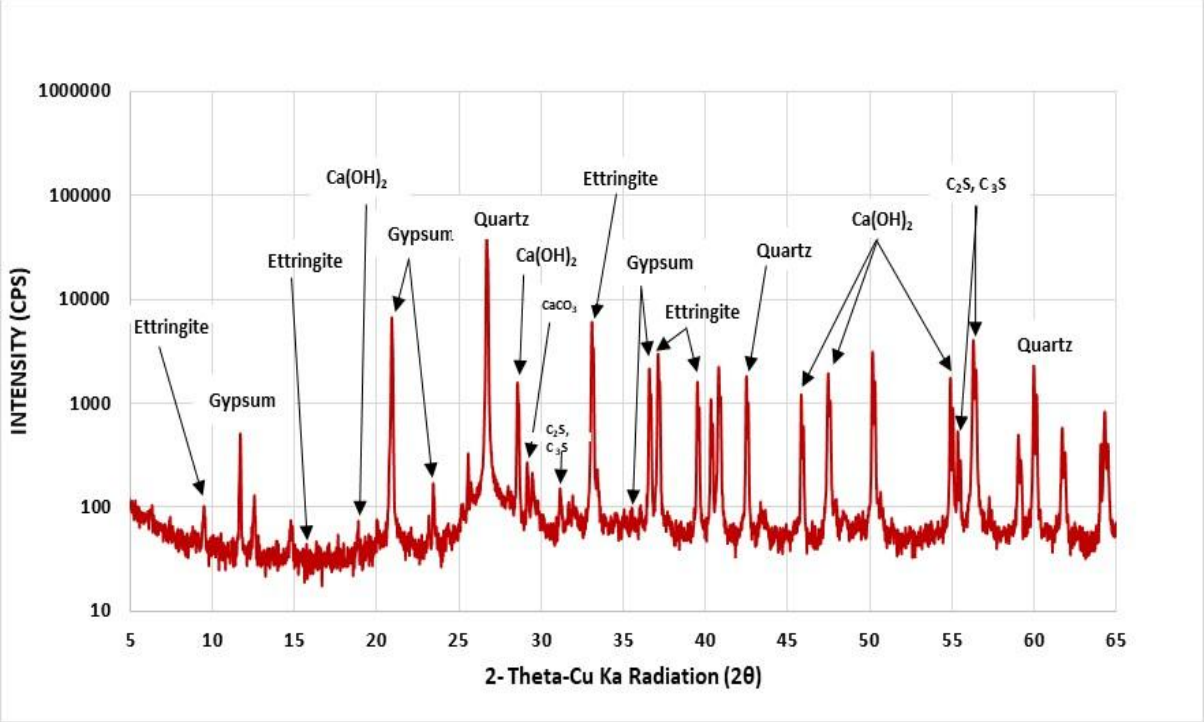

b)

Figure 3: X-ray diffraction (XRD) patterns of Cemented Paste Backfill (PC-CPB) at **(a)** 0% and **(b)** 45% pyrite content after a 150-day curing period.

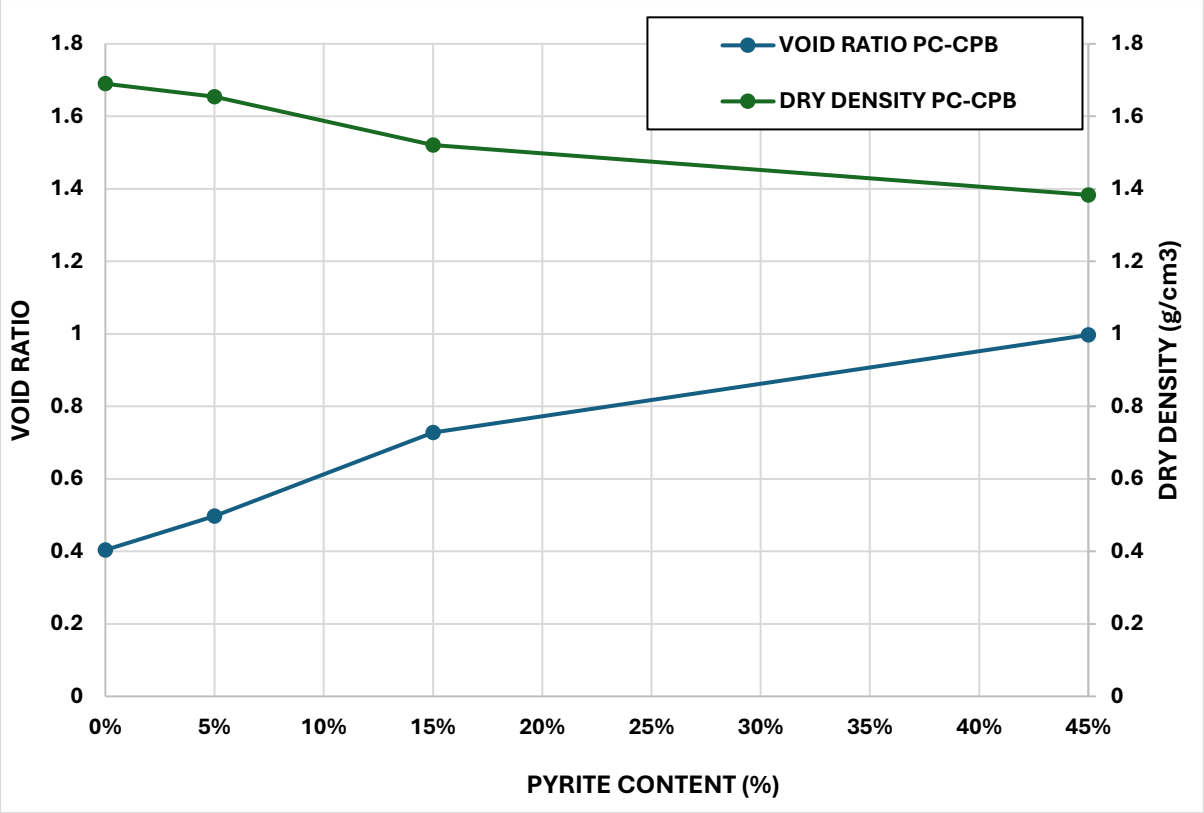

Figure 4: Effect of increased pyrite content on void ratio and dry density of PC-CPB after 150 curing days.

Figure 2 also shows the comparison between binder systems under the same curing condition of 150 days. The results (Figure 2b) revealed that permeability values were slightly higher in the SG-CPB mixtures than in the PC-based ones. At 0 % pyrite, the SG-CPB sample recorded a permeability of about 1.9×10^{-6} cm/s, which was higher than the 8.6×10^{-7} cm/s measured for the corresponding PC-CPB. At 45 % pyrite, both binders exhibited an increase in permeability, with the PC-CPB reaching approximately 2.5×10^{-6} cm/s, while the SG-CPB showed a slightly higher value of around 2.95×10^{-6} cm/s. Overall, the results indicate that the permeability of the CPB increases with increasing pyrite content regardless of the binder type. However, SG-CPB consistently displayed marginally higher permeability values than PC-CPB under no-air-drying conditions. The higher baseline permeability in SG-CPB can be linked to how the binder hydrates and how pyrite reacts within the mix. Portland cement reacts quickly

with water, forming dense compounds like calcium silicate hydrate, calcium hydroxide, and ettringite that create a compact structure and limit water flow (Celestin and Fall, 2009; Fall et al., 2009). Slag, on the other hand, hydrates more slowly and needs a highly alkaline environment to react fully. Under sealed curing, where moisture and alkalinity are limited, slag doesn't hydrate as completely, leaving more unreacted particles and a more open, porous structure (Demirboga, 2007; Fall et al., 2009; Haruna and Fall, 2022). In addition, the presence of trapped oxygen can oxidize pyrite (FeS_2), producing sulphates and sulphuric acid that lower the pH, weaken cement compounds, and form minerals like gypsum, which create small flow paths in the material (Moses et al., 1985; Whittaker and Black, 2015). Since slag hydration is sensitive to pH changes, these oxidation effects have a stronger impact on SG-CPB, leading to a slightly looser structure and higher permeability compared to PC-CPB. The XRD (Figure 5) and SEM (Figure 6) results for both SG-CPB and PC-CPB samples with 45% pyrite (Figure 5) further confirm the earlier assertions. In the SG-CPB sample, lower peaks of portlandite ($Ca(OH)_2$) were observed along with visible C_2S/C_3S and minor $Ca(OH)_2$ peaks. The presence of a lower amount of portlandite, together with unhydrated silicate phases, indicates incomplete hydration (Pokharel and Fall, 2013). This is likely due to the slower reaction rate of slag and the inhibitory effect of sulphate ions generated during pyrite oxidation. The PC-CPB sample showed intense $Ca(OH)_2$ (portlandite) and ettringite peaks, with moderate C_2S/C_3S reflections. The higher portlandite content reflects more complete hydration of silicate phases, which is typical of Portland cement systems (Li and Fall, 2018; Marchon et al., 2016). Although ettringite and residual gypsum were still detected, indicating the influence of sulphate reactions, the overall structure appeared denser and more consolidated due to greater C-S-H and portlandite formation. These XRD findings (Figure 5) align with the permeability results in Figure 2, confirming that under the same pyrite-rich and sealed curing conditions, SG-CPB

develops a more porous and permeable structure than PC-CPB. The XRD results are further corroborated by SEM results (Figure 6).

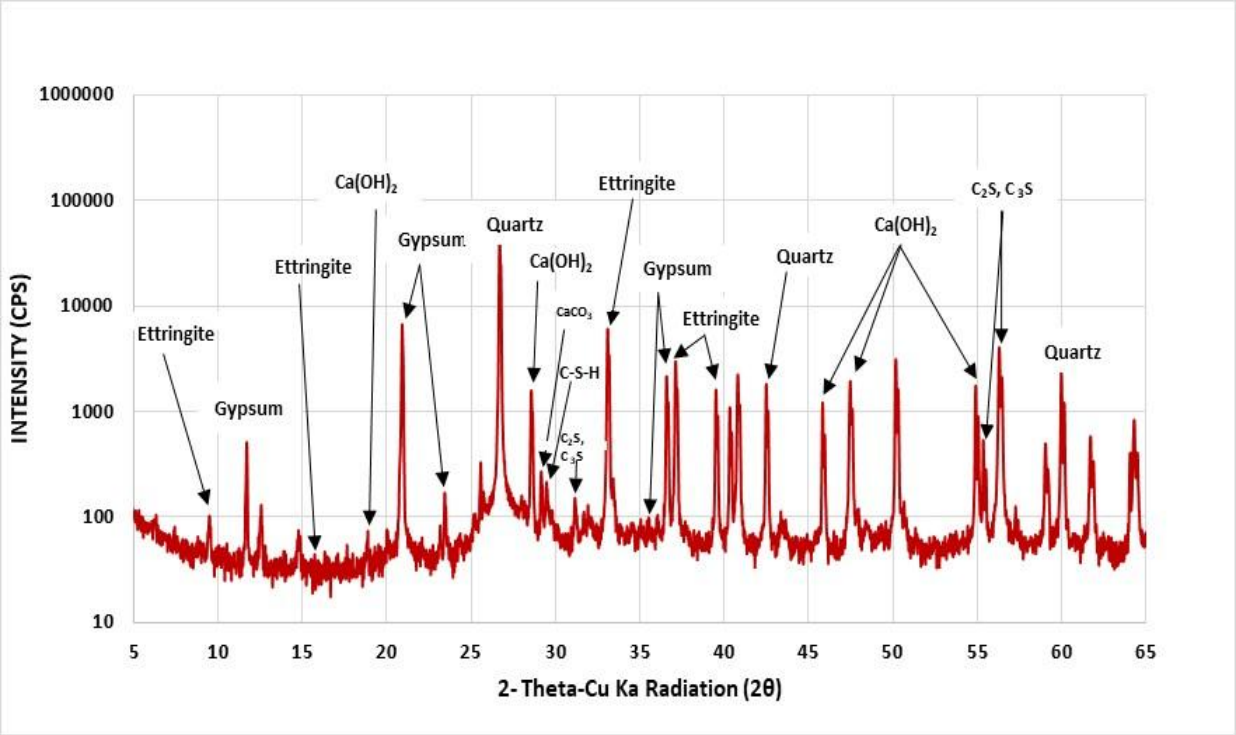

a)

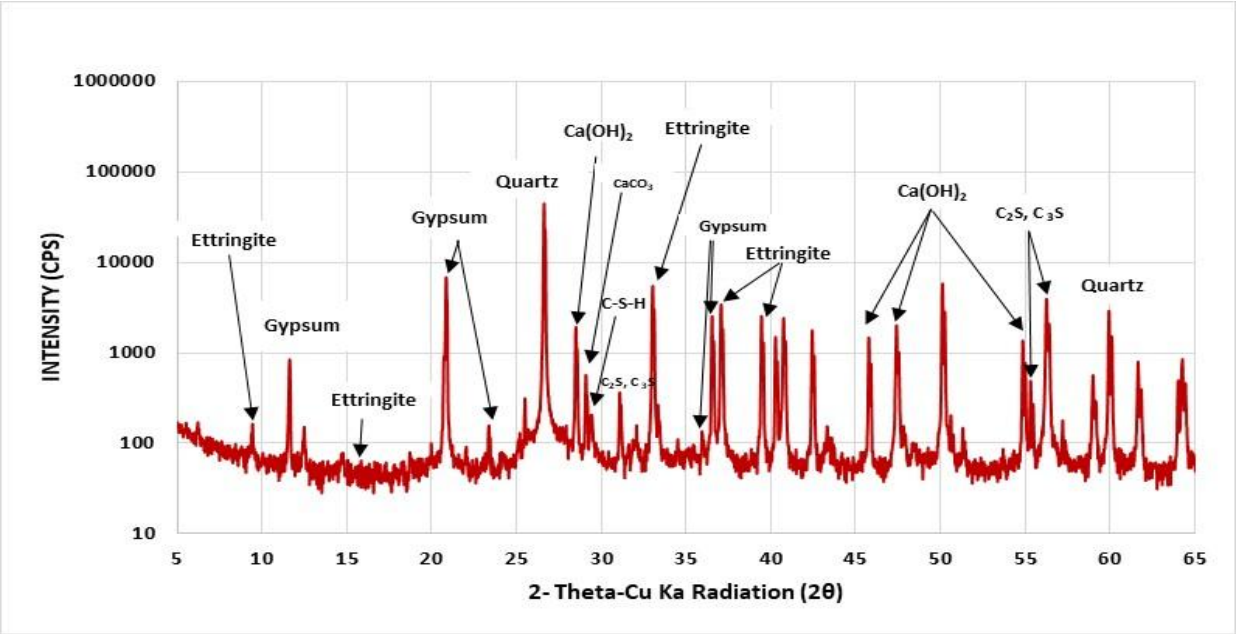

b)

Figure 5: X-ray diffraction (XRD) patterns of cemented paste backfill (CPB) samples with 45% pyrite content cured for 150 days, comparing **(a)** slag-based (SG-CPB) and **(b)** Portland cement-based (PC-CPB) systems.

The SEM observations provide direct visual evidence of the microstructural differences between the PC-CPB and pyrite SG-CPB samples under the 45% pyrite-rich sealed curing conditions. The PC-CPB sample (Figure 6a) showed a relatively dense and compact microstructure, with fewer and smaller pores. The matrix surrounding the tailings particles appears continuous, indicating that hydration products from Portland cement effectively filled and bridged inter-particle voids. The formation of C–S–H gel and portlandite (CH) improves particle bonding and refines the pore structure, producing a tighter matrix with limited pore connectivity, which restricts fluid flow (Celestin and Fall, 2009; Fall et al., 2009) and contributes to the lower permeability observed in PC-CPB. The SG-CPB sample (Figure 6b) exhibited a more heterogeneous and porous microstructure, with larger and more pores distributed within the matrix. The pores appear more open and interconnected, suggesting that the slag–cement binder did not fill the void spaces as effectively under the same curing conditions and pyrite content. This behaviour is associated with the slower hydration kinetics of slag-based binders, which delay the formation of dense hydration products and allow a greater number of voids to remain within the structure, resulting in a coarser pore network and greater pore connectivity (Demirboga, 2007; Fall et al., 2009; Haruna and Fall, 2022). Hence, the SEM observations support the XRD mineralogical findings and permeability results, indicating that SG-CPB develops a more porous and interconnected pore structure than PC-CPB, thereby facilitating water migration through the matrix and resulting in higher permeability.

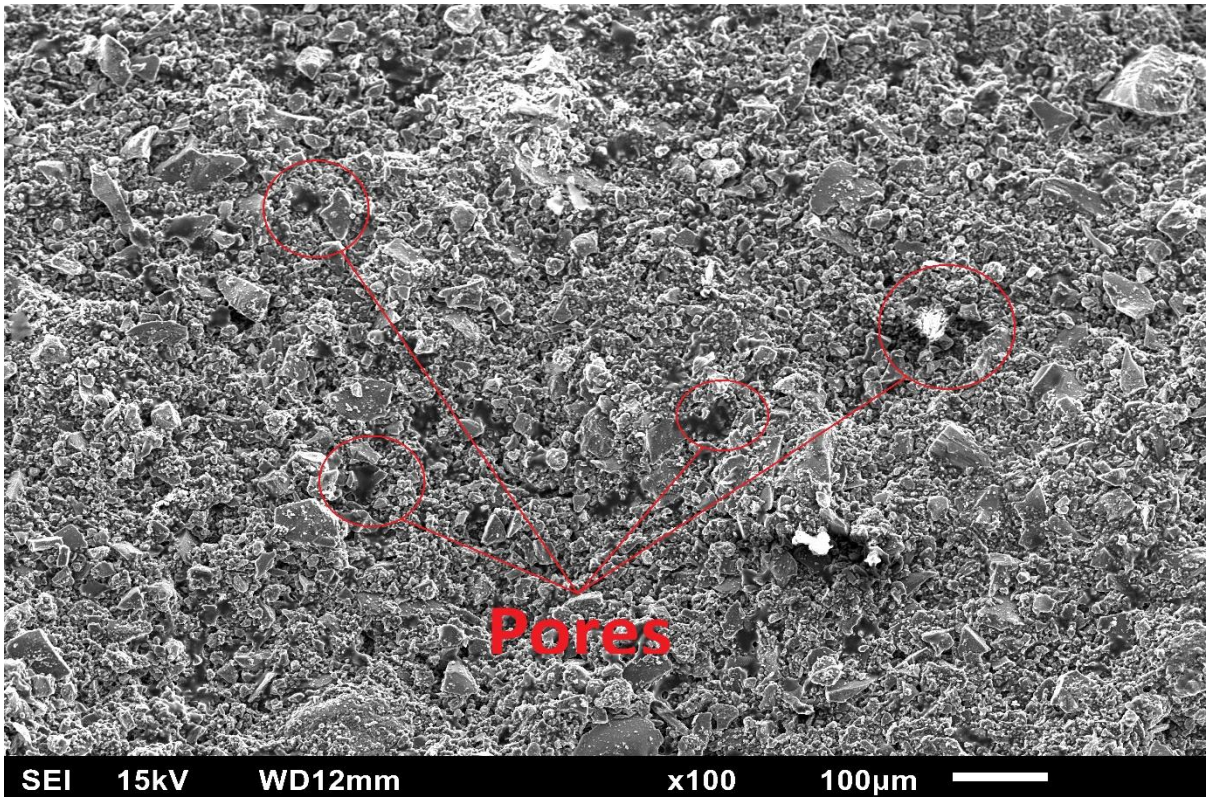

a)

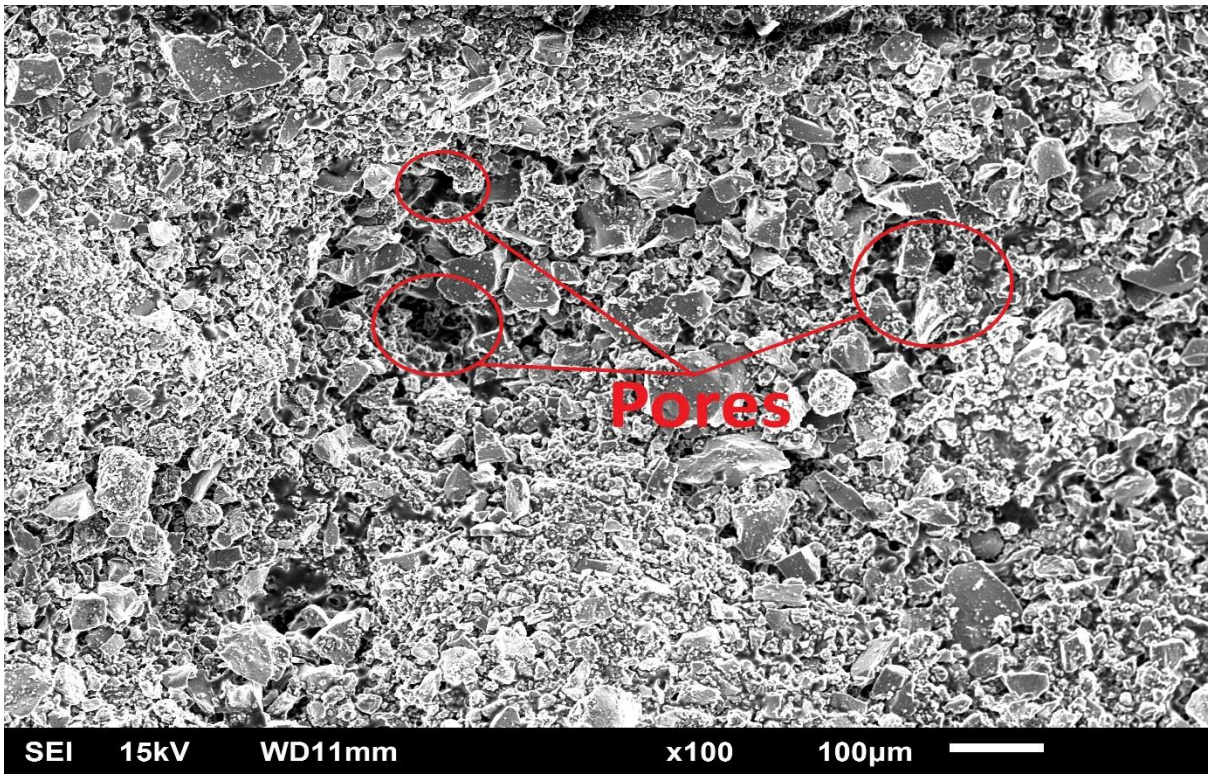

b)

Figure 6: SEM micrographs of 150-day-cured CPB specimens with 45% pyrite content, comparing **(a)** PC-CPB and **(b)** SG-CPB systems.

Furthermore, it can also be deduced from Figure 2b that the permeability of PC-CPB increases by approximately 191% as the pyrite content increases from 0% to 45%, whereas the corresponding increase in SG-CPB is about 53% over the same range. This indicates that PC-CPB is more sensitive to sulphate attack associated with pyrite oxidation. The greater susceptibility of PC-CPB is likely related to the more extensive formation of secondary sulphate-bearing phases, such as ettringite and gypsum, particularly in the 45% PC-CPB mixture. This interpretation is supported by the XRD patterns in Figure 5, where ettringite and gypsum peaks are more pronounced in PC-CPB than in SG-CPB, consistent with the greater permeability increase observed. The formation of these expansive sulphate phases can generate internal stresses within the cemented matrix, leading to microcracking, pore enlargement, and increased pore connectivity, which promote fluid migration and reduce durability. Thus, while SG-CPB may exhibit relatively higher permeability, it provides improved durability under pyrite-rich conditions by limiting sulphate-induced deterioration and slowing permeability development. These findings highlight the importance of binder selection in controlling the long-term environmental and geotechnical performance of cemented paste backfill systems.

6.4.2 INFLUENCE OF PYRITE OXIDATION ON THE PERMEABILITY CHARACTERISTICS OF CEMENTED PASTE TAILINGS UNDER SEALED AND AIR-DRIED CONDITIONS

In field scenarios, it's common for pyrite-bearing tailings to undergo oxidation prior to their backfill applications, primarily due to exposure to air. This oxidation process can lead to the release of a substantial quantity of sulphate ions into the pore water of the tailings intended for CPB preparation. Consequently, CPB produced from these tailings carries a notable sulphate content, potentially influencing its permeability. To evaluate the impacts of pyrite oxidation on CPB permeability, this study investigates the permeability effect of CPB with and without oxidation at varying pyrite concentrations. Based on the results presented in Figure 7, the samples with 0% pyrite concentration recorded the lowest permeability, approximately 9.7×10^{-7} cm/s for air-dried and 8.5×10^{-7} cm/s for sealed curing. This low permeability can be attributed to the formation of dense hydration products such as calcium silicate hydrate (C-S-H) and calcium hydroxide ($Ca(OH)_2$), which effectively fill the pore spaces within the backfill matrix, leading to a compact structure that restricts fluid flow (Li and Fall, 2018; Marchon et al., 2016). As the pyrite content increases to 5% and 15%, the permeability rises to about 1.6×10^{-6}–1.8×10^{-6} cm/s for air-dried samples and 1.4×10^{-6}–1.5×10^{-6} cm/s for those cured under sealed conditions. At 45% pyrite content, the permeability reaches its highest value, approximately 2.69×10^{-6} cm/s for air-dried and 2.5×10^{-6} cm/s for sealed samples, which represents almost a threefold increase relative to the 0% pyrite condition. The increment in permeability is primarily due to the oxidation of pyrite (FeS_2), which releases sulphate ions (SO_4^{2-}) that promote the formation of expansive secondary minerals such as ettringite and gypsum (Jana, 2022; Guirguis and Shehata., 2018; Jeyakaran et al., 2021). While these phases can initially fill voids and reduce permeability, their continued formation and expansion eventually cause microcracking and increased pore connectivity, resulting in higher permeability (Sicakova and Kovac,2020).

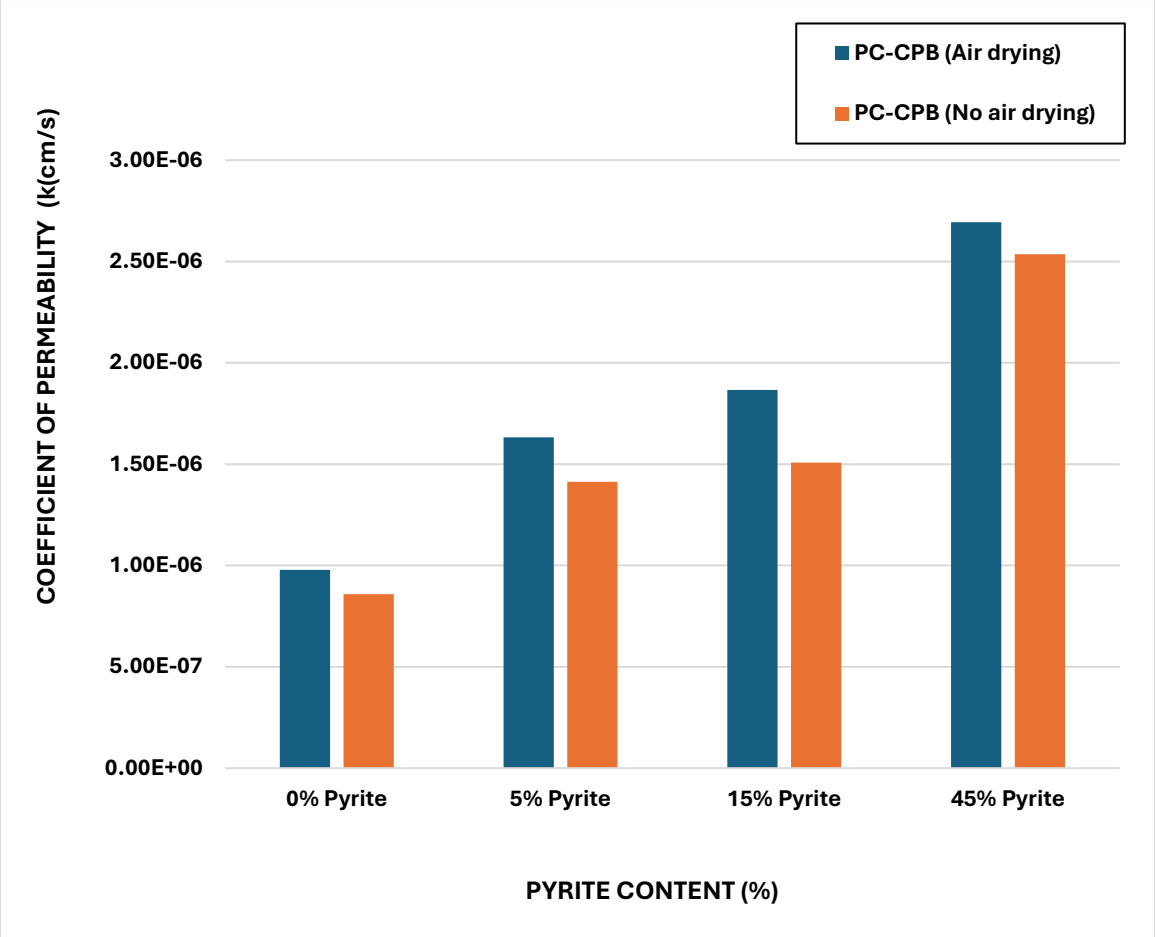

Figure 7: Effect of pyrite content and pyrite oxidation on the permeability of PC-CPB under air-drying and sealed conditions after 150 curing days.

These observed results find validity in the XRD results given in Figure 8, which illustrate that the non-air-dried (sealed) samples (8a) had dominant peaks of calcium silicate hydrate (C-S-H) and calcium hydroxide ($Ca(OH)_2$), with only minor traces of ettringite and gypsum, indicating normal cement hydration and a dense microstructure that reduces the flow of fluids. In contrast, the air-dried samples (8b) displayed stronger peaks of gypsum and ettringite alongside reduced C-S-H intensity, confirming that exposure to air accelerates pyrite oxidation and sulphate generation. The pronounced presence of these expansive sulphate-bearing minerals under air-drying conditions causes internal stress, cracking, and increased pore connectivity, consistent with the observed increase in permeability noted in the graphs and

the explanation for Figure 7. These results are consistent with the findings of Aldhafeeri and Fall (2016), who examined the oxidized and unoxidized layers of pyrite-bearing cemented paste backfill (CPB). Their XRD analysis revealed significantly higher concentrations of secondary expansive phases, such as gypsum and ettringite, in the oxidized layer compared to the unoxidized one. The authors further highlighted that the phases formed as a result of reactions between sulphate ions generated from pyrite oxidation and portlandite produced during cement hydration (Fall and Pokharel, 2010). Moreover, the appearance of calcium carbonate ($CaCO_3$) also reflects carbonation reactions from air exposure, further evidencing the chemical alterations induced by oxidation (Savija and Lukovic, 2016).

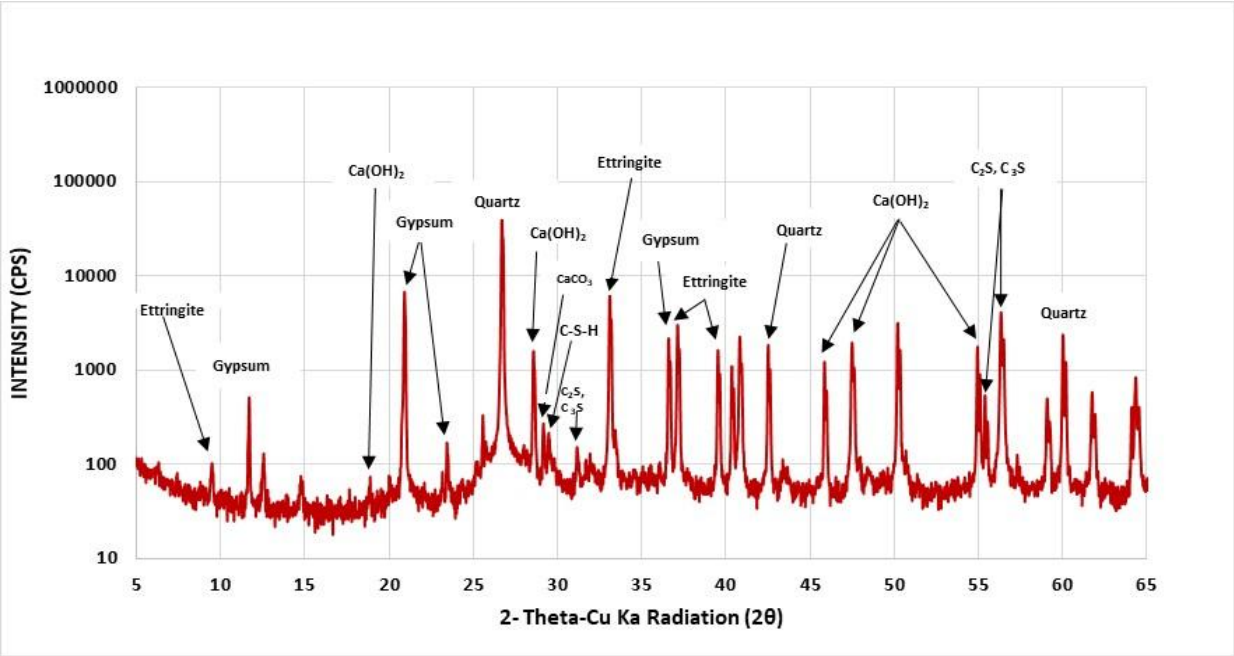

a)

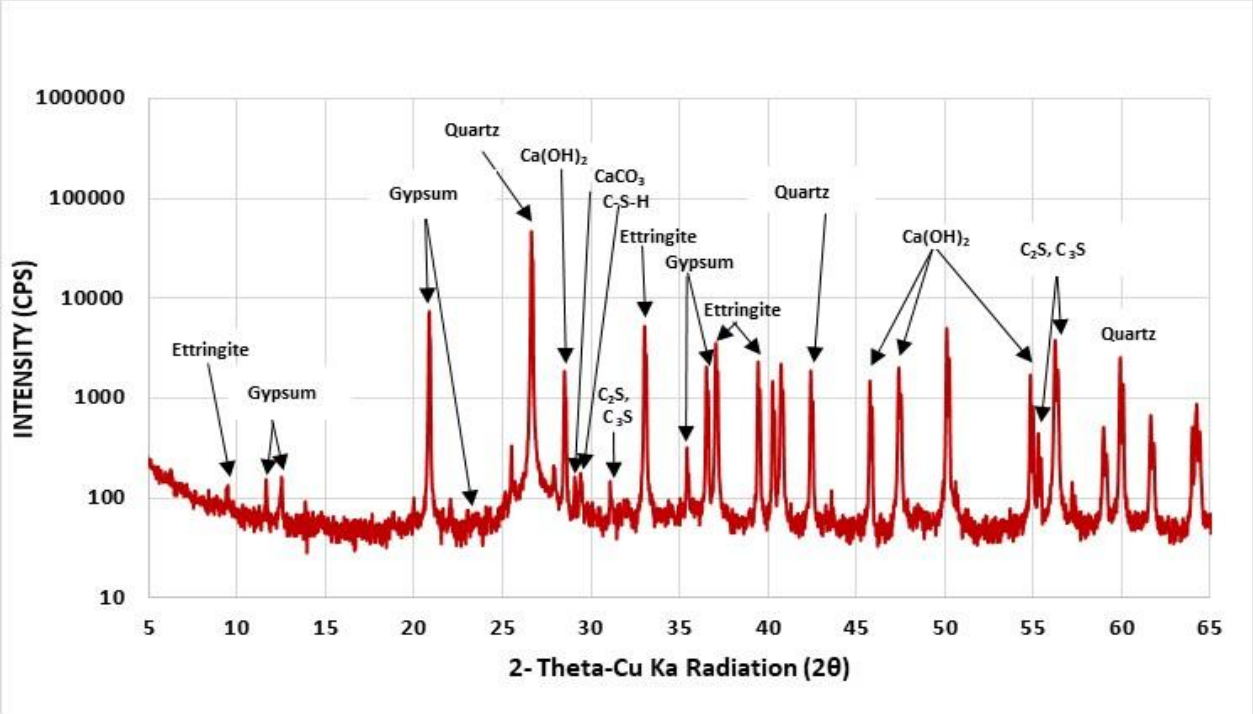

Figure 8: X-ray diffraction (XRD) patterns of **(a)** PC-CPB-45% pyrite (no air-drying) and **(b)** PC-CPB-45% pyrite (air-drying) after 150 curing days.

In agreement with the XRD results, the SEM observations presented in Figure (9) further provide additional microstructural evidence to support the role of oxygen ingress in promoting pyrite oxidation. The sealed 45% pyrite CPB specimen shows a relatively compact and continuous cementitious matrix, where tailings particles are partially embedded within hydration products and pore connectivity is limited, indicating restricted oxygen ingress and reduced pyrite oxidation. However, the air-dried samples show a more heterogeneous and porous structure, characterized by exposed particles, enlarged voids, and a less continuous matrix. This microstructural evolution reflects oxidation-induced deterioration, where sulphate released from pyrite oxidation promotes the formation of gypsum and ettringite, leading to microcracking and pore coarsening. Overall, the SEM, XRD, and permeability results confirm that oxygen ingress intensifies pyrite oxidation, progressively modifying the CPB

microstructure and increasing pore connectivity, which ultimately results in higher hydraulic conductivity.

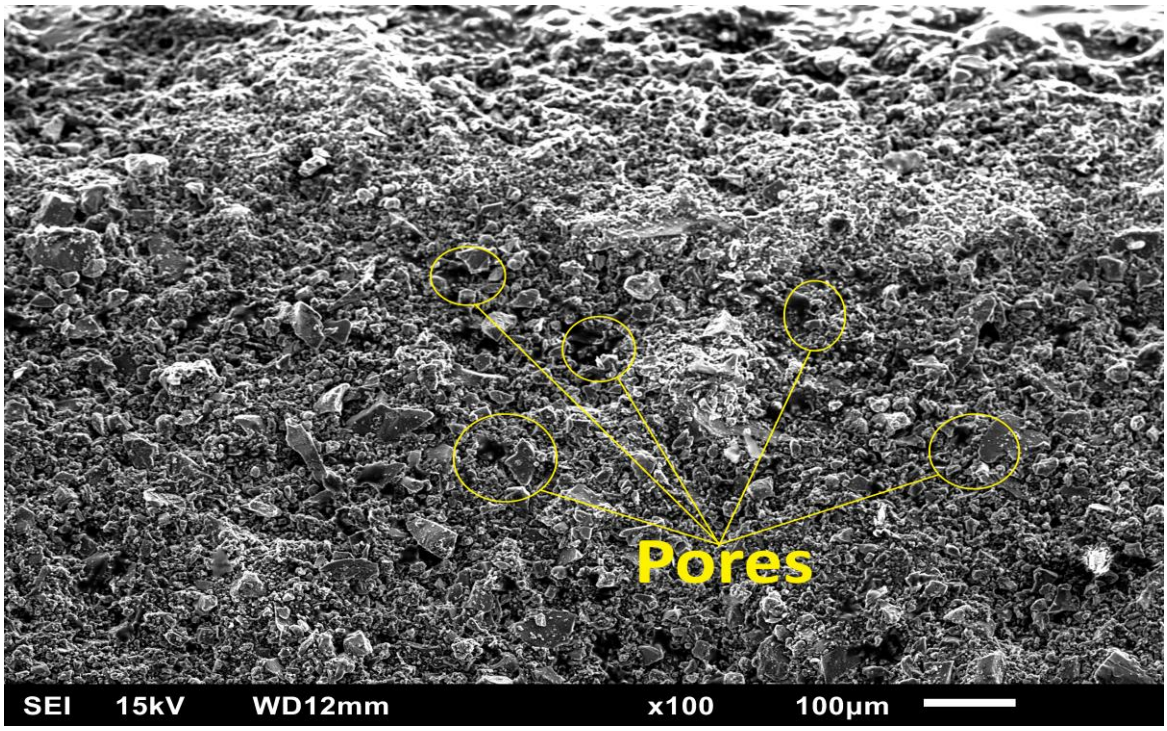

a)

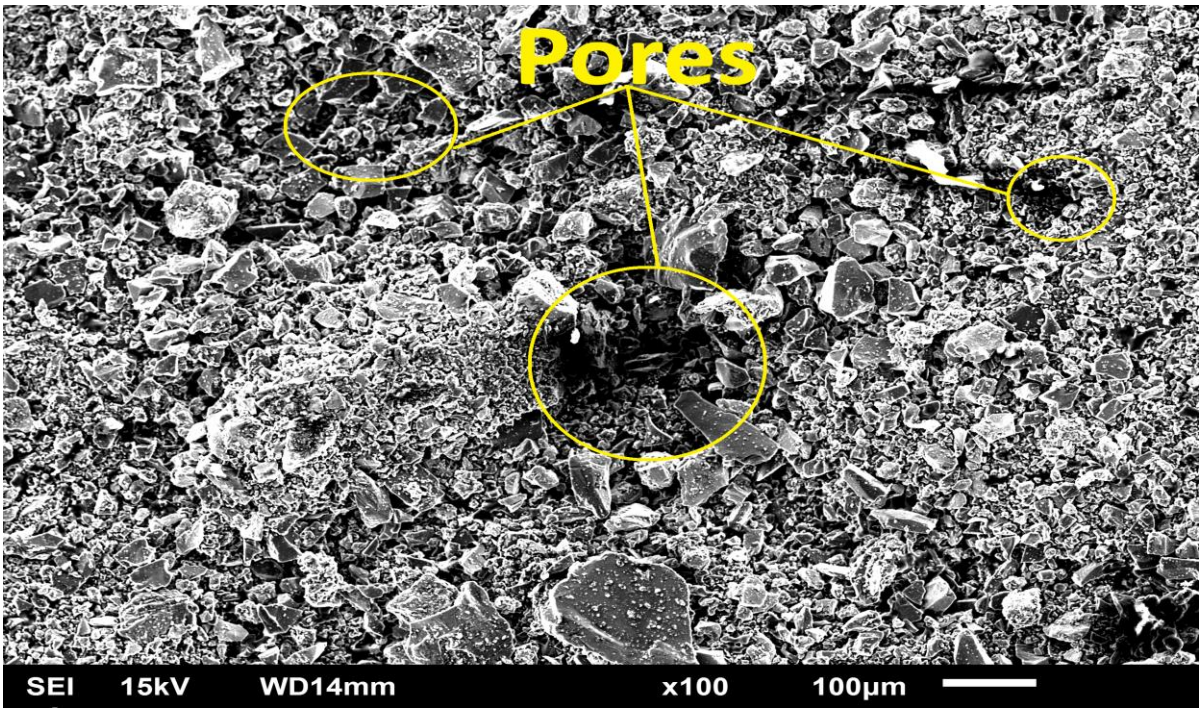

Figure 9: SEM micrographs of **(a)** PC-CPB-45% pyrite (no air-drying) and **(b)** PC-CPB-45%pyrite (air-drying) after 150 curing days.

This study also examined the effect of pyrite oxidation on different binder systems, and the results (Figure 10) show that the influence of pyrite oxidation follows the same pattern as the earlier findings, regardless of the binder type. As previously explained in the preceding sections, air-dried samples consistently displayed higher permeability due to accelerated pyrite oxidation, which promotes sulphate formation and the development of expansive minerals like gypsum and ettringite. The observed trend of slag-based CPB (SG-CPB) exhibiting higher permeability than Portland cement-based CPB (PC-CPB) is also attributed to the slower hydration rate of slag, which reduces matrix densification and increases its susceptibility to sulphate attack, as discussed earlier (Demirboga, 2007; Fall et al., 2009; Haruna and Fall, 2022). Thus, these results highlight the importance of considering oxidation effects during CPB preparation and placement, as prolonged exposure to air can compromise the material's durability and hydraulic performance.

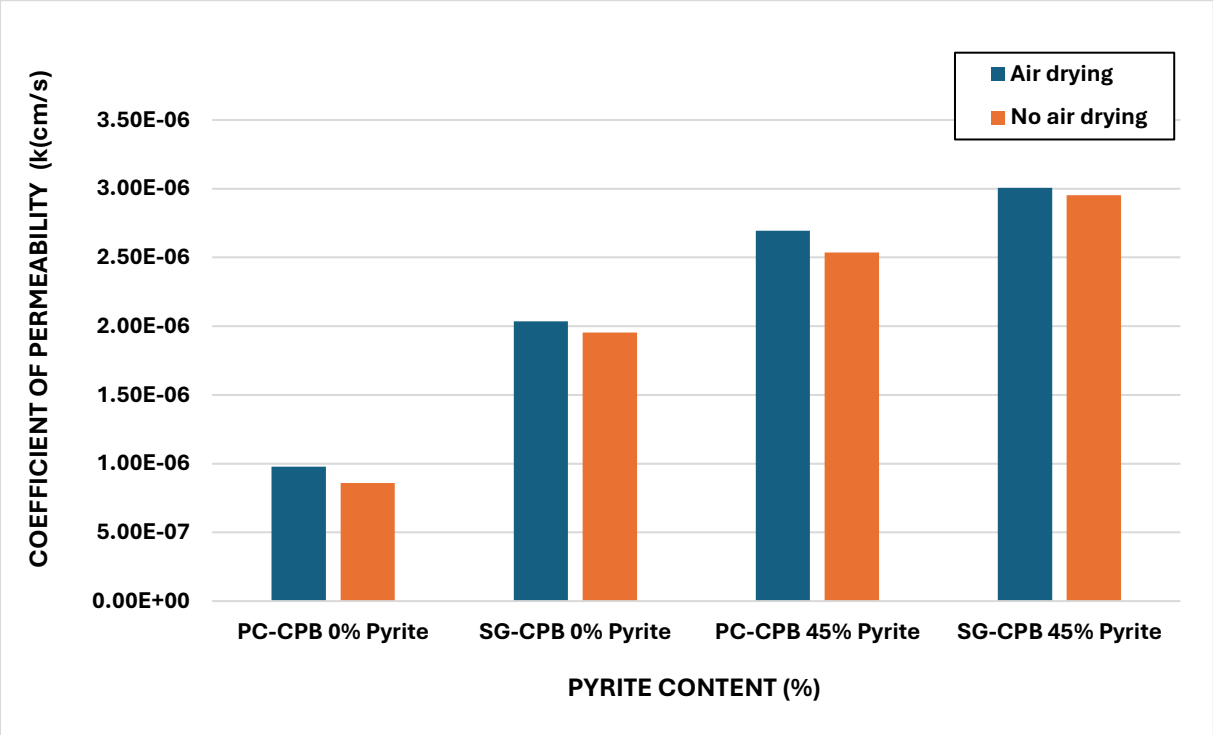

Figure 10: Effect of pyrite oxidation on the permeability of CPB stabilized with different binder types (PC-CPB and SG-CPB) at 150days curing time

6.4.3 INFLUENCE OF INITIAL SULPHATE CONCENTRATION ON THE PERMEABILITY BEHAVIOUR OF CEMENTED PASTE TAILINGS UNDER SEALED AND AIR-DRIED CONDITIONS

In practice, one of the key factors leading to the initial presence of sulphate ions in freshly prepared CPB is the presence and partial oxidation of sulphide minerals (e.g., pyrite). Therefore, the combined effects of sulphate concentration and pyrite content on CPB permeability were investigated. The results depicted in Figures 11(a) and 11(b) illustrate the role of initial sulphate content and pyrite content on the permeability response of CPB under sealed and air-dried conditions. Across all samples, the permeability coefficient increased progressively with increasing sulphate content and pyrite concentration, regardless of the binder type. However, the magnitude of increase varied notably between the different concentrations and binder systems.

Under sealed conditions, the permeability values remained generally lower compared to the air-dried samples, suggesting that limited oxygen availability under sealed curing slowed pyrite oxidation and subsequent sulphate generation. In the Portland cement-based CPB (PC-CPB), permeability increased from approximately 8.8×10^{-7} cm/s at 0 ppm sulphate to about 2.8×10^{-6} cm/s at 25,000 ppm for samples without pyrite, and further to around 3.5×10^{-6} cm/s when 15% pyrite was incorporated. A similar pattern was observed for the slag-based CPB (SG-CPB), where permeability increased sharply with sulphate enrichment, particularly at 25,000 ppm, reaching nearly 7.5×10^{-6} cm/s for samples containing 15% pyrite. This behaviour can be attributed to the release of sulphate ions from both the initial sulphate salts and partial oxidation of pyrite during mixing, which disrupted the microstructure by promoting the formation of expansive minerals such as ettringite and gypsum. These secondary products exert internal stress, induce microcracking, and increase pore connectivity within the backfill matrix, leading to higher hydraulic conductivity.

The air-dried samples consistently exhibited higher permeability across all binder and sulphate content combinations. This behaviour is attributed to the accelerated pyrite oxidation caused by greater oxygen exposure during the drying process. The oxidation process generates ferrous and ferric sulphates, as well as sulphuric acid, which attack key hydration products such as calcium silicate hydrate (C-S-H) and calcium hydroxide ($Ca(OH)_2$), weakening the cementitious matrix. The consequent formation of more abundant ettringite and gypsum crystals further expands the pore network, facilitating fluid flow. For instance, the permeability of SG-CPB with 25,000 ppm sulphate and 15% pyrite increased to nearly 1.0×10^{-5} cm/s, about twice that of its sealed counterpart.

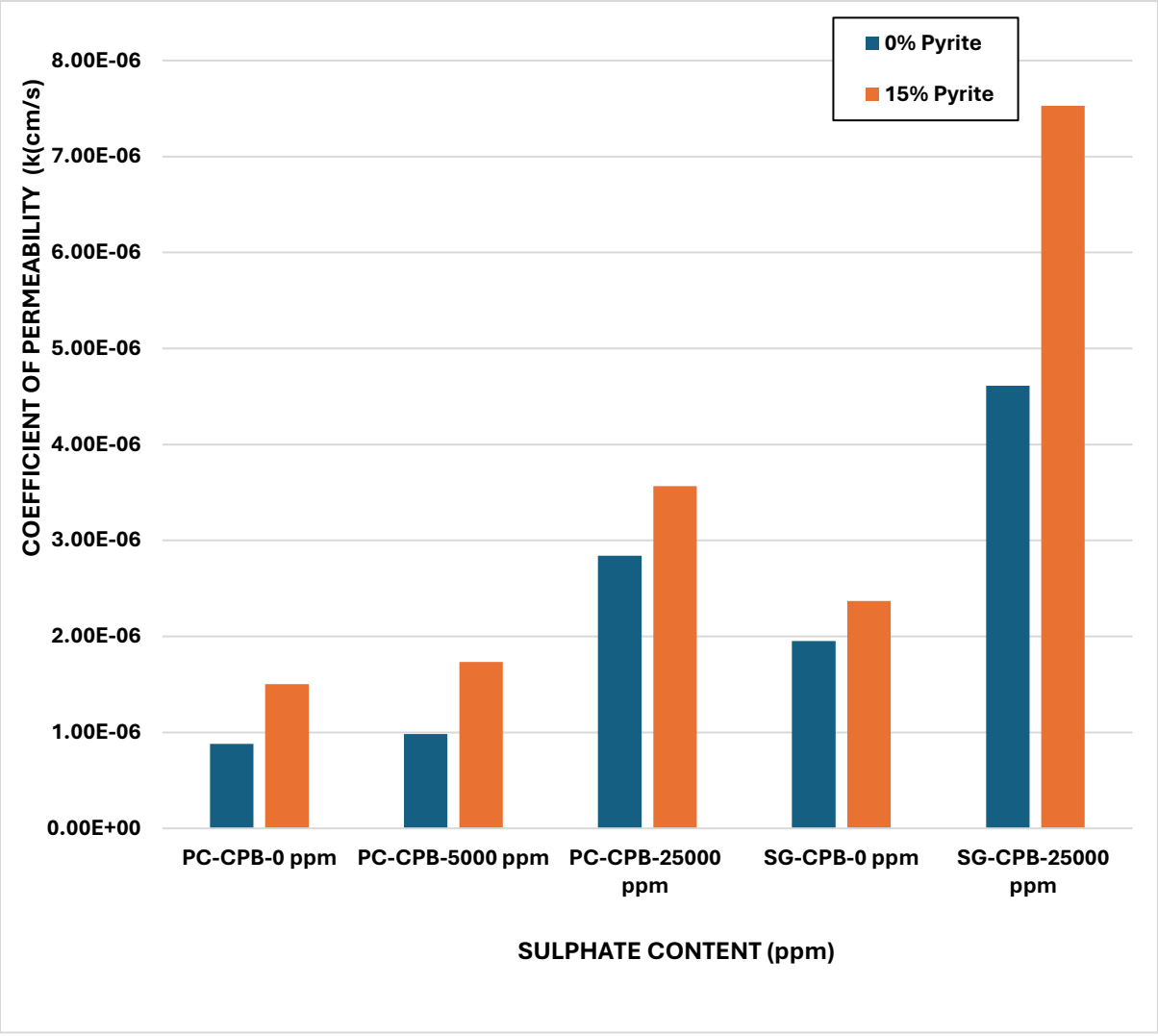

a)

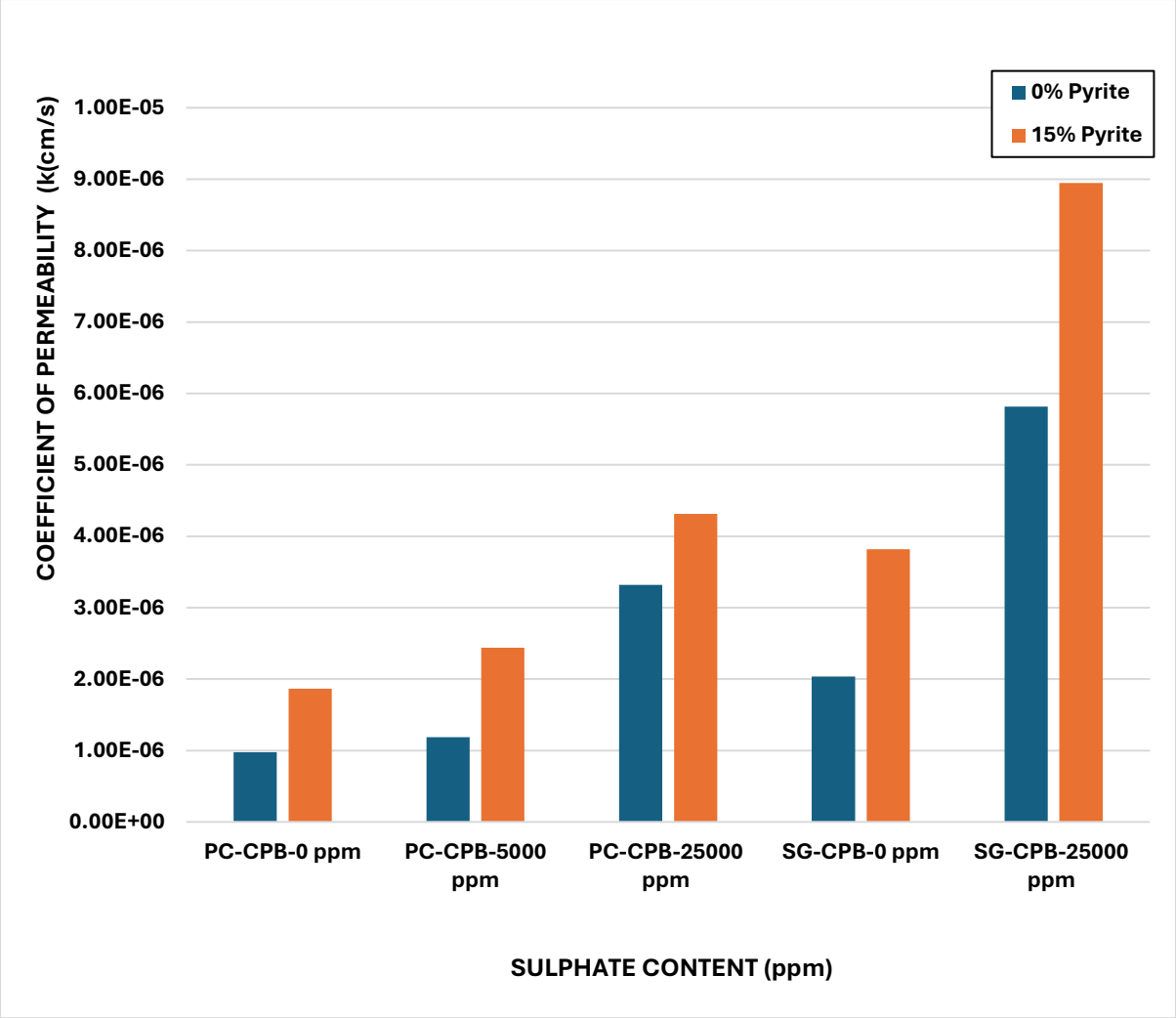

b)

Figure 11: Effect of initial sulphate, pyrite content and oxidation on the permeability of CPB exposed to **a)** No-air drying and **b)** Air-drying conditions.

In support of the permeability results presented in Figure 11(a), the void ratio and dry density trends shown in Figure 12 further confirm the microstructural degradation of CPB with increasing sulphate and pyrite contents. As sulphate concentration and pyrite content increased, there was a noticeable increment in the void ratio of PC-CPB, while the dry density decreased, particularly under air-dried conditions. This confirms a widened pore network and reduced matrix compactness due to the formation of expansive minerals such as ettringite and gypsum. Overall, these results demonstrate that both initial sulphate content and pyrite-induced sulphate

generation exert a strong influence on CPB permeability, with the effects being more pronounced under air-dried conditions and in slag-blended systems. The findings highlight the critical interplay between binder reactivity, curing environment, and sulphide oxidation processes in governing the hydraulic performance and long-term stability of sulphide-bearing backfill materials.

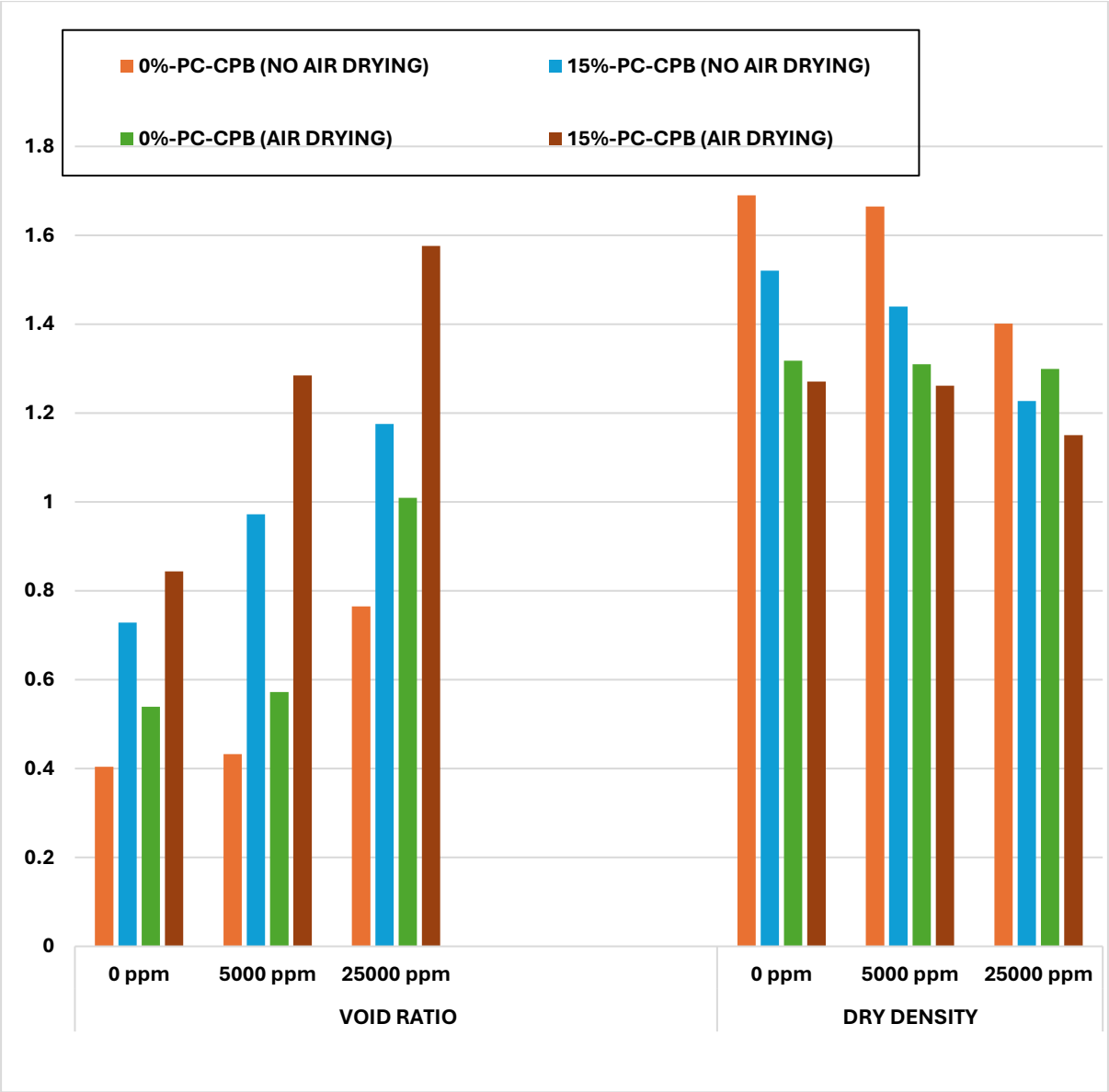

a)

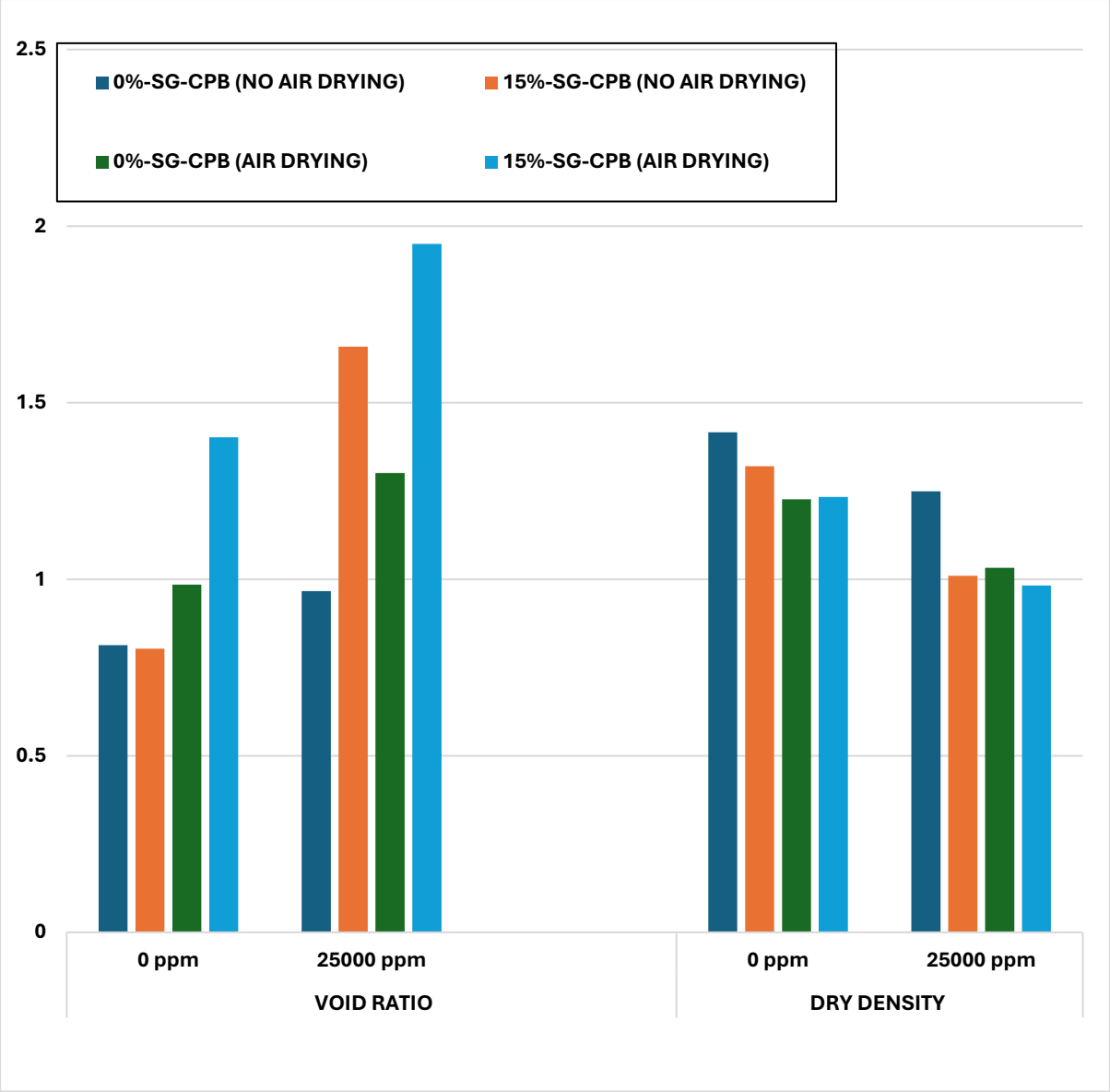

b)

Figure 12: Effect of initial sulphate content and pyrite content on the Void ratio and dry density of **a)** PC-CPB samples and **b)** SG-CPB samples after 150 curing days.

4.0 SUMMARY AND CONCLUSIONS

This study examined the effect of pyrite content, pyrite oxidation, initial sulphate concentration, and binder type on the permeability and microstructure of pyrite-bearing cemented paste tailings (CPB) under sealed and air-dried curing conditions. The key findings based on the results are summarized below;

- Increasing pyrite content significantly raised the permeability of CPB under both sealed and air-dried conditions. The rise was linked to pyrite oxidation, which created expansive minerals such as ettringite and gypsum. These secondary phases caused internal stress, cracking, and pore coarsening, leading to higher void ratios and lower dry densities.
- Air-dried samples consistently displayed higher permeability than sealed ones due to accelerated oxidation from oxygen exposure. Even under sealed conditions, limited internal oxidation caused microstructural weakening, demonstrating that pyrite-bearing systems remain vulnerable without strict oxygen control.
- Binder composition played a significant role in the hydraulic performance. Portland cement–based systems exhibited lower baseline permeability than slag-blended systems, owing to their higher portlandite content and faster hydration. In contrast, slag-blended binders showed lower susceptibility to sulphate-induced deterioration as pyrite and/or sulphate contents increased.
- Elevated initial sulphate concentrations further increased permeability, particularly when combined with high pyrite levels. The interaction between pre-existing sulphates and oxidation-derived ions intensified expansive mineral formation and microcracking.

In conclusion, this study shows that pyrite oxidation, sulphate content, and binder type have a significant impact on the hydraulic behaviour and long-term durability of cemented paste backfill (CPB). Hence, there is a strong need to select appropriate binders and minimize

oxidation and sulphate exposure during backfill preparation. Future research should focus on understanding the interactions between chemical processes and field conditions to further enhance the durability and sustainability of CPB systems.

5.0 REFERENCES

Abdul-Hussain, A., Fall, M., & Su, G. (2011, October 2–6). Evolution of hydraulic and mechanical properties of gelfill. *In* Proceedings of the 14th PanAmerican Conference on Soil Mechanics and Geotechnical Engineering (PCSMGE) and the 64th Canadian Geotechnical Conference (CGC), Toronto, ON, Canada.

Abdul-Hussain, N., & Fall, M. (2011). Unsaturated hydraulic properties of cemented tailings backfill that contains sodium silicate. *Engineering Geology*, *123*(4), 288–301. https://doi.org/10.1016/j.enggeo.2011.07.011

Abdul-Hussain, N., & Fall, M. (2012). Thermo-hydro-mechanical behaviour of sodium silicate-cemented paste tailings in column experiments. *Tunnelling and Underground Space Technology*, *29*, 85–93. https://doi.org/10.1016/j.tust.2012.01.004

Aldhafeeri, Z., & Fall, M. (2017). Sulphate induced changes in the reactivity of cemented tailings backfill. *International Journal of Mineral Processing*, *166*, 13–23. https://doi.org/10.1016/j.minpro.2017.06.007

Argane, R., Benzaazoua, M., Hakkou, R., & Bouamrane, A. (2015). Reuse of base-metal tailings as aggregates for rendering mortars: Assessment of immobilization performances and environmental behavior. *Construction & Building Materials*, *96*, 296–306. https://doi.org/10.1016/j.conbuildmat.2015.08.029

Benzaazoua, M., Ouellet, J., Servant, S., Newman, P., & Verburg, R. (1999). Cementitious backfill with high sulfur content Physical, chemical, and mineralogical characterization. *Cement and Concrete Research*, *29*(5), 719–725. https://doi.org/10.1016/S0008-8846(99)00023-X

Bian, J., Fall, M., & Haruna, S. (2021). Sulfate-induced changes in rheological properties of fibre-reinforced cemented paste backfill. *Magazine of Concrete Research*, *73*(11), Article 1900311. https://doi.org/10.1680/jmacr.19.00311

Boldt, C. M. K., Levens, R. L., & Marcy, A. D. (1996). *Environmental impacts of cemented mine waste backfill* (Mining Publications). United States Bureau of Mines. https://stacks.cdc.gov/view/cdc/9518

Bull, A. J., & Fall, M. (2020). Curing temperature dependency of the release of arsenic from cemented paste backfill made with Portland cement. *Journal of Environmental Management*, *269*, Article 110772. https://doi.org/10.1016/j.jenvman.2020.110772

Cacciuttolo Vargas, C., & Marinovic Pulido, A. (2022). Sustainable Management of Thickened Tailings in Chile and Peru: A Review of Practical Experience and Socio-Environmental Acceptance. Sustainability, 14(17), 10901. https://doi.org/10.3390/su141710901

Casanova, I., Aguado, A., & Agulló, L. (1997). Aggregate expansivity due to sulfide oxidation — II. Physico-chemical modeling of sulfate attack. *Cement and Concrete Research*, *27*(11), 1627–1632. https://doi.org/10.1016/S0008-8846(97)00148-8

Célestin, J. C. H., & Fall, M. (2009). Thermal conductivity of cemented paste backfill material and factors affecting it. *International Journal of Mining, Reclamation and Environment*, *23*(4), 274–290. https://doi.org/10.1080/17480930902731943

Czerewko, M. A., Cripps, J. C., Reid, J. M., & Duffell, C. G. (2003). Sulfur species in geological materials—sources and quantification. *Cement & Concrete Composites*, *25*(7), 657–671. https://doi.org/10.1016/S0958-9465(02)00066-5

Demirboga, R. (2007). Thermal conductivity and compressive strength of concrete incorporation with mineral admixtures. *Building and Environment*, *42*(7), 2467–2471. https://doi.org/10.1016/j.buildenv.2006.06.010

Edwards, K. J., Goebel, B. M., Rodgers, T. M., Schrenk, M. O., Gihring, T. M., Cardona, M. M., Hu, B., McGuire, M. M., Hamers, R. J., Pace, N. R., & Banfield, J. F. (1999). Geomicrobiology of Pyrite (FeS2) Dissolution: Case Study at Iron Mountain, California. Geomicrobiology Journal, 16(2), 155–179. https://doi.org/10.1080/014904599270668

Ercikdi, B., Cihangir, F., Kesimal, A., & Deveci, H. (2017). Practical Importance of Tailings for Cemented Paste Backfill. In M. Fall & E. Yilmaz (Eds.), *Paste Tailings Management* (pp. 7–32). Springer International Publishing AG. https://doi.org/10.1007/978-3-319-39682-8_2

Fall, M., & Benzaazoua, M. (2005). Modeling the effect of sulphate on strength development of paste backfill and binder mixture optimization. *Cement and Concrete Research*, *35*(2), 301–314. https://doi.org/10.1016/j.cemconres.2004.05.020

Fall, M., & Benzaazoua, M. (2005). Modeling the effect of sulphate on strength development of paste backfill and binder mixture optimization. *Cement and Concrete Research*, *35*(2), 301–314. https://doi.org/10.1016/j.cemconres.2004.05.020

Fall, M., & Pokharel, M. (2010). Coupled effects of sulphate and temperature on the strength development of cemented tailings backfills: Portland cement-paste backfill. *Cement & Concrete Composites*, *32*(10), 819–828. https://doi.org/10.1016/j.cemconcomp.2010.08.002

Fall, M., Adrien, D., Célestin, J. C., Pokharel, M., & Touré, M. (2009). Saturated hydraulic conductivity of cemented paste backfill. *Minerals Engineering*, *22*(15), 1307–1317. https://doi.org/10.1016/j.mineng.2009.08.002

Fall, M., Belem, T., Samb, S., & Benzaazoua, M. (2007). Experimental characterization of the stress–strain behaviour of cemented paste backfill in compression. *Journal of Materials Science*, *42*(11), 3914–3922. https://doi.org/10.1007/s10853-006-0403-2

Fall, M., Benzaazoua, M., & Saa, E. G. (2008). Mix proportioning of underground cemented tailings backfill. *Tunnelling and Underground Space Technology*, *23*(1), 80–90. https://doi.org/10.1016/j.tust.2006.08.005

Fall, M., Célestin, J. C., Pokharel, M., & Touré, M. (2010). A contribution to understanding the effects of curing temperature on the mechanical properties of mine cemented tailings backfill. *Engineering Geology*, *114*(3), 397–413. https://doi.org/10.1016/j.enggeo.2010.05.016

Ghirian, A., & Fall, M. (2013). Coupled thermo-hydro-mechanical–chemical behaviour of cemented paste backfill in column experiments. Part I: Physical, hydraulic and thermal processes and characteristics. *Engineering Geology*, *164*, 195–207. https://doi.org/10.1016/j.enggeo.2013.01.015

Ghirian, A., & Fall, M. (2014). Coupled thermo-hydro-mechanical—chemical behaviour of cemented paste backfill in column experiments Part II: Mechanical, chemical and microstructural processes and characteristics. *Engineering Geology*, *170*, 11–23. https://doi.org/10.1016/j.enggeo.2013.12.004

Godbout, J., 2005. Evolution des proprieties des remblais miniers cimentés en pate durant le curage. Mémoire de Maitrise, Ecole Polytechnique de Montréal (212 pp.).

Haruna, S., & Fall, M. (2022). Insight into Saturated Hydraulic Conductivity of Cemented Paste Backfill Containing Polycarboxylate Ether-Based Superplasticizer. *Minerals (Basel)*, *12*(1), Article 93. https://doi.org/10.3390/min12010093

Ke, X., Zhou, X., Wang, X., Wang, T., Hou, H., & Zhou, M. (2016). Effect of tailings fineness on the pore structure development of cemented paste backfill. *Construction & Building Materials*, *126*, 345–350. https://doi.org/10.1016/j.conbuildmat.2016.09.052

Kesimal, A., Ercikdi, B., & Yilmaz, E. (2003). The effect of desliming by sedimentation on paste backfill performance. *Minerals Engineering*, *16*(10), 1009–1011. https://doi.org/10.1016/S0892-6875(03)00267-X

Kesimal, A., Yilmaz, E., Ercikdi, B., Alp, I., & Deveci, H. (2005). Effect of properties of tailings and binder on the short-and long-term strength and stability of cemented paste backfill. *Materials Letters*, *59*(28), 3703–3709. https://doi.org/10.1016/j.matlet.2005.06.042

Klein, K., & Simon, D. (2006). Effect of specimen composition on the strength development in cemented paste backfill. *Canadian Geotechnical Journal*, *43*(3), 310–324. https://doi.org/10.1139/t06-005

Lee, H., Cody, R. D., Cody, A. M., & Spry, P. G. (2005). The formation and role of ettringite in Iowa highway concrete deterioration. *Cement and Concrete Research*, *35*(2), 332–343. https://doi.org/10.1016/j.cemconres.2004.05.029

Li, W., & Fall, M. (2018). Strength and self-desiccation of slag-cemented paste backfill at early ages: Link to initial sulphate concentration. *Cement & Concrete Composites*, *89*, 160–168. https://doi.org/10.1016/j.cemconcomp.2017.09.019

Mahlaba, J. S., Kearsley, E. P., & Kruger, R. A. (2011). Physical, chemical and mineralogical characterisation of hydraulically disposed fine coal ash from SASOL Synfuels. *Fuel (Guildford)*, *90*(7), 2491–2500. https://doi.org/10.1016/j.fuel.2011.03.022

Marchon, D., Sulser, U., Eberhardt, A., & Flatt, R. J. (2016). Molecular design of comb-shaped polycarboxylate dispersants for environmentally friendly concrete. Soft Matter, 12(3), 725–734. https://doi.org/10.1039/C5SM01913J

Martins, N. P., Helser, J., Plötze, M., Snellings, R., & Habert, G. (2024). Effect of sulfidic mine tailings used as mineral admixtures on the hydration of common and alternative cements. *Materials and Structures*, *57*(1), Article 19. https://doi.org/10.1617/s11527-023-02289-

Martins, N. P., Srivastava, S., Simão, F. V., Niu, H., Perumal, P., Snellings, R., Illikainen, M., Chambart, H., & Habert, G. (2021). Exploring the Potential for Utilization of Medium and Highly Sulfidic Mine Tailings in Construction Materials: A Review. Sustainability, 13(21), Article 12150. https://doi.org/10.3390/su132112150

Oyewale, Miracle., Fall, M., & Ghirian, A. (2025). Flow characteristics of paste tailings in surface disposal: the role of pyrite content. *Environmental Science and Pollution Research International*, *32*(11), 6446–6467. https://doi.org/10.1007/s11356-025-36051-w

Moses, C. O., Kirk Nordstrom, D., Herman, J. S., & Mills, A. L. (1987). Aqueous pyrite oxidation by dissolved oxygen and by ferric iron. *Geochimica et Cosmochimica Acta*, *51*(6), 1561–1571. https://doi.org/10.1016/0016-7037(87)90337-1

Nasir, O., & Fall, M. (2010). Coupling binder hydration, temperature and compressive strength development of underground cemented paste backfill at early ages. *Tunnelling and Underground Space Technology*, *25*(1), 9–20. https://doi.org/10.1016/j.tust.2009.07.008

Ouattara, D., Yahia, A., Mbonimpa, M., & Belem, T. (2017). Effects of superplasticizer on rheological properties of cemented paste backfills. *International Journal of Mineral Processing*, *161*, 28–40. https://doi.org/10.1016/j.minpro.2017.02.003

Pokharel M, Fall M (2013) Combined influence of sulphate and temperature on the saturated hydraulic conductivity of hardened cemented paste backfll. Cem Concr Compos 38:21–28. https:// doi.org/10.1016/j.cemconcomp.2013.03.015

Qi, C., & Fourie, A. (2019). Cemented paste backfill for mineral tailings management: Review and future perspectives. *Minerals Engineering*, *144*, Article 106025. https://doi.org/10.1016/j.mineng.2019.106025

Rodrigues A, Duchesne J, Fournier B, Durand B, Rivard P, Shehata M (2012) Mineralogical and chemical assessment of concrete damaged by the oxidation of sulfidebearing aggregates: importance of thaumasite formation on reaction mechanisms. Cem Concr Res 42(10):1336–1347. https://doi.org/10.1016/j.cemconres.2012.06.008

Schmidt T, Leemann A, Gallucci E, Scrivener KL (2011) Physical and microstructural aspects of iron sulfde degradation in concrete. Cem Concr Res 41(3):263–269. https://doi.org/10.1016/j.cemconres. 2010.11.011

Sheshpari, Morteza (Mori). (2015). A review of underground mine backfilling methods with emphasis on cemented paste backfill. Electronic Journal of Geotechnical Engineering. 20. 5183-5208.

Sicakova, Alena & Kovac, Marek. (2020). Relationships between Functional Properties of Pervious Concrete. Sustainability. 12. 6318. 10.3390/su12166318.

Tariq, A., & Nehdi, M. (2007). Developing durable paste backfill from sulphidic tailings. Proceedings of the Institution of Civil Engineers. Waste and Resource Management, 160(4), 155–166. https://doi.org/10.1680/warm.2007.160.4.155

Whittaker, M., & Black, L. (2015). Current knowledge of external sulfate attack. *Advances in Cement Research*, *27*(9), 532–545. https://doi.org/10.1680/jadcr.14.00089

Wu, A., Kang, Z., Ruan, Z., Wang, Y., Li, C., Wang, J., Wang, S., & Xiao, B. (2025). New development and frontiers of green mining with cemented paste backfill in China. In A. B. Fourie, A. Copeland, V. Daigle, & C. MacRobert (Eds.), Paste 2025: Proceedings of the 27th International Conference on Paste, Thickened and Filtered Tailings (pp. 607-614). Australian Centre for Geomechanics. https://doi.org/10.36487/ACG_repo/2555_43

Wu, D., Fall, M., & Cai, S. J. (2013). Coupling temperature, cement hydration and rheological behaviour of fresh cemented paste backfill. *Minerals Engineering*, *42*, 76–87. https://doi.org/10.1016/j.mineng.2012.11.011

Xiapeng P, Fall M, Haruna S (2019) Sulphate-induced changes of rheological properties of cemented paste backfill. Minerals Eng 141:105849. https://doi.org/10.1016/j.mineng.2019.105849

Yilmaz, E., & Fall, M. (2017). Introduction to Paste Tailings Management. In *Paste Tailings Management* (pp. 1–5). Springer International Publishing AG. https://doi.org/10.1007/978-3-319-39682-8_1

Yilmaz, E., Belem, T., & Benzaazoua, M. (2014). Effects of curing and stress conditions on hydromechanical, geotechnical and geochemical properties of cemented paste backfill. *Engineering Geology*, *168*, 23–37. https://doi.org/10.1016/j.enggeo.2013.10.024

Yilmaz, E., Belem, T., Benzaazoua, M., & Bussière, B. (2010). Assessment of the Modified CUAPS Apparatus to Estimate In Situ Properties of Cemented Paste Backfill. *Geotechnical Testing Journal*, *33*(5), 1–12. https://doi.org/10.1520/GTJ102689

Yilmaz, E., Benzaazoua, M., Belem, T., & Bussière, B. (2009). Effect of curing under pressure on compressive strength development of cemented paste backfill. *Minerals Engineering*, *22*(9), 772–785. https://doi.org/10.1016/j.mineng.2009.02.002

Zhong R, Wille K (2018) Deterioration of residential concrete foundations: the role of pyrrhotite-bearing aggregate. Cem Concr Compos 94:53–61. https://doi.org/10.1016/j.cemconcomp.2018.08.012

CHAPTER SEVEN.

INTEGRATION AND SYNTHESIS OF RESULTS.

7.1 INTRODUCTION

To comprehensively assess the overall influence of pyrite content on the engineering and environmental performance of paste tailings systems for both surface and underground mining applications, the findings from all four technical papers are synthesized and discussed in this chapter. Papers one and two examined the rheological behaviour of UPT, LCPT, and CPB. Specifically, Paper one investigated the effect of pyrite content on UPT and LCPT for surface mining operations, while Paper Two further evaluated how pyrite content influences CPB systems for underground mining applications. Papers Three and Four focused on the hydraulic behaviour of UPT, LCPT, and CPB under different oxidation and curing conditions. Overall, the four papers employed mineralogical transformations and microstructural evolution as the principal performance indicators to further validate results.

Across all studies, complementary parameters such as sulphate concentration, curing condition (sealed or air-dried), binder ratio, binder type, and oxidation environment were systematically investigated to develop a holistic understanding of the physicochemical mechanisms governing the evolution and long-term performance of pyrite-bearing tailings. A summary of the experimental parameters and variables examined throughout this PhD research is presented in Table 1.

Table 1: Factors and Tests studied in this PHD Research

STUDY REFERENCE		RHEOLOGICAL AND HYDRAULIC PROCESS								
Technical paper	**Chapter No**	**Tailings type**	**Mining application**	**Effect of Pyrite Content**	**Effect of Binder type**	**Effect of Sulphate**	**Effect of Curing time**	**Oxidative Condition**	**Microstructural tests**	**Monitoring Tests**
1	**3**	X	X	X	X		X		TG/DTG, XRD	Ph, EC, Zeta potential
2	**4**	X	X	X	X		X		TG/DTG, XRD	Ph, EC, Zeta potential
3	**5**	X	X	X	X	X		X	Void ratio, Dry density, Porosity	MIP, XRD
4	**6**	X	X	X	X	X		X	Void ratio, Dry density, Porosity	SEM, XRD

7.2 EFFECT OF SULPHIDE MINERALS (PYRITE) ON THE RHEOLOGICAL PROPERTIES OF UPT AND LCPT FOR SURFACE MINING APPLICATIONS.

Technical paper I investigates how pyrite, a common sulphide mineral in hard-rock mine tailings, governs the fresh-age flow of paste tailings used for surface disposal. The central aim was to determine how increasing pyrite content reshapes the rheology of both uncemented paste tailings (UPT) and lightly cemented paste tailings (LCPT), and to translate those effects into practical guidance for pipeline transport and surface paste deposition. To that end, four

specific objectives framed the work: quantify the influence of pyrite content on yield stress and viscosity; capture the time dependence of LCPT rheology over the first two hours after mixing at 20 °C; assess how binder type-100% Type I Portland cement (PC) versus a 50/50 PC–slag blend (SG) modulates pyrite's effects; and mechanistically link rheological shifts to concurrent chemical and microstructural changes using pH, zeta potential, electrical conductivity (EC), XRD, and TG/DTG.

In UPT, pyrite acted as a strong rheology accelerator. Yield stress and viscosity increased as pyrite increased from 0% to 45%. Two mechanisms were identified to explain this progressive rheological hardening. First, the presence of denser pyrite increases the overall packing density and solids volume per unit slurry volume, thereby elevating resistance to flow. Second, pyrite oxidation acidifies the suspension and increases sulphate ion concentration, which compresses the electrical double layer and weakens interparticle repulsion. Consistent with this, pH decreased with increasing pyrite content, while zeta potential also declined, thereby promoting particle flocculation and increasing the apparent viscosity of the mixture.

In LCPT, yield stress increased with curing time due to cement hydration, but at a slower rate in pyrite-bearing samples. Pyrite released sulphate ions that reacted with tricalcium aluminate (C_3A) to form ettringite, coating cement grains and hindering further hydration. As a result, LCPT with pyrite showed lower yield stress, fewer hydration products, and reduced calcium hydroxide formation. Electrical conductivity trends, XRD and TG/DTG analyses confirmed slower hydration and greater ettringite formation. Binder type also influenced rheology as blended PC–slag mixes had lower yield stress and viscosity than pure Portland cement due to slower pozzolanic activation, improving flowability but delaying early strength development.

Overall, the study concludes that pyrite content is a critical parameter controlling the pumpability and placement of paste tailings. High pyrite concentrations increase flow

resistance and hinder early hydration, particularly in cemented systems, while binder selection significantly influences rheological response and environmental performance. These findings contribute to the development of safer, more cost-effective, and sustainable tailings management practices by guiding material formulation, transport planning, and the use of alternative low-carbon binders in surface disposal operations.

7.3 EFFECT OF SULPHIDE MINERALS ON THE RHEOLOGICAL PROPERTIES OF PASTE TAILINGS (CPB) FOR UNDERGROUND MINING APPLICATIONS.

To further study the effect of pyrite content on paste tailings (PT) systems, technical paper II was conducted to evaluate the influence of pyrite content on the rheological behaviour of cemented paste backfill (CPB) for underground paste applications. The aim was to understand how varying pyrite concentrations and binder compositions affect the flowability, yield stress, and viscosity of CPB mixtures, as well as to identify the chemical and microstructural mechanisms governing these changes. The study also sought to provide practical insights for optimizing backfill transport, placement, and stability in underground mining operations.

The results demonstrated that pyrite content has a strong influence on the rheological properties of CPB. Both yield stress and viscosity increased significantly with higher pyrite concentrations, indicating that pyrite enhances the density and internal friction of the mixture. This behaviour was attributed to the high specific gravity and chemical reactivity of pyrite, which modifies particle packing and surface chemistry within the paste. Oxidation of pyrite produces sulphate ions and acidic conditions that lower pH and zeta potential, reducing repulsive electrostatic forces between particles and encouraging flocculation. Consequently, pyrite-rich CPB mixtures exhibited higher flow resistance and reduced workability, which has direct implications for pipeline transport and pumping efficiency in underground operations.

Curing time also played a significant role, as the rheological properties of all mixtures increased

with time due to the ongoing hydration of cement and the formation of binding products such as calcium silicate hydrate (C–S–H) and ettringite. However, pyrite-containing CPBs developed lower final yield stress values compared with pyrite-free mixtures. This reduction was caused by the inhibitory effect of pyrite on cement hydration: sulphate ions generated during pyrite oxidation react with tricalcium aluminate (C_3A) to form ettringite, coating unhydrated cement grains and slowing further hydration. Supporting tests, including electrical conductivity, X-ray diffraction (XRD), and thermogravimetric analysis (TG/DTG), confirmed slower hydration kinetics and fewer hydration products in pyrite-bearing samples. These findings indicate that the presence of pyrite not only increases initial flow resistance but also delays the development of structural strength within the backfill.

The results on binder type and ratio showed that replacing 50% of Portland cement with slag significantly lowered both yield stress and viscosity, particularly in pyrite-bearing mixtures. The slower pozzolanic reaction of slag produced fewer early hydration products, resulting in a less dense matrix. Although this reduced flow resistance and improved pumpability, it also delayed early strength development, which must be carefully considered during backfill design and mine scheduling.

Overall, the study highlights the importance of understanding how pyrite content and binder type interact to control the flow and setting behaviour of CPB systems used in underground mining. The findings provide a foundation for designing more efficient, cost-effective, and environmentally sustainable backfill mixtures that account for both short-term rheological performance and long-term durability.

7.4 EFFECT OF SULPHIDE MINERALS(PYRITE) ON THE PERMEABILITY PROPERTIES OF UPT AND LCPT FOR SURFACE MINING APPLICATIONS.

Paper III aimed to evaluate how pyrite content, oxidation conditions, sulphate

concentration, and binder composition influence the permeability and microstructural stability of uncemented and lightly cemented paste tailings (UPT and LCPT) used for surface disposal in mining operations. The central objective was to understand how sulphide minerals, especially pyrite, affect the hydraulic behaviour, durability, and environmental performance of these systems, which are crucial for predicting contaminant migration and long-term stability of tailings storage facilities.

The study systematically examined the permeability response of UPT and LCPT with varying pyrite contents (0–45%), under both sealed and air-dried curing conditions, and compared the performance of Portland cement (PC) and slag-blended (SG) binders. Complementary analyses, including void ratio, dry density, X-ray diffraction (XRD), and mercury intrusion porosimetry (MIP), were conducted to link hydraulic changes to microstructural and mineralogical transformations. Additional tests investigated how pre-existing sulphate ions (0–25,000 ppm) influence permeability, simulating tailings partially oxidized before mixing.

The key findings reveal that pyrite content plays a crucial role in the hydraulic performance of paste tailings systems. In uncemented tailings, increasing pyrite content caused a drastic rise in permeability due to higher void ratios and lower dry densities, reflecting looser, more open pore networks. In lightly cemented systems, the influence was less severe: at low pyrite levels (≤15%), cement hydration reduced permeability by refining the pore structure, but at 45% pyrite, permeability rose considerably compared to the mixes with 0-15% pyrite content. This increase was driven by sulphate ions released from pyrite oxidation, which reacted with calcium hydroxide and aluminates in cement to form expansive ettringite and gypsum. These reactions consumed hydration products, induced cracking, and coarsened the pore network, drastically weakening the matrix. Even under sealed conditions, internal oxidation was sufficient to impair matrix integrity, while air drying simulating field exposure

accelerated degradation.

Binder composition emerged as a critical control factor. PC-LCPT exhibited initially low permeability but was highly sensitive to sulphate and pyrite attack due to its higher C_3A and portlandite contents, which favour expansive mineral formation. In contrast, SG-LCPT displayed higher initial permeability under oxidative and sulphate-rich conditions. XRD and MIP analyses confirmed these trends. Additionally, high initial sulphate concentrations (particularly at 25,000 ppm) compounded the degradation effects, leading to significant permeability increases and matrix breakdown, especially when combined with pyrite oxidation and oxygen exposure. These synergistic interactions created interconnected voids and enlarged pore pathways, promoting solute transport and potential contaminant migration.

Overall, the research contributes significantly to understanding the coupled chemical-hydraulic processes governing the stability of sulphide-rich paste tailings. It demonstrates that permeability and environmental risk are closely linked to binder chemistry, oxidation potential, and sulphate load. By identifying the mechanisms driving permeability deterioration, this study provides a scientific basis for optimizing binder selection and controlling oxidation during surface paste disposal.

7.5 EFFECT OF SULPHIDE MINERALS (PYRITE) ON THE PERMEABILITY PROPERTIES OF CPB FOR UNDERGROUND MINING APPLICATIONS.

Technical paper IV was conducted to evaluate how pyrite content, pyrite oxidation, initial sulphate concentration, and binder composition govern the hydraulic behaviour and microstructural stability of cemented paste tailings (CPB) for underground mining applications. Type I Portland cement (PC) and a 50:50 PC–slag blend (SG) were adopted as binders at constant volumetric content, with pyrite dosed at 0, 5, 15, and 45 wt.% and initial sulphate in mixing water set to 0, 5,000, or 25,000 ppm. Curing conditions included: sealed (limited oxygen ingress) and air-dried (oxygen exposure). Permeability was measured with a

flexible-wall permeameter (ASTM D5084), while microstructure and mineralogy were tracked using void ratio/dry density, XRD, and supporting SEM analysis.

Key findings that under sealed curing conditions, permeability increased systematically with pyrite content, even without deliberate air exposure. This indicates that limited internal oxidation and sulphate release are sufficient to initiate secondary reactions. XRD patterns at high pyrite levels confirmed reduced portlandite and the emergence of ettringite/gypsum, consistent with sulphate consumption of $Ca(OH)_2$ and expansive crystallization. Physically, rising void ratio and declining dry density tracked the hydraulic deterioration, evidencing pore coarsening and loss of matrix compactness. Air-dried mixes exhibited higher permeability than sealed counterparts at equivalent pyrite contents, reflecting oxygen-driven oxidation and more vigorous sulphate generation. Correspondingly, XRD showed intensified ettringite/gypsum and diminished C–S–H/portlandite signatures, aligning with a shift toward larger, better-connected pores and microcracking that facilitates fluid flow.

Results on the effect of initial sulphate showed amplified degradation in both curing regimes. At 25,000 ppm, permeability rose sharply, especially when combined with pyrite and oxygen exposure. The synergy between pre-existing sulphate and oxidation-derived sulphate promoted excessive formation of expansive phases, internal stresses, and crack networks, which translated directly into higher void ratios, lower dry densities, and elevated permeability. Binder chemistry played a decisive moderating role. PC-based CPB recorded lower permeability and more refined pore systems due to faster hydration and greater portlandite availability; however, that same chemistry made PC more vulnerable to sulphate attack at high pyrite/sulphate levels because abundant C_3A and CH favour ettringite/gypsum formation. SG-based CPB, while showing higher baseline permeability and slower densification, proved less sensitive to sulphate- and pyrite-induced deterioration. The slag's pozzolanic consumption of CH and lower effective C_3A availability constrained expansive phase growth, limiting crack

development and mitigating permeability escalation relative to PC at elevated chemical stress. Taken together, these results contribute several advances to the CPB literature.

In sum, the study establishes that CPB permeability and by extension durability and environmental protection depends not only on pyrite content but also on oxygen availability, background sulphate load, and binder chemistry.

7.6 NOVEL CONTRIBUTION OF THE RESEARCH

This research presents novel information that advances the scientific understanding of how pyrite-driven chemical reactions influence flowability, permeability, microstructural evolution, and durability of PT, while providing engineering guidance for sustainable and resilient tailings management in mining environments.

The first paper established the rheological significance of pyrite in UPT and LCPT systems for surface disposal, revealing that increasing pyrite content substantially elevates yield stress and viscosity due to both physical densification and electrochemical destabilization of particle suspensions. The study identified that pyrite oxidation releases sulphate ions and lowers pH, compressing the electrical double layer and promoting flocculation, which increases flow resistance. Furthermore, in cemented mixtures, the release of sulphate retards hydration through premature ettringite formation. These findings introduced a mechanistic framework linking pyrite-induced chemical reactions to rheological performance, providing a predictive understanding of paste transport behaviour and the influence of binder selection, which is an advancement rarely quantified in previous CPB research.

Building upon this, the second paper extended the rheological study to underground CPB systems, demonstrating that pyrite content exerts dual control over early flowability and long-term structural development. The work showed that while pyrite-rich CPB mixtures exhibit high initial yield stress and viscosity, their strength gain is inhibited by the sulphate–

aluminate reaction that coats cement grains and slows hydration. The study was among the first to quantify how binder chemistry (Portland cement versus slag–cement blends) moderates these effects, showing that slag substitution mitigates pyrite-induced thickening and supports improved pumpability. This work provided design-relevant correlations between pyrite concentration, binder type, and rheological response, addressing a key gap in the geotechnical design of underground backfilling operations.

The third paper offered a novel understanding of how pyrite and associated sulphate reactions influence permeability and microstructural integrity in UPT and LCPT systems for surface disposal. It demonstrated that pyrite-rich tailings develop higher permeability due to acid generation and secondary mineralization, which disrupts the pore network. A particularly innovative contribution was the linkage of pyrite content degradation to mineralogical transformations identified through XRD and MIP analyses. The research established that permeability of pyrite-bearing tailings increases as a result of sulphate-induced ettringite and gypsum crystallization that expands and fractures the matrix, particularly under oxygen-exposed or high-sulphate conditions. This coupling of chemical and hydraulic processes advances predictive modelling of oxidation-driven permeability evolution in tailings impoundments, filling a long-standing research gap in mine waste geochemistry and geotechnics.

The fourth paper further advanced this field by examining the combined effects of pyrite content, oxidation potential, and pre-existing sulphate concentrations on the permeability and durability of underground CPB systems. It was the first to systematically differentiate permeability behaviour under sealed (oxygen-limited) and air-dried (oxidative) curing conditions, revealing that internal oxidation alone can significantly deteriorate the microstructure. Moreover, the study quantified how binder chemistry governs resistance to pyrite- and sulphate-induced degradation: while Portland cement produced denser matrices

with initially low permeability, it proved more vulnerable to sulphate attack at high pyrite levels; conversely, slag-blended binders, though slower to densify, better resisted chemical deterioration. These findings represent a new framework for durability-based design of CPB, integrating mineralogical reactivity, binder selection, and oxidation control into hydraulic performance predictions.

Together, these four studies establish a unified mechanistic understanding of pyrite's coupled chemical, mechanical, and hydraulic influences across various paste tailings systems. They introduce new correlations between pyrite reactivity, rheological evolution, and permeability degradation, while defining practical design guidelines for binder optimization, oxidation control, and sustainable tailings management. The research thus makes a significant and novel contribution to the body of knowledge on sulphide-bearing tailings, providing both theoretical advancement and applied relevance for geotechnical and environmental engineering practice in the global mining industry.

CHAPTER EIGHT.
CONCLUSIONS AND RECOMMENDATIONS.

8.1 CONCLUSIONS

The following conclusions are drawn from this study:

- Pyrite is a dominant factor governing the rheological, hydraulic, and chemical behaviour of paste tailings systems used in both surface and underground mining operations. Its high specific gravity increases packing density, while its oxidation releases sulphate ions that reduce pH and zeta potential, leading to particle flocculation, electrochemical destabilization, and greater flow resistance.
- Increasing pyrite content consistently elevated yield stress and viscosity in uncemented, lightly cemented, and cemented paste systems, resulting in reduced flow ability, higher pumping energy demand, and tighter operational windows for placement and pipeline transport.
- In cemented systems, pyrite retards hydration by forming ettringite and gypsum through sulphate (C_3A) reactions, which coat cement grains, reduce calcium hydroxide formation, and hinder the development of calcium silicate hydrate (C-S–H).
- Binder composition plays a key moderating role: pure Portland cement mixtures are more susceptible to sulphate-induced degradation, whereas slag-blended binders provide better flowability, slower hydration, and enhanced chemical resilience.
- Pyrite oxidation and sulphate release increase permeability and void ratio, particularly under air-dried or oxygen-exposed conditions, due to microcracking, pore coarsening, and matrix decomposition from expansive ettringite and gypsum formation. These effects are

magnified at high pyrite and sulphate concentrations, promoting permeability and potential contaminant migration.

- Sealed curing conditions help limit oxidation; however, internal reactions in high-pyrite systems can impair matrix integrity over time.
- The integrated results demonstrate that pyrite content, sulphate concentration, and binder type jointly control the evolution of permeability, and durability in paste tailings systems. Proper regulation of these parameters is essential for optimizing transportability, placement efficiency, and long-term environmental stability.
- The adoption of slag-blended binders offers a sustainable solution to mitigate sulphate attack, improve chemical stability, and reduce the carbon footprint of binder use.
- Overall, this research establishes a comprehensive framework linking the physicochemical processes of pyrite-bearing paste tailings to their engineering behaviour. It provides practical guidance for designing safer, cost-effective, and environmentally sustainable tailings management systems that ensure operational efficiency, structural integrity, and reduced environmental risk over the long term.

8.2 RESEARCH LIMITATIONS AND RECOMMENDATIONS FOR FUTURE RESEARCH STUDIES

Based on the findings of this research, future research work needs to;

- Investigate the long-term rheological evolution of pyrite-bearing paste tailings under varying temperature and humidity to simulate field conditions.
- Assess the interaction between pyrite oxidation and chemical admixtures (e.g., dispersants, superplasticizers) in improving flowability and controlling flocculation.

- Evaluate the use of alternative low-carbon binders (e.g., geopolymer, fly ash, or calcined clay blends) for mitigating pyrite-induced retardation and improving sustainability.
- Assess the environmental leachability and potential metal release from pyrite-bearing paste systems under different disposal and exposure scenarios.
- Conduct economic analyses to balance binder cost, energy demand, and environmental impact in designing sustainable pyrite-rich paste formulations.
- Given the scope of the present study, the investigation focused primarily on the influence of pyrite. However, in natural tailings systems, multiple sulphide minerals often coexist, including minerals such as pyrrhotite and chalcopyrite. As a limitation, the combined effects of these sulphide minerals on paste rheology and chemical reactivity were not examined. Therefore, future studies should investigate the interactive influence of multiple sulphide minerals, alongside pyrite, on the rheological behaviour and chemical reactivity of paste tailings systems.

APPENDIX-A

TEST MATERIALS, EQUIPMENT AND APPARATUS USED IN THIS STUDY

a) **(b)** **(c)**

Figure A-1: Test materials- a) Pyrite powder, b) Silica tailings c), Slag powder

a) **b)**

c)

Figure A-2: Testing equipment- a) Weighing balance, b) EC Monitoring Em50 data logger, c) pH Meter and probe

Figure A-3: Testing Apparatus-Brookfield digital viscometer (DV-E model)

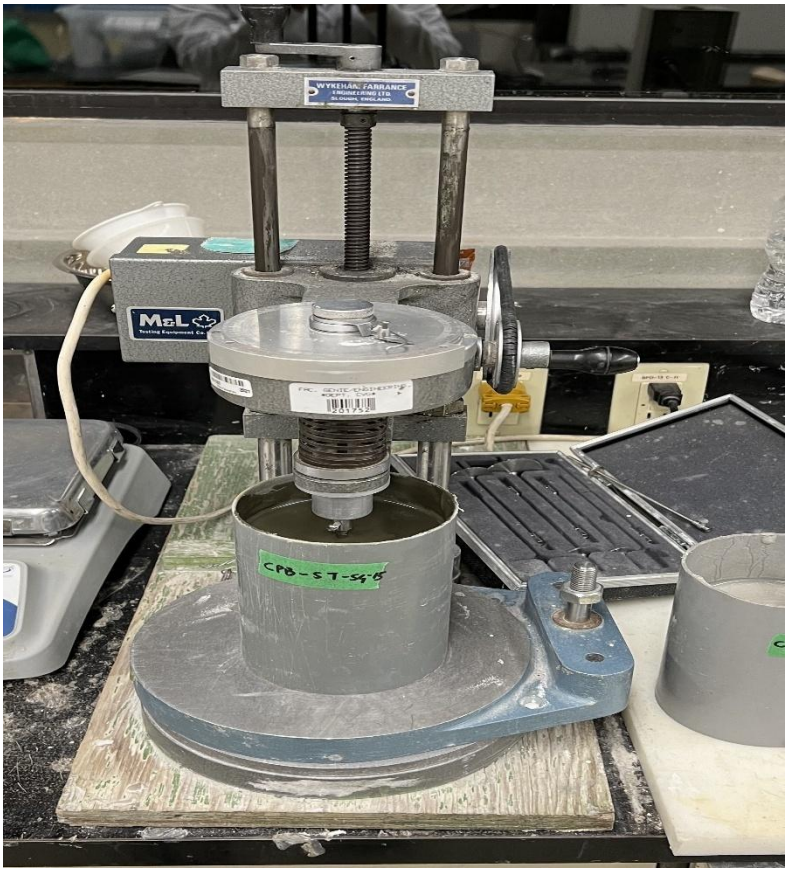

Figure A-4: Testing Apparatus-Wykeham-Farrance laboratory vane shear device

Figure A-5: Testing Apparatus- Tri-Flex 2 flexible wall permeameter

a)

b)

Figure A-6: Testing Equipment- a) Drying Oven, b) Kitchen aid mechanical mixer